Chronic pain and evoked responses in the brain

A magnetoencephalographic study in patients with Complex Regional Pain syndrome I and II

慢性疼痛和大脑的诱发反应
脑磁图的研究
复杂区域疼痛综合征I和II 患者

Colophon

Chronic pain and evoked responses in the brain
A magnetoencephalographic study in patients with Complex Regional Pain syndrome I and II
Peter J. Theuvenet

Utrecht: University Utrecht, Faculteit Geneeskunde, Thesis Utrecht University
With a summary in Dutch

ISBN/EAN: 978-90-70655-76-1

Printed by Number 58, Total Communications, Alkmaar, the Netherlands
Lay-out thesis: R.M. Blom (DPT department) Medical Center of Alkmaar, the Netherlands
Lay-out and graphics: P.J. Theuvenet, Medical Center of Alkmaar, the Netherlands

Part of the research conducted for this thesis was made possible by:

The University of Twente, Low Temperature Division, Hengelo, the Netherlands
Medtronic (Tolochenaz), Switzerland
The Royal Academy of Sciences, Amsterdam, the Netherlands

Production of the thesis was supported by The Pieter van Foreest Institute, Alkmaar, the Netherlands

Front cover: “A very cold place on earth”. The lowest temperature ever recorded at the surface of the earth was –89.2 °C (184.0 K) at the Soviet Vostok Station in Antarctica July 21, 1983.
Back cover: “The coldest place on earth”. In 1908 Kamerlingh Onnes at the University of Leiden, Dept. of Physics, managed to lower the temperature to less than four degrees above absolute zero, to –269 °C (4.15° Kelvin). The absolute zero is set by international agreement at -273.15 degrees Celsius. Photo with permission form Leiden University.

Chronic pain and evoked responses in the brain

A magnetoencephalographic study in patients with Complex Regional Pain Syndrome I and II

Chronische pijn en opgewekte activiteit in de hersenen
Een magnetoencephalografische studie bij patiënten met
Complex Regional Pain Syndrome I en II
(met een samenvatting in het Nederlands)

Proefschrift

ter verkrijging van de graad van doctor aan de Universiteit Utrecht op gezag van de rector magnificus, prof.dr. G.J. van der Zwaan, ingevolge het besluit van het college voor promoties in het openbaar te verdedigen op

woensdag 25 april 2012 des middags te 12.45 uur

door

Peter Johan Theuvenet

geboren op 17 december 1948
te Mataram, Lombok, Indonesië

Promotoren: Prof.dr. J.M. van Ree
Prof.dr. A.C. Chen

Co-promotor: Dr. J.C. de Munck

SCRIBONII LARGI
COMPOSITIONES
MEDICÆ.

IOANNES RHODIVS
recenſuit,
Notis illuſtrauit,
LEXICON SCRIBONIANVM
adiecit.

PATAVII, CIↃ IↃC LV.

Typis Pauli Frambotti Bibliopolæ.
SVPERIORVM PERMISSV.

C. J. Heise

"Vocatus, atque non vocatus, Deus aderit"
(Geroepen, en zelfs niet geroepen, God zal aanwezig zijn)
(Carl Gustav Jung 1875-1961)

In deep gratitude to my parents

Contributing authors

Prof. Dr. A.C. Chen
Human Brain Mapping and Cortical Imaging Laboratory, SMI, Aalborg University, Denmark (1998 – 2005)
Center for Higher Brain Functions, Capital Medical University, Beijing, China (2005 – present)

Prof. Dr. Z. Dunajski
Institute of Metrology and Biomedical Engineering, Warschaw University of Technology, Warschaw, Poland

Dr. J.C. de Munck
VU University Medical Center, Department of Physics and Medical Technology, Amsterdam, the Netherlands

Prof. Dr. F.L. Lopes da Silva
Swammerdam Institute for Life Sciences, Center of Neuroscience, University of Amsterdam, the Netherlands

Mevr. Prof. Dr. M.J. Peters
University of Twente, Low Temperature Division, the Netherlands

Drs. P.J. Theuvenet
Pain Clinic, Medical Center of Alkmaar, Alkmaar, the Netherlands

Dr. B.W. van Dijk,
MEG Center, VU University Medical Center, Amsterdam, the Netherlands

Prof. Dr. J.M. van Ree
Rudolf Magnus Institute of Neuroscience, Utrecht University and University Medical Center Utrecht, the Netherlands

Paranimphen
Dr. M.H. Hovingh, Reeuwijk, the Netherlands
Mrs. M.A. Dekkers, MSc, Alkmaar, the Netherlands

Table of contents

CHAPTER 1 INTRODUCTION

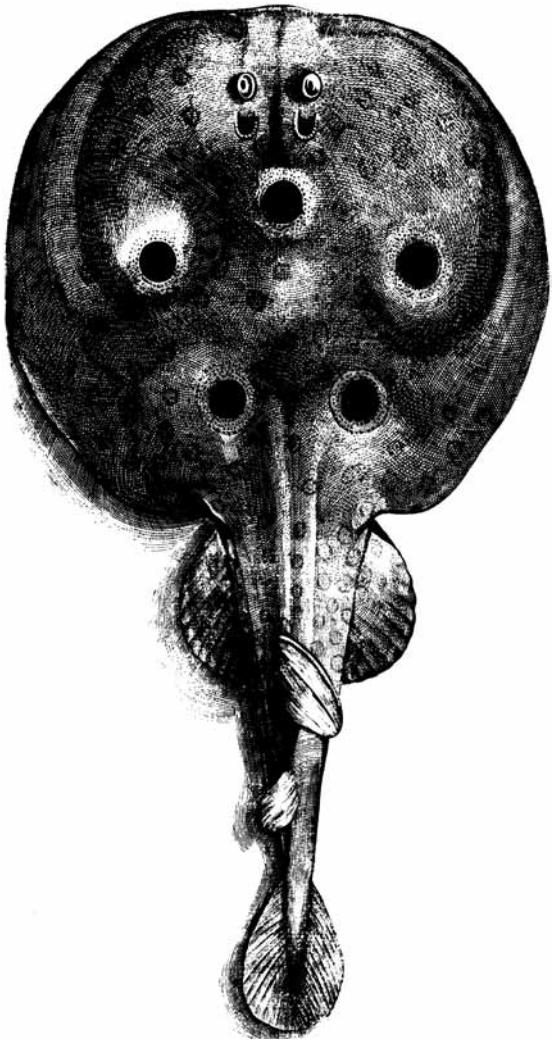

Torpedo fish
(Genus Torpedinidae)

The use of electrical energy to treat some types of pain dates back to Scribonius Largus, the Roman physician under the rule of emperor Claudius. In A.D 47 he described the use of electrical energy to treat some forms of pain by using the torpedo fish. Torpedo stems from Latin “torpere”, meaning “paralyzing or stiffening” and refers to the effects after human contact with the fish. The fish was used by the Greek to treat pain during childbirth and operations (Lazorthes et al., 1985; Bullock et al., 2005).

Neuromodulation is a recognized invasive therapy since its introduction in 1967 (Shealy et al., 1967). Two types are recognized in chronic non-oncological pain patients: Spinal Cord Stimulation (SCS) or Dorsal Column Stimulation (DCS), and the intrathecal administration of morphine (Spincemaille et al., 2004; Theuvenet et al., 2005).

Our clinical observation that after electrical dorsal column stimulation in some patients with chronic non-oncological pain, the pain alleviating effect diminished over time, triggered this research project. Besides the well known causes like scar tissue around the electrode, electrode migration and change in the course of the underlying disease, the therapy failed in some patients for unknown reasons.

Secondly, the fact that neuropathic pain due to traumatic peripheral nerve injury produces sensory disturbances and a volley of impaired afferent information (Woolf, 1993; Dellemijn, 1997; Woolf and Mannion, 1999), had to have demonstrable functional cortical effects. The study of both issues started in 1993. The first magnetoencephalograph (MEG) in The Netherlands was manufactured and made available for research at the Low Temperature Division of the Twente University, and the first MEG was measured on the 3rd of May, 1976.

General aims of the study

The general aim of the study was to investigate the cortically evoked responses after standard electrical median and ulnar nerve stimulation in two patient groups with either a Complex Regional Pain Syndrome (CRPS) type I or II, and compare the results with those in healthy subjects using identical measuring procedures. Five specific investigations were executed.

Specific investigations

I. to examine the stability and repeatability of evoked responses after standard electrical median, ulnar and posterior tibial nerve stimulation in the cortex of the brain in two studies of patients with a unilateral peripheral nerve injury and neuropathic pain.

II. to study the characteristics of the cortically evoked magnetic responses in healthy subjects after electrical median and ulnar nerve stimulation as a frame of reference for the measurements in the two patient groups.

III. to examine the characteristics of the cortically evoked responses in two patient groups: CRPS I and CRPS II.

IV. to compare the characteristics between the three groups: (a) healthy subjects; (b) CRPS I patients and (c) CRPS II patients.

V. to assess the functional cortical differences between these three groups and determine whether different cortical profiles exist.

In Chapter 2.1-2.4, an introduction into the neural circuitry involved in afferent information processing in the somatosensory nervous system is presented, including a short overview of neural plasticity changes and the body schema. In Chapter 2.5 an introduction is presented of CRPS I and II. Chapter 3.1 introduces and outlines magnetoencephalograph (MEG) as a neuroimaging and brain mapping technique. Chapter 3.2 presents the set up of the study, the materials and methods. Chapter 4 describes the results of the study in a group of patients with a peripheral nerve injury and chronic pain using MEG and EEG. Chapter 5 describes the cortical evoked characteristics of a group of healthy subjects after standard median nerve stimulation. Chapter 6 describes the cortical evoked magnetic responses after median and ulnar nerve stimulation in healthy subjects. Chapter 7 dealt with the question whether, like in motor handedness and lateralization, sensory handedness could be demonstrated. Chapters 5, 6 and 7 present the results after measuring healthy subjects and are to be considered as a normative database to this study. Chapter 8 describes the results of the study of patients with a proven peripheral nerve injury (PNI) and continuous neuropathic pain, some with full clinical CRPS II manifestation. Chapter 9 presents the results of comparisons in and between (a) a healthy control group; (b) patients with a PNI and (c) patients with a CRPS I. Chapter 10 presents Discussions and Conclusions.

References

Bullock TH, Hopkins CD, Popper AN, Fay RR (2005). In: Popper AN, Fay RR (Ed), Electroreception. Springer-Verlag, New York, pp 5-7.

Dellemijn, PLI (1997). Sensory disturbances in neuropathic pain. In: Dellemijn, Neuropathic pain (Thesis). Shaker Publishing, Maastricht: pp 45-62.

Lazorthes Y, Siegfried J, Upton RM. Basics on Biostimulation (1985). In: Lazorthes Y, Upton ARM (Ed), Neurostimulation, An Overview. Futura Publishing Company Inc. Mount Kisco, New York, pp 1-11.

Nuwer MR, Aminoff M, Desmedt J, Eisen AA, Goodin D, Matsuoka S, Mauguière F, Shibasaki H, Sutherling W, Vibert JF. IFCN recommended standards for short latency somatosensory evoked potentials. Report of an IFCN committee. International Federation of Clinical Neurophysiology. Electroencephalogr Clin Neurophysiol 1994; 91: 6-11.

Shealy CN, Mortimer JT, Reswick JB. Electrical inhibition of pain by stimulation of the dorsal columns: preliminary clinical report. Anesth Analg 1967; 46: 489-491.

Spincemaille GHJJ, Beersen, Dekkers MA, Theuvenet PJ. Neuropathic Limb Pain and Spinal Cord Stimulation: Results of the Dutch Perspective Study. Neuromodulation 2004; 3: 184-192.

Theuvenet PJ, Dekkers MA, Beersen N, Klazinga NS, MD, Spincemaille, GHJJ. The Development of a Quality System for Neuromodulation in The Netherlands. Neuromodulation 2005; 1: 28-35.

Woolf CJ. The pathophysiology of peripheral pain-abnormal peripheral input and abnormal central processing. Neurochir Suppl Wien 1993; 58: 125-130.

Woolf CJ, Mannion RJ. Neuropathic pain: aetiology, symptoms, mechanisms, and management. Lancet 1999; 353: 1959–1964.

CHAPTER 2 SOMATOSENSORY PROCESSING AND PAIN

2.1 The peripheral receptor

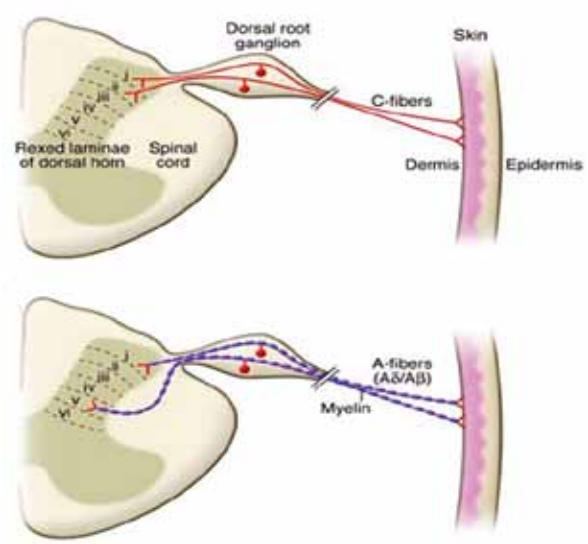

Fig.1. Nociceptor connections from the skin with Rexed areas I, II and V in the dorsal horn.
With permission: A. Dubin, Dept. of Biology, La Lolla, California, USA, J Clin Invest 2010.

Processing of information in the somatosensory nervous system, including pain, follows specialized neural pathways that start in the periphery of the body and end in the central nervous system ([2] Guyton, 1976; [2] Willis et al., 1985; Almeida et al., 2004). Neuroanatomy, neurochemistry and neurophysiology are basic areas of interest in relation to the function of the somatosensory system (Anand and Carr, 2005). All sensory systems have in common that perception starts in a specialized receptor ([1]Martin, 1991). Stimulation of a specialized receptor and the following transduction of the stimulus into the receptor potential, is the first step from perception towards sensation; this is common for vision, hearing, touch, taste, and smell. In the somatosensory system, receptors are distributed throughout the whole body (Kniyihar-Csillik, 1990; [1] Martin, 1991; Reichling and Levine, 2009).

Transduction is the conversion of energy from the stimulus into electrochemical energy (Fields, 1990; Lumpkin et al., 2007). The resulting encoded stimulus is transmitted along parallel and hierarchical pathways to e.g. the thalamus and from there to other subcortical and cortical areas ([3] Willis, 1985; Fields, 1990; Kaas, 2004) so that its meaning may become clear to the mind ([1] Guyton, 1976; Lumpkin et al., 2007). Stimulus information is enclosed in a series of action potentials by a process called neural encoding. These neural codes may arise from single neurons or a population of neurons ([2] Martin, 1991). Information in the somatosensory nervous system means e.g. the position of a limb, the intensity of pain, touch or temperature. Sensory systems are topographically organized, indicating that the different parts of the peripheral receptive sheet are orderly represented in subcortical and cortical areas. This is called somatotopy (Baumgartner et al., 1991; [3] Martin, 1991; Jain et al., 1998; Hlustík et al., 2001; Young et al., 2004), and is illustrated on the cortex by the homunculus (Penfield and Boldrey, 1937). The somatosensory homunculus, representing various body parts were studied non-invasively, using magnetoencephalography (Narici et al., 1991; Kakigi et al., 2000). While in other systems a single modality is mediated (vision or taste), in the somatosensory system many kinds of stimuli are processed. In this system, touch, proprioception, pain and thermal sensations are the four elementary modalities ([2]Martin et al., 1991; Dubin and Patapoutian, 2010).

Pain, like the other sensory modalities, depends on the activation of a discrete set of neural pathways, which includes primary afferent fibres that terminate distally in nociceptors (Kelly, 1991). C.S. Sherrington postulated in 1906 that part of the somatosensory system signals tissue injury which may result in pain sensation (Gebhart, 2004). It lasted another 60 years before the existence of two types of nociceptors in humans

was demonstrated. A nociceptor is defined as "a receptor sensitive to a noxious stimulus or to a stimulus which would become noxious if prolonged" (Perl, 1984). Nociceptors are the termination of small myelinated A-delta fibres (Burgess and Perl, 1967) or the non-myelinated C-fibres with bare endings (Bessou and Perl, 1969; Handwerker, 1991; Mason, 2007). C-fibre density in human skin is probably higher than A-delta fibre density (Bragard et al., 1996). Furthermore, in the different tissues, more than one type of nociceptor can be present (Perl, 1984; [2] Willis, 1985; Heppelman, 1990; Handwerker, 1991). Nociception is the neural process in the somatosensory nervous system that encodes and processes noxious stimuli (Loeser and Treede, 2008).

Recently, it was reported that in different species the proportion of nociceptors in cutaneous afferent A-beta fibers, may vary from 18% to 65%, and usually >50% in rodents. In rat, about 20% of all somatic afferent neurons with A-alpha/beta-fibers are nociceptive (Djouhri and Lawson, 2004; Dubin and Patapoutian, 2010). Proof that nociceptors mediate pain in humans comes from clinical and experimental observations following stimulation or ablative procedures ([5] Willis, 1995). In between, five classes of nociceptors in the skin and the subcutaneous tissue have been identified (Dubin and Patapoutian, 2010) which are activated by mechanical, thermal and chemical stimuli. Stimulation of cutaneous A- δ nociceptors will produce a "pricking pain" (Konietzny et al., 1981) in contrast to the dull burning pain after stimulation of C-nociceptors (Ochoa and Torebjörk, 1989). Nociceptors are also found in the supportive tissues of peripheral nerves and may give rise to nocigenic nerve pain (Asbury and Fields, 1984). In response to environmental circumstances (i.e. tissue damage), neuroplasticity changes occur from the peripheral receptor to the dorsal root ganglion (Kniyihar-Csillik, 1990; [1,2] Snow et al., 1991; Duggan et al., 1991; Reichling and Levine, 2009). In the dorsal root ganglion somatotopy is maintained (Hallin, 1990, 2001; Hlustík et al., 2001).

2.2 The afferent pathways

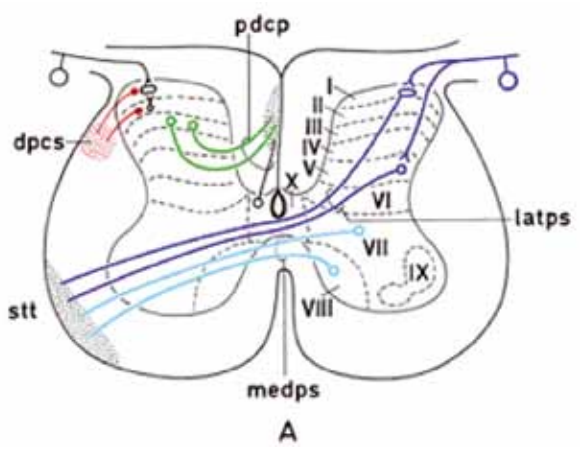

(with permission from Prof. Dr. R. Nieuwenhuys)
Roman numbers depict various cytoarchitectonic layers in the grey matter of the spinal cord according to Bror Rexed (1952). stt = spinothalamic tract (dark blue); medps = medial pain system (cyan); latps = lateral pain system; dpcs = descending pain control system (red); pdcp = postsynaptic dorsal column pathway (green). Blue lines depict connections from the dorsal root ganglion, through laminae I and V to the contralateral side of the spinal cord.

The central terminals of primary afferent fibres branch upon entering the spinal cord, and terminate in different ways and at different levels. Here the first relay point for somatic sensory information is found ([2] Willis, 1985; Rethelyi, 1990). This includes processing of nociceptive information (Heppelman et al., 1990). Lamination of the spinal cord was initially demonstrated in cats by Rexed, and later in humans (Rexed, 1952; [1] Nieuwenhuys, 2008). The trigeminal system will not be discussed since it is not relevant for the present study.

In humans, starting at the level of the spinal cord, several afferent pathways are distinguished ([3,4]

Willis, 1985; [1] Burt, 1993; [7] Willis and Westlund, 1997; Kaas, 2004; Almeida et al., 2004; [1,2] Nieuwenhuys, 2008). The AnteroLateral System (ALS) consists of three closely positioned afferent pathways in the white matter of the spinal cord and includes:

1) The spinothalamic tract (STT), arises from laminae I, IV-VIII and ascends in the contraleral anterolateral funiculus (see Fig. 1- latps), to the lateral part of the brainstem and ends in the lateral thalamus (Kaas, 2004; Almeida et al., 2004; [1] Nieuwenhuys, 2008). In monkeys, a smaller proportion of the fibres in the sacral cord do not cross the midline and run ipsilateral ([3] Willis, 1985). Afferent information from the arm and leg in healthy subjects, as confirmed by using Diffuse Tensor Imaging (DTI), is kept segregated in the ascending tracts and somatotopy is maintained (Hong et al., 2011). The STT conveys somatic information on pain, temperature and light touch ([1] Burt, 1993). The STT, originating from laminae I and V, is probably the most important human pathway involved in pain processing and constitutes the first part of the lateral pain system ([1] Willis, 1985). In humans, functional changes in the STT were demonstrated after a percutaneous cervical cordotomy in patients with pain due to a malignancy, indicating that pain modulation occurs rapidly after deafferentation (Rosso et al., 2003).

2) The spinoreticular tract (SRT) in monkeys arises from laminae VII and VIII, partly from laminae I and V ([3] Willis, 1985). The spinoreticular tract presents two projection components in the brain stem; (1) to the lateral reticular formation, involved in motor control and (2) the second directed to the medial reticular formation involved in mechanisms of nociception (Almeida et al., 2004). At the cervical enlargement, equal amounts of neurons cross contra laterally or run ipsilaterally. At the lumbar enlargement more cells project contralaterally ([1] Willis, 1985). This indicates that in monkeys the SRT pathway conveys information to the cortex bilaterally. The SRT ascends in the ALS more medially compared to the STT (see Fig. 1- medps), and terminates in the medial part of the thalamus ([2] Nieuwenhuys, 2008). Spinoreticular neurons, activated by antidrome stimulation were nociceptive ([3] Willis, 1985).

3) The spinomesencephalic tract (SMT) crosses the midline and conveys nociceptive information to the midbrain ([3] Willis, 1985; [2] Burt, 1993), among others the lateral peri-aquaductal grey, and the superior colliculus. Ablative procedures in humans have demonstrated that the SMT participates in pain mechanisms by activating midbrain neurons ([3] Willis, 1985). Most fibres of the ALS cross in the ventral white commissura, however a distinct ipsilateral part exists ([2] Nieuwenhuys, 2008).

4) The spino-parabrachio-amygdaloid pathway (SPAP) originates from cells in lamina I. Its trajectory is comparable to the ALS in that SPAP axons decussate. At the level of the pons, this pathway connects to the parabrachial nuclear complex and proceeds from there to the amygdala which are considered to be part of the limbic system ([2] Nieuwenhuys, 2008).

5) The spino-limbic projections arise from the SMT and SPAP and connect to the limbic system. This includes the cingulate cortex, amygdala and peri-aquaductal grey and the hypothalamus ([3] Burt, 1993).

6) The postsynaptic dorsal column pathway (PDCP) is located dorsally in the spinal cord, and was known to convey touch but in rats visceral nociceptive afferents have been demonstrated as well (Al-Chaer, 1998; [6] Willis et al., 1999). The PDCP ascends ipsilateral at the site of entry, and connects to either the nucleus gracilis or

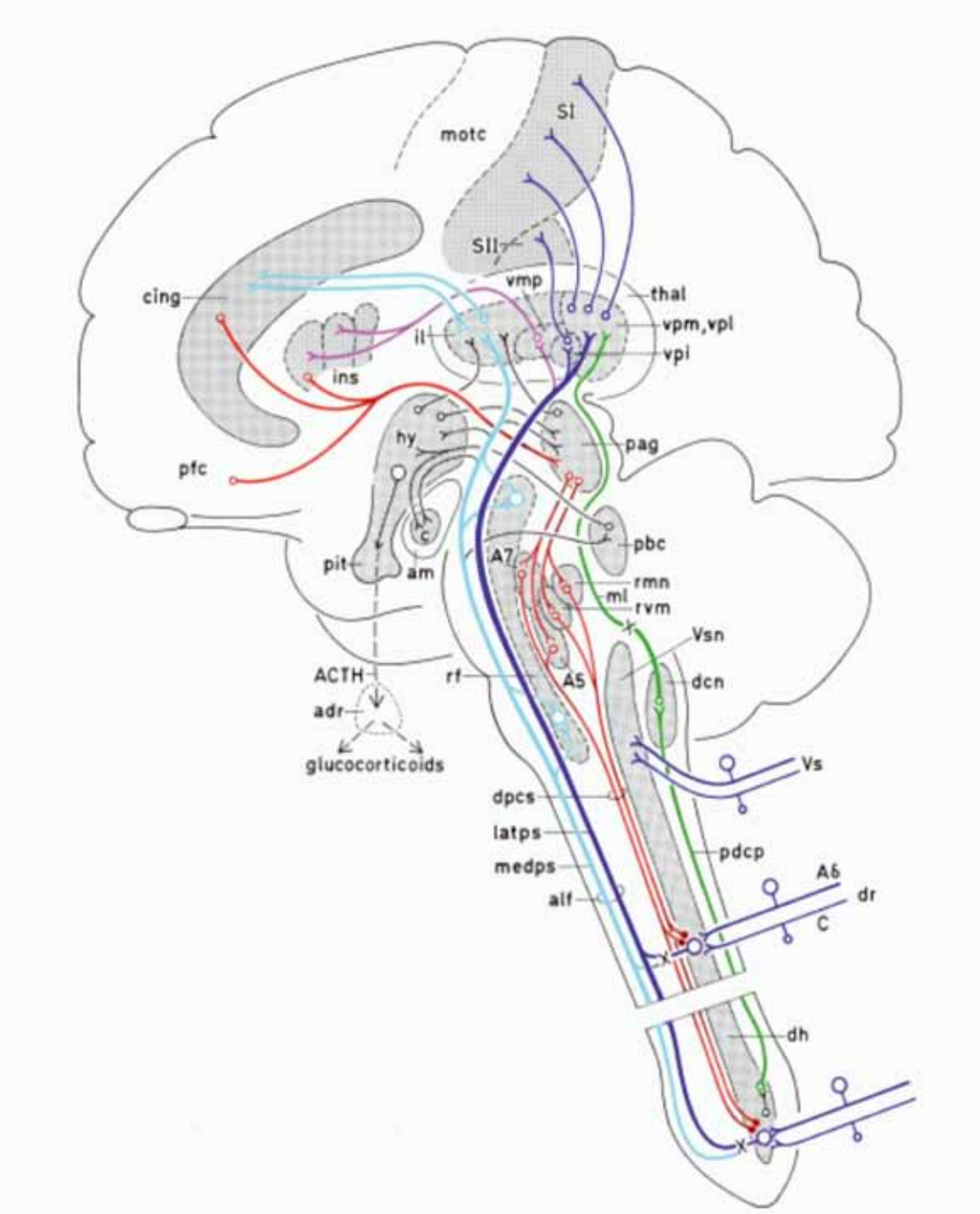

(with permission from Prof. Dr. R. Nieuwenhuys)

Fig. 1 presents a saggital overview of the ascending pathways in the spinal cord, subcortical and cortical structures and descending pathways. Alf = anterolateral funiculus; cing = cingulate cortex; dcn = dorsal column nuclei; dpcs (red) = descending pain control system; ins = insular cortex; Latps (dark blue) = lateral pain system; medps (cyan) = medial pain system; pdcp (green) = postsynaptic dorsal column pathway; pag = peri-aquaductal grey; rf = reticular formation; SI = primary somatosensory cortex; SII = secondary somatosensory cortex; vpi = ventral posterior inferior thalamic nucleus; vmp = ventral medial posterior thalamic nucleus; vpl = ventral posterior lateral thalamic nucleus; vpm = ventral posterior lateral thalamic nucleus.

cuneatus in the brainstem. Besides nocigenic visceral pain, nociceptive pathways in the PDCP are not essential for human pain ([5,6,7] Willis, 1995, 1999, 2001). Plasticity in this pathway was demonstrated ([3] Snow et al., 1991). Fig. 1 summarizes in a saggital overview afferent and efferent (red = descending) pathways, and cerebral structures involved in somatosensory processing of information, including nociception. The medial (medps) and lateral (latps) pathways of the pain system are depicted in different colors. Descending inhibition in red.

7) The spino-cerebellair pathway, arising from laminae I-VI, conveys mainly proprioceptive information to the ipsilateral cerebellum and has no direct relevance for the present study ([2]Burt, 1993).

In conclusion, the neuroanatomy reveals that in the afferent somatosensory nervous system, information is conveyed centrally both in a contralateral and ipsilateral way and in all afferent pathways, plasticity has been demonstrated.

2.3 Central processing

The pain system ([3] Willis, 1985) or *the pain matrix* (Melzack, 2001) originates from an extensive network of brain regions. The pain system is part of the somatosensory nervous system and is considered to represent a unique number of cerebral structures involved in pain perception (Guilbaud et al., 1994; Derbyshire, 2000; Schnitzler and Ploner, 2000; Iannetti, 2010; Legrain, 2011). From the level of the brainstem, medial and lateral thalamus, two major ascending projecting areas can be distinguished, a lateral and a medial pain system (Dubner, 1984; Jones et al., 1991; Sikes and Vogt, 1992; Vogt et al., 1993; Coghill et al., 1994; [2] Nieuwenhuys, 2008), each with a different task in the pain processing. The anatomical division in two pain systems was supported by work on morphine antinociception in animals (van Ree, 1977). In clinical practice, the demonstration of morphine antinociception throughout the neuraxis, initiated the epidural and intrathecal administration of morphine in non-malignant and malignant chronic pain in the home care situation (Boersma et al., 1992; Beersen et al., 2004). The thalamus, as an important subcortical relay centre (Almeida et al., 2004) and start of various thalamocortical connections, demonstrates plasticity as well ([4] Snow et al., 1991; Shyu and Vogt, 2009; Jetzer et al., 2009; Naumer et al., 2009). The structure and functional aspects of descending modulation of pain (Stanford, 1995; Gebhart, 2004) are not included in this overview since they are not relevant for the topic of this study.

The *medial pain system* starts in the medial part of the spinal cord and connects to the medial thalamic nuclei which show slower transmission and relatively poor spatial information (Jones and Derbyshire, 1996; Vogt and Sikes, 2000). In humans, the thalamus is involved in pain processing (Lenz, 1991; [2] Nieuwenhuys, 2008). The medial part (including deep brain stem structures, the peri-aquaductal grey, anterior cingulated and frontal cortex) is considered to be important for the emotional, cognitive and reflex processing of nociception ([5] Willis, 1995; Almeida, 2004). The *lateral pain system* on the other hand, passes the lateral part of the thalamus and projects to the primary and secondary somatosensory (SI and SII, respectively) and insular cortices (Jones et al., 1996; Wiech et al., 2000; Maihöfner et al., 2006). Although the role of the somatosensory cortex was debated in the past, its role in pain processing is now well accepted (Bushnell, 1999; Treede et al., 1999, 2000; Schnitzler and Ploner, 2000). The lateral system is somatotopically arranged and subserves relatively fast transmission.

After unilateral electrical stimulation in humans, contra- as well as ipsilateral SII somatotopy was found (Ruben et al., 2001). The lateral system is important for the sensory discriminative aspect of pain, especially acute pain mediated by A-delta fibres. In the lateral system (Fields, 1994) the thalamus is more than a simple relay station between the periphery and the cerebral cortex. Electronic microscope studies have revealed that numerous connections exist with surrounding structures (Ralston, 1984). The functional distinction in a medial and lateral pain system, supports the IASP definition of pain (Merskey et al., 1994) which states that pain comprises a "sensory and emotional experience. However, it remains difficult to differentiate the function of the pain systems from other functions of the same structures involved ([2] Nieuwenhuys, 2008).

The primary somatosensory cortex (SI) is anatomically and functionally well studied due to its proximity to the skull. In the saggital view (see Fig. 1), SI is positioned at the central sulcus in the postcentral gyrus and consists of four subsections, Brodmann areas 3a, 3b, 1 and 2 (Kaas, 2004). At the level of S I, somatotopy is maintained (Ogino et al., 2005; Okada et al., 1984). Electrocorticography in humans, after electrical median and ulnar nerve stimulation, demonstrated non-overlapping of the somatotopy of all digits despite relative spatial inter-digit differences (Baumgartner et al., 1991; Sutherling et al., 1992). Afferent pathways, via different thalamic nuclei are connected to these SI subsections and with SII (Kaas, 2004; Nieuwenhuys, 2008). Imaging and electrophysiological studies have provided additional evidence for a different role of the two pain systems and their respective subcortical and cortical areas (Treede et al., 1999, 2000). The functional neuroanatomical aspects will be discussed in Chapter 3.

Interhemispheric transmission of information

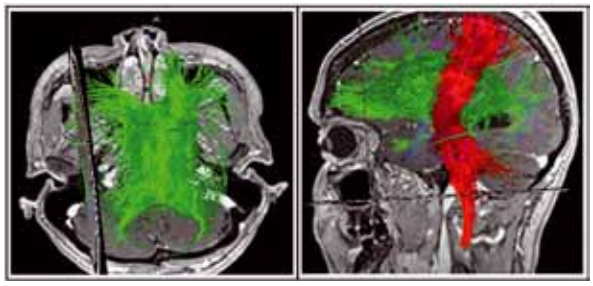

Diffuse Tensor Imaging (DTI) of the human corpus callosum (green) and pyramid tract (red).
(Courtesy: Dr. W.F. Tan, neurosurgeon – Medical Center Alkmaar, The Netherlands)

Each half of the body surface is represented topographically in the contralateral cerebral hemisphere (Calford and Tweedale., 1990; [3]Nieuwenhuys, 2008). In Chapter 2.2, bilateral neuroanatomical representation of somatosensory information in afferent somatosensory pathways was already mentioned ([2] Nieuwenhuys, 2008). Exchange of information in human adults between the neocortical parts of the two hemispheres, either through homotopic or heterotopic connections, is facilitated by the relatively large corpus callosum (CC) and the smaller commissura anterior ([3] Nieuwenhuys, 2008; Berlucchi, 2011). The corpus callosum is a thick band of nerve fibers that connects the left and right cerebral hemispheres allowing communication between both hemispheres. The CC is divided in three parts; from anterior to posterior (a) the genu, (b) the corpus and (c) the splenium. The CC transfers information between the two brain hemispheres ([4]Burt, 1993; [3] Nieuwenhuys, 2008) and in a fMRI study CC somatotopy was demonstrated (Salvolini et al., 2010). The posterior part of the CC exchanges somatosensory information (Fabri et al., 2005) between the two halves of the parietal lobe and visual center at the occipital lobe (Hofer and Frahm, 2006). The CC is also involved in the exchange in motor information.
In *animals*, evidence for interhemispheric transfer

was demonstrated. The evidence suggests that the pathways and mechanisms mediating this transfer are specific to the role of maintaining balance, or integration, between corresponding cortical fields (Calford and Tweedale, 1990). In the somatosensory homunculus, the representation of the hand and especially the digits is relatively large. In macaque monkeys, in this part of the somatosensory cortex a substantial number of neurons with receptive fields on the bilateral hands has been found. After lesioning the postcentral gyrus, neurons with bilateral receptive fields were not longer found, indicating that interhemispheric transfer of information occurs at higher hierarchical levels in each hemisphere (Iwamura et al., 1994). More recently it was found that a substantial number of neurons with bilateral receptive fields on extremities, hand/digits, shoulders/arms, or legs/feet in the caudal most part (areas 2 and 5) of the postcentral gyrus existed (Iwamura et al., 2001). This indicates that in monkeys a bilateral representation exists in the postcentral somatosensory cortices (Manzoni et al., 1984). Bilateral neuronal representation and interhemispheric transfer of information may explain why in unilateral deafferentation, bilateral changes occur in the cortex.

Clinical evidence in humans comes from patients with (a) callosal agenesis, (b) commissurotomies or (c) injury of the corpus callosum (Geffen et al., 1994; Berlucchi, 2011). In an fMRI study, differences between callosal agenesis and commissurotomy patients compared to a control group have been demonstrated after tactile and painful stimulation (Duquette et al., 2008). Bilateral tactile activation was found in SI and / or SII in controls and acallosal patients, in callosotomized patients no ipsilateral activation was observed. After painful stimuli, in all three groups ipsilateral responses in the target pain related areas have been demonstrated. Therefore, ipsilateral activation of pain related regions does not depend on an intact corpus callosum. Functionally, differences were found between total and partial callosotomy patients, indicating that posterior corpus callosum integrity is required for tactile information transfer (Fabri et al., 2005). In a female patient, body cognition was confined to the left side, she had difficulty in naming the fingers of the left hand. A MRI demonstrated involvement of the entire corpus callosum due to occlusion of a branch of the anterior cerebral artery (Nagumo and Yamadori, 1995). In callosotomy patients, a complex mosaic of mental processes that participate in human cognition, were observed (Gazzaniga, 2000).

Finally, in humans the question whether transcallosal interhemispheric influences are primarily excitatory ([2] Reggia et al., 2001), inhibitory or both, is still debated (Bloom and Hynd, 2005). There is evidence that both excitation and inhibition play a role in interhemispheric transmission of information (Brown et al., 1996; Bloom and Hynd, 2005; Knaap van der LJ, 2011). Altered interhemispheric transfer of information in patients with Tourette's disorder has been suggested, based on an altered MRI scan size of the corpus callosum in children and adults, possibly due to cortical plasticity changes (Plessen et al., 2004).

At a higher hierarchical level in somatosensory processing, the concept of the *body schema* is positioned. The body schema integrates multisensory information to maintain a real-time three-dimensional body representation (Maravita et al., 2003; Holmes and Spence, 2004; Naumer et al., 2009; De Vignemont, 2010; Mourauxa et al., 2010). In the context of the present study, multisensory integration is an important issue since it is not only operational under physiological conditions, but also in disease states with pain. Mechanisms that maintain the body schema are an important and renewed functional research area, they may explain some of the bilateral

changes encountered in animals and humans. The body schema is subserved by dedicated neural pathways from spinal cord and brain stem to the cortex (Berlucchi and Aglioti, 2010). Included are feelings such as pain, temperature, itch, sensual touch, muscular and visceral sensations, vasomotor activity, hunger, thirst and dyspnea. Some reports of body representations, postulate representation of the body in space generated by proprioceptive, somatosensory, vestibular and other sensory inputs (Schwoebel et al., 2005; Maravita et al., 2003).

Interoception or internal sense, is any sense that is normally stimulated from within the body, a sense of the physiological (homeostatic) condition of the body. Berlucchi (2010) points out that interoception, in addition to exteroception and proprioception is important for corporal awareness. However, the notion that corporeal awareness relates to a single cortical area, is far too simple. There is evidence for a cerebral organization based on a variety of distributed systems constituted by specifically interconnected areas in multiple locations (Berlucchi, 2010). Pain is part of this homeostatic system, our interoceptive consciousness (Birklein and Rowbotham, 2005). In a recent publication, body schema changes were described in two pain syndromes, CRPS and phantom limb pain (Reinersmann et al., 2011). Although two different pain syndromes, the body schema was equally disrupted. This suggests the involvement of complex central nervous system mechanisms (Reinersmann et al., 2010).

2.4 Neural plasticity and reorganization

The persistence of memory (Catalan: La persistència de la memòria). Dali's clocks aren't stopped or broken, they only adapt to the shape of every object they meet.

The notion that the human brain and its functions are not fixed throughout life was already suggested in 1890 (James, 1890; Berlucchi et al., 2009), but long forgotten. William James stated: "organic matter, especially nervous tissue, seems endowed with a very extraordinary degree of plasticity of this sort". The static view that the nervous system was relatively immutable after a critical period of gestation during early childhood, lingered during the first half of the twentieth century (Kaas, 1999). The first, allegedly to have used the term "neural plasticity" was Jerzy Konorski, Nencki Institute of Experimental Biology in Warschaw (Ledoux, 2002, 2003). Paralleled by the work of Donald Hebb, who rehabilitated the synaptic plasticity theory of learning in 1949 and stated that "when one cell repeatedly assists in firing another, the axon of the first cell develops synaptic knobs (or enlarges them if they already exist) in contact with the soma of the second cell" (Berlucchi et al., 2009). In other words: nerve cells may grow new connections and undergo metabolic changes that enable them to communicate: "neurons that fire together, wire together". These synaptic changes became known as long-term potentiation (LTP) and long-term inhibition (LTI). LTP is a long-lasting

enhancement in signal transmission between two neurons that results from stimulating them synchronously, LTI the opposite (Bliem et al., 2008; Sanderson et al., 2011). LTP and LTI in humans are regulated by homeostatic control mechanisms to maintain synaptic strength in a physiological range, as was demonstrated both for the motor and somatosensory cortex (Buonomano and Merzenich, 1998; Bliem et al., 2008). Our study aims are directed to functional cortical changes, therefore other basic mechanisms of cortical plasticity like axon growth (sprouting) or neurotransmitter changes, are not discussed (Florence, 1998, 2002).

Neuroplasticity, including cortical plasticity, is not a well defined concept, and frequently mixed with cortical reorganization. In humans, neuroplasticity under physiological and non-physiological circumstances, is an adaptation that may develop throughout the entire nervous system (Buonomano and Merzenich, 1998; Kaas, 1999; Zhuo, 2004; Sanderson, 2011). Neural reorganization occurs at a variety of levels, ranging from cellular changes, receptors and dorsal ganglia (Furue et al., 2004), sprouting of cortical connections (Florence, 1998) to large-scale changes involved in cortical remapping (Malmberg, 2001; Wall, 2002). Cortical plasticity may compensate the effects of the cortical degeneration associated with normal aging (Pellicciari et al., 2009). Interestingly, in clinical medicine, neuroplasticity has also been described after continuous intrathecal administration of an opioid and may be in involved in the phenomenon tolerance (Mao et al., 2001). In this study, an arbitrary distinction was made between cortical plasticity and cortical reorganization. Cortical plasticity has been defined as the central nervous systems ability (a quality) to adapt to environmental challenges or compensate for lesions, both in animals and humans (Donoghue, 1995; Buonomano and Merzenich, 1998; Rossini et al., 1994; Kaas, 2001). This signifies that the nervous system is able to react to changes, process the information and generate an appropriate behavioral response (Hummel et al., 2005). Cortical reorganization can be regarded as the quantification of cortical plasticity since it refers to measureable functional parameters, and addresses the question “what changed and what metric has been used to conclude that a plastic event has occurred ?” (Ebner et al., 2005).

Cortical plasticity affects human daily life much more than is realized. The most widely recognized forms of plasticity are learning, memory and recovery from neural damage (Byl, 2005). Cortical plasticity can occur within the same somatosensory modalities, e.g. vision, auditory or somatosensory system. The first to recognize that changes in one modality could influence and activate another modality, called *sensory substitution*, and offering technical opportunities was Paul Bach-y-Rita (1999). Patients with vestibular damage and loss of gravitational stability were treated with a small array of electrodes stimulating the tongue. After several weeks of treatment, patients regained their ability to remain balanced without the use of the equipment. Evidence for cortical reorganization comes from studies where changes in the somatotopy in the primary somatosensory and motor cortex after impaired afferent input occur (Kaas, 2005). Most contemporary knowledge on human cortical plasticity was initially derived from animal experiments ([1,2] Merzenich et al., 1983). Aspects of cortical plasticity changes in animals and humans will be discussed.

Animal studies

New World owl monkey

Animal research on cortical plasticity involved several kinds of animals, and evidence shows that their somatosensory maps can change. In particular New World owl and squirrel monkeys, which have most of the primary somatosensory cortex exposed close to the surface, have been studied (Jain et al., 1998). On the somatosensory cortex of owl monkeys, after myelin staining, morphological maps for each finger were found. In response to peripheral stimulation using microelectrodes, an orderly somatotopic presentation was found from lateral to medial (Jain et al., 1998). After injury, these maps did not change morphologically but only physiologically. In normal monkeys, using a learning paradigm, cortical plasticity changes were found in a use-dependant task setting (Jenkins,1990; Nudo, 1996). Besides cortical changes, plasticity changes at the subcortical level in the brainstem and thalamus have been described (Garraghty et al., 1991; Jones and Pons, 1998; Wall et al., 2002).

Following *peripheral nerve injury*, plasticity changes include both motor and somatosensory map reorganization. Facial nerve transection in rats produced a *functional shift* from the denervated area towards a new group of innervated muscles within hours. A stable, functional change that lasted for months. One of the striking observations was the activation of neighbouring receptive fields to compensate for the deafferentiated area (Sanes et al., 1988). *Bilateral cortical changes* were demonstrated by Calford and Tweedale (1990). In their study with flying foxes and monkeys, a local anesthetic was used for peripheral denervation of a digit. Linking homotopic regions of the primary somatosensory cortex, the bilateral effects of denervation were monitored. They found that plasticity induced in one hemisphere, in the form of receptive field *expansion* brought about by a relatively small peripheral denervation, was immediately (within minutes) mirrored in the other hemisphere. The mechanisms that induce multilevel changes may result from altered peripheral afferent activity. The altered activity induced a central release of inhibition which facilitates interhemispheric processing of information (Xu and Wall, 1999).

Human studies

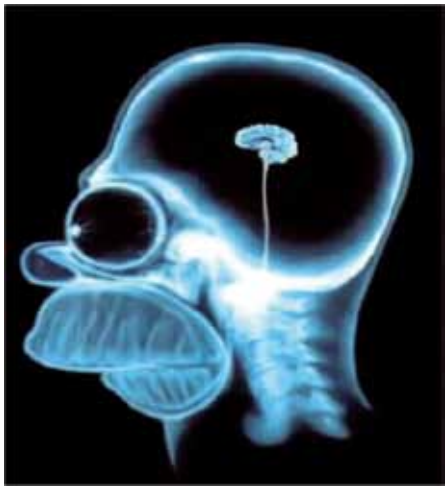

"An abnormally shrunken hand area was observed in three syndactyly patients"

Adult human and patient studies demonstrate that rapid cortical plasticity changes occur under physiological conditions and after injury. Cortical

plasticity was found in violin players, and witness the amazing capacity of the nervous system to meet the environmental demands in human life (Byl et al., 2000; Pantev et al., 2003). The use-dependent enlargement of the *area* of the left hemisphere representation in the sensorimotor cortex of right handed violin players was noticed. While the significant right-larger-than-left asymmetry of the motor and somatosensory cortex was lacking in right handed non-musician controls (Schwenkreis et al., 2007). In a use-dependant learning study, using a unilaterally trained tactile discrimination task model, cortical plasticity was demonstrated using MEG. The parameter demonstrating reorganization was the *dipole strength*, after training a dipolar strength decrease was observed (Spengler et al. 1997). Short-term neuroplastic changes were described in healthy humans. After transient sensory deprivation using an ischemic nerve block (INB), rearrangement of the magnetic finger representations in the primary somatosensory cortex was observed (Rossini et al., 1994). Using an Equivalent Current Dipole (ECD) model (Fuchs et al., 2004), an increase in *dipole strength and a position shift* in the coronal plane was observed for the thumb and little finger. In these three human studies, different reorganizational parameters were found.

In another MEG study, three patients underwent a surgical syndactyly correction of the hand (Mogilner, 1993). Preoperatively, *an abnormally shrunken hand area* was found on the primary somatosensory cortex without distinct borders between the webbed fingers. Compared to controls, somatosensory map restoration was observed after the operation for each finger. This suggested that after operation, functional plasticity changes in the primary somatosensory cortex restored non-overlapping. Functional non-overlapping of the fingers in humans, after electrical median and ulnar nerve stimulation, was demonstrated by electrocorticography (Sutherling et al., 1992). This affirms that under physiological circumstances, somatotopy in the somatosensory map is maintained. *However*, cortical restoration after nerve repair differed between adults and children. After suturing a transected peripheral nerve in adults, sensory perception remained abnormal. In children, the superior recovery from nerve injury presumably depended on restoration of somatotopy in the central sensory maps. This was supported by experiments in immature monkey (Florence et al., 1996). These two examples indicate that the different tissues involved (skin versus nerve tissue), produced different cortical effects.

Under experimental circumstances in humans, like an ischemic nerve block (INB) producing deafferentation, fast cortical plasticity changes occurred (Rossini, 1994). After using an INB block, an increased bilateral cerebral blood flow was observed in the motor cortex, as well as an increased excitability of the *ipsilateral* hemisphere and decreased interhemispheric transmission (Sadato, 1995). In two human studies, acute deafferentation was reached with the use of a local anaesthetic block or a unilateral INB block. Increased tactile discrimination was found in the non-anesthetized somatosensory cortex ([1,2]Werhahn, 2002). Other studies demonstrate immediate task-dependant cortical changes that fade away after 3-4 weeks, possibly due to a learning effect (Spengler et al., 1997). *Unilateral* changes in afferent somatosensory inputs, not only produced cortical plasticity in the contralateral hemisphere (Mogilner, 1993; Karl, 2001) but also in the ipsilateral sensorimotor cortex (Hummel, 2005). Therefore, the functional sensory hand index (Theuvenet et al., 2005) is not a fixed but rather a dynamic entity, and the inter-digit somatosensory map distances may adapt

in response to altered circumstances. These rapid and bilateral reorganizations generally are attributed to a rebalancing of excitatory and inhibitory factors within a dynamically maintained system in humans (Burton, 2005). The mechanisms operational in bilateral changes, facilitated by altered interhemispheric transmission, induce somatosensory and motor cortical functional adaptations (Kaas, 1999). Interhemispheric transmission is facilitated by transcallosal fibres (see 2.4). The question whether these fibres are primarily excitatory, inhibitory or both is still debated (Bloom and Hynd, 2005). Possibly, in subcortical areas competitive processes drive intercallosal transfer of information ([1] Reggia et al., 2001).

Acute deafferentation, e.g. after nerve injury, elucidates the cortical induced changes (Kaas, 2003). After deafferentation, a reduction in the activity in the motor cortex is quickly induced (minutes to hours), which causes a down regulation of the inhibitory gamma amino butyric acid (GABA) neurotransmitter level ([2] Levy et al., 2002). This enhances activation of inhibited horizontally oriented pathways and leads to altered cortical motor maps as was demonstrated by transcranial motor stimulation (Kaas, 2005). Evidence that GABA might play a role comes from the effects of a single dose of a GABA receptor agonist. The plasticity effect was downregulated, suggesting that decrease of inhibition plays a role ([2] Werhahn et al., 2002). In focal dystonia, as seen i.e. in CRPS I patients, a significant GABA level decrease was observed in the sensorimotor cortex and lentiform nuclei contralateral to the affected hand. In the ipsilateral hemisphere, only a small nonsignificant decrease was found ([1] Levy et al., 2002).

After upper limb amputation in humans, two types of cortical plasticity were observed; an input-increase and input-decrease type (Elbert et al., 1997). Magnetic source imaging revealed that after tactile stimulation the decreased area of the somatosensory cortex of the amputated hand was invaded by increasing the facial area. This “invasion” of the cortical amputation zone was accompanied by a significant increase in the size of the representation of the digits of the *intact hand*. This demonstrates again bilateral cortical changes after a unilateral intervention. Wall and coworkers (2002) suggested that sensory dysfunctions after nerve, root, dorsal column and amputation injuries can be viewed as diseases of reorganization. In arm amputees, it was demonstrated that adaptive changes in the somatosensory cortex in humans were strongly positively correlated with pain (Flor et al., 1995). This indicates that in phantom pain, pain may be a consequence of cortical plasticity in the primary somatosensory cortex.

All presented studies on neuroplasticity, both in animals and humans, express cortical reorganizational changes in the primary somatosensory cortex (SI) and changes are based on different parameters. Animal and human studies share a common feature: cortical plasticity changes and reorganizations were both described under physiological and pathological circumstances.

Cortical reorganization: functional correlates

The characteristics of cortical reorganization, the parameters (Ebner, 2005) that describe cortical plasticity changes will differ for each research project, research aim and measuring technique. High resolution techniques like electroencephalography (EEG), magnetoencephalography (MEG), functional magnetic resonance imaging (fMRI) or transcranial magnetic stimulation (TMS) analyze electromagnetic properties of neural

activation (Rossini and Melgari, 2011). Nowadays, combinations of techniques are used to compensate for the technical limitations of each technique. The study of cortical plasticity and reorganization in humans, using MEG, may include cortical evoked responses. In these studies, parameters like peak latency, dipole position, dipole strength and somatosensory map changes have been described (Tecchio et al., 2002; Huttunen et al., 2006). In the present research project, the parameters studied are described in Chapter 3.

2.5 Complex Regional Pain Syndrome (CRPS)

CRPS I in the left hand after soft tissue bruising

In "The Classification on Chronic Pain" (Merskey et al., 1994) by IASP, CRPS I and II are defined as two chronic pain syndromes with comparable symptomatology and potential severe disability (Albrecht et al., 2006). The chronic pain in CRPS is often disproportionate to the inciting event, a seemingly innocent soft tissue bruising may initiate the syndrome and it is underdiagnosed in children. In this population, up to 90% of the cases include females in the age between 8-16 years (Stanton-Hicks, 2010). By IASP definition, CRPS I is without and CRPS II with peripheral nerve injury (PNI). There is accumulating evidence that in both syndromes, neuroanatomical (Baron, 2000; Oaklander et al., 2006, 2009), neurochemical (Birklein 2001, 2008; Hettne et al., 2007; Tannemaat et al., 2007; Obata et al., 2008; Baron, 2009) and adaptive functional changes occur from the peripheral receptor, the spinal cord to subcortical and cortical areas (Dykes, 1984; Das, 1997; Tinazzi et al., 2000; Juottonen et al., 2002; Schwenkreis et al., 2003; Maihöfner et al.,2003; Forss et al., 2005; Devor, 2006; Drummond and Finch, 2006; Stern et al., 2006; Krause et al., 2006; Larbig et al., 2006; Schaible, 2007; Navarro et al., 2007; Vartiainen et al., 2008; Baron 2009). Basically, tissue injury results in the release of pro-nociceptive mediators. Injury sensitizes peripheral nerve terminals and evokes an increased excitability of spinal cord dorsal horn neurons - peripheral and central sensitization, respectively (Jarvis et al., 2009). Nevertheless, there is still no clear explanation why after a seemingly innocent bruising of a hand, a cascade of serious changes is set into motion that result in CRPS I.

CRPS I is mainly based on clinical signs and symptoms, objective diagnostic tests to study the syndrome are still lacking (Geertzen et al., 2006), and as a consequence the incidence of CRPS I varies considerably. Since the publication by Bruehl (1999), several efforts were made to improve the list of criteria supporting the diagnosis CRPS (Harden et al., 2006, 2007, 2010; Brunner et al., 2008; van Bodegraven Hof et al., 2010). CRPS I, using the IASP criteria (Merskey et al., 1994) was diagnosed in 46% after wrist fractures (Sandroni et al., 2003) and especially in patients who complained of pain after the use of a cast (Fields and Basbaum, 1994). In the Sandroni study, the female to male ratio was 4:1. The costs of health care are high, caused by the fact that an adequate treatment is lacking (Taylor et al. 2006;

Kemler et al., 2010). In CRPS I symptoms like pain, edema, vasomotor and sudomotor disturbances may develop (Veldman et al., 1993; Baron et al., 1998; Bruehl et al.,1999; Jänig et al., 1991, 2003; Stanton-Hicks, 2003; Kandi et al., 2007; Harden et al., 2007; Schürmann et al., 2007; Perez et al., 2007; Albazaz et al., 2008). Interestingly, peripheral neuropathological changes displaying abnormal thin fibre axons in the skin and vascular bed were described in CRPS I (Albrecht et al., 2006) and a genetic predisposition is suspected (Birklein et al., 2008). Neuroimaging techniques like Magnetic Resonance Imaging (MRI), fMRI (functional MRI) and Positron Emission Tomography (PET) have no added value and are not recommended on a routine basis (Geertzen et al., 2006). In the last decade, few publications on CRPS I and functional neuroimaging techniques (EEG or MEG with MRI) have been published indicating that the central nervous system in CRPS I plays a role in the pathogenesis of the disease (Maihöfner et al., 2003; Forss et al., 2005; Birklein and Rowbotham, 2005; Schwenkreis et al., 2009). This supports the view that CRPS I is a syndrome that involves the peripheral and central nervous system (Tinazzi, 2000; Jänig et al., 2002, 2003).

CRPS II may result from peripheral nerve injury (PNI) but the incidence of CRPS II is relatively low, ranging from 2 - 2,5% (Kline et al., 1995; Bryant et al., 2002). Nerve injury originates from many causes, it is often traumatic but e.g. radiation, chemical, electrical and iatrogenic injuries have been described (Maggi et al., 2003; Devor, 2006; Kretschmer et al., 2009). Peripheral nerve damage is classically divided in three ways, from neuropraxia, and axonotmesis to neurotmesis. This classification describes whether or not there is discontinuity in the integrity of the connective tissues and/or the axon and its myelin framework (Sunderland, 1945; Kline et al., 1995) PNI not necessarily results in CRPS II or neuropathic pain and may present less severe forms comparable to CRPS I (Kline et al., 1995). Neuropathic pain was recently redefined as, “pain arising as a direct consequence of a lesion or disease affecting the somatosensory nervous system” (Treede et al., 2008). The original IASP definition of neuropathic pain (Merskey et al., 1994) was challenged since e.g. it did not differentiate neuropathic dysfunction from physiological neuroplasticity in the somatosensory nervous system. The mechanisms after traumatic nerve injury leading to pain are complex and not fully understood. Even though PNI patients presented comparable symptoms, their sensory profiles differed. This supports the concept of different underlying mechanisms leading to chronic pain in PNI patients (Baron, 2000; Schüning et al., 2009).

Volleys of abnormal peripheral inputs start shortly after the nerve injury. It begins with spontaneous ectopic discharges in the resealed proximal nerve stump (end bulbs), and in response to mechanical and chemical stimulation (McAllister et al., 1995). In this state of increased excitability or sensitization (Woolf, 1993), ephaptic communication and crossed after-discharge attribute to abnormal inputs. Abnormal discharge from cross-talk with sympathetic fibres may produce autonomic dysfunction (Drummond, 2001,2004; Devor, 2006; Baron, 2006). Besides plasticity changes at the level of the nociceptor and in response to impaired nociceptive inputs, a “wind up” phenomenon in the spinal cord has been described leading to sensitization (Woolf, 2007, 2011). Central sensitization is the next change leading to less reversible changes and during this development the N-methyl-D-asparate (NMDA) receptor is activated and pain may arise (Latremoliere, 2009; Woolf, 2004, 2011). In this stage, not only propagation of afferent information is facilitated but also descending inhibition is decreased (Bee and Dickenson, 2008).

In conclusion: neuropathic pain may be due to abnormal peripheral input and/or abnormal central processing (Chen et al., 2002; Woolf, 2004; Costigan et al., 2009; Latremoliere et al., 2009). In humans, an impaired flow of afferent information evokes adaptive cortical responses (Das, 1997; Tecchio et al., 2002). These changes are more extensively described under cortical plasticity (Chapter 2.1.4). However, in a neuropathic pain review study, using fMRI and PET, no unique pain matrix could be defined (Chen et al., 2008).

The distinction between CRPS I and II patients, with identical symptomatology but a nerve injury in CRPS II patients only, is still under debate. Some consider CRPS I also as a neuropathic pain syndrome (Bruehl, 2010). This is supported by decreased cutaneous C-fibre (Oaklander et al., 2006) and A-delta fibres in the affected limb in CRPS I patients (Albrecht et al., 2006). The question remains whether these changes initiated CRPS or resulted from CRPS, and whether CRPS I is a true neuropathic pain syndrome. In clinical practice, it may be difficult to recognize minimal fiber injury and for that reason fiber injury will remain unnoticed (Ochoa, 2006; Oaklander et al., 2006).

References

- Albazaz R, Wong YT, Homer-Vanniasinkam S. Complex regional pain syndrome: a review. Ann Vasc Surg 2008; 22: 297-306.
- Albrecht PJ, Hines S, Eisenberg E, Pud D, Finlay DR, Connolly MK, Paré M, Davar G, Rice FL. Pathologic alterations of cutaneous innervation and vasculature in affected limbs from patients with complex regional pain syndrome. Pain 2006; 120: 244-266.
- Al-Chaer ED, Feng Y, Willis WD. A role for the dorsal column in nociceptive visceral input into the thalamus of primates. J Neurophysiol 1998; 79: 3143-3150.
- Almeida TF, Roizenblatt S, Tufik S. Afferent pain pathways: a neuroanatomical review. Brain Research 2004; 1000: 40-56.
- Anand KJ, Carr DB. The neuroanatomy, neurophysiology, and neurochemistry of pain, stress, and analgesia in newborns and children. Pediatr Clin North Am 1989; 36: 795-822.
- Asbury AK, Fields HL. Pain due to peripheral nerve damage: an hypothesis. Neurology 1984; 34: 1587-1590.
- Bach-y-Rita P. Theoretical aspects of sensory substitution and of neurotransmission related reorganization in spinal cord injury. Spinal Cord 1999; 37: 465-474.
- Baron R, Jänig W. Pain syndromes with causal participation of the sympathetic nervous system. Anaesthesist 1998; 47: 4-23.
- Baron R: Peripheral neuropathic pain: from mechanisms to symptoms. Clin J Pain 2000; 16: 12-20.
- Baron R. Mechanisms of disease: Neuropathic pain, a clinical perspective. Nat Clin Pract Neurol 2006; 2: 95-106.
- Baron R. Neuropathic pain: a clinical perspective. Handb Exp Pharmacol 2009; 194: 3-30.
- Baumgartner C, Doppelbauer A, Deecke L, Barth DS, Zeitlhofer J, Lindinger G, Sutherling WW. Neuromagnetic investigation of somatotopy of human hand somatosensory cortex. Exp. Brain Res 1991; 87: 641-648.
- Bee LA, Dickenson AH. Descending facilitation from the brainstem determines behavioral and neuronal hypersensitivity following nerve injury and efficacy of pregabalin. Pain 2008; 140: 209-223.
- Beersen N, de Bruijn JHB, Dekkers MA, Ten Have P, Hekster GB, Redekop WK, Spincemaille GH, Theuvenet PJ, Berg M, Klazinga NS. Developing a National Continuous Quality Improvement System for Neuromodulation Treatment in The Netherlands. Jt Comm J Qual Saf 2004; 30: 310-321.
- Berlucchi G, Buchtel HA. Neuronal plasticity: historical roots and evolution of meaning. Exp Brain Res 2009; 192: 307-19.
- Berlucchi G, Aglioti SM. The body in the brain revisited. Exp Brain Res 2010; 200: 25-35.
- Berlucchi G (2011). What is callosal plasticity ?. In: Chalupa LM, Berardi N, Caleo M, Galli-resta L, Pizzorusso T (Ed), Cerebral Plasticity, new perspectives, 1st Edn. Massachusetts Institute of Technology, Toppan Best-set Premedia Limited, USA, pp 235-246.
- Bessou P, Perl ER. Response of cutaneous sensory units with unmyelinated fibers to noxious stimuli. J Neurophysiol 1969; 32: 1025-1043.
- Birklein F, Riedl B, Neundorfer B, Handwerker HO. Sympathetic vasoconstrictor reflex pattern in patients with complex regional pain syndrome. Pain 1998; 75: 93-100.
- Birklein F, Riedl B, Sieweke N, Weber M, Neundörfer B. Neurological findings in complex regional pain syndromes--analysis of 145 cases. Acta Neurol Scand 2000; 101: 262-269.
- Birklein F, Schmelz M, Schifter S, Weber M. The important role of neuropeptides in complex regional pain syndrome. Neurology 2001; 57: 2179-2184.
- Birklein F, Rowbotham MC. Does pain change the brain? Neurology 2005; 65: 666-667.
- Birklein F, Schmelz M. Neuropeptides, neurogenic inflammation and complex regional pain syndrome (CRPS). Neurosci Lett 2008; 437: 199-202.
- Bliem B, Müller-Dahlhaus JF, Dinse HR, Ziemann U. Homeostatic metaplasticity in the human somatosensory cortex. J Cogn Neurosci 2008; 20: 1517-1528.

- Bloom JS, Hynd GW. The role of the corpus callosum in interhemispheric transfer of information: excitation or inhibition? Neuropsychol Rev 2005; 15: 59-71.
- Boersma FP, Bosma ES, Giezen LM, Theuvenet PJ. Cancer pain control by infusion techniques in the home situation in the Northern Netherlands: an innovative project on the use of medical technology in the home situation. J Pain Symptom Manage 1992; 7: 155-159.
- Brown P, Ridding MC, Werhahn KJ, Rothwell JC, Marsden CD. Abnormalities of the balance between inhibition and excitation in the motor cortex of patients with cortical myoclonus. Brain 1996; 119: 309-317.
- Buonomano, DV, Merzenich MM. Cortical Plasticity: From Synapses to Maps. Annu Rev Neurosci 1998; 21:149-186.
- Burgess PR, Perl ER. Myelinated afferent fibres responding specifically to noxious stimulation of the skin. J Physiol 1967; 190: 541-562.
- [1] Burt AM (1993). Brain stem and Cerebellum. In: Burt AM (Ed), Textbook of Neuroanatomy, 1st edn. W.B. Saunders and Company, Philadelphia, pp 132-155.
- [2] Burt AM (1993). General somatic and general visceral afferent pathways. In: Burt AM (Ed), Textbook of Neuroanatomy, 1st edn. W.B. Saunders Company, Philadelphia, pp 193-223.
- [3] Burt AM (1993). The limbic system. In: Burt AM (Ed) Textbook of Neuroanatomy, 1st edn. W.B. Saunders Company, Philadelphia, pp 479-502.
- [4] Burt AM (1993). Telencephalon. In: Burt AM (Ed), Textbook of Neuroanatomy, 1st edn. W.B. Saunders Company, Philadelphia, pp 479-502.
- Burton H (2005). Cerebral cortical regions devoted to the somatosensory system. In: Nelson RJ (Ed), The somatosensory system: deciphering the brains own body image. Methods and new frontiers in neuroscience. CRC Press, Boca Raton, USA, pp 27-73.
- Bushnell MC, Duncan GH, Hofbauer RK, Ha B, Chen JI, Carrier B. Pain perception: is there a role for primary somatosensory cortex? Proc Natl Acad Sci USA 1999; 96: 7705-7709.
- Bragard D, Chen AC, Plaghki L. Direct isolation of ultra-late (C-fibre) evoked brain potentials by CO2 laser stimulation of tiny cutaneous surface areas in man. Neurosci Lett 1996; 209: 81–84.
- Bruehl S, Harden RN, Galer BS, Saltz, S. External validation of IASP diagnostic criteria for Complex Regional Pain Syndrome and proposed research diagnostic criteria. International Association for the Study of Pain. Pain 1999; 81: 147-154.
- Bruehl S. An update on the pathophysiology of complex regional pain syndrome. Anesthesiology 2010; 113: 713-725.
- Brunner F, Lienhardt SB, Kissling RO, Bachmann LM, Weber U. Diagnostic criteria and follow-up parameters in complex regional pain syndrome type I--a Delphi survey. Eur J Pain 2008; 12: 48-52.
- Bryant PR, Kim CT, Millan R. The rehabilitation of causalgia (complex regional pain syndrome-type II). Phys Med Rehabil Clin N Am 2002; 13: 137-157.
- Byl NN, McKenzie A and Nagarajan SS. Differences in somatosensory hand organization in a healthy flutist and a flutist with focal hand dystonia: a case report. J Hand Ther 2000; 13: 302-309.
- Byl NN (2005). Behavioral basis of focal hand dystonia: aberrant learning in the somatosensory cortex. In: Ebner FF (Ed), Neural plasticity in adult somatic sensory-motor systems, 1st edn. Boca Raton, Taylor & Francis Group, USA, pp 227-263.
- Calford MB, Tweedale R. Interhemispheric transfer of plasticity in the cerebral cortex. Science 1990; 249: 805-807.
- Chen R, Cohen LG, Hallett M. Nervous system reorganization following injury. Neuroscience 2002; 111: 761-73.
- Chen FY, Tao W, Li YJ. Advances in brain imaging of neuropathic pain. Chin Med J 2008; 121: 653-657. (English).
- Coghill RC, Talbot JD, Evans AC, Meyer E, Gjedde A, Bushnell MC, Duncan GH. Distributed processing of pain and vibration by the human brain. J Neurosci 1994; 14: 4095-4108.

- Cook ND. Callosal inhibition: the key to the brain code. Behav Sci 1984; 29: 98-110.
- Costigan M, Scholz J, Woolf CJ. Neuropathic pain: A maladaptive response of the nervous system to damage. Annu Rev Neurosci 2009; 32: 1-32.
- Das A. Plasticity in adult sensory cortex: A review. Network Comput Neural Syst 1997; 8: 33-76.
- Derbyshire, SWG. Exploring the pain "Neuromatrix". Current Review of Pain 2000; 4: 466-477.
- De Vignemont F. Body schema and body image--pros and cons. Neuropsychologia 2010; 48: 669-680.
- Devor M. Sodium channels and mechanisms of neuropathic pain. J Pain 2006; 7 (1 Suppl 1): S3-S12.
- Djouhri L, Lawson SN. A-beta-fiber nociceptive primary afferent neurons: a review of incidence and properties in relation to other afferent A-fiber neurons in mammals. Brain Res Rev 2004; 46: 131-145.
- Donoghue JP. Plasticity of adult sensorimotor representations. Curr Opin Neurobiol 1995; 5: 749-754.
- Drummond PD, Finch PM, Skipworth S, Blockey P. Pain increases during sympathetic arousal in patients with complex regional pain syndrome. Neurology 2001; 57: 1296-1303.
- Drummond PD. Involvement of the sympathetic nervous system in complex regional pain syndrome. Int J Low Extrem Wounds 2004; 3: 35-42.
- Drummond PD, Finch PM. Sensory changes in the forehead of patients with complex regional pain syndrome. Pain 2006; 123: 3-5.
- Dubin AE, Patapoutian A. Nociceptors: the sensors of the pain pathway. J Clin Invest 2010; 120: 3760-3772.
- Dubner R, Ruda MA, Miletic M, Hoffert MJ, Bennet GJ, Nishikawa N, Coffield J (1984). Neural Circuitry Mediating Nociception in the Medullary and Spinal Dorsal Horns. In: Kruger L, Liebeskind JC (Ed), Neural Mechanisms of Pain, Vol. 6. Raven Press, New York, pp 151-166.
- Duggan AW, Weihe E (1991). Central transmission of impulses in nociceptors: events in the superficial dorsal horn. In: Basbaum AI, Besson JM (Ed), Towards a new pharmacotherapy of pain, 1st edn. John Wiley & Sons, Chicester, pp 35-68.
- Duquette M, Rainville P, Alary F, Lassonde M, Lepore F. Ipsilateral cortical representation of tactile and painful information in acallosal and callosotomized subjects. Neuropsychologia 2008; 46: 2274-2279.
- Dykes RW. Central consequences of peripheral nerve injuries. Ann Plast Surg 1984; 13: 412-22.
- Dykes RW. Mechanisms controlling neuronal plasticity in somatosensory cortex.
  Can J Physiol Pharmacol 1997; 75: 535-545.
- Ebner FF, Amstrong-James, M (2005). The effects of sensory deprivation on sensory function of SI barrel cortex. In: Ebner FF (Ed), Neural plasticity in adult somatic sensory-motor systems, 1st edition. Boca Raton, Taylor & Francis Group, USA, pp 109-139.
- Elbert T, Sterr A, Flor H, Rockstroh B, Knecht S, Pantev C, Wienbruch C, Taub E: Input-increase and input-decrease types of cortical reorganization after upper extremity amputation in humans. Exp Brain Res 1997; 117: 161-64.
- Fabri M, Del Pesce M, Paggi A, Polonara G, Bartolini M, Salvolini U, Manzoni T. Contribution of posterior corpus callosum to the interhemispheric transfer of tactile information. Cogn Brain Res 2005; 24: 73-80.
- Fields HL (1984). Brainstem Mechanisms of Pain Modulation. In: Kruger L, Liebeskind JC (Ed), Neural Mechanisms of Pain, Vol. 6. Raven Press, New York, pp 241-252.
- Fields HL, Basbaum AI (1994). Central nervous system mechanisms of pain modulation. In: Wall PD, Melzack R (Ed), Textbook of Pain, 3rd edn. Churchill Livingston, Edinburgh, pp 243-260.
- Flor H, Elbert T, Knecht S, Wienbruch C, Pantev C, Birbaumer N, Larbig W, Taub E. Phantom-limb pain as a perceptual correlate of cortical reorganization following arm amputation. Nature 1995; 375: 482-484.
- Florence SL, Garraghty PE, Wall JT, Kaas JH. Sensory afferent projections and area 3b somatotopy following median nerve cut and repair in macaque monkeys. Cereb Cortex 1994; 4: 391-407.

- Florence SL, Jain N, Pospichal MW, Beck PD, Sly DL, Kaas JH. Central reorganization of sensory pathways following peripheral nerve regeneration in fetal monkeys. Nature 1996; 381: 69-71.
- Florence SL, Taub HB, Kaas JH. Large-scale sprouting of cortical connections after peripheral injury in adult macaque monkeys. Science 1998; 282: 1117-1121.
- Florence SL (2002). The changeful mind: Plasticity in the Somatosensory system. In: Nelson RJ (Ed), The somatosensory system. CRC Press, Boca Raton, pp 335-367.
- Forss N, Kirveskari E, Gockel M. Mirror-like spread of chronic pain. Neurology 2005; 65: 748-750.
- Fuchs M, Wagner M, Kastner J. Confidence limits of dipole source reconstruction results. Clin Neurophysiol 2004; 6: 1442-1451.
- Furue H, Katafuchi T, Yoshimura M. Sensory processing and functional reorganization of sensory transmission under pathological conditions in the spinal dorsal horn. Neurosci Res 2004; 48: 361-368.
- Garraghty, PE; Kaas, JH. Functional reorganization in adult monkey thalamus after peripheral nerve injury. Neuroreport 1991; 2: 747-750.
- Gazzaniga MS. Cerebral specialization and interhemispheric communication: does the corpus callosum enable the human condition? Brain 2000;123:1293-1326.
- Gebhart GF. Descending modulation of pain. Neurosci Biobehav Rev 2004; 27: 729-37.
- Geertzen JHB; Perez RSGM (2006). Diagnostics, Epidemiology and Etiology. In: Geertzen JHB; Perez RSGM; Dijkstra PU; Kemler MA; Rosenbrand CJGM (Ed), Evidence Based Guideline Complex regional Pain Syndrome I. Van Zuiden, Utrecht, The Netherlands, pp 29-55. In Dutch.
- Geffen GM, Jones DL, Geffen LB. Interhemispheric control of manual motor activity. Behav Brain Res 1994; 64: 131-140.
- Guilbaud G, Bernard JF, Besson JM (1994). Brain areas involved in nociception. In: Wall PD, Melzack R (Ed), Textbook of Pain, 3rd edn. Churchill Livingston, Edinburgh, pp 113-128.
- [1]Guyton AC (1976). Transmission and processing of information in the nervous system. In: Guyton AC (Ed), Medical Physiology, 5th edn. W.B. Saunders Company, Philadelphia, pp 626-638.
- [2]Guyton AC (1976). Sensory receptors and their basic mechanisms of action. In: Guyton AC (Ed), Medical Physiology, 5th edn. W.B. Saunders Company, Philadelphia, pp 640-676.
- Hallin RG. Microneurography in relation to intraneural topography: somatotopic organisation of median nerve fascicles in humans. J Neurol Neurosurg Psychiatry 1990; 53: 736-744.
- Hallin RG, Wu G. Fitting pieces in the peripheral nerve puzzle. Exp Neurol 2001; 172: 482-492.
- Handwerker HO (1991). What peripheral mechanisms contribute to nociceptive transmission and hyperalgesia. In: Basbaum AI, Besson JM (Ed), Towards a new pharmacotherapy of pain, 1st edn. John Wiley & Sons, Chicester, pp 5-20.
- Harden RN, Bruehl SP. Diagnosis of complex regional pain syndrome: signs, symptoms, and new empirically derived diagnostic criteria. Clin J Pain 2006; 22: 415-419.
- Harden RN, Bruehl S, Stanton-Hicks M, Wilson PR. Proposed new diagnostic criteria for complex regional pain syndrome. Pain Med 2007; 8: 289-292.
- Harden RN, Bruehl S, Perez RS, Birklein F, Marinus J, Maihofner C, Lubenow T, Buvanendran A, Mackey S, Graciosa J, Mogilevski M, Ramsden C, Chont M, Vatine JJ. Validation of proposed diagnostic criteria (the “Budapest Criteria”) for Complex Regional Pain Syndrome. Pain 2010; 150: 268-274.
- Heppelman B, Messlinger K, Neiss WF, Schmidt RF (1990). The sensory terminal tree of “free nerve endings” in articular capsule of the knee. In: Zenker W, Neuhuber WL (Ed), The Primary Afferent Neuron,1st edn. Plenum Press, New York and London, pp 73-85.
- Hettne KM, de Mos M, de Bruijn AG, Weeber M, Boyer S, van Mulligen EM, Cases M, Mestres J, van der Lei J. Applied information retrieval and multidisciplinary research: new mechanistic hypotheses in complex regional pain syndrome. J Biomed Discov Collab 2007; 2: 2.

- Hlustík P, Solodkin A, Gullapalli RP, Noll DC, Small SL. Somatotopy in human primary motor and somatosensory hand representations revisited. Cereb Cortex 2001; 11: 312-21.
- Hofer S, Frahm J. Topography of the human corpus callosum revisited--comprehensive fiber tractography using diffusion tensor magnetic resonance imaging. Neuroimage 2006; 32: 989-994.
- Holmes N; Spence C. The body schema and multisensory representation(s) of peripersonal space. Cognitive processing 2004; 5: 94–105.
- Hong JH, Kwon HG, Jang SH. Probabilistic somatotopy of the spinothalamic pathway at the ventroposterolateral nucleus of the thalamus in the human brain. Am J Neuroradiol 2011; 32: 1358-1362.
- Hummel F, Gerloff C, Cohen LG (2005). Modulation of Cortical Function and Plasticity in the Human Brain. In: Ebner FF (Ed), Neural plasticity in adult somatic sensory-motor systems, 1st edition. Boca Raton, Taylor & Francis Group, USA, pp 207-227.
- Huttunen J, Komssi S, Lauronen L. Spatial dynamics of population activities at S1 after median and ulnar nerve stimulation revisited: a MEG study. NeuroImage 2006; 32: 1024-1031.
- Iannetti GD, Mouraux A. From the neuromatrix to the pain matrix (and back). Exp Brain Res 2010; 205: 1-12.
- Iwamura Y, Iriki A, Tanaka M. Bilateral hand representation in the postcentral somatosensory cortex. Nature 1994; 369: 554-556.
- Iwamura Y, Taoka M, Iriki A. Bilateral activity and callosal connections in the somatosensory cortex. Neuroscientist 2001; 7: 419-429.
- Jain N, Catania KC, Kaas JH. A histologically visible representation of the fingers and palm in primate area 3b and its immutability following long-term deafferentations. Cereb Cortex 1998; 8: 227-236.
- James, W (1890). Habit. In: James W (Ed), The Principles of Psychology. Henry Holt & Company, New York, 104-128.
- Jänig W, Koltzenburg M (1991). What is the interaction between the sympathetic terminal and the primary afferent. In: Basbaum AI, Besson JM (Ed), Towards a new pharmacotherapy of pain,1st edn. John Wiley & Sons, Chichester, pp 331-352.
- Jänig W, Baron R. Complex regional pain syndrome is a disease of the central nervous system. Clin Auton Res 2002; 12: 150-164.
- Jänig W, Baron R. Complex regional pain syndrome: mystery explained ? Lancet Neurol 2003; 2: 687-697.
- Jarvis MF, Boyce-Rustay JM. Neuropathic pain: Models and mechanisms. Curr Pharm Des 2009; 15: 1711-1716.
- Jenkins WM, Merzenich MM, Ochs MT, Allard T, Guíc-Robles E. Functional reorganization of primary somatosensory cortex in adult owl monkeys after behaviorally controlled tactile stimulation. J Neurophysiol 1990; 63: 82-104.
- Jetzer AK, Morel A, Magnin M, Jeanmonod D. Cross-modal plasticity in the human thalamus: evidence from intraoperative macrostimulations. Neuroscience 2009; 164: 1867-1875.
- Jones AKP, Brown WD, Friston KJ, QI LY and Frackowiak RSJ. Cortical and subcortical localization of response to pain in man using positron emission tomography. Proc R Soc Lon B 1991; 224: 39-44.
- Jones AKP, Derbyshire SWG. Cerebral mechanisms operating in the presence and absence of inflammatory pain. Ann Rheum Dis 1996; 5: 411–420.
- Jones, EG, Pons, TP. Contributions to large-scale plasticity of primate somatosensory cortex. Science 1998; 282: 1121-1125.
- Juottonen K, Gockel M, Silén T, Hurri H, Hari R, Forss N. Altered central sensorimotor processing in patients with complex regional pain syndrome. Pain 2002; 98: 315-323.
- Kaas JH. Is most of neural plasticity in the thalamus cortical? Proc Natl Acad Sci 1999; 96: 7622-7623.
- Kaas JH (2001): Functional implications of plasticity and reorganizations in the somatosensory and motor systems of developing and adult primates. In: Nelson RJ (Ed), The somatosensory system. Boca Raton, CRC Press, pp 367-82.

- Kaas JH, Collins CE. Anatomic and functional reorganization of somatosensory cortex in mature primates after peripheral nerve and spinal cord injury. Adv Neurol 2003; 93: 87-95.
- Kaas, JH. Somatosensory system (2004). In: Paxinos G, Mai JK (Ed), The human nervous system, 2nd edn. Elsevier, Amsterdam, Heidelberg, Tokyo, pp 1061-1086.
- Kaas, JH (2005). Reorganization of motor cortex after damage to the motor system. In: Neural plasticity in adult somatic sensory-motor system. In: Ed. Ebner, FF (Ed), Frontiers in Neuroscience. CRC Press, Taylor and Francis Group, Boca Raton, pp 189-207.
- Kaas JH, Qi HX, Burish MJ, Gharbawie OA, Onifer SM, Massey JM. Cortical and subcortical plasticity in the brains of humans, primates, and rats after damage to sensory afferents in the dorsal columns of the spinal cord. Exp Neurol 2008; 209: 407-416.
- Kakigi R, Hoshiyama M, Shimojo M, Naka D, Yamasaki H, Watanabe S, Xiang J, Maeda K, Lam K, Itomi K, Nakamura A. The somatosensory evoked magnetic fields. Prog Neurobiol 2000; 61: 495-523.
- Kandi B, Kaya A, Turgut D, Ozgocmen S, Cicek D. Clinical presentation of cutaneous manifestations in complex regional pain syndrome (type 1). Skinmed 2007; 6: 118-121.
- Karl A, Birbaumer N, Lutzenberger W, Cohen LG, Flor H. Reorganization of motor and somatosensory cortex in upper extremity amputees with phantom limb pain. J Neurosci 2001; 21: 3609-3618.
- Kelly, JP (1991). Functional anatomy of the central nervous system. In: Kandel ER, Schwartz JH, Jessel TM (Ed), Principles of Neural Science, 3rd edn. Elsevier, Amsterdam, pp 283-295.
- Kemler MA, Raphael JH, Bentley A, Taylor RS. The cost-effectiveness of spinal cord stimulation for complex regional pain syndrome. Value Health 2010; 13: 735-742.
- Kline DG, Hudson AR (1995). Basic considerations. In: Kline DG, Hudson AR (Ed), Nerve injuries. Operative Results for Major Nerve Injuries, Entrapments, and Tumors. W.B. Saunders Company. Philadelphia, London, pp 1-29.
- Knaap van der LJ, van der Ham IJ.How does the corpus callosum mediate interhemispheric transfer? A review. Behav Brain Res 2011; 223: 211-221.
- Kniyihar-Csillik E, Csillik B (1990). Structural, functional and cytochemical plasticity of primary afferent terminals in the upper dorsal horn. In: Zenker W, Neuhuber WL (Ed), The primary afferent neuron. Plenum Press, New York, pp 227-251.
- Konietzny F, Perl ER, Trevino D, Light A, Hensel H. Sensory experiences in man evoked by intraneural electrical stimulation of intact cutaneous afferent fibers. Exp Brain Res 1981; 42: 219-222.
- Krause P, Förderreuther S, Straube A. TMS motor cortical brain mapping in patients with complex regional pain syndrome type I. Clin Neurophysiol 2006; 117: 169-176.
- Kretschmer T, Heinen CW, Antoniadis G, Richter HP, König RW. Iatrogenic nerve injuries. Neurosurg Clin N Am 2009; 20:73-90.
- Larbig W, Montoya P, Braun C, Birbaumer N. Abnormal reactivity of the primary somatosensory cortex during the experience of pain in complex regional pain syndrome: a magnetoencephalographic case study. Neurocase 2006; 12: 280-285.
- Latremoliere A, Woolf CJ: Central sensitization: A generator of pain hypersensitivity by central neural plasticity. J Pain 2009; 10: 895-926.
- LeDoux, JE. (2002). Small change. In: LeDoux JE (Ed), Synaptic self. Viking, New York, United States, pp. 137.
- LeDoux JE. The self: clues from the brain. Ann N Y Acad Sci 2003; 1001: 295-304.
- Legrain V, Iannetti GD, Plaghki L, Mouraux A. The pain matrix reloaded: a salience detection system for the body. Prog Neurobiol 2011; 93: 111-124.
- Lenz FA (1991). Evidence that the thalamus is involved in the generation of sensory abnormalities observed in human central pain syndromes. In: Nashold BS, Ovelmen - Levitt J (Ed), Deafferentation pain syndromes, Vol. 19. Raven Press, New York, pp 141-150.
- [1] Levy LM, Hallett M. Impaired brain GABA in focal dystonia. Ann Neurol 2002; 51 : 93-101.

- [2] Levy LM, Ziemann U, Chen R, Cohen LG. Rapid modulation of GABA in sensorimotor cortex induced by acute deafferentation. Ann Neurol 2002; 52: 755-761.
- Loeser JD, Treede RD. The Kyoto protocol of IASP Basic Pain Terminology. Pain 2008; 31; 137: 473-477.
- Lumpkin EA, Caterina MJ. Mechanisms of sensory transduction in the skin. Nature 2007; 445: 858-865.
- Maggi SP, Lowe JB 3rd, Mackinnon SE. Pathophysiology of nerve injury. Clin Plast Surg 2003; 30: 109-126.
- Maihöfner C, Handwerker HO, Neundörfer B, Birklein F. Patterns of cortical reorganization in complex regional pain syndrome. Neurology 2003; 23: 1707-1715.
- Maihöfner C, Handwerker HO, Birklein F. Functional imaging of allodynia in complex regional pain syndrome. Neurology 2006; 66: 711-717.
- Malmberg A (2001). Central Changes. In: Reichmann H (Ed), Pain in Peripheral Nerve Diseases, 1st edition. Basel, Karger, pp 149-167.
- Mao J, Mayer DJ. Spinal cord neuroplasticity following repeated opioid exposure and its relation to pathological pain. Ann N Y Acad Sci 2001; 933: 175-84.
- Maravita A, Spence C, Driver J. Multisensory integration and the body schema: close to hand and within reach. Curr Biol 2003; 13: 531-539.
- [1] Martin JH (1991). Coding and processing of sensory information. In: Kandel ER, Schwartz JH, Jessel TM (Ed), Principles of Neural Science 3rd edn. Elsevier, Amsterdam, pp 329-340.
- [2] Martin JH, Jessel TM (1991). Modality coding in the somatic sensory system. In: Kandel ER, Schwartz JH, Jessel TM (Ed), Principles of Neural Science, 3rd edn. Elsevier, Amsterdam, pp 341-352.
- [3] Martin JH, Jessel TM (1991). Anatomy of the somatic sensory system. In: Kandel ER, Schwartz JH, Jessel TM (Ed), Principles of Neural Science, 3rd edn. Elsevier, Amsterdam, pp 353-366.
- Manzoni T, Barbaresi P, Conti F. Callosal mechanism for the interhemispheric transfer of hand somatosensory information in the monkey. Behav Brain Res 1984; 11: 155-70.
- Mason P. Placing pain on the sensory map: classic papers by Ed Perl and colleagues. J Neurophysiol 2007; 97: 1871-1873.
- McAllister RM, Calder JS. Paradoxical clinical consequences of peripheral nerve injury: a review of anatomical, neurophysiological and psychological mechanisms. Br J Plast Surg 1995; 48: 384-395.
- Melzack R. Pain and the Neuromatrix in the Brain. Journal of Dental Education 2001; 65: 1378 -1383.
- Merskey H, Bogduk N. Classification of Chronic Pain. In: Merskey H, Bogduk N (Ed), IASP Task Force on Taxonomy. IASP Press, Seattle, 1994; pp. 40-43.
- [1] Merzenich, MM; Kaas, JH; Wall JT; Nelson RJ; Sur, M; Felleman, DJ. Topographic reorganization of somatosensory cortical areas 3b and 1 in adult monkeys following restricted deafferentation. Neuroscience 1983; 8: 33-55.
- [2] Merzenich, MM; Kaas, JH; Wall JT; Sur, M; Nelson RJ; Felleman, DJ. Progression of change following median nerve section in the cortical representation of the hand in areas 3b and 1 adult owl and squirrel monkeys. Neuroscience 1983; 10: 639–665.
- Mogilner A, Grossman JAI, Ribary U, Joliot M, Volkmann J, Rappaport D, Beasley RW, Llinas RR. Somatosensory cortical plasticity in adult humans revealed by magnetoencephalography. Proc Natl Acad Sci 1993; 90: 3593-3597.
- Mourauxa A, Diukovac A, Leea MC, Wisec RG, Iannettie GD. A multisensory investigation of the functional significance of the “pain matrix”. NeuroImage 2010; 3: 2237-2249.
- Nagumo T, Yamadori A. Callosal disconnection syndrome and knowledge of the body: a case of left hand isolation from the body schema with names. J Neurol Neurosurg Psychiatry 1995; 59: 548–551.
- Narici L, Modena I, Opsomer RJ, Pizzella V, Romani GL, Torrioli G, Traversa R, Rossini PM. Neuromagnetic somatosensory homunculus: a non-invasive approach in humans. Neurosci Lett 1991; 121: 51-54.
- Naumer MJ, van den Bosch JJ. Touching sounds: thalamocortical plasticity and the neural basis of multisensory integration. J Neurophysiol 2009; 102: 7-8.
- Navarro X, Vivó M, Valero-Cabré A. Neural plasticity after peripheral nerve injury and regeneration. Prog Neurobiol 2007; 82: 163-201.

- [1] Nieuwenhuys R, Voogd J, van Huijzen C (2008). Ascending Reticular System. In: Nieuwenhuys R, Voogd J, van Huijzen C (Ed), The Human Central Nervous System, 4th edn. Springer Verlag, Berlin, pp 268-271.
- [2] Nieuwenhuys R, Voogd J, van Huijzen C (2008). General Sensory Systems and taste. In: Nieuwenhuys R, Voogd J, van Huijzen C (Ed), The Human Central Nervous System, 4th edn. Springer Verlag, Berlin, pp 683-715.
- [3] Nieuwenhuys R, Voogd J, van Huijzen C (2008). Telencephalon: Neocortex. In: Nieuwenhuys R, Voogd J, van Huijzen C (Ed), The Human Central Nervous System, 4th edn. Springer Verlag, Berlin, pp 595-600.
- Nudo RJ, Milliken GW, Jenkins WM, Merzenich MM. Use-dependent alterations of movement representations in primary motor cortex of adult squirrel monkeys. J Neurosci 1996; 16: 785-807.
- Oaklander AL, Rissmiller JG, Gelman LB, Zheng L, Chang Y, Gott R. Evidence of focal small-fiber axonal degeneration in complex regional pain syndrome-I (reflex sympathetic dystrophy). Pain 2006; 120: 235-243.
- Oaklander AL, Fields HL. Is reflex sympathetic dystrophy/ complex regional pain syndrome type I a small-fiber neuropathy ? Ann Neurol 2009; 65:629-638.
- Obata K, Noguchi K. Contribution of primary sensory neurons and spinal glial cells to pathomechanisms of neuropathic pain. Brain Nerve 2008; 60: 483-492.
- Ochoa J, Torebjörk E. Sensations evoked by intraneural microstimulation of C nociceptor fibres in human skin nerves. J Physiol 1989; 415: 583-599.
- Ochoa JL. Is CRPS I a neuropathic pain syndrome? Pain 2006; 123: 334–335.
- Ogino Y, Nemoto H and Goto F. Somatotopy in human primary somatosensory cortex in pain system. Anesthesiology 2005; 103: 821-827.
- Okada YC, Tanenbaum R, Williamson SJ, Kaufmann L. Somatotopic organization of the human somatosensory cortex revealed by neuromagnetic measurements. Exp Brain Res 1984; 56: 197-205.
- Pantev C, Ross B, Fujioka T, Trainor LJ, Schulte M, Schulz M. Music and learning-induced cortical plasticity. Ann N Y Acad Sci 2003; 999: 438-450.
- Pellicciari MC, Miniussi C, Rossini PM, De Gennaro L. Increased cortical plasticity in the elderly: changes in the somatosensory cortex after paired associative stimulation. Neuroscience 2009; 163: 266-276.
- Penfield W, Boldrey E. Somatic motor and sensory representation in the cerebral cortex of man as studied by electrical stimulation. Brain 1937; 60: 389-443.
- Perez RS, Collins S, Marinus J, Zuurmond WW, de Lange JJ. Diagnostic criteria for CRPS I: differences between patient profiles using three different diagnostic sets. Eur J Pain 2007; 11: 895-902.
- Perl ER (1984). Characterization of nociceptors and their activation of neurons in the superficial dorsal horn: first steps for the sensation of pain. In: Kruger L, Liebeskind JC (Ed), Neural Mechanisms of Pain, Vol. 6. Raven Press, New York, pp 23-52.
- Plessen KJ, Wentzel-Larsen T, Hugdahl K, Feineigle P, Klein J, Staib LH, Leckman JF, Bansal R, Peterson BS. Altered interhemispheric connectivity in individuals with Tourette‘s disorder. Am J Psychiatry 2004; 161: 2028-2037.
- Ralston III, HJ (1984). Synaptic Organization of Spinothalamic Tract Projections to the Thalamus with Special Reference to Pain. In: Kruger L, and Liebeskind JC (Ed), Neural Mechanisms of Pain, Vol. 6. Raven Press, New York, pp 183-215.
- [1] Reggia JA, Goodall SM, Shkuro Y, Glezer M. The callosal dilemma: explaining diaschisis in the context of hemispheric rivalry via a neural network model. Neurol Res 2001; 23: 465-471.
- [2] Reggia JA, Goodall S, Levitan S. Cortical map asymmetries in the context of transcallosal excitatory influences. Neuroreport 2001; 12: 1609-1614.
- Reichling DB, Levine JD. Critical role of nociceptor plasticity in chronic pain. Trends Neurosci 2009; 32: 611–618.
- Rethelyi M (1990). Ultrastructure of primary afferent terminals in the spinal cord. In: Zenker W, Neuhuber WL (Ed), The Primary Afferent Neuron, 1st edn. Plenum Press, New York, pp 213-225.
- Rexed B. The cytoarchitectonic organization of the spinal cord in the cat. J Comp Neurol 1952; 96: 414-495.

- Reinersmann A, Haarmeyer GS, Blankenburg M, Frettlöh J, Krumova EK, Ocklenburg S, Maier C. Left is where the L is right. Significantly delayed reaction time in limb laterality recognition in both CRPS and phantom limb pain patients. Neurosci Lett 2010; 486: 240-245.
- Reinersmann A, Haarmeyer GS, Blankenburg M, Frettlöh J, Krumova EK, Ocklenburg S, Maier C. Comparable disorder of the body schema in patients with complex regional pain syndrome (CRPS) and phantom pain. Schmerz 2011; 25: 558-562.
- Rossini PM, Martino G, Narici L, Pasquarelli A, Peresson M, Pizzella V, Tecchio F, Torrioli G, Romani GL. Short-term brain 'plasticity' in humans: transient finger representation changes in sensory cortex somatotopy following ischemic anesthesia. Brain Res 1994; 642: 169-177.
- Rossini, PM, Melgari, J-M (2011). Neurophysiological correlates of cortical plasticity in the normal and diseased human brain. In: Chalupa LM, Berardi N, Caleo M, Galli-resta L, Pizzorusso T (Ed), Cerebral Plasticity, new perspectives, 1st Edn. Massachusetts Institute of Technology, Toppan Best-set Premedia Limited, USA, pp 291-302.
- Rosso T, Aglioti SM, Zanette G, Ischia S, Finco G, Farina S, Fiaschi A, Tinazzi M. Functional plasticity in the human primary somatosensory cortex following acute lesion of the anterior lateral spinal cord: neurophysiological evidence of short-term cross-modal plasticity. Pain 2003; 101: 117-27.
- Ruben J, Schwiemann J, Deuchert M, Meyer R, Krause T, Curio G, Villringer K, Kurth R, Villringer A. Somatotopic organization of human secondary somatosensory cortex. Cereb Cortex 2001; 11: 463-473.
- Sadato N, Zeffiro TA, Campbell G, Konishi J, Shibasaki H, Hallett M. Regional cerebral blood flow changes in motor cortical areas after transient anesthesia of the forearm. Ann Neurol 1995; 37: 74-81.
- Salvolini U, Polonara G, Mascioli G, Fabri M, Manzoni T. Functional topography of the human corpus callosum. Bull Acad Natl Med 2010; 194: 617-631.
- Sanderson JL, Dell'Acqua ML. AKAP signaling complexes in regulation of excitatory synaptic plasticity. Neuroscientist 2011;17: 321-36.
- Sandroni P, Benrud-Larson LM, McClelland RL, Low PA. Complex regional pain syndrome type I: incidence and prevalence in Olmsted county, a population-based study. Pain 2003; 103: 199-207.
- Sanes JN, Suner S, Lando JF, Donoghue JP. Rapid reorganization of adult rat motor cortex somatic representation patterns after motor nerve injury (cerebral motor cortex/motor system/neural plasticity/motor control). Proc. Nail Acad Sci USA 1988; 85: 2003-2007.
- Schaible HG. Peripheral and central mechanisms of pain generation. Handb Exp Pharmacol 2007; 177: 3-28.
- Schnitzler A, Ploner M. Neurophysiology and functional neuroanatomy of pain perception. J Clin Neurophysiol 2000; 17: 592-603.
- Schüning J, Scherens A, Haussleiter IS, Schwenkreis P, Krumova EK, Richter H, Maier C. Sensory changes and loss of intra-epidermal nerve fibers in painful unilateral nerve injury. Clin J Pain 2009; 25:683-690.
- Schürmann M, Zaspel J, Löhr P, Wizgall I, Tutic M, Manthey N, Steinborn M, Gradl G. Imaging in early posttraumatic complex regional pain syndrome: a comparison of diagnostic methods. Clin J Pain 2007; 23: 449-457.
- Schwenkreis P, Janssen F, Rommel O, Pleger B, Völker B, Hosbach I, Dertwinkel R, Maier C, Tegenthoff M. Bilateral motor cortex disinhibition in complex regional pain syndrome (CRPS) type I of the hand. Neurology 2003; 61: 515-519.
- Schwenkreis P, El Tom S, Ragert P, Pleger B, Tegenthoff M, Dinse HR. Assessment of sensorimotor cortical representation asymmetries and motor skills in violin players. Eur J Neurosci 2007; 26: 3291-3302.
- Schwenkreis P, Maier C, Tegenthoff M. Functional Imaging of Central Nervous System Involvement in Complex Regional Pain Syndrome. AJNR Am J Neuroradiol 2009; 30: 1279-1284.
- Schwoebel J, Coslett HB. Evidence for multiple, distinct representations of the human body. J Cogn Neurosci 2005; 17: 543–553.
- Sikes RW, Vogt BA. Nociceptive neurons in area 24 of rabbit cingulate cortex. Journal of Neurophysiology 1992; 68: 1720-1732.

- [1] Snow PJ, Wilson P (1991). Plasticity in the dorsal horn. In: Autrum H, Ottoson D, Perl ER, Schmidt RF, Shimazu H, Willis WD (Ed), Progress in Sensory Physiology 11. Springer Verlag, Berlin, pp 117-224.
- [2] Snow PJ, Wilson P (1991). Plasticity in the peripheral somatosensory nervous system. In: Autrum H, Ottoson D, Perl ER, Schmidt RF, Shimazy H, Willis WD (Ed), Sensory Physiology, Vol. 11. Springer Verlag, Berlin, pp 6-55.
- [3] Snow PJ, Wilson P (1991). Plasticity and the dorsal column nuclei. In: Autrum H, Ottoson D, Perl ER, Schmidt RF, Shimazy H, Willis WD (Ed), Sensory Physiology, Vol. 11. Springer Verlag, Berlin, pp 225-282.
- [4] Snow PJ, Wilson P (1991). Plasticity and the somatosensory thalamus. In: Autrum H, Ottoson D, Perl ER, Schmidt RF, Shimazy H, Willis WD (Ed), Sensory Physiology, Vol. 11. Springer Verlag, Berlin, pp 286-310.
- Spengler F, Roberts TP, Poeppel D, Byl N, Wang X, Rowley HA, Merzenich MM. Learning transfer and neuronal plasticity in humans trained in tactile discrimination. Neurosci Lett 1997; 232: 151-154.
- Stanford JA. Descending control of pain. British Journal of Anesthesia 1995; 75: 217-227.
- Stanton-Hicks M. Complex regional pain syndrome. Anesthesiol Clin North America 2003; 21: 733-744.
- Stanton-Hicks M. Plasticity of complex regional pain syndrome (CRPS) in children. Pain Med 2010; 11: 1216-1223.
- Stern J, Jeanmonod D, Sarnthein J: Persistent EEG overactivation in the cortical pain matrix of neurogenic pain patients. NeuroImage 2006; 31: 721-31.
- Sunderland S. The intraneural topography of the radial, median and ulnar nerves. Brain 1945; 68: 243–299.
- Sutherling WW, Levesque MF, Baumgartner C. Cortical sensory representation of the human hand: size of finger regions and non-overlapping digit somatotopy. Neurology 1992; 42: 1020-1028.
- Tannemaat MR, Korecka J, Ehlert EM, Mason MR, van Duinen SG, Boer GJ, Malessy MJ, Verhaagen J. Human neuroma contains increased levels of semaphorin 3A, which surrounds nerve fibers and reduces neurite extension in vitro. J Neurosci 2007; 27: 14260-14264.
- Taylor RS, Van Buyten JP, Buchser E. Spinal cord stimulation for complex regional pain syndrome: a systematic review of the clinical and cost-effectiveness literature and assessment of prognostic factors. Eur J Pain 2006; 10: 91-101.
- Tecchio F, Padua L, Aprile I, Rossini PM: Carpal tunnel syndrome modifies sensory hand cortical somatotopy: a MEG study. Hum Brain Mapp 2002; 17: 28-36.
- Tinazzi M, Priori A, Bertolasi L, Frasson E, Mauguière F, Fiaschi A. Abnormal central integration of a dual somatosensory input in dystonia. Evidence for sensory overflow. Brain 2000; 123: 42-50.
- Treede RD, Kenshalo DR, Gracely RH and Jones AKP. The cortical representation of pain. Pain 1999; 79: 105-111.
- Treede RD, Apkarian AV, Bromm B, Greenspan JD, Lenz FA. Cortical representation of pain: functional characterization of nociceptive areas near the lateral sulcus. Pain 2000; 87: 113-119.
- Treede RD, Jensen TS, Campbell JN, Cruccu G, Dostrovsky JO, Griffin JW, Hansson P, Hughes R, Nurmikko T, Serra J. Neuropathic pain: Redefinition and a grading system for clinical and research purposes. Neurology 2008; 29: 1630-1635.
- Van Bodegraven Hof EA, Groeneweg GJ, Wesseldijk F, Huygen FJ, Zijlstra FJ. Diagnostic criteria in patients with complex regional pain syndrome assessed in an out-patient clinic. Acta Anaesthesiol Scand 2010; 54: 894-899.
- Van Ree JM. Multiple brain sites involved in morphine antinociception. J Pharm Pharmacol 1977; 29: 765-767.
- Vartiainen NV, Kirveskari E, Forss N. Central processing of tactile and nociceptive stimuli in complex regional pain syndrome. Clin Neurophysiol 2008; 119: 2380-2388.
- Veldman PH, Reynen HM, Arntz IE, Goris RJ. Signs and symptoms of reflex sympathetic dystrophy: prospective study of 829 patients. Lancet 1993; 342: 1012-1016.
- Vogt BA, Sikes RW, Vogt LJ (1993). Anterior cingulate cortex and the medial pain system. In: Vogt BA, Birkhauser GM (Ed), Neurobiology of Cingulate Cortex and Limbic Thalamus. Birkhäuser, Boston, pp 313–344.

- Vogt BA, Sikes RW. The medial pain system, cingulate cortex, and parallel processing of nociceptive information. Prog Brain Res 2000; 122: 223-235.
- Wall, JT, Xu J, Wang X. Human brain plasticity: an emerging view of the multiple substrates and mechanisms that cause cortical changes and related sensory dysfunctions after injuries of sensory inputs from the body. Brain Res Brain Res Rev 2002; 39: 181-215.
- [1] Werhahn KJ, Mortensen J, van Boven RW, Zeuner KE, Cohen LG. Enhanced tactile spatial acuity and cortical processing during acute hand deafferentation. Nat Neurosci 2002; 5: 936-938.
- [b] Werhahn KJ, Mortensen J, Kaelin-Lang A, Boroojerdi B, Cohen LG. Cortical excitability changes induced by deafferentation of the contralateral hemisphere. Brain 2002; 125: 1402-1413.
- Wiech K, Preissl H, Lutzenberger W, Kiefer RT, Topfner S, Haerle M, Schaller HE, Birbaumer N. Cortical reorganization after digit-to-hand replantation. J Neurosurg 2000; 93: 876-883
- [1] Willis WD, Jr (1984). Modulation of Primate Spinothalamic Tract Discharges. In: Kruger L, Liebeskind JC (Ed), Neural Mechanisms of Pain, Vol 6. Raven Press, New York, pp 217-240.
- [2] Willis WD (1985). Peripheral nerves and sensory receptors. In: Willis WD, Coggeshall RE (Ed), Sensory mechanisms of the spinal cord. Plenum Press, New York, pp. 13-47.
- [3] Willis WD (1985). Ascending nociceptive tract. In: Willis WD (Ed), The Pain System. Karger, Basel, Paris, London, pp 145-206.
- [4] Willis WD (1991). The Spinothalamic Tract and other Ascending Nociceptive Pathways of the Spinal Cord. In: Shimoji K, Kurokawa T, Tamaki T, Willis WD (Ed), Spinal Cord Monitoring and Electrodiagnosis. Springer Verlag, Berlin, Heidelberg, pp 1-7.
- [5] Willis WD, Jr (1995). From Nociceptor to Cortical Activity. In: Bromm B, Desmedt JE (Ed), Pain and the Brain: From Nociception to Cognition, Vol 22. Raven Press, New York, pp 1-19.
- [6]Willis WD, Al-Chaer ED, Quast MJ, Westlund KN. A visceral pain pathway in the dorsal column of the spinal cord. Proc Natl Acad Sci USA 1999; 96: 7675-7679.
- [7] Willis WD Jr, Westlund KN. The role of the dorsal column pathway in visceral nociception. Curr Pain Headache Rep 2001; 5: 20-26.
- Woolf CJ. The pathophysiology of peripheral pain-abnormal peripheral input and abnormal central processing, Neurochir Suppl Wien, 1993, 58: 125-130.
- Woolf CJ. Dissecting out mechanisms responsible for peripheral neuropathic pain: implications for diagnosis and therapy. Life Sci 2004; 74: 2605-2610.
- Woolf CJ. Central sensitization: uncovering the relation between pain and plasticity. Anesthesiology 2007; 106 :864-867.
- Woolf CJ. Central sensitization: implications for the diagnosis and treatment of pain. Pain 2011; 152: S2-15.
- Xu J, Wall JT. Evidence for brainstem and supra-brainstem contributions to rapid cortical plasticity in adult monkeys. J Neurosci 1999; 19: 7578-7590.
- Young JP, Herath P, Eickhoff S, Choi J, Grefkes C, Zilles K, Roland PE. Somatotopy and attentional modulation of the human parietal and opercular regions. J Neurosci 2004; 24: 5391-5399.
- Zhuo M. Central plasticity in pathological pain. Novartis Found Symp 2004; 261: 132-45.

CHAPTER 3 MATERIALS AND METHODS

3.1 Magnetoencephalography (MEG)

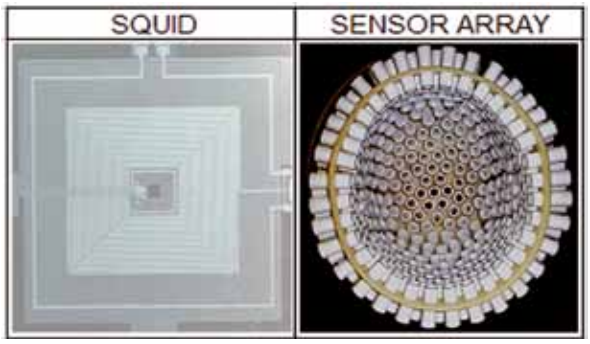

The SQUID as was used in Twente (1 x 1 mm). It consists of niobium, aluminium and palladium. SENSOR array: Courtesy MEG CTF International Services Ltd.

The discovery of superconductivity in 1911 by Nobel Prize winner Heike Kamerlingh Onnes (1853 – 1926), has retrospectively been fundamental to the development of MEG. From 1882 to 1923 Kamerlingh Onnes served as professor of experimental physics at the Leiden University (van Delft, 2001). In 1911, after his ability to liquefy helium, he found that at 3.0 Kelvin the resistance in a solid mercury wire immersed in liquid helium suddenly vanished and superconductivity was demonstrated. A second invention was equally fundamental for MEG. In 1973, Brian David Josephson, Nobel Prize winner in physics, discovered that super conducting loops with a small junction can be used to measure magnetic field changes with unprecedented precision, these devices are the basis of a Superconducting Quantum Interference Device (SQUID).

MEG is a completely non-invasive technique that measures magnetic field changes in the human brain induced by natural occurring electrical activity or in response to artificial stimulation (Okada et al. 1983; Lopes da Silva and van Rotterdam, 1993; Volegov et al., 2004; Huttunen, 1988; Babiloni et al., 2009). MEG was first measured in 1968 by David Cohen using a million turn induction magnetometer (Cohen, 1968; Orrison et al, 1995). Initially, the signal to noise (S/N) ratio was poor and the shielded room required technical improvements. The improved shielded room was build shortly later at the Massachusetts Institute of Technology (Cohen, 1972). It was not until the SQUID became available (Zimmerman et al., 1970) in combination with the improved shielded room that measurements were qualitatively comparable to electroencephalography (EEG). A SQUID is a very sensitive sensor able to measure the strength and direction of extremely small magnetic fields (Vrba and Robinson, 2001). A SQUID is a superconducting ring that is interrupted at one or two point contacts (the Josephson junctions) where the current is concentrated in a very small cross-sectional area (Vrba and Robinson, 2001; Raij, 2005). The sensitivity of a SQUID is based on the quantum mechanic properties of these junctions at liquid helium temperatures (4.2 Kelvin), where the ring is superconducting. Therefore, the SQUID's used in a MEG are installed in a highly isolating barrel with liquid helium called a dewar (Babiloni et al., 2009). New technological improvements made it possible to place an increasing number of SQUID sensors in the same dewar, leading to today's whole-head MEG systems containing 150 to 300 SQUIDS and hence becoming a valuable diagnostic tool (Erwin et al., 1993; Hämäläinen et al., 1993; Baumgartner et al., 2004; Kakigi et al., 2004; Funke et al., 2009).. Whole-head MEG devices made evoked bilateral hemispherical measurements possible with improved spatial resolution (Kakigi, 2004) and facilitated clinical research in e.g. somatosensory function, pain and epileptic surgery (Funke et al., 2009). All MEG measurements are performed in a shielded room to limit external noise from far-away sources as traffic, elevators and nearby (medical) electrical devices. The SQUID's used in a MEG do not directly measure the magnetic fields of the brain. SQUID's are connected through

a magnetic flux transformer to superconducting coils called magnetometers or a pair of coils called gradiometers that are placed inside the dewar as close as possible to the brain. A gradiometer consist of two coils, a pickup coil and a compensation coil, with opposite orientation. This configuration makes the system insensitive for homogenous magnetic fields, or for relatively far away sources. In this way the signal to noise ration (SNR) is largely increased compared to a magnetometer, which consists of a single pickup coil (Vrba, 1991). Because MEG measurements encounter no distortion from fluid, skin or bone its spatial resolution is much better than EEG, (Babiloni et al., 2009) allowing for routine measurements of evoked cortical magnetic responses (Hari et al., 1983; Huttunen et al., 2006). Contrary to EEG, for which a reference electrode is required, MEG is completely reference free (Williamson and Kaufman, 1988; Barkley and Baumgartner, 2003). MEG measurements can be performed in the sitting and supine position. Preparations for MEG measurements are relatively easy because no electrodes have to be attached, which increases patient comfort. As was rightfully pointed out, the use of MEG in the clinical setting unlike the use of e.g MRI, still suffers from a poor user interface that hampers clinical use. This, in addition to the high costs of the purchase of MEG and its maintenance, is probably a major reason for its limited clinical applications (Parra et al., 2004).

3.1.1 The generation of cortical responses

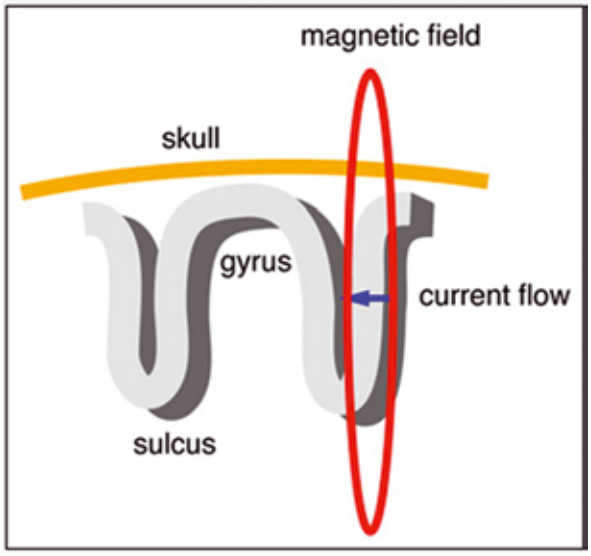

Courtesy MEG CTF International Services Ltd.

The neuronal generation mechanism underlying MEG is very similar to EEG, the only physical difference being the type of electromagnetic fields by which neural currents are transferred to the physical sensor, magnetometer/gradiometer or electrode. Therefore, the same neuron anatomical properties of the brain need to be considered when studying the generators of MEG ([5]Hari, 1993; Lopes da Silva and van Rotterdam, 1993). At the neocortical level of mammals, two categories of neurons can be distinguished: pyramidal and non-pyramidal cells. The pyramidal cell population accounts for at least 70% of the neocortical neurons (Nieuwenhuys, 1994, 2008). Pyramidal cells (in e.g. lamina IV and V) have dendritic trees that run parallel to each other, they are perpendicularly oriented to the cortical surface and have an axon that descends in the subcortical white matter. The pyramidal neurons constitute a network all over the neocortex and are the largest output and input system of the neocortex (Nieuwenhuys, 2008).

During synchronized synaptic activation along the proximal dendrites of the neurons, extracellular currents will arise to close the current loops, which were opened to activated ion channels at the postsynaptic cells. These ionic currents pass through conductive tissues as brain, cerebrospinal fluid, skin, where they reach the EEG sensors and are recorded as potential differences. Both the primary currents at the activated synapses and the resulting secondary currents through the conductive tissues, contribute to the brain's magnetic field by Biot-Savard's law (Ioannides and Fenwick, 2005). The parallel orientation of the pyramidal cells is of crucial importance here, because the resulting electromagnetic fields of multiple synchronized pyramidal cells will add up, whereas the fields due to the other, randomly oriented cells, will cancel. In this way, synchronized neuronal currents cause measurable electric and magnetic fields in the brain (Lopes da Silva et al., 1987; Parra et al., 2004; Babiloni et al., 2009). It has been estimated that to detect a measurable MEG or EEG signal, approximately 50.000 active neurons are needed (Okada, 1983). This neuronal synchronization of neighboring pyramidal cells, can in a clinical setting be obtained by stimulating one of the nerves repeatedly. Because of the one-to-one neuron anatomic organization, such stimulation results in a simultaneous activation of neighboring cell in the cortex. As a result, one can obtain a magnetic field in the order of 10^{-12} to 10^{-13} T at a distance of about 15 mm from the scalp, peak-to-peak (Vrba, 2002). By applying the stimulus repeatedly and averaging the resulting MEG or EEG signal, a stable response can be obtained with high signal to noise ratio.

The cortically evoked responses

Electrical stimulation of a peripheral nerve in humans produces measurable and repeatable cortically evoked responses. Over the last four decades, electrical stimulation of the median, ulnar and posterior tibial nerve were well studied, and in humans using EEG and MEG.

Using EEG, short latency and long latency evoked potentials have initially been described after electrical *median* nerve stimulation ([1,2] Allison et al., 1989). The evoked responses were studied using cortical-surface and transcortical recordings obtained during neurosurgery ([1] Allison et al., 1989). In 54 patients, three groups of evoked responses were found in the contralateral hemisphere at around 20 ms, 30 ms and 90 ms. Contraleral somatosensory responses at these latencies were localized in the primary somatosensory cortex (SI), probably Brodmann area 3b ([2] Allison et al., 1989). Ipsilateral responses were not found in this area but possibly in 4, 1,2 and 7. Surface and transcortical recordings suggest that ipsilateral responses originate from transcallosal inputs from the contralateral hemisphere ([2] Allison et al., 1989). At latencies around 125 ms, results suggested that the secondary somatosensory cortex was involved and a radial generator was active. These findings were confirmed in later studies (Frot and Mauguière, 1997). An interesting finding in the EEG studies is the latency difference in activation between SI and SII of around 40 ms (Frot and Mauguière, 1999).

Using MEG, several studies describe results of cortical evoked responses to either non-noxious (Baumgartner, 1991; Kawamura et al., 1996; Kakigi, 2000; Babiloni et al., 2004; Hoshiyama et al., 1995, 1996; [6] Hari et al., 1999; Huttunen et al., 2006; Tecchio et al., 1997, 1998, 2000, 2005; Theuvenet et al., 2005, 2006, 2011; Chen et al., 2011) or noxious stimulation ([1,3] Hari et al., 1983, 1984; Huttunen et al., 1995; Kakigi, 1995). After electrical non-noxious median nerve stimulation, major magnetic field characteristics in terms of

peak latencies, peaks and generator localization were comparable to EEG studies. In the first 90 ms post-stimulus, sources are located in SI, and around 125 ms in SII ([2,4] Hari et al., 1983, 1984; Simões et al., 1999, 2002). It has to be realized that EEG measures both radial and tangential oriented generators in contrast to MEG where only tangential generators can be measured (Barkley and Baumgartner, 2003). Therefore, sensitivity to tangential sources makes MEG more fit to measure activity in the sulci (Barkley and Baumgartner, 2003). MEG studies of human evoked cortical responses have improved our understanding of somatosensory processing in healthy subjects (Rossini et al., 1989; Tecchio et al., 1997, 1998, 2000). However, also of patients with cerebral injuries like stroke (Rossini et al., 2001), epilepsy (van der Meij et al., 2001; Lopes da Silva, 2008) and pain (Flor et al., 1995; Treede et al., 1999; Bromm, 2001).

The inverse problem and dipole localization

Cortically evoked responses, either recorded by EEG and MEG, are caused by multiple synchronized pyramidal cell activations (Meijs et al., 1988). The aim of multichannel EEG and MEG is to study brain function through the analysis of the spatial distribution of the evoked fields and the localization of the underlying sources ([2] Lopes da Silva, 1994; [5] Hari, 1994). The determination of these sources is usually called the "inverse problem" (Barkley and Baumgartner, 2003; Parra et al., 2004; Darvas et al., 2004). A key property of the inverse problem is that, due to the fact that there are generally several current distributions that produce identical magnetic and/or electric field patterns, its solution is non-unique ([5] Hari, 1993). This indicates, that due to non-uniqueness, several current distributions can in principle produce identical magnetic field patterns, in contrast to e.g. MRI where the inverse problem can be solved uniquely ([5] Hari, 1993;). This non-uniqueness was already pointed out by Helmholtz in 1853 who stated that a current distribution inside a conductor, cannot uniquely be retrieved from the measured magnetic field outside the head (Leonardelli, 2006). The increasing number of sensors in MEG however improved the accuracy of MEG inverse solution significantly (Koenig et al., 2008).

Given the constraints of the inverse problem but based on known anatomy and neurophysiology of the brain, meaningful solutions can be found by using the equivalent current dipole (ECD) model ([5] Hari, 1993; Fuchs, 2004). An equivalent current dipole can be considered as "the brain area that is responsible for a given potential or magnetic field scalp distribution or brain map". In this formulation of the inverse problem it is assumed that a set of neighbouring activated dendrites in the cortex, can be mathematically described as an equivalent current dipole, of which the position parameters describe the activated cortical area. The dipole fitting procedure attempts to find these dipole position and orientation parameters in such a way that the observed magnetic field distribution is, in statistical terms, matched as closely as possible to the magnetic/electric field pattern predicted by the dipole. ([2] Lopes da Silva, 1993).

Because dipole fitting is based on the prediction of magnetic/electric fields for a given dipole source, assumptions are needed regarding the geometry and conductivity of the brain, skull and skin. Often these assumptions are formulated as a realistic head model (wherein the anatomy is described in a geometrically precise way), or as a homogeneously conducting sphere which is less accurate, but allows much faster computations (Meijs et al., 1988). With the use of the CTF manufacturer's software, a compromise between these two head models is made, by fitting a

series of spheres to the MRI of the individual subject. This head model has to be constructed only once and can then be saved on disk for later use. Because head model and MRI share the same coordinate system, results of dipole fit calculations can be mapped onto the MRI scan and related to anatomical information.

3.1.2 Cortical human brain mapping

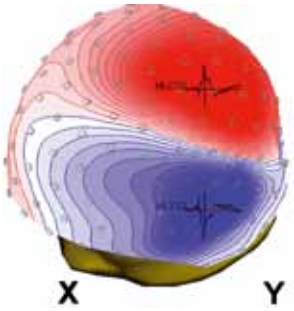

Left Hemispherical dipolar brain map after median nerve stimulation at 70 milliseconds post stimulus.

Functional human brain mapping is the technique to measure and map cortical brain function, under physiological and non-physiological circumstances, and in relation to anatomical structures (Lehmann, 1990; Maurer and Dierks, 1991; Baumgartner, 1993). Unlike electrocorticography (ECoG), where during a neurosurgical procedure direct cortical stimulation is performed, new non-invasive techniques became available (Rossini and Pauri, 2000; Rossini and Dal Forno, 2004). The functional topography of the somatosensory evoked electrical and magnetic responses after non-noxious median nerve (Allison et al., 1989; Kakigi, 1994; Tecchio et al., 1997, 1998, 2000; Theuvenet et al., 2005, 2006), ulnar nerve (Baumgartner et al., 1991; Vanni et al., 1996; Huttunen et al., 2006) and posterior tibial nerve stimulation (Kakigi et al., 1995; Kany et al., 1997; Theuvenet et al., 1999; Willemse et al., 2007) are well studied. MEG enabled clinicians to study and visualize functional "images" of the brain non- invasively (Berman et al., 1995; Parra et al., 2004). In the present MEG study, a MEG equivalent current dipole was electronically superimposed on an individual MRI based head model, MRI and MEG had a common coordinate system (Theuvenet et al., 2005, 2006). The brain

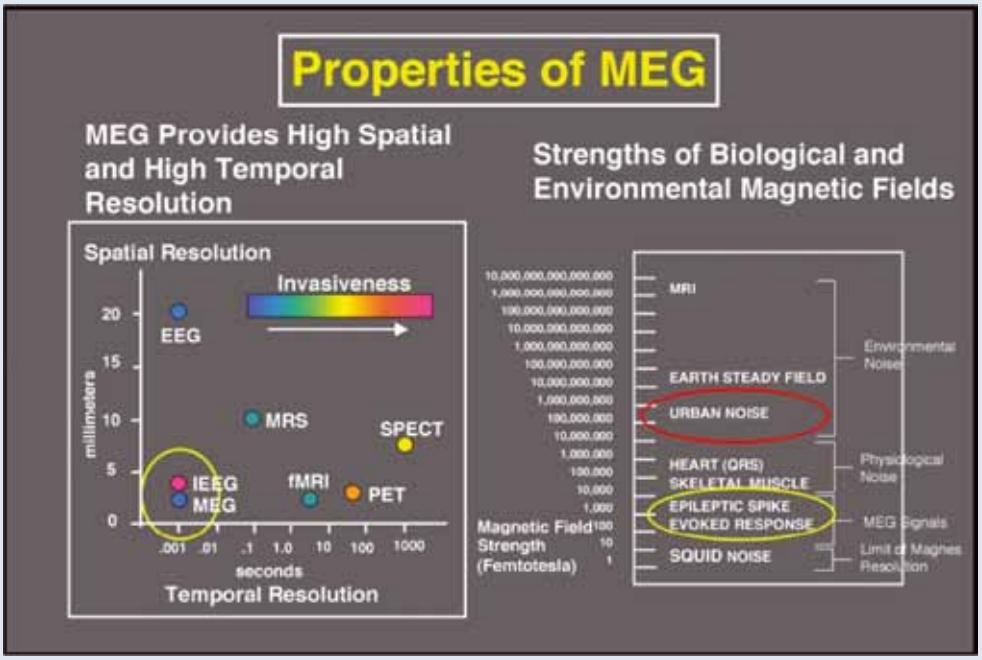

Courtesy MEG CTF International Services Ltd.

map that can be retrieved at each desired peak latency has a dipolar configuration presenting the magnetic outflow (see map above: the efflux in red) and inflow (in blue). For each individual in this study and for each hemisphere, brain maps were produced. In the time window of 400 ms, the series of brain maps depicted the sequence and orientation of brain activation.

3.1.3 Functional non-invasive neuroimaging techniques

Over the last three decades, new non-invasive techniques became available that increased our knowledge of the human brain and its function. These include e.g. EEG, HD-EEG, MEG, TMS, fMRI, and PET (Jones et al., 1991; Casey et al., 1994; Cherry and Phelps, 1996; Rossini and Pauri, 2000; Bandettini, 2009). In the above figure (Properties of MEG) on the left side, the relative spatial and temporal resolutions are depicted for different imaging techniques (*see Acronyms*). HD-EEG (High Definition EEG) is not included in this overview but is supposed to have an improved spatial resolution of 1-3 cm (Babiloni, 2009). In the spatial and temporal domain, MEG proved to reflect accurately evoked magnetic responses with however functional limitations (Parra et al., 2004). In induced pain (noxious stimulation), MEG offered a better spatial resolution compared to EEG (Kakigi et al., 2004). Similar to EEG, MEG does not require exposure to a radiation dose and therefore repeated measurements are easily performed presenting an important clinical advantage of MEG compared to PET and Single Photon Emission Computed Tomography (SPECT). For the study of deeper localized sources, like thalamic activation in neuropathic pain, MEG is not a suitable technique since it is mostly sensitive to neocortical tangential sources (Huttunen, 1998). SPECT offers better opportunities despite the relatively poor temporal resolution (Ushida et al., 2010). In contemporary research and clinical practice, combined techniques or multimodal imaging by eliminating limitations posed by an individual technique, may offer depending on the research question, offer advantages in the clinical setting (Pichler et al., 2008). Cortically evoked responses using MEG, suggested single activation of only one map in SI. However, combining fMRI and PET demonstrated multiple foci of activation in SI after cutaneous finger stimulation (Schnitzler et al., 2000).

CHAPTER 3.2 DESIGN OF THE STUDY

This study is dedicated to the question to what extent the cortically evoked responses in two well known chronic pain syndromes, CRPS I and II, are different. At the start of the study (1993) the only MEG system available in The Netherlands was at the University of Twente since 1976. Therefore, the current study started with first MEG measurements done at University of Twente. Data analysis software was still under development. In 1996, a new, commercially manufactured 151 channel whole head MEG system became available at the VU University Medical Center, Amsterdam,. Therefore, the project was continued in Amsterdam from 2000 onwards.

3.2.1 Organization of the measurements

All measurements in this study were approved by medical ethical committees. Measurements at the University of Twente (Enschede) were approved by the Medical Ethical Committee of University of Twente, as part of cooperation with the Medical Spectrum Twente. Measurements at the Medical Center Alkmaar were approved by the medical ethical committee (NH04-196) and VU University Medical Center. Prior to the measurements, an informed consent was obtained from all

participants. Each patient was allowed to stop participation in the project, without any consequences for the patient and without the need for explanation.

The present study consisted of three phases:

Phase 1: the first phase from 1993 – 1999 at the University of Twente (Low Temperature Division): 35 measurements divided over three patient groups (Peripheral Nerve Injury [PNI], entrapment neuropathies in an upper extremity, essential trigeminal neuralgia). The questions in 1993 that initiated this project were:

(a) "why the effects of electrical spinal cord stimulation fade away in time apart from evident causes like scar tissue forming at the tip of the electrode, dislocations, change of disease, low battery of the pulsegenerator?" and (b) "would it be possible to monitor cortically evoked changes in the pain and pain free state after spinal cord stimulation?"

Since no MRI's were simultaneously made of the patients in this phase, MRI based assessment of dipole characterization was not feasible. EEG was measured after implantation of the pulsegenerator because it was not possible to use MEG since the switch in the pulsegenerator produced too much noise. Results of the this study, but only of the peripheral nerve injury group, were published in 1999 and are presented in Chapter 4. Massive spontaneous muscle movement disturbances as in trigeminal neuralgia, not continuous pain as in the nerve entrapment group were the main reasons why the focus concentrated on the PNI group for further study. This part of the study was financed by the University of Twente.

Phase 2: a second phase was financed by the KNAW and performed between 2000 - 2001 at the MEG Center, VU Medical Hospital, Amsterdam (Dept. of Clinical Neurophysiology). Eight magnetoencephalographic measurements, using a 151 channel whole head MEG system were performed. Patients with a unilateral peripheral nerve injury of an upper extremity were measured to confirm repeatability and consistency of earlier findings at Twente University, since in Twente a different MEG was used. In this phase individual MRI's were made. At the same time preparations were made for the third phase.
Phase 3: the third phase started late 2004 after financial support was made available and the measurements ended summer 2008. This phase was built on earlier experiences (phase 1 and 2). The main goal of phase 3 was to systematically compare the cortically evoked responses in Complex Regional Pain syndrome I and II, and to assess the functional differences in comparison to a healthy control group. This phase consisted of three parts:
(3A). Measurements were performed in a group of twenty healthy subjects to be studied under identical measuring conditions as the two patient groups. In the healthy subject group, at random standard electrical stimulation (Nuwer et al., 1994, 1995) of the median and ulnar nerves of both hands was performed. In this study, results of these measurements were used as reference database for the patient's measurements. Chapter 5,6 and 7 present the questions addressed and results after standard electrical median and nerve stimulation in this group.
(3B). CRPS II. This group consisted of twenty patients with an assessed peripheral nerve injury and continuous pain. In this group at the time of the measurements 4 patients had clinical symptoms of CRPS, from the other 16 the medical history indicated that CRPS was present. The target nerve to stimulate electrically was either the median or ulnar nerve, away from the initial trauma and not directed at the injured nerve. Thus

after ulnar nerve injury, median nerve stimulation followed etc. The first measurement was at the uninjured hand, the second at the injured hand (pain state). A third measurement after a local anesthetic block with 1 -2 ml Lidocaine 1% followed until the patient was fully pain free. The third measurement was performed to study the cortical effects of the anesthetic block. Report of this phase is presented in Chapter 8.
(3C) By definition of the International Association for the Study of Pain (IASP), presented in the Classification of Chronic Pain (Taskforce on Taxonomy, 1994), a type I and II is distinguished although clinical symptoms presented in the definition are identical. In CRPS II a peripheral nerve injury is present. The CRPS I group inclusion criteria in this study were based on the Bruehl research questionnaire (Bruehl et al., 1999) and patients in this group had to suffer from continuous pain. After inclusion standard electrical nerve stimulation was directed either to the median or ulnar nerve. If i.e. CRPS I developed after a metacarpal fracture of the fifth digit, median nerve stimulation was chosen in order not to aggravate pain. Part 3C of this thesis is presented in chapter 9 which combines the results of this group and the CRPS II group (see 2). This part of the study (1 to 3) was technically supported by the Medical Center Alkmaar (Department of Radiology) and University Medical Center (MEG Center).

3.2.2 Measuring setup and registration of the data

Phase 1: magnetoencephalographic measurements were performed at the University of Twente (Low temperature division) in a magnetically shielded room (Vacuum Schmeltze GmbH, Hanau, Germany) using a 19-channel magnetometer system, allowing for the measurement of only one hemisphere at the time. To cover a larger part of the brain, MEG measurements from multiple

The 19 channel MEG used at Twente University

positions were combined. For each patient position with respect to the dewar, three coils, placed at the nasion, left and right ear were activated and their position was determined with respect to the MEG system. A POLHEMUS position tracker was used to define these coil positions, as well as the EEG electrodes positions, with respect to landmarks on the head. The x, y and z axes system used for all measurements was based on three coils, one each at the nasion and right and left ear. The posterior (negative) – anterior (positive) x-axis runs from inion to the nasion. Placements of the coils was performed and supervised by the same investigator to ensure comparable coil placement within patients. After changing the lateral position of each patient in order to stimulate the other hand or foot, before each measurement the position of the coils was redefined.

The EEG measurements were also performed in the magnetically shielded room in order to diminish external noise. Potentials were recorded using a thirty-two or more electrode system

placed on the scalp according to the international 10-20 system. Resistance at each electrode had to be < 5 k Ohm. Signals from the electrodes were amplified and fed through the same systems as the signals from the magnetometer. During magnetic measurements the subjects were lying comfortably in lateral position. The subjects and patients were given no specific task to perform, but were asked not to move and to stay awake with the eyes open and to fixate on the same spot. The position of the head was stabilized with a vacuum pillow. Between the measurements patients were allowed enough time to rest. Standard electrical nerve stimulation was applied by means of two cotton disk electrodes at the ankle (posterior tibial nerve) or at the wrist (median nerve), the cathode proximal (Nuwer et al., 1994). Square-wave constant current pulses with a duration of 0.6 ms were applied. The stimulus rate was randomly varied between 0.9 and 1.2 Hz or was fixed at 0.6 Hz. The amplitude of the stimulus was slightly above the motor threshold (about 7 mA) producing a clear painless twitch and paraesthesias in the thumb or the big toe. First the unaffected median or posterior tibial nerve was stimulated, then the affected side. All measurements were repeated twice, in order to detect possible artifacts and check reproducibility. In patients using a spinal cord stimulator, measurements at the affected hand or foot were repeated in the pain free state. The latency of the response was measured from the onset of the stimulus to the time instant of peak amplitude in the chosen wave. The data acquisition equipment contained an artifact rejector that deleted disturbed epochs. Off-line averaging was performed after 200-300 responses.

During the study, three (3/8) patients were treated for their pain with unilateral spinal cord stimulation (SCS). SCS is an invasive technique whereby an electrode is introduced percutaneously into the posterior part of the spinal canal, positioned extradurally in order to stimulate the dorsal columns. During implantation and positioning of the electrode under local anaesthesia and fluoroscopy, in each patient paraesthesias in the affected area have to be found in close cooperation with the patient. Once stimulation was achieved in the pain overlapping area, the time needed for each patient to become pain free was monitored. The subcutaneously implantable pulse generator normally used for spinal cord stimulation after positive testing, contains a magnetic switch which generates high magnetic disturbances. Consequently, magnetic measurements could not be carried out once the pulse generator had been implanted. Therefore, after implantation of the spinal electrode, evoked magnetic fields were recorded using an external pulse generator. The latter was placed outside the shielded room and was connected to the patient by means of long cables. Patients who underwent SCS were measured before SCS and after SCS. The second measurement was performed once the patient was pain free. EEG measurements were also performed months later in time to assure that the results were reproducible.

Between the measurements of each hemisphere, the patient was allowed a rest since during a measurement the patient remained in the lateral position. Coils at nasion, left and right ear remained in position and before each measurement the head to the MEG device position was reassessed electronically producing comparable data. For EEG, positioning of the electrodes and gaining acceptable resistance took around 30 minutes. Data registration and processing was achieved using ANS software (ANT, Enschede, The Netherlands). Dipole calculations were made numerically and projected to a sphere. Since no MRI's were made, projections on an individual MRI was not performed. Off-line data management

was executed using local software programs like SPSS.

Phase 2: in phase 2 the measurements performed at the University of Twente were repeated for consistency and repeatability at the MEG Center, VU University Medical Center, Amsterdam. Eight patients with a peripheral nerve injury were enrolled. In this phase, the consistency and reproducibility of Twente results were assessed and supported earlier findings at Twente. The protocol of the main study, measuring setup was defined as well as the protocol to produce the MRI's.

Whole head MEG setup in the shielded room
Courtesy MEG CTF International Services Ltd.

Phase 3: in phase 3 MEG - MRI recordings (VU University Medical Center) were performed.
A 151-channel whole-head magnetoencephalography system (CTF, Port Coquitlam, Canada) was used and measurements were performed in a 3-layer magnetically shielded room (Vacuum Schmeltze GmbH, Hanau, Germany). The x, y and z coordinate system, common to each individual MEG and MRI, was based on three anatomical landmarks and positioning coils were fixed to the nasion, and left and right pre-auricular points. Using the positions of these fiducials a head centered coordinate frame was defined. Placements of the coils was according to instructions of the MEG center and supervised by the same technician, as much as possible, to avoid inter-technician differences. The (+) axis was directed to the nose, the (+) y-axis to the left ear and the (+) axis to the vertex. MEG signals were sampled at 1250 Hz, triggered by the synchronization pulse of the electric stimulator. On-line, filters were set at direct current for high-pass and at 400 Hz (4^{th} order Butterworth filter - IMST GmbH, Kamp-Lintfort, Germany) for anti-aliasing low-pass. Off-line the magnetoencephalography data were screened for artifacts, averaged and Direct Current-corrected using the pre-trigger interval to determine the recording offset. Furthermore, +/- averages were calculated to obtain noise-level estimates. The raw data were visually inspected after data acquisition. Trials showing clear artifacts caused by eye blinks or by muscle activity, e.g. due to swallowing, were removed from the dataset.

Brain MRI registration was performed with a 1.5T 3d-MRI (Siemens Sonata, Erlangen, Germany). The following parameter settings were used in the Medical Center Alkmaar and VU University Medical Center: sagittal slice orientation, slice thickness 2 mm, FOV 256mm, scanmode fl3d, scan technique 20 magnitude, TR 11,8 ms, echoes no. 1, TE 5ms, flip angle 30 degrees

and contrast enhancement was applied. Lastly, the number of signals averaged was 2, scan matrix 256, reconstruction matrix 256, TI 0 and frequency 63,6 MHz. The MEG-MRI common reference system was defined on the basis of three anatomical landmarks (vitamin E capsules, 5 mm of diameter) fixed on nasion, left and right pre-auricular points. The MRI scan planes were set parallel to the above defined MEG localization coordinate system. In this way, we achieved superimpositions on MRI images with a precision of 2–3 mm as previously shown using simulations with artificial "dipoles" within a skull. The entire MRI procedure lasted about 30 min and was well tolerated by all subjects. Data storage was performed and made available on CD for off line data processing.

3.2.3 Collection and processing of the data

On line data monitoring and acquisition, and off line data averaging and rejection of too disturbed channels was performed at the MEG Center. MRI's were used for individual head modelling using manufacturers MEG software (CTF software, Port Coquitlam, Canada). Based on each MRI, an individual head model was defined that was used for dipole calculations and electronic display of the brain maps. Together with Advanced Neuro Technology software (ANT A/S, Enschede, The Netherlands) used for graphical display, CTF software was employed for the assessment of peak latencies, peaks, compressed waveform profiles (CWP), global field power (GFP), six dipole characteristic calculations (three dipole position, two orientation and strength) and graphical display. All MRI's and averaged datasets, using CTF and ASA software, were processed. From these results, all parameters (N=10) were either calculated or converted into plots (e.g. the GFP plots for each individual or a group) or into maps (e.g. all brain maps).

3.2.4 Statistical analysis

This study was designed as an explorative, observational study of the parameters that describe the cortical evoked responses in healthy subjects, CRPS I and CRPS II – PNI patients. Since no prior experimental and quantitative results as to the magnitude of the expected effects were available, a formal calculation of a prespecified power was not possible. Absence of an a priori sample size calculation based on power analysis emphasizes that a statistically nonsignificant result must be interpreted with caution since an existing difference may not be detected due to excess variability in the data and / or too small sample sizes. Therefore posterior powers have been calculated where appropriate. Owing to the moderate availability of PNI patients with continuing pain, groups of only twenty subjects and patients were selected. Experimental design consisted in all cases of simple two independent or dependent groups comparisons. Only contralateral hemispherical activity was analyzed in this study for comparison of the subject and patient groups. Statistical tests used were the independent groups t-test (or its non-parametric equivalent the Mann-Whitney rank sum test where appropriate) for between groups comparisons, and the paired t-test (or its non-parametric equivalent the Wilcoxon signed ranks test where appropriate) for within groups comparisons. A p-value less than 0.05 was considered as a statistically significant rejection of the null-hypothesis specified with two-tailed alternative hypotheses. Effect sizes and p-values are reported wherever relevant magnitudes of effects existed. Effect size (ES) is a numerical way of expressing the strength or magnitude of a reported relationship (Olejnik et al.,2000; Nakagawa et al., 2007) be it causal or not, and is defined as:

$$\text{Effect Size (E.S.)} = \frac{\text{mean experimental group} - \text{mean control group}}{\text{standard deviation control group}}$$

By offsetting the effect against the standard deviation of the controls, effect size is a measure of clinical relevance. An ES of plus or minus one unit means that the size of the effect is plus or minus 1 standard deviation, i.e. about two thirds of the normal biological variation. In addition to the effect size, the statistical power of a test was computed in cases where the test was negative (null hypothesis not rejected) and it was considered important to report the probability that the effect found in the sample could be excluded as a measure of the population value. Control for multiple testing was deemed unnecessary since in this explorative study no common hypothesis or theory covering two or more individual statistical tests was present. Control for the family wise error rate is important only when a conclusion based on several statistical tests is falsified, if at least one of the underlying tests is negative (Benjamini et al., 1995, Perneger, 1998). Given the clinical significance of our results and the likelihood of an increase of type II errors, control for the family wise error rate, i.e. a Bonferroni correction, was not performed. Statistical analysis was performed using SigmaStat 3.5v software (Systat Software, Inc. Point Richmond, CA, USA). Powers have been computed with the program PASS 6.0 (NCSS, Kaysville, UT, USA).

References

[1] Allison T, McCarthy G, Wood CC, Darcey TM, Spencer DD, and Williamson PD. Human Cortical Potentials Evoked by Stimulation of the Median Nerve I. Cytoarchitectonic Areas Generating Short-Latency Activity. Journal of Neurophysiology 1989; 694-722.

[2] Allison T, McCarthy G, Wood CC , Williamson PD and Spencer DD. Human Cortical Potentials Evoked by Stimulation of the Median Nerve II. Cytoarchitectonic Areas Generating Long-Latency Activity. Journal of Neurophysiology 1989; 62: 711-722.

Babiloni F, Babiloni C, Carducci F, Romani GL, Rossini PM, Angelone LM, Cincotti F. Multimodal integration of EEG and MEG data: A simulation study with variable signal-to-noise ratio and number of sensors. Hum Brain Mapp 2004, 22: 52-62.

Babiloni C, Pizzella V, Gratta CD, Ferretti A, Romani GL. Fundamentals of electroencefalography, magnetoencefalography, and functional magnetic resonance imaging. Int Rev Neurobiol 2009; 86: 67-80.

Bandettini PA. What's new in neuroimaging methods? Ann N Y Acad Sci 2009; 1156: 260-93.

Flor H, Braun C, Birnbaumer N, Elbert T, Ross B, Hoke M (1995). Chronic pain enhances the magnitude of the magnetic field evoked at the site of pain. In: Baumgartner C, Deecke L, Stroink G, Williamson SJ (Eds), Biomagnetism: Fundamental Research and Clinical Applications, Vol. 7, Elsevier Science, IOS Press, Amsterdam, pp 107-111.

Baumgartner C, Doppelbauer A, Deecke L, Barth DS, Zeitlhofer J, Lindinger G and Sutherling WW. Neuromagnetic investigation of somatotopy of human hand somatosensory cortex. Exp Brain Research 1991; 87: 641-648.

Baumgartner C (1993). Functional anatomy of the human somatosensory cortex. In: Baumgartner C (Ed), Clinical Electrophysiology of the somatosensory cortex. Springer Verlag, Vienna, pp. 1-13.

Baumgartner C. Controversies in clinical neurophysiology. MEG is superior to EEG in the localization of interictal epileptiform activity. Con Clin Neurophysiol 2004; 115: 1010-1020.

Barkley GL, Baumgartner C. MEG and EEG in epilepsy. J Clin Neurophysiol 2003; 20: 163-178.

Benjamini Y, Hochberg Y: Controlling the False Discovery Rate: A practical and Powerful Approach to Multiple testing. The Journal of the Royal Statistical Society. Series B (Methodological) 1995; 57: 289-300

Brett M, Johnsrude IS, Owen AM. The problem of functional localization in the human brain. Nat Rev Neurosci 2002; 3: 243-249.

Bromm B. Brain Images of Pain. News Physiol Sci 2001; 16: 244-249.

Bruehl S, Harden RN, Galer BS, Saltz, S. External validation of IASP diagnostic criteria for Complex Regional Pain Syndrome and proposed research diagnostic criteria. International Association for the Study of Pain. Pain 1999; 81: 147-154.

Casey KL, Minoshima S, Berger KL, Koeppe RA, Morrow TJ and Frey K.A. Positron Emission Tomographic Analysis of Cerebral Structures activated specifically by Repetitive Noxious Heat Stimuli, Journal of Neurophysiology, 1994 (71); 802-807.

Chen AC, Theuvenet PJ, de Munck JC, Peters MJ, van Ree JM, Lopes da Silva FL. Sensory Handedness is not Reflected in Cortical Responses After Basic Nerve Stimulation: A MEG Study. Brain Topogr 2011 Nov 12. [Epub ahead of print].

Cherry SR, Phelps ME. Imaging brain function with positron emission tomography. Brain Mapping: The Methods 1996; 191-221.

Cohen D. Magnetoencephalography: evidence of magnetic fields produced by alpha-rhythm currents. Science 1968; 161: 784-786.

Cohen D. Magnetoencephalography: detection of the brain's electrical activity with a superconducting magnetometer. Science 1972; 175: 664-666.

Darvas F, Pantazis D, Kucukaltun-Yildirim E, Leahy RM. Mapping human brain function with MEG and EEG: methods and validation. Neuroimage 2004; 23 Suppl 1:S289-99.

Delft van D, Kes P. The discovery of superconductivity. Physics today. The American Institute of Physics 2001; 38-44.

Disbrow E, Roberts T, Poeppel D, Krubitzer L. Evidence for interhemispheric processing of inputs from the hands in human S2 and PV. J Neurophysiol 2001; 85: 2236-2244.

Erwin CW, Rozear MP, Radtke RA, Erwin AC (1993). Somatosensory evoked potentials and surgical monitoring. In: Niedermeyer E, Lopes da Silva FH (Ed), Electroencephalography. Williams & Wilkins, Baltimore, Philadelphia, Hong Kong, 957-974.

Flor H, Braun C, Birnbaumer N, Elbert T, Ross B, Hoke M (1995). Chronic pain enhances the magnitude of the magnetic field evoked at the site of the pain. In:

Frot M, Mauguière F. Timing and spatial distribution of somatosensory responses recorded in the upper bank of the Sylvian fissure (SII area) in humans. Cereb Cortex 1999; 9: 854-863.

Fuchs M, Wagner M, Kastner J. Confidence limits of dipole source reconstruction results. Clin Neurophysiol 2004; 6: 1442-1451.

Funke M, Constantino T, Van Orman C, Rodin E. Magnetoencephalography and magnetic source imaging in epilepsy. Clin EEG Neurosci 2009; 40: 271-80.

Gevins AS, Bressier SL (1988). Functional topography of the human brain. In: Pfurtscheller G, F.H.Lopes da Silva (Ed), Functional Brain Imaging. Hans Huber Publishers, pp 99-116.

Hämäläinen M, Hari R, Ilmoniemi R, Knuutila J, Lounasmaa OV. Magnetoen- cephalography – theory, instrumentation, and applications to noninvasive studies of signal processing in the human brain. Reviews of Modern Physics 1993; 65: 413–497.

[1] Hari R, Kaukoranta E, Reinikainen K, Huopaniemie T, Mauno J. Neuromagnetic Localization of Cortical Activity evoked by Painful Dental Stimulation in Man. Neuroscience Letters 1983: 42: 77-82.

[2] Hari R, Hämäläinen M, Kaukoranta E, Reinikainen K, Teszner D. Neuromagnetic responses from the second somatosensory cortex in man. Acta Neurol Scand 1983; 68: 207-212.

[3] Hari R, Hamalainen M, Ilmoniemi R, Kaukoranta E, Reinikainen K (1984). Magnetoencephalographic Localization of Cortical Activity Evoked by Somatosensory and Noxious Stimulation. In: Bromm B (Ed), Pain Measurement in Man. Neurophysiological Correlates of Pain. Elsevier Science Publishers B.V., Amsterdam, pp 317-324.

[4] Hari R, Reinikainen K, Kaukoranta E, Hämäläinen M, Ilmoniemi R, Penttinen A, Salminen J, Teszner D. Somatosensory evoked cerebral magnetic fields from SI and SII in man. Electroencephalogr Clin Neurophysiol 1984; 57: 254-263.

[5]Hari, R (1993). Magnetoencephalography as a Tool of Clinical Neurophysiology. In: Niedermeyer E, Lopes da Silva FL (Ed), Encephalography, Basic Principles, Clinical Application, and related Fields, 3d Edn. Williams & Wilkins, Baltimore (USA), pp. 1035-62.

[6] Hari R, Forss N. Magnetoencephalography in the study of human somatosensory cortical processing. Philos Trans R Soc Lond B Biol Sci 1999; 1387: 1145-1154.

Hoshiyama M, Kakigi R, Kitamura Y, Shimojo M, Watanabe S. Somatosensory evoked magnetic fields after mechanical stimulation of the scalp in humans, Neuroscience Letters 1995; 29-32.

Hoshiyama M, Kakigi R, Koyama S, Kitamura Y, Shimojo M, Watanabe S. Somatosensory evoked magnetic fields following stimulation of the lip in humans. Electroencephalography and Clinical Neurophysiology 1996: 96-104.

Huttunen J (1988). Evoked magnetic fields in the study of somatosensory cortical areas. In: Pfurtscheller G, Lopes da Silva FH (Ed), Functional Brain Imaging. Hans Huber Publishers, Toronto, pp. 61-69.

Huttunen J, Komssi S, Lauronen L. Spatial dynamics of population activities at S1 after median and ulnar nerve stimulation revisited: a MEG study. NeuroImage 2006; 32: 1024-1031.

Ioannides AA, Fenwick PB, Liu L. Widely distributed magnetoencephalography spikes related to the planning and execution of human saccades. J Neurosci 2005; 25: 7950-7967.

Jones AKP, Brown WD, Friston KJ, QI LY, Frackowiak RSJ. Cortical and subcortical localization of response to pain in man using positron emission tomography, Proc R Soc Lon B 1991; 224: 39-44.

Kakigi R. Somatosensory evoked magnetic fields following median nerve stimulation, Neuroscience Research 1994: 165-174.

[1] Kakigi R, Koyama S, Hoshiyama M, Kitamura Y, Shimojo M, Watanabe S. Pain-related magnetic fields following painful CO2 laser stimulation in man, Neuroscience Letters 1995; 45-48.

[2] Kakigi R, Koyama S, Hoshiyama M, Shimojo M, Kitamura Y, Watanabe S. Topography of somatosensory evoked magnetic fields following posterior tibial nerve stimulation. Electroencephalography and Clinical Neurophysiology 1995; 127-134.

Kakigi R, Hoshiyama M, Shimojo M, Naka D, Yamasaki H, Watanabe S, Xiang J, Maeda K, Lam K, Itomi K, Nakamura A. The somatosensory evoked magnetic fields. Progress in Neurobiology 2000; 61: 495-523.

Kakigi R, Inui K, Tran DT, Qiu Y, Wang X, Watanabe S, Hoshiyama M. Human brain processing and central mechanisms of pain as observed by electro- and magneto-encephalography. J Chin Med Assoc 2004; 67: 377-86.

Kawamura T, Nakasato N, Seki K, Kanno A, Fujita S, Fujiwara S, Yoshimoto T. Neuromagnetic evidence of pre- and post-central cortical sources of somatosensory evoked responses. Electroencephalography and Clinical Neurophysiology 1996; 100: 44-50.

Koenig T, Melie-García L, Stein M, Strik W, Lehmann C. Establishing correlations of scalp field maps with other experimental variables using covariance analysis and resampling methods. Clin Neurophysiol 2008; 119: 1262-1270.

Lehmann D. Past, present and future of topographic mapping. Brain Topography 1990; 3: 191-202.

Leonardelli, E. A multimodal neuroimaging study of the somatosensory system. Thesis, 2010. University Padova, Italy, Chapter 4, pp 70-74.

[1] Lopes da Silva FH, van Rotterdam A (1993). Biophysical Aspects of EEG and Magnetoencephalography Generation. In: Niedermeyer E, Lopes da Silva FH (Ed), Electroencephalography. Williams & Wilkins, Baltimore - Philadelphia, pp 78-91.

[2] Lopes da Silva FH, van Rotterdam A (1993). EEG analysis: theory and practice. In: Niedermeyer E, Lopes da Silva FH (Ed), Electroencephalography. Williams & Wilkins, Baltimore - Philadelphia, pp 1117-1118.

Maurer K, Dierks Th (1991). Definition and Terminology. In: Maurer K, Dierks Th (Ed), Atlas of Brain Mapping. Springer-Verlag, Berlin-Heidelberg, pp 1-9.

Meijs JWH, ten Voorde BJ, Peters MJ, Stok CJ, Loes da Silva FH (1988). The influence of various head models on EEG's and MEG's. In: Pfurtscheller G, Lopes da Silva FH (Ed), Functional brain Imaging. Hans Huber Publishers, Toronto, pp 31-45.

Nieuwenhuys R. The neocortex. An overview of its evolutionary development, structural organization and synaptology. Anat Embryol 1994; 190: 307-337.

Nieuwenhuys R, Voogd J, van Huijzen C (2008). Telencephalon: Neocortex. In: Nieuwenhuys R, Voogd J, van Huijzen C (Ed), The Human Central Nervous System, 4th edn. Springer Verlag, Berlin, pp 595-600.

Nakagawa S, Cuthill IC: Effect size, confidence interval and statistical significance: A practical guide for biologists". Biological Reviews Cambridge Philosophical Society 2007; 82: 591-605

Nuwer MR, Aminoff M, Desmedt J, Eisen AA, Goodin D, Matsuoka S, Mauguière F, Shibasaki H, Sutherling W, Vibert JF. IFCN recommended standards for short latency somatosensory evoked potentials. Report of an IFCN committee. International Federation of Clinical Neurophysiology. Electroencephalogr. Clin. Neurophysiol 1994; 91: 6-11.

Olejnik S, Algina, J: Measures of Effect Size for Comparative Studies: Applications, Interpretations and Limitations. Contemporary Educational Psychology 2000; 25: 241-86

Okada,Y (1983). Neurogenesis of evoked magnetic fields. In: Williamson SH; Romani GL; Kaufman L; Modena I (Ed), Biomagnetism: an Interdisciplinary Approach. Plenum Press, New York, pp 399-408.

Orrison WW, Lewine JD (1995). Functional Brain Imaging. Magnetoencephalography and Magnetic Source Imaging. In: Orrison WW, Lewine JD, Sanders JA, Hartshorne MF (Ed), Mosby Yearbook Inc. St. Louis (USA), pp 369 - 418.

Perneger TV. What's wrong with Bonferroni adjustments. BMJ 1998; 18:1236-38.

Parra J, Kalitzin SN, da Silva FH. Magnetoencephalography: an investigational tool or a routine clinical technique? Epilepsy Behav 2004; 5: 277-285.

Pichler BJ, Wehrl HF, Kolb A, Judenhofer MS. Positron emission tomography/magnetic resonance imaging: the next generation of multimodality imaging? Semin Nucl Med 2008; 38: 199-208.

Raij T (2005). Pain processing in the human brain: views from magnetoencephalography and functional magnetic resonance imaging. Thesis, Brain research unit, Helsinki University of technology, pp. 16-21.

Rossini PM, Narici L, Romani G-L, Traversa R, Cecchi L, Cilli M, Urbano A. Short latency somatosensory evoked responses to median nerve stimulation in healthy humans: electric and magnetic recordings. Intern J Neuroscience 1989; 46: 67-76.

Rossini PM, Nerici L, Martino G, Pasquarelli A, Peresson M, Pizella V, Tecchio F, Romani G-L. Analysis of interhemispheric asymmetries of somatosensory evoked magnetic fields to right and left median nerve stimulation., Electroencephalography and Clinical Neurophysiology 1994; 91: 476-482.

Rossini PM, Pauri F. Neuromagnetic integrated methods tracking human brain mechanisms of sensorimotor areas 'plastic' reorganization. Brain Res Brain Res Rev 2000; 33: 131-154.

Rossini PM, Tecchio F, Pizzella V, Lupoi D, Cassetta E, Pasqualetti P. Interhemispheric Differences of Sensory Hand Areas after Monospheric Stroke: MEG/MRI Integrative Study. NeuroImage 2001; 474-485.

Rossini PM, Dal Forno G. Integrated technology for evaluation of brain function and neural plasticity. Phys Med Rehabil Clin N Am 2004; 15: 263-306.

Schnitzler A, Seitz RJ, Freund HJ (2000). The somatosensory system. In: Toga AW, Mazziotta JC (Ed), Brain Mapping, The Systems. Academic Press, London, pp. 291-309.

Simões C, Hari R. Relationship between responses to contra- and ipsilateral stimuli in the human second somatosensory cortex SII. NeuroImage 1999; 10: 408-416.

Simões C, Alary F, Forss N, Hari R. Left-hemisphere-dominant SII activation after bilateral median nerve stimulation. NeuroImage 2002; 15: 686-690.

Skrandies W. Global field power and topographic similarity. Brain Topogr 1990; 3: 137-141.

Tecchio F, Rossini PM, Pizzella V, Cassetta E, Romani GL. Spatial properties and interhemispheric differences of the sensory hand cortical representation: a neuromagnetic study. Brain Research 1997; 767: 100-108.

Tecchio F, Rossini PM, Pizella V, Cassetta E, Pasqualetti P, Romani G-L. A neuromagnetic normative dataset for hemispheric sensory hand cortical representation and their interhemispheric differences. Brain Research Protocols 1998; 306-314.

Tecchio F, Pasqualetti P, Pizzella V, Romani G, Rossini PM. Morphology of somatosensory evoked fields: inter-hemispheric similarity as a parameter for physiological and pathological neural connectivity. Neurosci Lett 2000 ; 287 : 203-206.

Theuvenet PJ, van Dijk BW, Peters MJ, van Ree JM, Lopes da Silva FL, Chen AC. Whole-head MEG analysis of cortical spatial organization from unilateral stimulation of median nerve in both hands: No complete hemispheric homology. NeuroImage 2005; 28: 314-325.

Theuvenet PJ, van Dijk BW, Peters MJ, van Ree JM, Lopes da Silva FL, Chen AC. Cortical characterization and inter-dipole distance between unilateral median versus ulnar nerve stimulation of both hands in MEG. Brain Topogr 2006; 19: 29-42.

Theuvenet PJ, de Munck JC, Peters MJ, van Ree JM, Lopes da Silva FL, Chen AC. Anesthetic block of pain-related cortical activity in patients with peripheral nerve injury measured by magnetoencephalography. Anesthesiology 2011; 115: 375-86.

Treede RD, Kenshalo DR, Gracely RH, Jones AKP. Cortical representation of pain. Pain 1999; 79: 105-111.

Ushida T, Fukumoto M, Binti C, Ikemoto T, Taniguchi S, Ikeuchi M, Nishihara M, Tani T. Alterations of contralateral thalamic perfusion in neuropathic pain. Open Neuroimag J. 2010; 4:182-6.

Van der Meij W, Huiskamp GJ, Rutten GJ, Wieneke GH, van Huffelen AC, van Nieuwenhuizen O. The existence of two sources in rolandic epilepsy: confirmation with high resolution EEG, MEG and fMRI. Brain Topogr 2001; 13: 275-82.

Vanni S, Rockstroh B, Hari R. Cortical sources of human short-latency somatosensory evoked fields to median and ulnar nerve stimuli. Brain Res 1996; 737: 25-33.

Vrba J, Haid G, Lee S, Taylor B, Fife AA, Kubik P, McCubbin J, Burbank MB. Biomagnetometers for unshielded and well shielded environments. Clin Phys Physiol Meas 1991; 12 Suppl B: 81-6.

Vrba J, Robinson SE. Signal Processing in Magnetoencephalography. Methods 2001; 25: 249-71.

Willemse RB, de Munck JC, van't Ent D, Ris P, Baayen JC, Stam CJ, Vandertop WP. Magnetoencephalographic study of posterior tibial nerve stimulation in patients with intracranial lesions around the central sulcus. Neurosurgery 2007; 61: 1209-1217.

Zimmerman, J.E., Theine, P., and Harding, J.T. Design and operation of stable rf-biased superconducting point-contact quantum devices. Journal of Applied Physics 1970; 41: 1572-1580.

Chapter 4

Responses to Median and Tibial Nerve Stimulation in Patients with Chronic Neuropathic Pain

P.J. Theuvenet, Z. Dunajski, M.J. Peters, J.M. van Ree

Brain Topography, 1999, vol. 11, no. 4, pp. 305-313 (9).

Abstract

Somatosensory evoked magnetic fields and electrical potentials were measured in eight patients with unilateral neuropathic pain. After median nerve stimulation on the painful side, the amplitudes of the evoked responses were enhanced 2 to 3 times at a latency of about 100 ms compared to the responses of the contralateral, unaffected side. After posterior tibial nerve stimulation an enhancement was found at latencies around 110 ms and 150 ms. The scalp distribution of the magnetic field at the latencies of “abnormal” responses was dipolar and the responses could be ascribed to a current dipole. Three (of the eight) patients underwent spinal cord stimulation (SCS) for their pain. The enhancement of the evoked responses to stimulation of the painful side decreased after spinal cord stimulation. After a long period of spinal cord stimulation only (e.g., a year) during which the patient reported to be pain free, these “abnormal” responses were no longer observed.

Introduction

Electrical potentials and magnetic fields experimentally evoked by painful stimuli ("douleur laboratoire") have been investigated extensively (Hattunen et al. 1986; Dowman 1994 a,b,c; Bromm 1995). The waveforms of early components, i.e., the components at latencies less than 90 ms, are related to sensory aspects of pain perception. The later components such as the electrical N150 and P250 are ascribed to the appraisal of the painful stimulus (Bromm 1984; Joseph et al. 1991; Laudahn et al. 1995; Flor et al. 1995). The aim of our work was to study evoked responses in a group of patients who suffered from the sequelae of traumatic neuropathic pain and the responses once the patient became pain free after spinal cord stimulation (SCS). We investigated the magnetic fields and electrical potentials evoked by stimulation of the median nerve or the posterior tibial nerve in eight patients suffering from unilateral neuropathic pain. Ten healthy volunteers were also examined as a reference group. The responses to stimulation of the unaffected and injured sides were compared. During our study three (of the eight) patients underwent spinal cord stimulation (SCS). Patients who underwent SCS were measured before SCS and after SCS. SCS is an invasive technique whereby an electrode is introduced percutaneously into the spinal canal in order to stimulate the dorsal columns for pain relief. During implantation and positioning of the electrode under local anesthesia and fluoroscopy, paraesthesias in each patient in the affected area have to be found in close cooperation with the patient. Both MEG and EEG are due to the same sources, although EEGs are generated by sources irrespective of their directions while MEGs are principally generated by sources that are oriented tangentially with respect to the skull. Consequently, similarities between the waveforms of evoked potentials and evoked fields are to be expected. Usually, magnetic field measurements require fewer trials for averaging to obtain a sufficiently high signal-to-noise ratio than measurements of the potentials. Moreover, they may offer a better spatial resolution of the underlying sources if more sensors are used.

Subjects and methods

Subjects

Brain responses to median or posterior tibial nerve stimulation were examined in ten healthy right-handed volunteers (1 woman; 9 men; in the range 20 to 55 years; mean age 29 ±9 SD) and eight patients who suffered from unilateral neuropathic (traumatic) pain (4 women; 4 men; in the range 35-70 years; mean age 46 ± 11 SD). All patients gave their consent to this non-invasive study. Three patients had a spinal cord stimulator implanted and measurements were carried out before (3 days), immediately after SCS (within one week after electrode implantation), and again after a longer period of SCS (from six months to three years). The level of the four electrode tips of the Quad electrode (Medtronic) was between C5-C7 for arm and hand and Th10-Th12 for the leg, just outside the midline of the vertebra (on fluoroscopy) on the affected side. After a period of about 2 weeks of successful stimulation an Itrell-2 or 3 pulse generator (Medtronic) was implanted subcutaneously. SCS was the only therapy for all three patients after implantation. The case histories of these three patients are presented below in detail.

Patient A was a 47-year-old female who had had an accident in 1993. After the accident she suffered from pain at the ankle. The right superficial sural nerve was transected and embedded in the fibula. The operation failed to relieve her pain, the original

pain at the ankle recurred. The EMG showed a good response after stimulation of the sural nerve on the left side, but there was no reaction on the right (injured) side. Sensation both on the back of the right foot and laterally in the area of the sural nerve was lowered. There was also a paresis of the plantar flexors of the right foot (grade 4).

Patient B was a 69-year-old male who suffered a serious accident to his right hand in 1979 so that the fourth and fifth finger had to be amputated. Subsequent operations to the hand failed to relieve his pain. The patient complained of hyperpathia, allodynia, a shooting and burning pain and intolerance to cold in the area of amputation. He was unable to use the remaining three fingers and had to protect his hand continuously in daily life. All earlier therapies like transcutaneous electrical nerve stimulation (TENS), stellate ganglion blocks and tricyclic anti-depressant drugs failed to relieve his pain.

The general condition of the patient was good. In 1993 the patient underwent SCS at the cervical level (entrance of the electrode at Th2 - Th3) and became pain free.

Patient C was a 50-year-old male with damage to the posterior tibial nerve on the left side after several tendon operations to the ankle in 1991. In 1992, the posterior tibial nerve was found to be entrapped in scar tissue. The neurolysis that was performed failed to relieve the patient' s complaints. These consisted of persistent pain at the medial side of the ankle and in the foot, stiffness and inability to walk. After the neurolysis there was neither motor weakness nor sensory loss. During exercise the patient described that he had the impression that the area of the pain was enlarging. This patient was in a good general condition. After SCS in 1995 (entrance electrode between L2-L3 and the four electrode tips over Th10) and paraesthesia in the area of the pain, he experienced pain relief and was able to walk over longer distances.

Methods

Magnetic field measurements were carried out in a magnetically shielded room using a 19-channel magnetometer (Brake et al. 1990). The component of the magnetic induction perpendicular to the head was measured. The signals from the magnetometer were amplified and filtered by a high-pass digital filter at 0.1 Hz and a low pass filter at 450 Hz. The data acquisition equipment contains an artefact rejector that deletes disturbed epochs. The implantable pulse generator normally used for spinal cord stimulation contains a magnetic switch which generates high magnetic disturbances. Consequently, magnetic measurements cannot be carried out once the pulse generator is implanted. After implantation of the spinal cord electrode, evoked magnetic fields were recorded using an external pulse generator. The latter was placed outside the shielded room and was connected to the patient by means of long cables. The position of the magnetometer in relation to the head is illustrated in figure 3. The measurements of potentials were also performed in the magnetically shielded room in order to diminish external noise. Potentials were recorded using thirty-two or more electrodes placed on the scalp according to the international 10-20 system. Signals from the electrodes were amplified and fed through the same filters as the signals from the magnetometer. During magnetic measurements the subjects were lying in the lateral position. The volunteers and patients were given no specific task to perform, but were asked not to move and to stay awake with the eyes open. The position of the head was stabilized with a vacuum pillow. The electrical stimulus was applied by means of two cotton disk electrodes at the ankle (posterior tibial nerve) or at the wrist (median nerve). Square-wave constant current pulses with duration of 0.6 ms were applied. The stimulus rate was randomly varied between 0.9 and 1.2 Hz or it was fixed at 0.6 Hz. The amplitude of the stimulus was

slightly above the motor threshold (about 7 mA) producing a painless twitch and paraesthesias in the thumb or the big toe. A POLHEMUS position indicator was used to define the location and orientation of the magnetometer coils and the electrode positions relative to landmarks on the head. Off-line averaging was done after 200-300 responses. All measurements were repeated twice, in order to detect possible artefacts and check reproducibility.

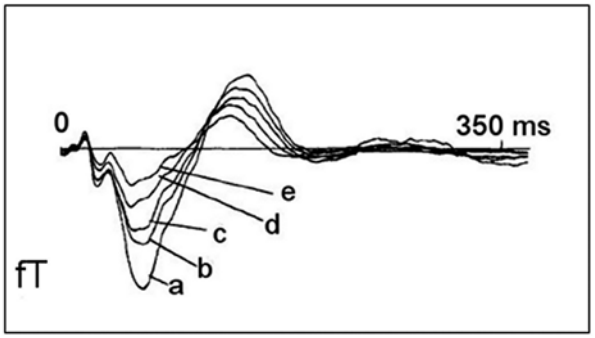

Fig. 1. presents the magnetic responses to median nerve stimulation as a function of the interstimulus interval ISI; a) ISI=3 sec, b) ISI=2 sec ± 50% randomisation, c) ISI= 2 sec, d) ISI= 1 sec, e) ISI= 0.5 sec. Timeframe is 350 ms post stimulus and vertically the amplitude in femto tesla.

The latency of the response was measured from the onset of the stimulus to the time instant of peak amplitude in the chosen wave. Increases of the evoked responses were characterized by the ratio of the signals measured under varying circumstances at a chosen time instant. A two-way ANOVA (analysis of variance) was performed to compare the responses, evoked at both the painful and unaffected sides, and the responses of healthy volunteers and patients. Statistical data based on the paired t-test are presented for periods of interest in which distribution patterns of the magnetic field or electrical potentials were stable. All reported p-values are two tailed. From the magnetic field measurements an equivalent dipole was localized by means of Advanced Source Analysis program using the Marquardt algorithm (Marquardt 1963). Three concentric spheres described the head.

Results

The measured electrical and magnetic responses of the ten healthy volunteers to the median and posterior tibial nerve stimulation showed waveforms which were consistent with those presented in the literature and are considered to be normal (e.g., Rossini at al. 1994; Kany and Treede 1997; Hoshiyama et al. 1997). Responses after stimulation of the nerves on both sides were similar, in the sense that they showed the same waves, although the polarity and amplitude of the waves is position dependent. All waveforms of the responses of healthy subjects showed some common features:

a) the responses were maximal over the contralateral hemisphere
b) after median nerve stimulation, the first peaks were found around 20 and 40 ms after stimulus onset
c) after posterior tibial nerve stimulation the first peaks were found at a latency around 40 ms
d) the topographical maps of the potential or the magnetic field of the middle-latency components did not change considerably in a period of 20 ms around the peak latencies, suggesting that the generators were not changing their position

An example of an SEF to median nerve stimulation as a function of the interstimulus interval, measured over the contralateral side is shown in figure 1. It was found that after a break of only a minute between stimulation sequences, the amplitudes of the next sequence would start somewhere between the initial and final values of the first, “fresh” sequence. A recovery time of 3-5 minutes was required to ensure that the signals were not influenced by the former sequence of

measurements. Typical peak values of the evoked responses measured at the contralateral side at a latency of about 80 ms after median nerve stimulation were 10 uV for SEP and 800 fT for SEF. Typical peak values of the evoked potentials measured at the contralateral side at a latency of about 110 ms after tibial nerve stimulation were 8 uV. Eigenvalue decomposition was performed for the distributions found in the period of 20 ms around a peak. It was found that the largest eigenvalue could explain more than 80% of the signal.

Patients.

Magnetic measurements were preferred whenever possible to avoid extended measurement sessions. The responses following median and tibial nerve stimulation of the unaffected side of the eight patients were similar to those of the healthy volunteers. However, the responses following stimulation of the painful side differed substantially. In all eight patients, the amplitudes of both the magnetic and the electrical responses at a latency of 90 -100 ms after stimulation of the median nerve were enhanced 2 to 3 times compared to those in the control group. The responses after stimulation of the posterior tibial nerve were increased mainly at latencies of 115 and 150 ms. This increase of amplitude was seen as an “additional wave” with an amplitude of about 400 fT in the channel with the highest response. During source analysis, the waves peaking at latencies of interest were compared with the 40 ms wave. The equivalent dipole at a latency of 40 ms is presumed to be located at the highest and most medial portion of the postcentral gyrus, in areas 1, 2 and 3b (Fujita et al. 1995; Wikstrom et al. 1997). For this reason the location of this dipole is used as a reference for the equivalent dipole found at the latencies of enhanced responses. The measurements obtained from patients A, B and C are described below in detail.

Patient A. Magnetic responses to posterior tibial nerve stimulation measured over the contralateral hemisphere are shown in figure 2. Responses to stimulation of the (injured side) right posterior tibial nerve (red lines) and the left tibial nerve (blue lines) are superimposed. The responses in both records are about the same at latencies of 40 ms, 60 ms, and 75 ms but they are different at latencies of 110 ms and 150 ms. The enhanced 110 ms wave is best seen in channels 1, 2, 7,17, and 18, and

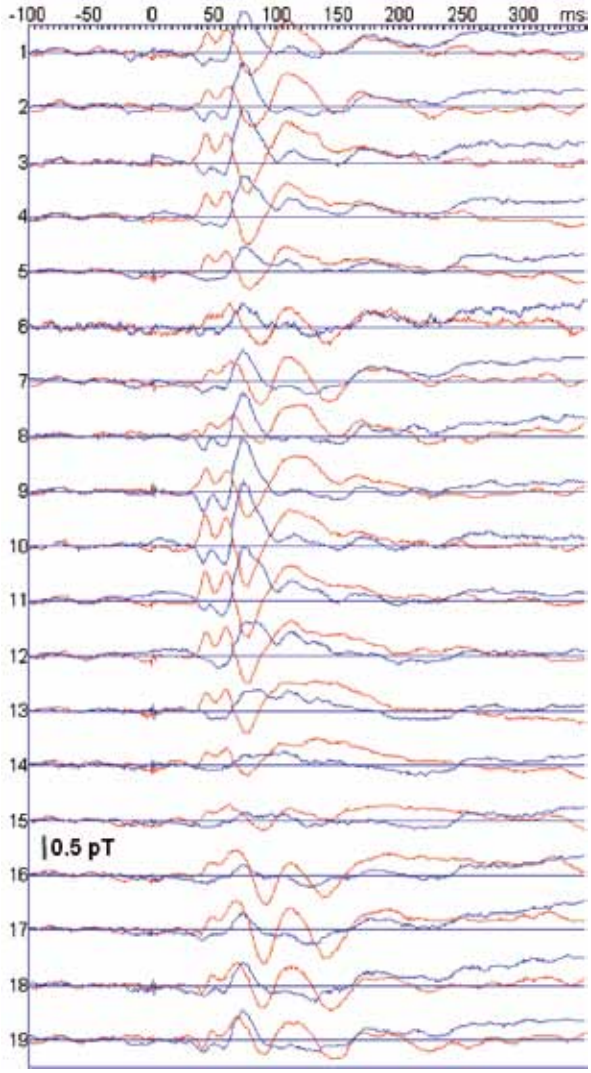

Figure 2. Magnetic responses to the posterior tibial nerve stimulation of patient A, while the patient was in pain; red lines - the injured leg stimulated; blue lines - the healthy leg stimulated. The measuring positions of the channels are indicated in figure 3.

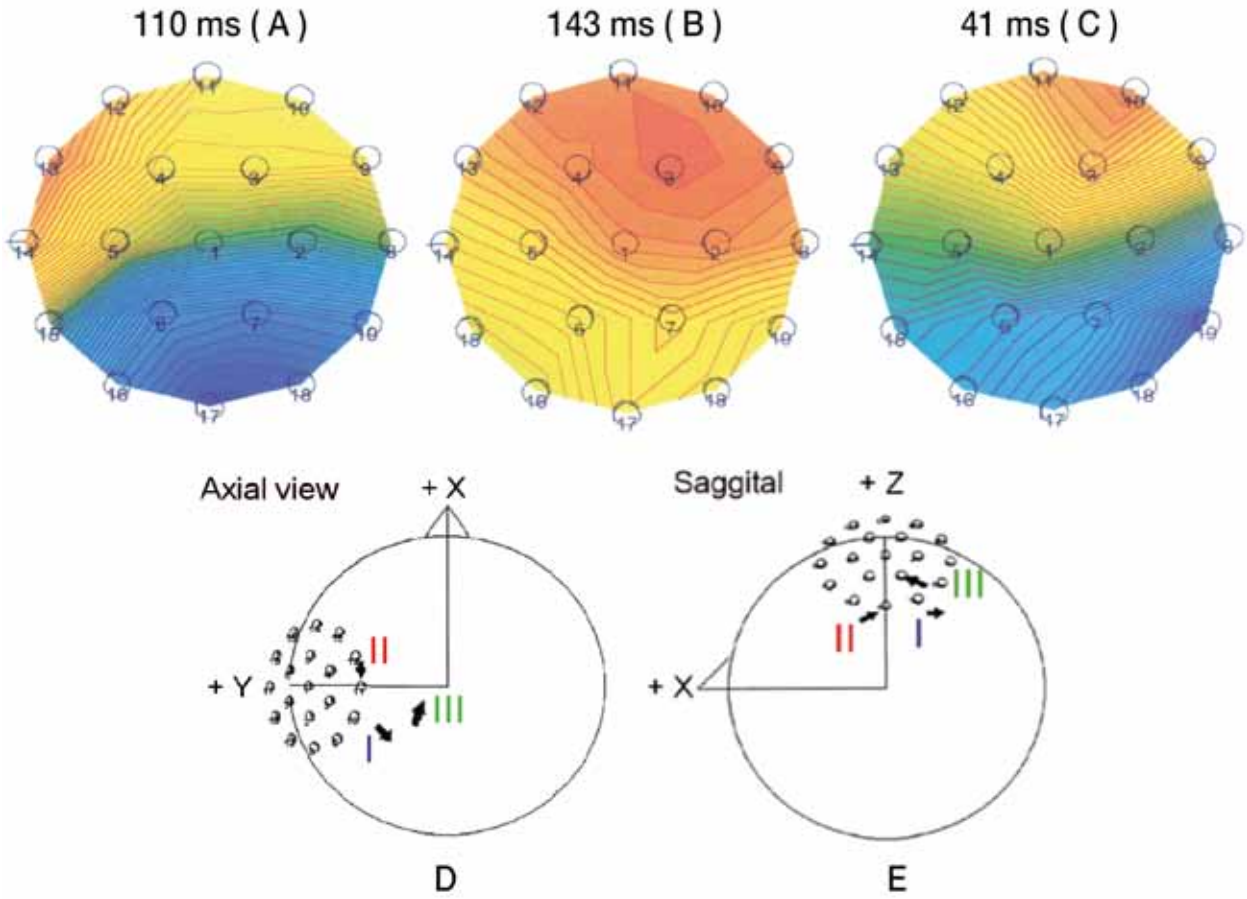

Fig. 3. Isomagnetic field maps measured at latencies of: (A) 110 ms, (B) 143 ms, and (C) 41 ms; (D) and (E) the sources indicated by arrows explain the magnetic responses: I) for 110 ms; II) for 143 ms; III) for 41 ms. The head is described by a spherical model. The 19 channels used to measure the magnetic field are depicted. The axes are oriented as follows: x - toward the nasion, y - ear canal, z - vertex.

the 150 ms wave in channels 1,7,17,18, and 19.

These waves can also be seen in the responses of corresponding channels after stimulation of the healthy leg. However, the ratio of the amplitudes of the responses of the injured side to the corresponding responses of the healthy side is high. An ANOVA performed on these data showed that the differences are statistically significant, $t=4.05$ and $p<0.0001$. Isomagnetic field maps for latencies of 110 ms and 143 ms after stimulation are shown in figures 3a and 3b. Source analysis showed that they could be ascribed to a single equivalent current dipoles within the brain. The dipoles are depicted in figures 3d and 3e. At a latency of 110 ms the measurements are for 98% and at 143 ms for 92.5 % determined by the current dipole. For comparison, the dipole location found at a latency of 41 ms is also shown. This dipole explains the measurement for 99%. The dipole found at 143 ms latency is shifted about 4 cm in the frontal direction. No enhanced activity at the latencies mentioned above was observed in the evoked potentials measured nine months after SCS and the patients report to be pain free. The amplitudes of the responses after stimulation of the tibial nerve at the right and left side were about the same as illustrated in figure 4.

As was mentioned before, nine months after pulse generator implantation only evoked potentials could be obtained.

During short intervals the pulse generator was switched off in order to perform measurements. Figure 5b shows the results after 15 minutes and figure 5c after 30 minutes of stimulation when the patient reported to be pain free. We summarized these findings in figure 5d (for one channel), the upper trace was recorded when the patient was in pain, the second, third and fourth interval after 7, 20 and 30 minutes of stimulation, respectively.

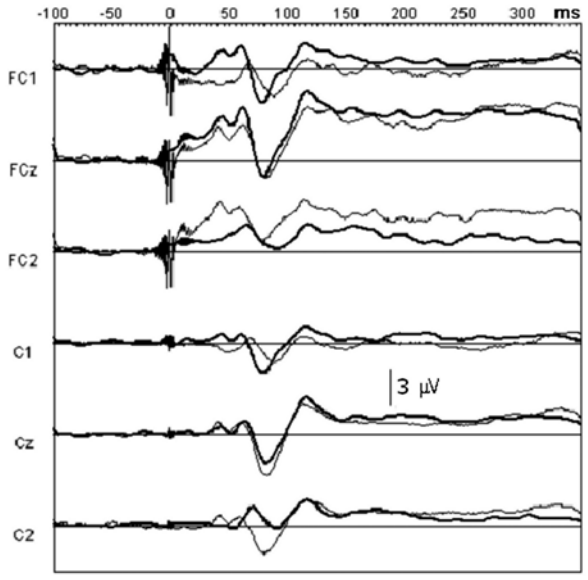

Figure 4. SEPs to the posterior tibial nerve stimulation in patient A, after 9 months of SCS treatment. Thin line: injured leg; bold line: healthy leg stimulated. SEPs were measured simultaneously in 64 channels. Only a few of the measurements are shown. Comparing the responses, measured while the patient was pain free, with those shown in figure 2, which were measured while the patient was in pain, it may be concluded that the 110 and 150 ms waves have disappeared.

Patient B. The following experiments were carried out after the implantation of the spinal electrode. In a single session evoked fields were measured: a) with the electrode in situ, without stimulation and the patient in pain, b) while stimulating with an external pulse generator and the pain fading away, and c) after switching the external pulse generator off and the patient was pain free. Records, after stimulation of the injured hand and measured with the magnetometer system in the same position above the left hemisphere, are shown in figures 5a-5d. Channel 1 is over C3. The positions of the other channels correspond to those shown in figure 3. Figure 5a presents the responses to median nerve stimulation before SCS was applied and the patient was in pain, though the SCS electrode was already implanted. The cortical responses at the latencies 20 ms and 40 ms are similar to those of the normal subjects. At latency around 100 ms the evoked fields at the painful side differed considerably from those evoked at the unaffected (left) side, (shown in figure 5e). Next the pulse generator was switched on and the patient was stimulated for 30 minutes. Similar changes were found in the other measuring channels. Comparison of the responses shown in figure 5a with those shown in figure 5c shows an additional wave at latency around 100 ms when the patient was in pain. Measurements of this patient were repeated six months, two years, and three years after pulse generator implantation. At this stage only evoked potentials could be measured because of the magnetic switch. In the pain free situation the 100 ms components in the responses to median nerve stimulation of the right hand were not enhanced compared to the (unaffected) left hand or the healthy volunteers. An ANOVA showed that the observed differences were statistically not significant.

Patient C. Responses to posterior tibial nerve stimulation of the injured leg were measured before, during the session of SCS, and after 30 minutes once the patient was pain free and the pulse generator was switched off. Responses after tibial nerve stimulation when the patient was

in pain (before SCS) and after SCS (patient was pain free) are shown in figure 6. Channels with the same number are at the same position over the head (channel1 is over electrode position C2). When the patient was in pain an increase of the amplitudes at latencies 110, 150 and 210 ms was observed. The activity at the latency of 150 ms is the most prominent for this patient and may be considered as an additional wave. This additional wave diminished after spinal cord stimulation. The statistical analysis of the waves when the patient was in pain or pain free showed significant differences, t=3.1, p=0.0022.

DISCUSSION

The typical features of the responses after median and posterior tibial nerve stimulation in healthy volunteers, (as described by Kany and Treede 1997) were comparable with the responses from the unaffected side of our pain patients. In all studied patients with longstanding neuropathic pain (in one case since 1979) an enhancement of the amplitudes, at latencies between 80 and 150 ms, was seen in evoked fields and potentials compared to the unaffected side and the reference group. In MEG's the increase in amplitudes at these latencies was 2 to 3 times higher to around 400 fT. Because such a high enhancement was not observed in responses after stimulation of the nerve on the unaffected side, this non-painful side can be used as a control. In three patients who underwent SCS this enhancement was found to be reversible once the patient reported to be pain free. This was still true after considerable time. We also found that the magnetic field distributions of the enhanced waves were dipolar and the responses could be ascribed to a single current dipole. Similar findings were reported by Flor et al. (1995), who studied a group of low back pain patients, category XXVII. (IASP 1994). When painful and non-painful electrical stimuli were given to a finger at the painful side, the 100 and 150 ms components of the evoked field were enhanced for both kind of stimuli, although for the latter the enhancement was less. The component at 100 ms was selectively enhanced to the stimuli of the painful site. Flor et al. assumed that chronic noxious stimulation would lead to an increased representation of the painful area in the somatosensory cortex. In their study nociceptive rather than neuropathic pain was studied. We used only non-painful stimuli and at a different site of stimulation. Differences in SEP in another group of low back pain patients were also reported by Knutsson et al. (1988).

Peripheral nerve injury gives rise to abnormal peripheral input and/or central processing and may persistently induce a state of central sensitization and pain (Woolf 1993). At the same time deafferentation produces neuroplastic changes in a period from days to weeks, a.o. a reorganization of cortical representations (Merzenich 1983 and 1991).

We argued that if abnormal peripheral and/or central input is an underlying cause in neuropathic pain resulting in central sensitization (Woolf 1993), we could perhaps find evidence for this over the cortex and at the same time study the effects of SCS. The Gate Control Theory (Melzack and Wall 1965; Willis 1995) has provided a theoretical basis for electrostimulation. The exact way in which SCS alleviates pain is still unknown, a segmental as well as a supraspinal neuromodulatory mechanism has been proposed (Linderoth 1994; Meyerson 1975). Our findings are in agreement with the literature that chronic pain produces changes at the cortical level, in this study in neuropathic pain patients.

The disappearance of the amplitude enhancement of the middle latency components, after SCS and the patients report to be pain free, suggests that

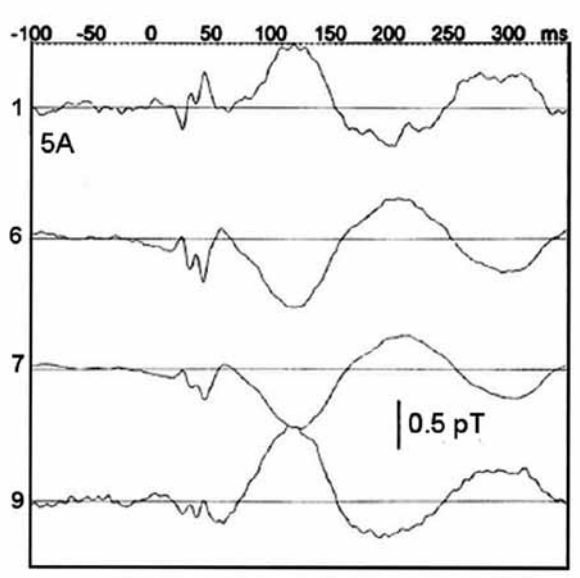

Fig. 5A

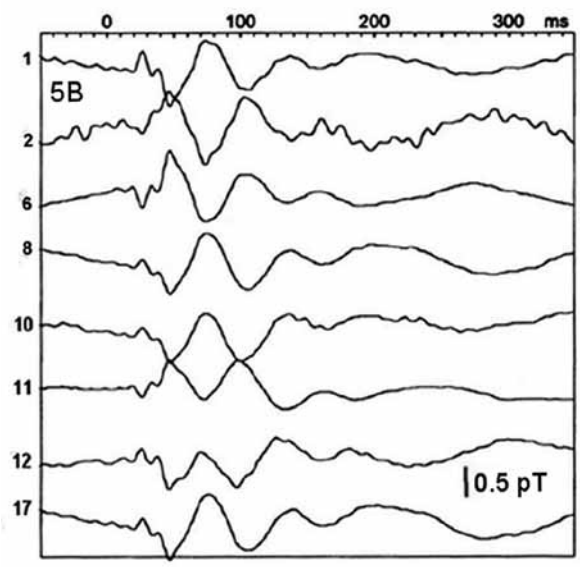

Fig. 5B

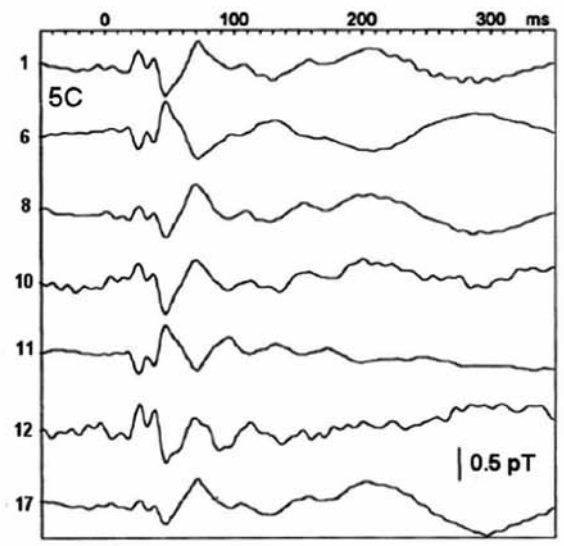

Fig. 5C

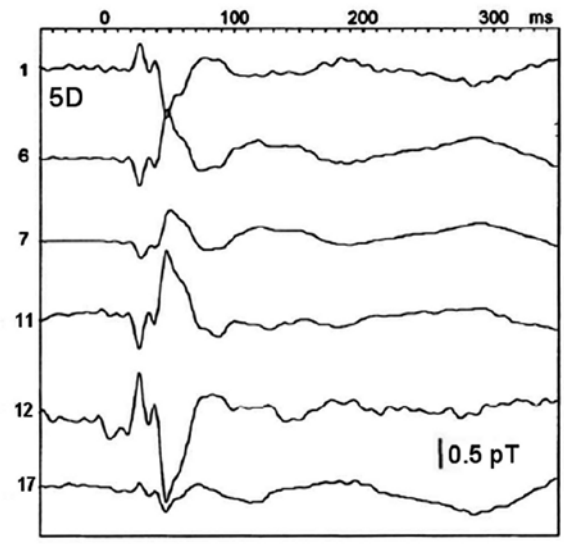

Fig. 5D

Fig. 5A-5D. Records of the magnetic field measured at the same position over the contralateral hemisphere for median nerve stimulation of the injured hand of patient B; ***5A)*** *records of SEFs measured over the contralateral hemisphere for median nerve stimulation of the healthy left hand,* ***5B)*** *before SCS when the patient was in pain,* ***5C)*** *after 15 minutes of SCS,* ***5D)*** *after 30 minutes of SCS, when the patient reported to be pain free.*

these components are related to chronic pain. In Flor's study this was shown for chronic nociceptive pain. Evoked magnetic fields and/or potentials may in time offer a way to monitor chronic pain and the effects of SCS since an objective way to study chronic pain is not so far available. This could have practical importance as it is known that the effects of SCS diminish in time (North, 1991). We summarized these findings in Fig. 5E (only channel 11), the upper trace was recorded when the patient was in pain, the second, third and fourth interval after 7, 20 and 30 minutes of stimulation, respectively.

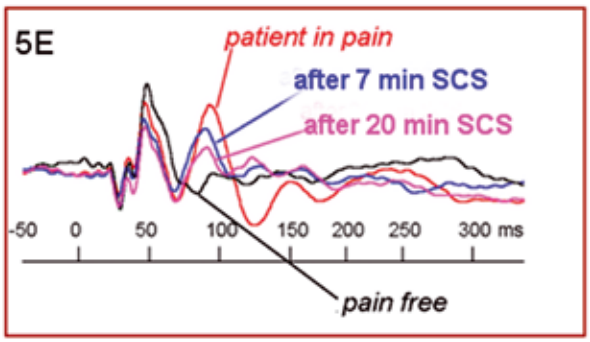

Fig 5E. Superimposed records of the magnetic field measured at different moments over the contralateral hemisphere after median nerve stimulation of the injured hand of patient B; ***a)*** *first moment when the patient was in pain without SCS (red),* ***b****) the second after 7 minutes of SCS (blue),* ***c)*** *the third after 20 minutes of SCS (purple) hardly pain but with a cold hand and* ***d)*** *the fourth after 30 minutes of SCS, and the patient in a completely pain free condition with a warm hand* ***(black)****.*

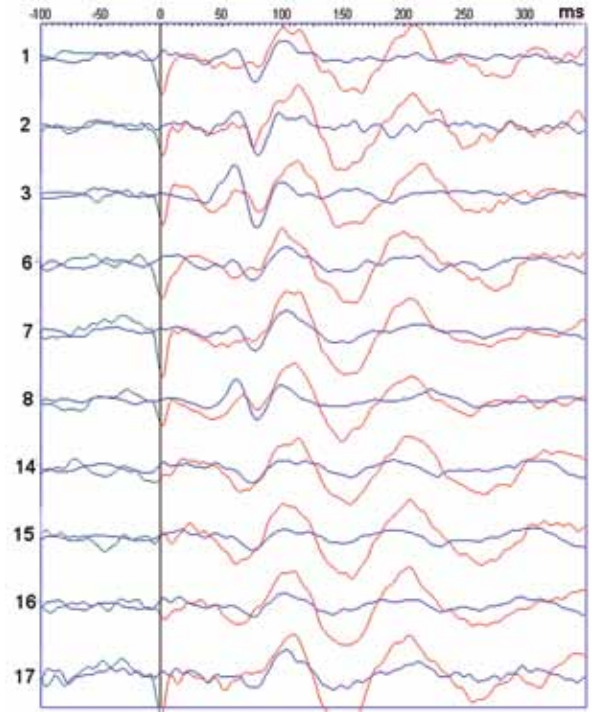

Fig. 6. Records of the magnetic field measured at eight different positions over the contralateral hemisphere for posterior tibial nerve stimulation of the injured leg of patient III: before SCS - red line, and after 30 minutes of SCS and the patient was pain free - blue line. The observation points were the same during all measurements.

ACKNOWLEDGMENTS

The authors would like express their gratitude to professor dr. F.H. Lopes da Silva for his comment and Mrs. M.A. Dekkers, MSc and Mr. E. Krooshoop for their technical support. The study was supported by Medtronic b.v., The Netherlands.

References

Brake HMJ, Flokstra J ter, Jaszczuk W, Stammis R, Ancum GK van, Martinez A and Rogalla H. The UT 19-channel DC SQUID based neuromagnetometer. Clin. Phys. and Physiol. Meas., 1990, 12B: 45-50.

Bromm B. Pain-related components in the cerebral potential. Experimental and multivariate statistical approaches. In: B. Bromm (Ed.) Pain measurements in man. Neurophysiological correlates of pain. Amsterdam: Elsevier, 1984: 257-290.

Bromm B. Consciousness, pain, and cortical activity. In: B. Bromm and J.E. Desmedt (Eds.), Pain and the Brain: From Nociception to Cognition, Advances in Pain Research and Therapy Vol. 22, Raven Press, New York, 1995: 35-59.

Dowman R. SEP topographies elicited by innocuous and noxious sural nerve stimulation. I. Identification of stable periods and individual differences, Electroenceph. Clin. Neurophysiol., 1994a, 92: 291-302.

Dowman R. SEP topographies elicited by innocuous and noxious sural nerve stimulation. II. Effects of stimulus intensity on topographic pattern and amplitude. Electroenceph. Clin. Neurophysiol., 1994b, 92: 303-315.

Dowman R, Darcey TM. SEP topographies elicited by innocuous and noxious sural nerve stimulation. III. Dipole source localization analysis. Electroenceph. Clin. Neurophysiol., 1994c, 92: 373-391.

Flor H, Braun C, Birbaumer N, Elbert T, Ross B and Hoke M. Chronic pain enhances the magnitude of the magnetic field evoked at the site of pain. In: Biomagnetism: Fundamental Research and Clinical Applications, C. Baumgartner et al. (Eds) Elsevier Science, IOS Press, 1995: 107-111.

Fujita S, Nakasoto N, Matani A, Tamura I and Yoshimoto T. Short latency somatosensory evoked field for tibial nerve stimulation: rotation of dipole pattern over the whole head. In; Biomagnetism: Fundamental Research and Clinical Applications, C. Baumgartner et al. (Eds.) Elsevier Science, IOS Press, 1995: 95-98.

Huttunen J, Kobal G, Kaukoranta E and Hari R. Cortical responses to painful CO2 stimulation of nasal mucosa; a magnetoencephalographic study in man, Electroenceph. Clin. Neurophysiol., 1986, 64: 347-349.

Hoshiyama M, Kakigi R, Koyama S, Watanabe S and Shimojo M. Activity in posterior parietal cortex following somatosensory stimulation in man: Magnetoencephalographic study using spatio-temporal source analysis, Brain Topography 1997, 10: 23-30.

IASP (International Association for the Study of Pain), Task Force on Taxonomy: Classification of Chronic Pain 1994.

Joseph J, Howland EW, Wakai R, Backonja M, Baffa O, Potenti FM and Cleeland, CS. Late pain-related magnetic fields and electric potentials evoked by intracutaneous electric finger stimulation. Electroenceph. Clin. Neurophysiol., 1991, 80: 46-52.

Kany C and Treede RD. Median and tibial nerve somatosensory evoked potentials: middle-latency components from the vicinity of the secondary somatosensory cortex in humans, Electroenceph. Clin. Neurophysiol., 1997, 104: 402-410.

Knutsson E, Skoglund CR and Natchev E. Changes in voluntary muscle strength, somatosensory transmission and skin temperature concomitant with pain relief during autotraction in patients with lumbar and sacral root lesions. Pain, 1988, 33: 173-179.

Laudahn R, Kohlhoff H and Bromm B. Magnetoencephalography in the investigation of cortical pain processing. In: B. Bromm and J.E. Desmedt (Eds.), Pain and the Brain: From Nociception to Cognition, Advances in Pain Research and Therapy Vol. 22. Raven Press, New York, 1995: 267-282.

Linderoth B. Dorsal column stimulation and pain, Ph D Thesis, Karolinska Institute, Stockholm, Sweden, 1994.

Marquardt DW. An algorithm for least-squares estimation of non-linear parameters. J. Soc. Indust. Appl. Math., 1963, 11: 431-441.

Melzack R and Wall PD. Pain mechanisms: a new theory, Science, 1965: 150: 971-979.

Merzenich MM, Kaas JH, Wall J, Nelson RJ, Sur M and Felleman D. Topographic reorganization of somatosensory cortical areas 3B and 1 in adult monkeys following restricted deafferentation. Neurosci. 1983, 8: 3-55.

Merzenich MM, Recanzone G, Jenkins WM Allard TT and Nudo RJ. Cortical Representational Plasticity. In: P. Rakic, P and W. Singer (Eds), Neurobiology of Neocortex, 2nd edition 1991: 41-67.

Meyerson BA. Dorsal column stimulation for chronic pain. Acta Neurochirugica, 1975, 31: 264-265.

North RB, Ewend MG, Lawton MT, Kidd DH and Piantadosi S. Failed back surgery syndrome: 5-year follow-up after spinal cord stimulator implantation, Neurosurgery, 1991, 28: 692-699.

Rossini PM, Nerici L, Martino G, Pasquarelli A, Peresson M, Pizella V, Tecchio F and Romani GL. Analysis of intrhemispheric asymmetries of somatosensory evoked magnetic fields to right and left median nerve stimulation. Electroenceph. clin. Neurophysiol., 1994, 91: 476-482.

Tecchio F, Pasqualetti P, Pizzella V, Romani G and Rossini PM. Morphology of somatosensory evoked fields: inter-hemispheric similarity as a parameter for physiological and pathological neural connectivity. Neurosci Lett., 2000, 287: 203-6.

Wikstrom H, Roine RO, Salonen O, Aronen HJ, Virtanen J, Ilmoniemi RJ and Huttunen J. Somatosensory evoked magnetic fields to median nerve stimulation: interhemispheric differences in a normal population, Electroenceph. clin. Neurophysiol., 1997, 104: 480-487.

Willis WD. From nociceptor to cortical activity. In: B. Bromm and J.E. Desmedt (Eds.), Pain and the Brain: From Nociception to Cognition, Advances in Pain Research and Therapy, Vol. 22. Raven Press, New York, 1995: 1-19.

Woolf CJ. The pathophysiology of peripheral pain-Abnormal peripheral input and abnormal central processing, Neurochir. Suppl. Wien, 1993, 58: 125-130.

Chapter 5

Whole head MEG analysis of cortical spatial organization from unilateral stimulation of median nerve in both hands: No complete hemispheric homology.

Peter J. Theuvenet, Bob W. van Dijk , Maria J. Peters, Jan M. van Ree,
Fernando L. Lopes da Silva and Andrew C.N. Chen. NeuroImage 2005; 28: 314-325

Abstract

We examined the contralateral hemispheric cortical activity in MEG (151 ch) after unilateral median nerve stimulation of the right and left hand in twenty healthy right-handed subjects. The goal was to establish parameters to describe cortical activity of the hemispheric responses and to study the potential ability to assess differences in volunteers and patients. We focused on the within-subject similarity and differences between evoked fields in both hands. Cortical activity was characterized by the overlay display of waveforms (CWP), number of peak stages, loci of focal maxima and minima in each stage, 3D topographic maps and exemplified equivalent current dipole characteristics. The paired-wise test was used to analyze the hemispheric differences. The waveform morphology was unique across the subjects, similar CWPs were noted in both hemispheres of the individual. The contralateral hemispheric responses showed a well defined temporal-spatial activation of six to seven stages in the 500 ms window. Consistent (in over 80% of subjects) the six stages across the subjects were M20, M30, M50, M70, M90 and M150. A M240 was present in the Left Hemisphere (LH) in 15/20 subjects and in the Right Hemisphere (RH) in 10/20. Statistics of the latencies and amplitudes of these seven stages were calculated. Our results indicated that the latency was highly consistent and exhibited no statistical mean difference for all stages. Also no mean amplitude differences between both hemispheres at each stage were found. The patterns of magnetic fields in both hemispheres were consistent in 70% of the subjects. A Laterality Index (L.I.) was used for defining the magnetic field amplitude differences between two hemispheres for each individual. Overall, the absolute amplitude of the brain responses was larger in the left than in the right hemisphere in the majority of subjects (16/20), yet a significant portion (4/20) exhibited right dominance of the N20m activity. Each individual exhibited a unique CWP, there was reliable consistency of peak latencies and mean amplitudes in median nerve MEG. Nevertheless, this study indicates the limitations of using the intact hemisphere responses to compare with those from the affected (brain) side and suggests caution in assuming full homology in the cortical organization of both hemispheres. This study provides some results to address clinical issues like which parameter describes individual differences best. Whether a genuine difference is found or whether any difference may simply represent the variability encountered in a normal population.

Introduction

In the past 30 years of magnetoencephalography (MEG) research, the hardware technology changed from a single sensor to over 300 SQUID sensors and the software from simple signal detection to complex MEG/MRI co-registration with various types of source analyses. This advance has greatly improved our appreciation of the brain organization in health and its reorganization after disease conditions (Rossini et al., 2001). MEG is reputed with special sensitivity to generators that reside in the sulcus and gyrus of the cortex, favoring a tangential orientation of the equivalent dipole representing 80% of the human brain sources (Flemming et al., 2001). It is almost independent of the electrical resistance distribution in the head and doesn't need a reference. Thus, MEG is suitable to localize brain activities in spite of its difficulty to detect both radial generators and deep sources. One major field of MEG studies is focused on somatosensory research from healthy subjects to patients afflicted with a diversity of diseases and traumas. A better understanding how cortical plasticity in brain reorganization is related to the use (e.g. training effects) or disuse (e.g. deafferentation or stroke) and practical applications of MEG for clinical diagnosis/prognosis of disease sequelae can be anticipated. In MEG source imaging of clinical applications, caution is being discussed in recent publications (Babiloni et al., 2004; Fuchs et al., 2004; Rossini and Dal Forno, 2004). Particularly, the use of MEG in tracing the source (Wheless et al., 2004) is drawing a significant debate (Barkley and Baumgartner, 2003; Barkley, 2004; Baumgartner, 2004; Lesser, 2004; Parra et al., 2004).

The first MEG report on somatosensory evoked fields, SEFs (Baumgärtner et al.,1991), demonstrated the anterior-parietal pattern of N20m-P20m and the reversal of the P30m-N30m in the contralateral hemisphere in response to median nerve stimulation in one hand. Rossini et al. (1994) compared the hemispheric differences of the evoked fields to unilateral hand stimulation of both hands and the homology implications were reported in a study on phantom limb pain (Karl et al., 2001; Schaefer et al., 2002). Rossini et al. (1994) focused on the location and strength of the equivalent sources activated in the primary somatosensory cortex (<50 ms) contralateral to the stimulated nerve. The Equivalent Current Dipole (ECD) model was used with the main aim of making a quantitative comparison between the responses of the two hemispheres. The spatial coordinates of the equivalent sources did not differ statistically significantly in the two hemispheres, but the strengths (in nAm) of the equivalent sources were significantly higher in the left hemisphere. This contralateral effect was confirmed in a small group of subjects (Soros et al.,1999).

A "normative" data set was established in another Italian sample (Tecchio et al.,1998 and 2000) using the interhemispheric correlation coefficient as a parameter to study physiological and pathological neural connectivity. It was noted that consistency of SEFs across a hemisphere within a subject is far greater than among subjects. In the wave morphology, the similarity across the hemisphere is well defined as an individual signature between subjects. Wikström et al. (1997) studied the primary sensorimotor (SM1) and secondary somatosensory (SII) activation. The conclusion was that at the individual level the median nerve SEFs from the contralateral primary sensorimotor cortex (SMI) could be used to detect abnormally large interhemispheric asymmetries. The window of analysis has extended beyond the early stages to mid-latency somatosensory activation, from <50 ms to >100 ms. Kakigi et al. (1994) demonstrated that the deflections,

N90m-P90m, were generated in the contralateral second sensory cortex (SII), a small N90m-P90m was identified in the hemisphere ipsilateral to the stimulation site. It is emphasized that the lack of responses in the sensory association cortices (parietal areas) may be due to radial oriented dipoles. The majority of the studies use Equivalent Current Dipole (ECD) modeling to examine the sources of M20 and M30 in the SEFs. It is important to note that various assumptions are inherently imbedded in different methods of dipole analysis. For example, the N20m-P20m and P30m-N30m have often been explored with a single moving dipole model as a generator residing at the posterior bank of 3b for M20 (Kanno et al., 2003). In contrast, the generator of the M30 remains undetermined in case it is modeled by a single generator (Hari et al.,1993; Kakigi et al.,1994; Wikström et al.,1996; Hoshiyama and Kakigi, 2001), however the measurements can be explained by assuming two generators (Kawamura et al.,1996) in the SI-MI area. When dealing with mid-latency and late stages of SEP/SEF, the spatio-temporal dynamics become even more complicated than at short latency stages. We question whether source localization and related parameters are the only way for the study of pathological conditions. In this study therefore we examined the normal state of cortical activities (evoked magnetic fields) in both hemispheres in response to standard median nerve stimulation in a window of 450 ms. We aimed at identifying the major parameters that practically could be used in a descriptive and analytical way for future clinical studies of neurological dysfunction and disease in patients. These studied parameters are important and based on the quantified hemispherical differences of the measured data. The parameters of the study deemed to be compact and easy to use in a clinical context. Finally we aimed at comparing the differential effects between the right and left hemisphere (RH and LH) in response to contralateral hand stimulation under identical stimulation conditions.

Materials and Methods

Subjects and Median Nerve Stimulation

Twenty volunteers (14 males and 6 females, age range 32-45 years, all right handed) were recruited from the hospital staff, adequately informed and gave their consent. The Medical Ethical Committee of the Free University Hospital approved of this study. All subjects were healthy without neurological dysfunction. Handedness was established both using lists from the VU Medical Center which included arm and leg performance, secondary the Edinburgh Inventory which produced a lowest value of 0,8 (7/20 subjects). Median nerve stimulation was performed at the wrist with a bipolar electrode, the cathode proximal (IFCN Guideline: Nuwer et al, 1994). Electrical stimulation was used since it is a very precise and common way of stimulation and it can induce the early components. To stimulate the median nerve in a standard way we employed an electrical stimulator (Grass, USA; model S48) using a photoelectric stimulus isolation unit (Grass, USA; model SIU7). The stimulation current was pulsed, at a repetition rate of 2 Hz and with a pulse duration of 0.2 ms. All subjects were studied in one session, lasting about 45 minutes. Stimulation was in counter-balanced order between right and left hand across the subjects. Between stimulation of both hands, a resting period of 5-10 minutes was ensured. Stimulus intensity was tailored to the individual twitching level of each separate hand and reached a 1.5 x motor twitching level. The twitch threshold varied with the subject, was well tolerated and painless. Typical values were 6,1 - 7,7 mA (± 1,1 mA). Five hundred events were recorded from the wrist surface of the median nerve in each hand.

MEG Recordings

MEG measurement data were recorded using a 151-channel whole-head VSM gradiometer system (VSM MedTech Ltd., Canada) in a 3-layer magnetically shielded room (Vacuum Schmeltze GmbH, Germany). The layout of the recording montage and coordinate system is illustrated in Fig.1.

The x, y and z coordinate system is based upon the nasion, left and right ear, the location where the coils are positioned that are used to determine the distance between the head and the measurement system. Using the positions of these fiducials a head centered coordinate frame is defined. The positions of all MEG sensors in head coordinates are thus known. Using the coordinates of the sensors in multiple recording sessions, corresponding to multiple head positions, we determined the best recording position, as the position in which the smallest rotation and translations were necessary to align all data sets. For the recordings per subject the positional variations were quite small; the mean rotation angle amplitude was 3.8 degrees, the mean translation distance was 0.4 cm. For the recordings of the entire group the variations were larger, the mean rotation angle amplitude was 5.6 degrees, the mean translation distance was 0.8 cm. The average subjects head was positioned 0.02 cm left from the centre of the helmet. Recordings were performed in synthetic 3rd-order gradient mode, using the manufacturers real-time software (Vrba, 1996). All subjects were in a comfortable supine position with the head well positioned in the helmet without much space left to move which might alter the position. The MEG signals were sampled at 1250 Hz, triggered on the synchronization pulse of the electric stimulator. The peri-stimulus interval was 50 ms pre-trigger and 450 ms post-trigger. On-line filters were set at DC for high-pass and at 400 Hz (4th order Butterworth) for anti-aliasing low-pass. No on-line or off-line high pass filters were used that might influence the outcome of the data, only a correction for DC based on the pre-stimulus interval of 50 ms. The system has a baseline of 5 cm. Off-line the MEG data were screened for artifacts, averaged and DC-corrected using the pre-trigger interval to determine the recording offset. Also +/- averages were calculated to obtain noise-level estimates. The estimated distance between two neighboring sensors in the area of our interest is 2,67 cm.

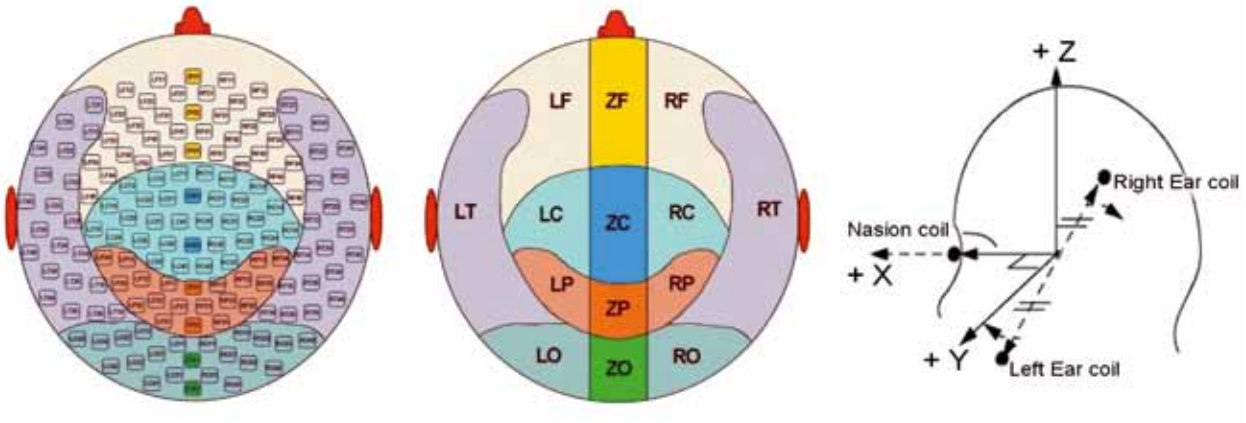

Fig. 1A-C. In the left panel (1A) montage of the 151 sensors is displayed and in the middle panel (1B) the spatial relations. In the right panel (1C) the x, y and z coordinate system of the VSM – MEG. Left (L) and Right (R) are the hemispherical sides, Z is for the midline, F (frontal), C (central), T (temporal), P (parietal) and O (occipital) depict the sensor groups related to different cortical areas. With permission: VSM MedTech Ltd. (Canada).

MRI Recordings

Of all 20 subjects a MRI was made with a 3D-1.5T (Siemens Sonata) MRI using the same measuring protocol in two hospitals. The protocol was as follows: slice orientation was sagittal, thickness 2mm, TR11.8ms, nr. of echoes 1, TE 5ms, flip angle 30 degrees, nr of signals averaged 2, scan matrix 256 and reduction matrix 256. The results presented in Table 3 are based upon twenty individual MRI's.

Compressed Waveform Profile (CWP)

When the responses of all sensors are superimposed, a butterfly-like overlay plot is produced. We termed this whole head overlay plot the compressed waveform profile (CWP) from which the peak activation stages were isolated. It is conventional to define the somatosensory activities in the time domain into three different phases, an early (<50ms), mid-latency (50-90ms), and late (90-400ms) phase, each containing peak stages. The compressed waveform profile can effectively provide characteristics of the brain dynamics of the sensory, motor and perceptual brain regions. Moreover, it can exhibit individual patterns for the different subjects.

Focal Extrema

At each peak stage, the extrema reflect the sites of magnetic efflux and influx, respectively. From the topographic SEF pattern, the magnetic gradients and the locus of underlying current dipole can be deduced. The amplitudes of the focal extrema were used for statistical analyses.

Laterality Index (L.I.)

A conventional index of the differences and the level of lateralization between the left hemisphere (LH) and right hemisphere (RH) responses is computed as the Laterality Index, L.I. (Jung et al., 2003) according to the formula:

$$L.I. = (LH-RH) / (LH+RH)$$

where (LH – RH) in this study is the difference in amplitudes between the LH and the RH response at the focal extrema (efflux and influx) expressed in femtotesla, fT (see also Fig.5). This means that in each hemisphere at a given peak latency two values are computed , the efflux (red) having a positive value and the influx (blue) as a negative one. All N20 (blue bars) depict the indices of the LH and RH based upon the influxes, all P20 (red bars) represent the effluxes. We focused on two latencies, 20 and 30 ms, since these two early peak latencies are well studied. When both hemispheres are equal in SEF magnitude of a subject, the L.I. on the y-axis should be zero. Thus, a positive L.I. indicates a higher magnitude in left (dominant) hemisphere than in the right one. If the L.I. is negative (down), there is less activation in LH than in the (dominant) RH.

Equivalent Current Dipole and Dipole Parameters

VSM (CTF) software was used to obtain the equivalent current dipoles (ECD) describing the MEG data collected with the VSM-whole-cortex MEG/EEG System (151 sensors) and based upon the coordinate system depicted in Fig. 1C. The head was approximated with a spherical volume conductor for source analysis of MEG data. A conventional single equivalent current (moving) dipole analysis (e.g. Lin et al., 2003; Fuchs et al., 2004) was used in this study for data evaluation. MEG data were co-registered with MR images using fiducial coils and vit. E markers. The head model was chosen to match the inner contour of the skull. This matching was done by eye. Epochs in the post stimulus 450ms time window, with clear SEF deflections (as judged by comparison of average and plus minus average signal

amplitudes), were visually identified to select the cortical areas of interest for further analysis. At each of the peak stages the dipole characteristics were determined, data are only presented of the M20 and M30.

Data management and statistical analysis

First stage data-analysis was done during measurements using the VSM software (release v4.16). The analysis window was 50 ms before and 450 ms after the stimulation. Each subject was asked to relax, to ignore the stimuli as much as possible, to keep the eyes open and refrain from blinking during the recording. A small number (max 50) of events containing too much disturbances due to movement or blinking was rejected for each dataset manually. All further data-analysis and presentation was performed employing software from ASA (Advanced Source Analysis, ANT A/S, The Netherlands) for graphical display.

Only the contralateral activity was analyzed in this study for comparison of the hemispheric activation in response to both right and left hand stimulation. In the first step, we created the compressed waveform profile (CWP) of all 151 channels of SEFs in each subject and identified the (peak) stages. In our study we employed the following parameters: the latency and the number of the (peak) stages, site of activity (x, y and z), focal activity (magnitude) and the patterns of activation

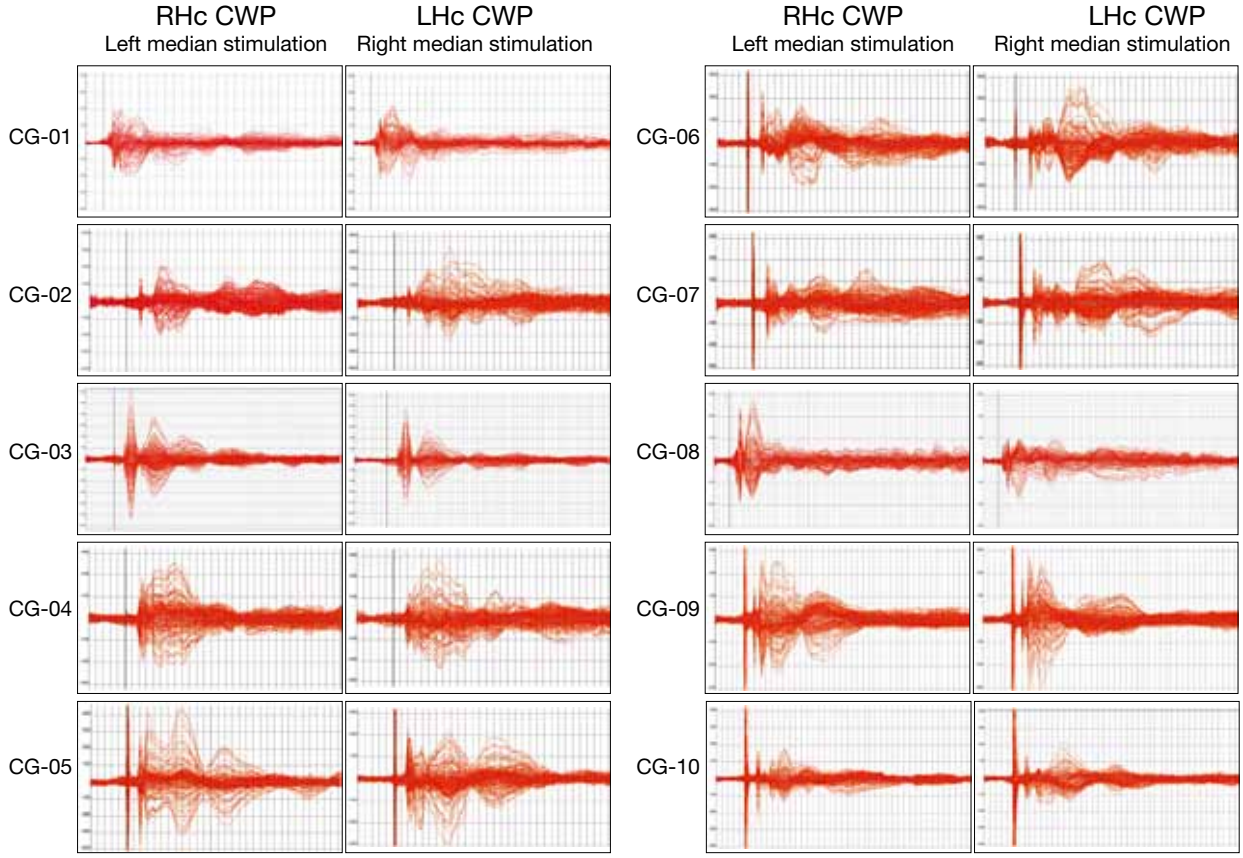

Fig. 2. Compressed Waveform Profiles (CWP), the superimposed channel waves for the 151 sensors in 20 normal healthy subjects. The magnetic field strength (amplitude in fT) is vertical and the time window (0 - 350 msec) is horizontal. Most CWPs have an amplitude range from –350 to 350 fT, where necessary another scale was used, i.e. CG-05 where the range was from –50 to 500 fT. CG-01 and CG-08 are based upon a time window of 1sec during measurements and produced a different horizontal scaling.

(3D – topographic maps). In order to compare the two hemispheres we derived the following parameters: latency differences, laterality indices and the coefficient of variation (cv), an index of measurement consistency. All these parameters could be extracted without retort to dipole analyses. We finally studied overlay plots and grand averages of all subjects and established the dipole localizations of the M20 and M30 peak stages in relation to an individual MRI. A series of statistical analysis was conducted to compare these parameters in the hemispheres from right vs. left hand stimulation of the median nerve. Pair-t test was employed to evaluate the studied effects, with alpha of 0.05 adopted as significant.

Results

Compressed Waveform Profile (CWP) in SEFs
Fig.2 depicts the morphology of the CWPs between the right (RHc) and left hemispherical (LHc) cortex in response to contralateral median nerve stimulation and contrast of CWPs in each hemisphere among twenty subjects.

The left panel (RHc) displays the contralateral activation in response to left median nerve stimulation while the right panel shows the contralateral hemispherical (LHc) activation to right median nerve stimulation. The maximum amplitude (vertically presented) was between 300 - 400 fT and the time window presented was restricted in all CWPs to 350 ms (horizontal axis). CG is the code for the volunteers, the results of 10 are depicted. Inspection of Fig. 2 demonstrates large inter-subjects variability in CWPs, a relatively high intra-individual consistency of the two CWPs however in response to contralateral activation of both hands. It is noted that each subject revealed his/her unique signature. In all subjects both sharp early peaks can be distinguished as stages of high activity at later latencies, which extended over many milliseconds (i.e. CG01 and CG04).
In our subjects up to 6 - 7 stages could be identified (see Table I). The initial one was a M20 and M30 stage in all subjects, followed by the M50 stage in the left (18/20 subjects) and right (17/20subjects) hemisphere. The largest energy is found in the mid-latency M70 (all 20 subjects) and at the later stage M90 (both sides 18/20 subjects). The first two peaks (M20 / M30) are quite sharp but the fourth peak (around 70 ms, see Table 2), apart from its high amplitude, may extend over 50 - 80 ms in duration, see Fig. 2 subject CG-04. At 150M another peak can be identified (left 18/20 and right 20/20 subjects) as a 240M (left 15/20 and right 10/20, respectively). Identification of the peaks at these stages was not only based upon the morphology alone but also upon maximum Root Mean Square (RMS) values. The RMS value is calculated over a data range that is selected from the overlay traces (CWPs) of all artifact free channels that are displayed and is an indication of power. We can identify appreciable differences in both morphology and (peak) stages between RH and LH in each subject. Thus, for detailed analysis of brain measures it is more accurate to examine the individual profile than to describe the averaged event related SEF as is often reported in the literature. Statistical analysis indicates no difference in the number of stages between the two stimulated hands (Table 1). However, when comparing the two hemisphere peak activations, some values (in bold-italics) were not homologous though there was a large agreement.

Median Left hemisphere (LHc)						
20ms	30ms	40ms	70ms	90ms	150ms	240ms
20/20	**20/20**	18/20	**20/20**	18/20	18/20	15/20

Median Right hemisphere (RHc)						
20ms	30ms	40ms	70ms	90ms	150ms	240ms
20/20	**20/20**	17/20	**20/20**	18/20	20/20	10/20

Table 1. Peak activation stages observed for all 20 subjects in both hemispheres. At different latencies different number of (peak) stages were found.

Overlay Plot vs. Grand Averaged compressed waveform profiles

To appreciate the similarity and differences of the CWPs across the subjects, an overlay display was created which can be compared to the CWP of the grand average of the group. Fig. 3 illustrates the differences in CWP between two displays showing larger and more differentiated signals in the overlay plot than in the grand average.

3D Topography of Somatosensory Evoked Fields

At three peak latencies, 20, 30 and 70 ms the 3D topography of SEF's is displayed to illuminate the spatio-temporal dynamics of the cortical evoked magnetic field. These cortical dynamics are shown in Fig. 4 for a typical subject (CG-09).

In the upper part of Fig. 4 (CH), the evoked fields on the contra-lateral cortex after median nerve stimulation are shown. A clear dipolar configuration is found at these three latencies, the polarities in the RHc and LHc are in general opposite. The well known polarity reversal between 20 and 30 ms is clearly seen, as is the stability of the polarity and magnetic field localization until 90 ms (also see Fig.5). In the lower part of Fig. 4, in

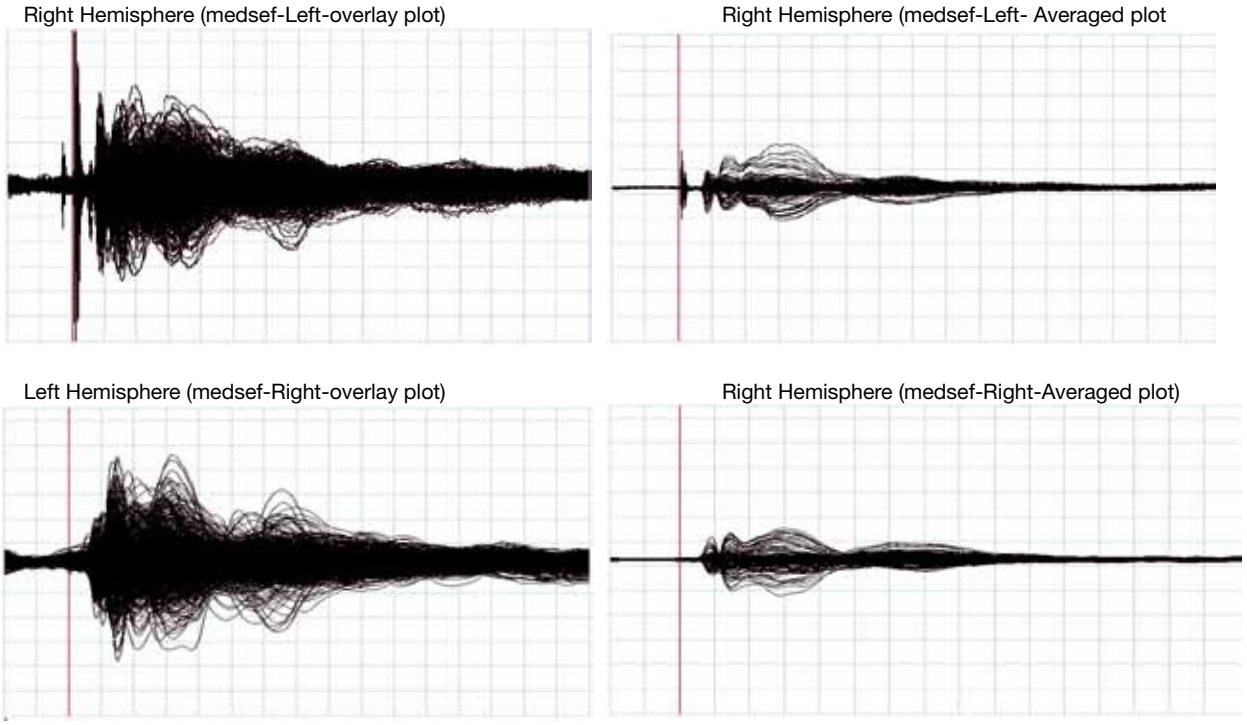

Fig. 3. The left part of the figure presents the overlay plot of the CWPs of 20 healthy volunteers after left and right electrical median nerve stimulation. The right part depicts the averaged CWPs of the same group. The enclosed scales: 100 ft in magnitude bar, 250 ms in time bar.

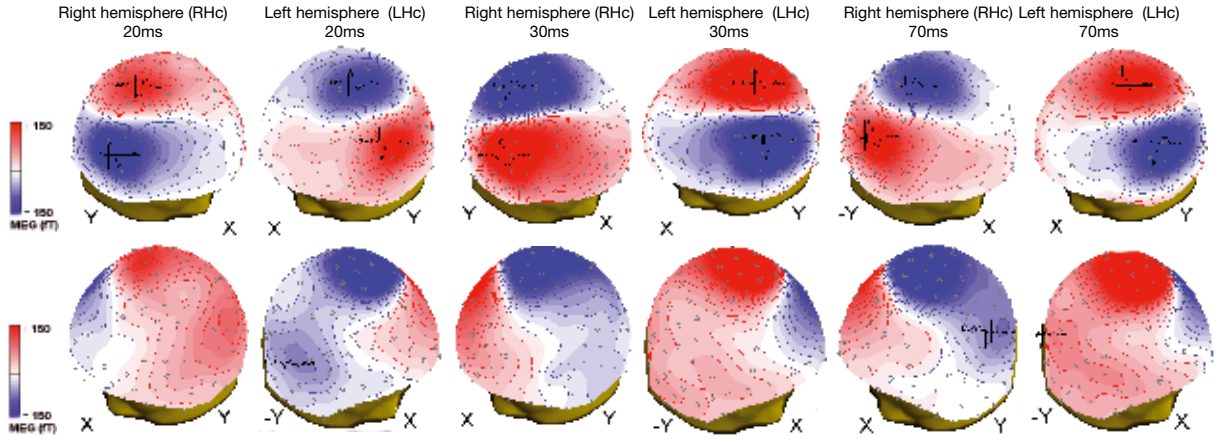

Fig. 4. Comparison of the patterns observed in the contra-lateral (C.H.) and the ipsilateral hemisphere (I.H.) in response to a left and right median nerve stimulation, in one single subject at the 20 ms, 30 ms, and 70 ms.

the ipsi-lateral hemisphere (IH), cortical activity is shown at the same latencies. Cortical responses on the ipsi-lateral side display activity that is not simply dipolar. These responses are initially more temporo-parietal but from 30 ms on more frontally localized. To appreciate the full range of brain activity the results of one subject are presented in detail. In Fig. 5 the isofield contour maps of a typical volunteer (CG-09) are depicted at different latencies. The field distribution shows a dipolar configuration from the fast first peak at 20 ms until 250 ms. This is true for both hemispheres at comparable peak maxima at around 20, 30, 50, 70, 90, 150 and 240 ms.

Across the time window of 0-350 ms, 7 sequential activations are observed as a bipolar pair at 20, 30, 50, 70, 90, 150 and 240 ms. Between 20 and 30 ms the evoked field polarity begins to invert and this is seen in both hemispheres. This first polarity reversal is seen in 17/20 subjects. In 3/20 subjects however two early peak latencies are seen in the period of 20-24 ms. In these three subjects the polarity reversal was observed already between these to early peaks. In two subjects the reversal occurred later, between 40 and 52 ms, in one subject in both hemispheres, in two subjects only in the LH or RH. In the LHc

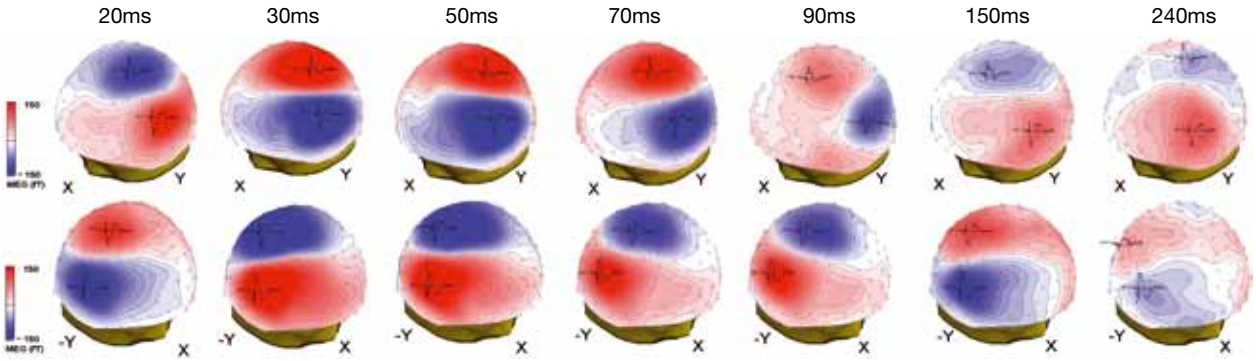

Fig. 5. The hemispheric spatial pattern of the evoked fields to median nerve stimulation for the contralateral left hemisphere (LHc) to the right hand stimulation and the contralateral right hemisphere (RHc) to the left hand stimulation in a single representative subject (HCG-09). In the top bar the different latencies are depicted, from M20 to M240. Efflux is depicted in red, influx in blue. Polarity reversal is both observed between 20/30 ms and 90/150 ms. A new observation of polarity reversal of the evoked field at 90/150 ms is also shown in both hemispheres.

Latencies (ms)	M20	M30	M50	M70	M90	M150	M240
Stages	**1**	**2**	**3**	**4**	**5**	**6**	**7**
Right Hemisphere (mean)	20,9	32,8	44,2	68,6	92,0	148,5	252,5
(Standard deviation - Std)	1.8	2,4	4,9	6,4	9,0	18,3	30,5
c.v. (mean/Std)	*0,08*	*0,07*	*0,11*	*0,09*	*0,09*	*0,10*	*0,12*
LH (mean)	21,0	32,1	48,4	73,3	93,2	150,8	235,5
(Std)	1,9	2,3	4,3	5,4	8,6	22,1	15,9
c.v.	*0,09*	*0,07*	*0,08*	*0,07*	*0,09*	*0,12*	*0,06*
Latency Diff. (absolute)	*0,1*	*0,7*	*4,2*	***4,7***	*1,2*	*2,3*	***17,0***

Efflux in MEF (fT)							
Stages	**1**	**2**	**3**	**4**	**5**	**6**	**7**
RH (mean)	140,0	198,0	154,7	214,9	169.5	116,4	68,1
(Std)	87,5	105,3	84,3	82,8	56,2	50,6	19,5
c.v.	*0,62*	*0,53*	*0,54*	*0,38*	*0,33*	*0,43*	*0.3*
LH (mean)	174.6	210,8	166,8	220,8	168,5	122,5	68,8
(Std)	81.8	120,3	101,0	92,3	100,3	60,9	42,4
c.v.	*0.50*	*0,57*	*0,60*	*0,41*	*0,59*	*0,49*	*0.6*
Ratio RH/LH	0.8	0,93	0,92	0,97	1,0	0,95	1.0
Amplitude Diff.	***34.6***	***12,8***	***12,1***	5,9	1,0	6,1	0,7

Influx in MEF (fT)							
Stages	**1**	**2**	**3**	**4**	**5**	**6**	**7**
RH (mean)	-168,9	-204,4	-150,4	190,6	-151.5	-112,6	-62,9
(Std)	69,1	122,6	91,5	77,3	66.7	55,1	31,0
c.v.	*-0,40*	*-0.6*	*0.6*	*0,40*	*0.4*	*0.5*	*0.5*
LH (mean)	-173.7	-206,9	-155,7	-200,7	-176,3	-107,3	-67,4
(Std)	99.0	107,6	92,6	67,7	76,5	74,6	24,8
c.v.	*0.6*	*0.5*	*0,59*	*0,33*	*0,43*	*0,69*	*0.4*
Ratio RH/LH	1.0	1.0	0,96	0.9	0.9	1,04	0.9
Amplitude Diff.	4.8	2,5	5,3	***10,1***	***24,8***	5,3	4,5

Table 2. Parameter values of the hemispheric responses to the uni-lateral median nerve stimulation (the italic bold values are the major differences between the two hemispheres). c.v = coefficient of variation.

the evoked field remains stable up to around 90 ms where the amplitude decreases and at around 150 ms the field is inverted again and a second polarity reversal is observed, again cortical activity is dipolar but not as clear. In the RHc similar evolution can be seen. The corresponding SEF waveforms at each maximum and minimum site are illustrated in Fig. 5. The second polarity reversal is seen in 17/20 subjects, in 2 subjects no reversal at all is seen and in 1 subject only over the left hemisphere.

SEF maxima and minima, Peak Latencies and Amplitudes

Table 2 provides an overview of the 7 peaks; their averaged latencies, the standard deviations

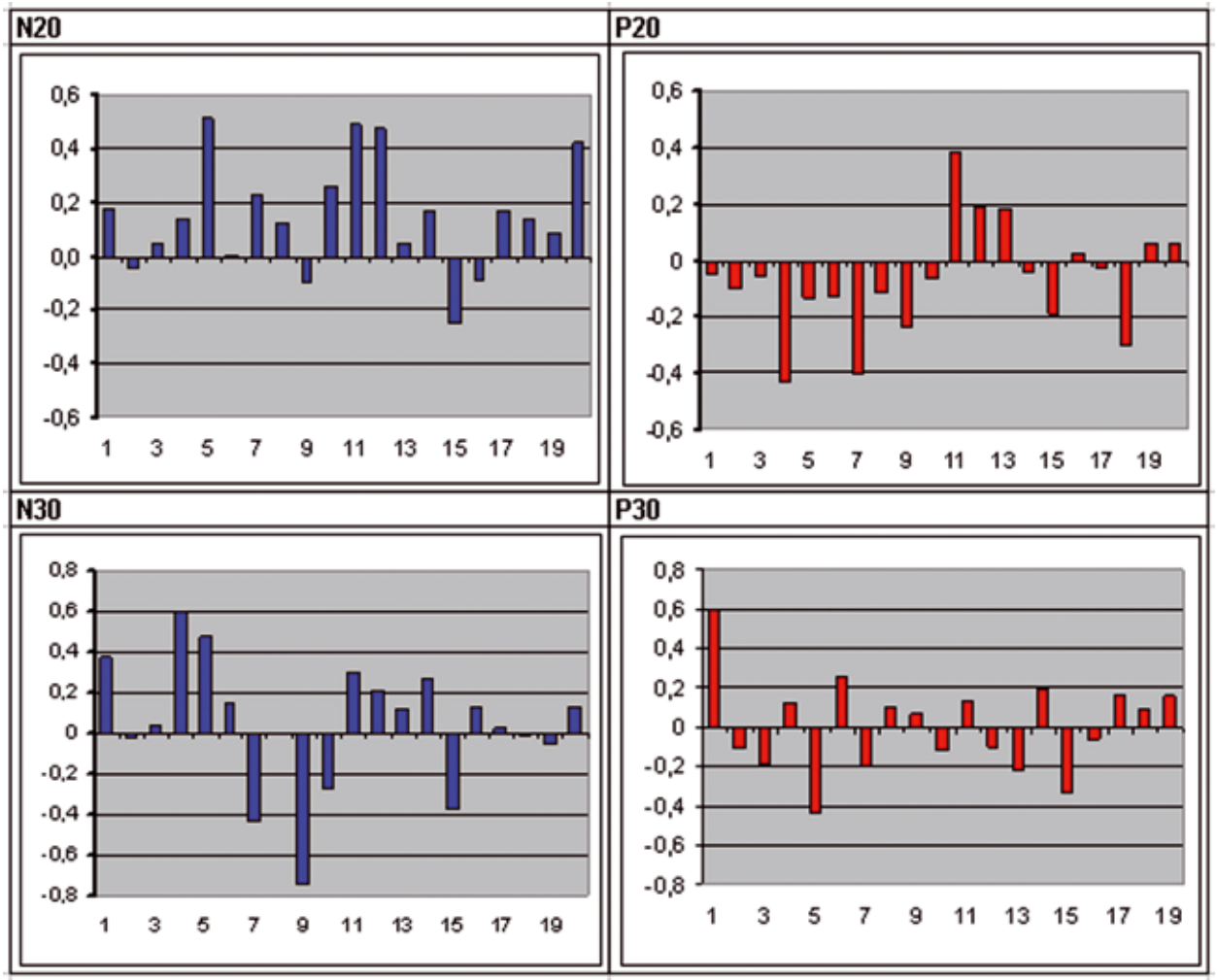

Fig. 6. This figure demonstrates the distribution of the laterality index of 20 healthy subjects. Laterality Index of the Early Cortical Activation is defined as the (L.I. =<LH-RH>/<LH+RH>) at the early M20 and M30 peak stages. Scales: amplitudes in fT in the vertical magnitude bar, numbers in horizontal bar.

over both hemispheres, the absolute latency and amplitude differences. From these data it follows that there are no statistically discernible differences between the two hemispheres. The dispersion of variability across subjects is noticeable (c.v), especially in the later stages. Large interhemispheric variations within each activation stage are found. These values (in bold-italic) in Table 2 clearly illustrate substantial differences between two hemispheres at the latencies of M70 (mean of 4.7 ms) and M240 (mean of 17.0 ms), as well as differences larger than 10 fT in some amplitudes.

However in the left hemisphere the values of the positive amplitudes are shown in the majority of subjects. These results clearly indicated there was no complete hemispheric homology in brain activation magnitudes, even though the mean values in each stage were consistently larger compared with those in the right hemisphere.

Laterality Index of hemispheric activities

The Laterality Index (L.I.), i.e. (LH-RH)/(LH+RH), is used to express the proportion of the “left-

					Position (cm)		Orientation in degrees		Strenght
Peak	**Nerve**	**N = 20**		**X**	**Y**	**Z**	**Declination**	**Azimuth**	**nAm**
20ms	L. Med.	20 / 20	mean	0,83	-3,56	8,7	76,7	19,9	23,19
			sd	0,93	1,71	0,6	13,8	12	8,29
			cv (sd/mean)	1,12	0,47	0,06	0,17	0,6	0,35
			95% c.i.	-7,9 to 9,49	-18,7 to 11,5	3,37 to 14,3	46,1 to 199,5	-86,7 to 126,5	-50,6 to 97
	R. Med.	20 / 20	mean	0,4	4,3	8,6	78,2	307,6	26,5
			sd	0,76	0,39	0,7	9,2	109,2	11,1
			cv	2	0,09	0,1	0,11	0,35	0,41
			95% c.i.	-6,3 to 7,1	0,84 to 7,76	2,37 to 14,83	-92,7 to 249,1	-665,1 to 1280,3	-72,2 to 125,2

				X	**Y**	**Z**	**Declination**	**Azimuth**	**nAm**
30ms	L. Med.	20 / 20	mean	0,8	-3,5	9,1	106,2	210,4	30,3
			sd	0,87	2,06	0,7	10,3	72,8	18,3
			cv	1,12	0,6	0,1	0,09	2,89	0,6
			95% c.i.	-6,96 to 8,54	-21,84 to 14,84	2,87 to 15,33	14,5 to 197,9	-438,1 to 858,9	-132,5 to 197,7
	R. Med.	20 / 20	mean	0,6	3,5	9,0	101,6	169,6	29,5
			sd	0,98	1,98	0,9	14,82	72,18	14,03
			cv	1,6	0,57	0,1	0,14	0,42	0,47
			95% c.i.	-7,15 to 8,35	-14,3 to 21,3	0,99 to 17,01	-30,3 to 232,7	-473,4 to 812,6	-95,1 to 154,1

Table 3. The dipole parameters in the right and left hemispheres in response to unilateral median nerve stimulation at M20 and M30. Position (x, y and z axis – see Table 1C), orientation (declination and azimuth) and strength (nanoAmperemeter - nAm).

Scalp MEF		**M20**	**M30**	**M50**	**M70**	**M90**	**M150**	**M240**
Efflux	***r***	0.057	0.057	0.595	0.291	0.162	0.463	0.421
	p	0.009	0.009	0.015	n.s.	n.s.	0.05	n.s.
Influx	***r***	0.057	0.675	0.695	0.367	0.088	0.566	0.543
	p	0.009	0.001	0.003	n.s.	n.s.	0.014	n.s.
Dipole Moment	***r***	0.27	0.308	0.673	0.635	0.126	0.248	0.036
	p	n.s.	n.s.	0.004	0.006	n.s.	n.s.	n.s.

Table 4A. Correlations of field focal amplitudes and dipole moments between two hemispheres. At the early stages (M20 and M30), the SEFs between LHc (contralateral left hemisphere) and RHc (contralateral right hemisphere) were significantly correlated for both magnetic efflux and influx in MEG (r for Pearson correlation, p for p-value; significant values of p<0.05 are painted in shadows, n.s. for not significant)

Efflux/ Moment		M20	M30	M50	M70	M90	M150	M240
LH	***r***	0.697	0.707	0.772	0.617	0.605	0.286	0.313
	p	0.001	0.0005	0.001	0.008	0.01	n.s.	n.s.
RH	***r***	0.629	0.778	0.621	0.755	0.564	0.288	0.099
	p	0.003	0.0001	0.005	0.0001	0.015	n.s.	n.s.
Influx/ Moment								
LH	***r***	-0.622	0.707	-0.881	-0.818	-0.534	0.289	0.092
	p	0.003	0.0005	0.0001	0.0001	0.027	n.s.	n.s.
RH	***r***	-0.727	0.446	-0.777	-0.582	-0.472	0.312	0.14
	p	0.0003	0.048	0.0001	0.007	0.048	n.s.	n.s.

Table 4B. Correlations between SEFs and dipole moments within Right Hemisphere or Left Hemisphere

hemispheric dominance" and is only based on the amplitudes of the focal maxima and minima. Fig. 6 clearly demonstrates a majority of subjects having left-hemispheric dominance based upon amplitude although some subjects, i.e. 4/20 in N20 and 5/20 in N30, have a right-hemispheric dominance. The N20 and P20 showed distinctive patterns. The L.I. of N20 and N30 in the group are not the same, though both exhibited left hemisphere dominance (positive L.I.). In some subjects a 50 % higher amplitude in one hemisphere was found over the other. Such results would be considered "pathological" (Jung et al., 2003). These results clearly indicate there is no complete hemispheric homology in brain activation magnitudes even in our healthy subjects.

Dipole parameters and hemispheric differences

Table 3 lists the mean of the parameters of the equivalent dipoles at the time instants of M20 and M30 of all 20 subjects using a single moving dipole model. The Confidence Intervals (C.I) for all parameters are listed. The 95% C.I. is defined as

$$CI = \text{mean} \pm 1{,}96 \times SE$$

and the Standard Error (S.E.) as $SE = SD/\sqrt{n}$, n is the number of subjects in the group and SD is the Standard Deviation. Few of these parameters showed significant difference of means between the left and right hemisphere to contralateral median nerve stimulation. Though no group difference was shown statistically, there remained an appreciable absolute difference between two hemispheres within each subject when the values are examined on their individual basis (shown in Table 3).

Correlations of field magnitudes and dipole moments between two hemispheres

At the early phase (M20-M50), the SEF influx and efflux were significantly correlated between two hemispheres, but not at the middle phase (M70, M90). At the late stage, only the activities at M150 of both hemispheres were correlated (see Table 4A). No correlation of the dipole moments (see Table 4B) was found between the two hemispheres in the very early stages, M20 and M30.

Correlations of field magnitudes and dipole moments within each hemisphere

Even more revealing was the consistent high correlations (r= .45-.88 and p< 0,001) between the extracranial magnetic fields and the intracranial dipole moments. For both hemispheres, in the early stages, at 20M and 30M.

Discussion

The main focus of our study was on the intra-subject difference between the two hemispheres of each subject regarding the MEG responses to unilateral median nerve stimulation. The objective of our study was not primarily to explain differences between the evoked fields in the two hemispheres, but to identify parameters that can be used to describe the observed differences. From the results it follows that none of the chosen parameters was in itself sufficient to describe all differences and that probably a combination is necessary in case pathologies are studied. We questioned whether there was complete hemispheric homology in activation stages, patterns, and strength of the two hemispheric responses given the unilateral stimulation on the median nerve of both hands. To that purpose we examined the similarities and differences of the contralateral cortical responses after left and right hand median nerve stimulation in healthy volunteers. Only under the assumption of absolute hemispheric homology, it would be possible to apply the recorded activities from one intact site to infer the affected side of the brain in patients. To this end, the results of this study would contribute to elaborate a normative parameter set to be applied in clinical practice

The number of peak stages

Although the SEF to median nerve stimulation has been studied over a decade, there is no generally accepted nomenclature yet for the description of the compressed waveform profile. From the literature it followed that experimental settings were different with respect to the number of MEG sensors (4-306), pulse duration (0,2-0,3 ms), stimulus frequency (2,0-2,7 Hz) interstimulus interval (150-1200 ms), sampling rate (125-4096 Hz), number of trials (100-300), the time window (100-700 ms) and the offline processing of the data (filter settings) including differences in software used to process the data. Changes in the evoked fields were shown for example to be dependent on the interstimulus interval (Wikström et al., 1996). Another source of confusion can be the orientation of the used coordinate system. Tecchio et al.(1998) used x, y and z axes that differ from the ones used in the VSM or ASA software. In the latter software programs the x-axis is through the nose and the y-axis from the left to right ear. In Tecchio's experiments the x-axis runs through the ears and the y is through the nose), their x - axis is therefore 90 degrees rotated clockwise.

Furthermore not all authors described the parameters consistently. Kakigi et al.(2000) described in a time window of 160 ms, 6 peak activations after median nerve stimulation. Hari et al.(1993) described in a time window of 325 ms, 3 peak activations including SII. Tecchio et al.(1997) studied mainly the first two peaks. Wikström et al.(1997) studied peaks in a time window of 400

ms and described 4 major peaks. Lastly Rossini et al.(1994) also worked on normative datasets and described in a time window of 50 ms the 2 major peak activations.

The present study provides maximally seven SEF stages. The nature of the individual differences remains unclear. Out of these stages the most consistent peak activations are the M20, M30, M50, M70, M90 and M150. Late activation includes a 240M. The first two reflect the classical fast stages examined in the literature. Our results indicate the importance of the mid-latency and late stages in cortical response to median nerve stimulation. In fact the largest magnitude in cerebral response to median nerve stimulation occurs at the M70. The fast stages of M20 and 30M are known to be of somatosensory origin, while the mean latency M70 may be of sequential sensorimotor origin.

The spatial characterization of the SEFs

Two main observations of spatial organisation from this study have not been reported previously. First, the regular bipolar patterns throughout the recording window as seen in Fig. 5, from early M20 to late M250, as the MEG in the literature is often limited to a shorter window. Perhaps, the classical studies have been focused on the intrinsic sensory processing while considering the late stages as extrinsic cognitive related potentials. In our view, the M70, being largest in magnitude, may likely reflect the sensorimotor processing of the frontal motor stage. Additional later stages are also the continuation of sensory-perceptual processing that last from 90 ms to 250 ms in this study. The 90-130 ms being the period of SII processing, while from the 130 ms on being the SII to insular-cingulate limbic integration.

The second new observation is that following the well-known polarity reversal between M20 and M30, an additional and second polarity reversal between M90 and M150 is observed. First, the magnetic field in the LHc (left hemisphere) at 20 ms consisting of a dorsal negativity and ventral positivity, reverses at 30 ms. The field pattern of dorsal positivity and ventral negativity remains relatively stable until about M90, although the field strength decreases between M30 and M90, in both hemispheres. Second, between 90 ms and 150 ms a second polarity reversal is observed. In this way the field patterns at M20 and the M150 have approximately the same polarity, although the orientation of the fields is slightly different. The RH (right hemisphere), from M20 to M240 depicts the same double polarity reversal but the polarities are opposite to the LH. It is as yet unclear how these changes relate to somatosensory processing between SI and SII (Hari and Forss,1999; Kakigi et al., 2000).

Since little has been reported on the individual patterns of cortical activities, this study effectively demonstrates the great individual characteristics of cortical activation from the waveform measured in the CWP and associated topographic maps. The CWP is considered to be highly valuable in examining the hemispheric consistency of two hemispheres within the individuals and across the subjects (Tecchio et al., 2000).

Overlay Plot vs. Grand Averaged compressed waveform profiles

Usually only the group grand average is used to present measurements showing the main similarities across the subjects. The overlay display of the individual subjects greatly accentuates the differences among the subjects. The display of both the overlay plot and the grand average has been reported in pain research (Inui et al., 2003) The use of both plots as in Fig. 3 is advantageous and both can be effective to convey information

on brain activities.

Inter-Subject and Intra-Subject Consistency

Based on the CWP, number of stages in SEF and amplitude parameters, our study concurs with the findings of high inter-subject variability of SEF morphology and an intra-subject inter-hemispheric consistency in cortical responses (Tecchio et al., 2000). In addition to the Tecchio report, this study is a major confirmation on the quantitative and normative description of the SEF values in a group of twenty healthy subjects. However, our results of the Laterality Index (L.I.) of focal field magnitude lend against use of sample mean (no significant difference) in comparison of two hemispherical activities. In fact, a significant minority (4/20 subjects) exhibited a right-hemisphere dominance. Our result is largely in agreement with a recent study (Jung et al., 2003) proclaiming that only a single subject (i.e. 1/16) presented a right hemisphere dominance. Their conclusion was based on the laterality of the dipole moment of the N20/SEPs only, while we examined the full spectrum from early to late phase and were likely to show a higher number of subjects with a right hemispheric dominance. However 2 out of 16 subjects in that report had a “pathological condition” with more than a side difference of over 50 % in N20 in one hemisphere compared with the amplitude in the other (Jung et al., 2003). Our results exhibited a similar number of subjects with clear asymmetric amplitudes (4/20 at over 40%, 2/20 at 50%; see the N20 in Fig.6). These results of “abnormality” of a 50% side difference in normal subjects may have to take into account when examining the hemispheric differences in stroke patients (Rossini et al., 2001).

The results in this study are complementary to a similar ECD study by Wikström et al. (1997). Though other studies on the unilateral stimulation of human hands were reported by SEPs (Niddam et al., 2000) and by MEG (Simões and Hari, 1999), none of them examined the laterality or homology of both hemispheres pertinent to the discussion of this study.

Nevertheless, recent reports and the results of this study strongly advocate the need to examine (a) the unilateral stimulation of one hand alone, (b) unilateral stimulation of both hands independently and (c) the relation of the hemispheric responses to hand dominance (Jung et al. 2003). In this way, we may further extent our understanding on the functional relations between hand and brain in health and in disease.

Correlation between scalp field and dipole strength

At the early stages, M20 and M30, there was a high correlation between the observed extracranial magnetic fields and fields due to a single intracranial current dipole. In other words, a single dipole describes the source of the field adequately. The fact that there is a lower correlation at later time instants may simply reflect the fact that then more sources are active.

Between hemispheric and within hemispheric correlations of dipole moments

The results in this study of correlations (Table-4) of SEFs led to the unexpected finding that no correlation of the dipole moments was present between the two hemispheres in the early phase. This effect, in turn may hamper the interpretation of dipole moments as measures of functional strengths of intact and affected brain sides. The degree of left hemispheric predominance in sensorimotor responses in the right-handed subjects has been described recently (Jung et al., 2003) using equivalent current dipoles.

Practical Implications

Any intra- and inter-individual comparison between studies requires at least the same or a comparable

measuring protocol. This is true for accurately relating function and localization since the sub-areas (3a, 3b and 1) of the human somatosensory cortex SI vary topographically to a certain extent (Geyer et al., 2000). Furthermore we have to bear in mind that sensory activation also depends on the type of stimulated nerve (Kaukoranta et al., 1986). The results from our study may provide a step toward a normative database comprising parameters that describe hemispheric activation in response to both left and right median nerve stimulation. Such an intra-subject inter-hemispheric comparison has been established for studying the cortical reorganization in stroke patients (Tecchio et al., 2000; Rossini et al., 2001; Ossenblok et al., 2001), and is potentially useful in studies of spatial attention (Braun et al., 2002), sensory-motor gating (Wasaka et al., 2003), writer's cramp (Braun et al., 2003) in normal healthy subjects. But it will also be useful for the assessment of paraplegic patients (Ioannides et al., 2002), and of chronic pain patients (Maihofner et al., 2003; Theuvenet et al., 1999). The question which parameters should be preferred to describe differences in patients after evoked cortical activation depends on the objectives of the study. In the pain studies differences in amplitudes were measured and the result of pain therapy was established by looking at amplitude changes. Studying differences in patient groups may provide important information for clinical practice. By way of inference from normal and pathological conditions, the results of our study are of value in order to asses abnormal activation of neuronal systems and/or brain reorganization.

Conclusion

Individual subjects exhibited unique waveform morphology in their CWP. Using complex waveform profile analysis, 6-7 peaks or stages were isolated and the activation segments were extracted from the CWP. Intra-subject inter-hemispheric consistency was found in 3D topography of somatosensory evoked magnetic fields, and dipole parameters. Quantitative data showed reliable consistency in latency and amplitude across the hemispheres at each peak stage. Within each activation segment, focal maximal of magnetic efflux and re-entrance could be clearly isolated. In order to assess an affected brain side, this study indicates that the following items should be taken into consideration (a) compressed waveform profile, (b) dipole parameters related to loci, orientations, and moments, (c) laterality index, and (d) spatial topography and parameters of scalp field parameters in peak latencies, peak maxima, and peak strength. The correlations of the extracranial SEF and intracranial dipole moments in either hemisphere indicate systematic and differential processing of somatosensory information in both hemispheres. While group averages (inter-individual differences) tend to rule out differences, intra-individual characteristics are more consistent. The result of our study clearly indicates that the healthy unaffected side cannot be taken fully as the "normal reference" for the affected side of the hemisphere.

Acknowledgements

This study was supported by the MEG Center, Royal Netherlands Academy of Science, Amsterdam, and Medtronic b.v., The Netherlands.

References

Baumgartner C, Doppelbauer A, Sutherling WW, Zeitlhofer J, Lindinger G, Lind C, Deecke L., Human somatosensory cortical finger representation as studied by combined neuromagnetic and neuroelectric measurements. Neurosci Lett. 16 (1991), pp. 103-108.

Baumgartner C. Controversies in clinical neurophysiology. MEG is superior to EEG in the localization of interictal epileptiform activity: Con. Clin Neurophysiol. 115 (2004), pp. 1010-1020.

Babiloni F, Babiloni C, Carducci F, Romani GL, Rossini PM, Angelone LM, Cincotti F. Multimodal integration of EEG and MEG data: A simulation study with variable signal-to-noise ratio and number of sensors. Hum Brain Mapp. 22 (2004), pp. 52-62.

Barkley GL, Baumgartner C. MEG and EEG in epilepsy. J Clin Neurophysiol. 20 (2003), pp. 163-78.

Braun C, Haug M, Wiech K, Birbaumer N, Elbert T, Roberts LE. Functional organization of primary somatosensory cortex depends on the focus of attention. NeuroImage 3 (2002), pp. 1451-1458.

Braun C, Schweizer R, Heinz U, Wiech K, Birbaumer N, Topka H. Task-specific plasticity of somatosensory cortex in patients with writer's cramp. NeuroImage 2 (2003), pp.1329-1338.

Flemming L, Haueisen J, Tenner U, Giessler F and Eiselt M., Source Localization in an animal model, Proceedings 3rd Int. Symposium on Non-invasive Functional Source Imaging (NFSI 2001), Innsbruck, Austria, Biomedizinische Technik 46 (2001), pp. 138-140

Fuchs M, Wagner M, Kastner J. Confidence limits of dipole source reconstruction results. Clin Neurophysiol. 6 (2004), pp. 1442-1451.

Forss N, Hari R, Salmelin R, Ahonen A, Hamalainen M, Kajola M, Knuutila J, Simola J. Activation of the human posterior parietal cortex by median nerve stimulation. Exp Brain Res. 2 (1994), pp. 309-315.

Forss N, Hietanen M, Salonen O, Hari R. Modified activation of somatosensory cortical network in patients with right-hemisphere stroke. Brain. 122 (1999), pp. 1889-1899.

Geyer S, Schormann T, Mohlberg H, Zilles K. Areas 3a, 3b and 1 of Human Primary Somatosensory Cortex, NeuroImage 11 (2000), pp. 684 - 696

Hari R, Karhu J, Hamalainen M, Knuutila J, Salonen O, Sams M, Vilkman V. Functional organization of the human first and second somatosensory cortices: a neuromagnetic study. Eur J Neurosci. 6 (1993), pp. 724-34.

Hari R. and Forss,B. Magnetoencephalography in the study of human somatosensory cortical processing. Philos Trans R Soc Lond B Biol Sci. 354 (1999), pp. 1145-1154.

Hoshiyama M, Kakigi R. Correspondence between short-latency somatosensory evoked brain potentials and cortical magnetic fields following median nerve stimulation. Brain Res. 908 (2001), pp.140-148.

Ioannides AA, Liu L, Khurshudyan A, Bodley R, Poghosyan V, Shibata T, Dammers J, Jamous A. Brain activation sequences following electrical limb stimulation of normal and paraplegic subjects. NeuroImage 16 (2002), pp.115-29.

Jung P, Baumgärtner U, Bauermann T, Magerl W, Gawehn J, Stoeter P, Treede RD. Asymmetry in the human primary somatosensory cortex and handedness. Neuroimage 19 (2003), pp. 913-923.

Kakigi, R, Somatosensory evoked magnetic fields following median nerve stimulation. Neurosci Res. 20 (1994), pp. 165-174.

Kakigi R, Hoshiyama M, Shimojo M, Naka D, Yamasaki H, Watanabe S, Xiang J, Maeda K, Lam K, Itomi K, Nakamura A., The somatosensory evoked magnetic fields, Progress in Neurobiology, 61 (2000), 495 - 523

Kanno A, Nakasato N, Hatanaka K, Yoshimoto T. Ipsilateral area 3b responses to median nerve somatosensory stimulation. Neuroimage. 1 (2003), pp. 169-177.

Karl A, Birbaumer N, Lutzenberger W, Cohen LG, Flor H. Reorganization of motor and somatosensory cortex in upper extremity amputees with phantom limb pain. J Neurosci. 2001 May 15;21(10):3609-18.

Kaukoranta E, Hämäläinen J, Sarvas J, Hari R. Mixed and sensory nerve stimulation activate different cytoarchitectonic areas in the human primary somatosensory cortex SI. Exp. Brain Research (1986), pp. 60-66

Kawamura T, Nakasato N, Seki K, Kanno A, Fujita S, Fujiwara S, Yoshimoto T. Neuromagnetic evidence of pre- and post-central cortical sources of somatosensory evoked responses. Electroencephalogr. Clin. Neurophysiol. 100 (1996), pp. 44-50

Lesser RP. MEG: good enough. Clin Neurophysiol. 115 (2004) 995-7.

Maihofner C, Handwerker HO, Neundorfer B, Birklein F. Patterns of cortical reorganization in complex regional pain syndrome. Neurology. 61 (2003), pp. 1707- 1715.

Niddam DM, Arendt-Nielsen L, Chen AC. Cerebral dynamics of SEPS to non-painful and painful cutaneous electrical stimulation of the thenar and hypothenar. Brain Topogr. 13 (2000), pp. 105-114.

Nuwer MR, Aminoff M, Desmedt J, Eisen AA, Goodin D, Matsuoka S, Mauguiere F, Shibasaki H, Sutherling W, Vibert JF. IFCN recommended standards for short latency somatosensory evoked potentials. Report of an IFCN committee. International Federation of Clinical Neurophysiology. Electroencephalogr. Clin. Neurophysiol. 91 (1994), pp. 6-11.

Ossenblok P, Leijten F.S.S. , de Munck J.C., Huiskamp G.J., Barkhof F., Boon P., Magnetic source imaging contributes to the presurgical identification of sensorimotor cortex in patients with frontal lobe epilepsy, Clinical Neurophysiology 114 (2003) pp. 221-232.

Parra J, Kalitzin SN, da Silva FH. Magnetoencephalography: an investigational tool or a routine clinical technique? Epilepsy Behav. 5 (2004), pp. 277-85.

Rossini PM, Narici L, Martino G, Pasquarelli A, Peresson M, Pizzella V, Tecchio F, Romani GL. Analysis of interhemispheric asymmetries of somatosensory evoked magnetic fields to right and left median nerve stimulation. Electroencephalogr Clin Neurophysiol. 91 (1994) pp. 476-482.

Rossini PM, Tecchio F, Pizzella V, Lupoi D, Cassetta E, Pasqualetti P, Interhemispheric differences of sensory hand areas after monohemispheric stroke: MEG/MRI integrative study. NeuroImage. 14 (2001), pp. 474-485. Erratum in: Neuroimage 14(5) (2001) 1230. Paqualetti P

Rossini PM, Dal Forno G. Integrated technology for evaluation of brain function and neural plasticity. Med Rehabil Clin N Am. 15 (2004), pp. 263-306.

Schaefer M, Muhlnickel W, Grusser SM, Flor H. Reliability and validity of neuroelectric source imaging in primary somatosensory cortex of human upper limb amputees. Brain Topogr. 2002 Winter;15(2):95-106.

Simões C and Hari R, Relationship between Responses to Contra- and Ipsilateral Stimuli in the Human Second Somatosensory Cortex SII, NeuroImage 10 (1999) 408 – 416.

Soros P, Knecht S, Imai T, Gurtler S, Lutkenhoner B, Ringelstein EB, Henningsen H. Cortical asymmetries of the human somatosensory hand representation in right- and left-handers. Neurosci Lett. 271(1999), pp. 89-92.

Tecchio F, Rossini PM, Pizzella V, Cassetta E, Romani GL. Spatial properties and interhemispheric differences of the sensory hand cortical representation: a neuromagnetic study. Brain Research , 767 (1997), pp. 100 - 108.

Tecchio F, Rossini, P.M. ,Pizella V, Cassetta E, Pasqualetti P, Romani G. A neuromagnetic normative data set for hemispheric sensory hand cortical representation and their interhemispheric differences. Brain Research Protocols, 2 (1998), pp. 306 - 314

Tecchio F, Pasqualetti P, Pizzella V, Romani G, Rossini PM. Morphology of somatosensory evoked fields: inter-hemispheric similarity as a parameter for physiological and pathological neural connectivity. Neurosci Lett. 287 (2000), pp. 203-6.

Theuvenet PJ. , Dunajski Z, Peters MJ, van Ree JM., Responses to median and tibial nerve stimulation in patients with chronic neuropathic pain. Brain Topogr. 11(1999), pp. 305-313.

Vrba, J, Robinson, S.E, Signal Processing in Magnetoencephalography, Methods 25 (2001), pp. 249-271.

Wasaka T, Hoshiyama M, Nakata H, Nishihira Y, Kakigi R. Gating of somatosensory evoked magnetic fields during the preparatory period of self-initiated finger movement. NeuroImage. 20 (2003), pp. 1830-8.

Wheless JW, Castillo E, Maggio V, Kim HL, Breier JI, Simos PG, Papanicolaou AC. Magnetoencephalography (MEG) and magnetic source imaging (MSI). Neurologist. 10 (2004), pp. 138-153.

Wikström H, Roine RO, Salonen O, Aronen HJ, Virtanen J, Ilmoniemi RJ, Huttunen J. Somatosensory evoked magnetic fields to median nerve stimulation: interhemispheric differences in a normal population. Electroencephalogr Clin Neurophysiol. 104 (1997), pp. 480-487.

Chapter 6

Hemispheric Discrimination in MEG between median versus ulnar nerve in unilateral stimulation of left and right hand.

Peter J. Theuvenet, Bob W. van Dijk, Maria J. Peters, Jan M. van Ree,
Fernando L. Lopes da Silva and Andrew C.N. Chen.

Brain Topography 2006; 19: 29-42

Abstract

Contralateral somatosensory evoked fields (SEF) by whole head MEG after unilateral median and ulnar nerve stimulation of both hands were studied in 10 healthy right-handed subjects. Major parameters describing cortical activity were examined to discriminate median and ulnar nerve evoked responses. Somatic sensitivity showed high similarity in the 4 study conditions for both hand and nerve. The brain SEFs consisted of 7-8 major peak stages with consistent responses in all subjects at M20, M30, M70 and M90. Comparable inter-hemispheric waveform profile but high inter-subject variability was found. Median nerve induced significantly shorter latencies in the early activities than those of the ulnar nerve. The 3D cortical maps in the post stimulus 450 ms timeframe showed for both nerves two polarity reversals, an early and a late one which is a new finding. Dipole characteristics showed differential sites for the M20 and M30 in the respective nerve. Higher dipole moments evoked by the median nerve were noticed when compared to the ulnar. Furthermore, the results of the dipole distances between both nerves for M20 were calculated to be at 11,17 mm ± 4,93 (LH) and 16,73 mm ± 5,66 (RH), respectively after right hand versus left hand stimulation. This study showed substantial differences in the cortical responses between median and ulnar nerve. Especially the dipole distance between median and ulnar nerve on the cortex was computed accurately for the first time in MEG. Little is known however of the cortical responses in chronic pain patients and the parameter(s) that may change in an individual patient or a group. These results provide precise basis for further evaluating cortical changes in functional disorders and disease sequelae related to median and ulnar nerves.

Introduction

The primate hand occupies a special significance in human evolution. The use of and functional difference between the right and left hand is a major focus for understanding the organization of the brain somatotopy of the human hand (Baumgärtner et al., 1991 and 1993; Biermann et al., 1998; Druschky et al., 2002; Nakamura et al., 1998). The cortical representation of the sensory hand extension (Baumgartner et al.,1993), that is the distance between the dipole location of the 1st and 5th finger, estimated using SEPs, averaged 12,5 mm. In a comparable MEG study, the sensory hand extension was 22 mm (Tecchio et al.,1997), which presents a substantial difference. In a recent study with evoked potentials (Chen et al., 2005) the hand extension was estimated 15mm. It is known that the cerebral cortex in reaction to pathological conditions, i.e. deafferentation, develops cortical plasticity (Buonomano and Merzenich, 1998; Garraghty et al., 1994; Kaas et al., 1991 and 1999; Wall et al., 2002). In this process deprived cortical neurons can acquire new receptive fields producing topographical changes in cortical maps. The distance of the cortical representation of the median and ulnar nerve was described to be a sensitive index of cortical plasticity and reorganization in tactical co-activation of fingers (Ziemus et al., 2000). One way to assess normal function and sequelae of disease or injury of the these major peripheral nerves of the human hand is by way of EEG, and more recently MEG, for non-invasive measurement of the SEPs and SEFs, respectively (Hämäläinen et al.,1993).

Current MEG technology is a powerful means for the investigation of somatosensory and nociceptive processing (Hari et al., 1999; Kakigi et al., 1994; Kawamura et al., 1996; Nakamura et al., 1998; Rossini et al., 1994) but also has limitations (Parra et al., 2004). Functional analysis has to be based upon accurate characterization and localization of neural activity and has to take into consideration the known asymmetrical aspects of the two hemispheres. The left and right hemispheres of the brain may differ in their anatomy (i.e. the morphology of the central sulcus) and function, brain asymmetry was described in both animals (Riddle et al., 1995) and humans (White et al., 1997; Amunts et al., 2000; Jung et al., 2003; Toga et al., 2003). White et al. (1997) showed that the surface morphology of the central sulcus varied widely within and between subjects. In two recent studies (Theuvenet et al., 2005; Tecchio et al., 2005) the within subject similarity and between subjects variability of the dipole parameters after median nerve stimulation was demonstrated in both hemispheres.

In earlier studies on the cortical representation of median and ulnar somatotopy, the ulnar evoked responses have been found to be situated medially and superiorly to the position of the median nerve responses, likely at the posterior bank of area 3b (Baumgartner et al., 1991, Forss et al., 1996; Vanni et al., 1996) confirming the somatotopic organization of SI. These results focused on the characterization of early components and their source generators in the brain. The N20, and P30 have largely been attributed to the primary somatosensory (SI) generators of area 3b and area 1 for P33 components (Inui et al., 2003). While the early components in SEPs have been relatively well investigated for neural generators (Babiloni et al., 2001), the middle latency components have not been yet fully elucidated. For accurately relating function and localization, careful examination of an individual is needed (Geyer et al., 2000) since the sub-areas (3a, 3b and 1) of the human somatosensory cortex SI vary topographically to a certain extent. A major effort has been the establishment of a set of normative brain responses to standard peripheral nerve

stimulation (Hari et al., 1999; Rossini et al., 1994 and 2001; Tecchio et al., 1997, 1998 and 2000). In order to study the affected hemisphere, compared to the intact hemisphere in peripheral and central somatosensory processing, unilateral stimulation of both hands has been evaluated (Forss et al., 1999; Rossini et al., 2001; Theuvenet et al., 2005). To a large extent, only the median nerve has been examined but little is known about the ulnar nerve in this aspect. Furthermore, no detailed parameters in comparison of both functional nerves of hand in the human cortex have been reported and their relations between the two hemispheres remains unclear.

The aim of this study was to describe the major parameters of the evoked responses measured by whole head MEG after electrical stimulation of the *median and ulnar nerve* in a time window of 500 ms (including a 50 ms pre-stimulus interval) in both hemispheres. First we studied the full spectrum of well known parameters including quantified hemispherical differences of the measured data. We aimed at identifying the major parameters that could be used in a descriptive and analytical way for clinical studies of neurological dysfunction and disease in patients. Second, we assessed the variation of these parameters for a group and for individual subjects since group means may wipe out individual differences. It is important to assess the variability of inter-hemispherical differences in order to determine the range of normal variation and differences for each parameter. What has to be regarded as normal variation, what is a true (pathological) difference and then which parameter remained to be examined. Lastly, we question whether in cases of unilateral damage, the unaffected side can safely be taken as a reference for identifying pathological states. This question is important since the answer may be informative regarding the central mechanisms of somatosensory processing in chronic pain and will be published separately.

Materials and Methods

Subjects

Ten healthy volunteers (7 males and 3 females, age range 26-45 years, mean 33.5 ± 5.9 years, all Caucasian *right* handed) were recruited from two hospital staffs. All volunteers were adequately informed and gave their consent. Handedness was established both using lists from the VU Medical Center which included arm and leg performance and the Edinburgh Inventory (value of 0.8).The Medical Ethical Committee of the VU Medical Centre approved of this study.

Counter balanced median and ulnar nerve stimulation

Stimulation between right and left hand was in a counter-balanced order between right and left hand across the subjects. Median and ulnar nerve stimulation was performed at the wrist with a bipolar electrode, the cathode was placed proximally according to the international guidelines (IFCN Guideline: Nuwer et al.,1994). To stimulate both nerves we employed an electrical stimulator (Grass, USA; model S48) using a photoelectric stimulus isolation unit (Grass, USA; model SIU7). The stimulation current was pulsed, at a repetition rate of 2 Hz and with a pulse duration of 0.2 ms. All subjects were studied in one session (totally 45 minutes) and a resting period of 5-10 minutes was ensured between each nerve. Stimulus intensity was tailored individually and was set to 1.5 x the motor twitching level. The twitch threshold varied with the subject, was well tolerated and painless. Five hundred events were recorded from the median and ulnar nerve in each hand.

MEG Recordings

A 151-channel whole-head gradiometer system (VSM, Canada) was used and measurements were performed in a 3-layer magnetically shielded room (Vacuum Schmeltze Gmbh, Germany). The VSM x, y and z coordinate system is based upon the nasion, left and right ear where coils are positioned that are used to determine the distance between the head and the measurement system. The origin of the coordinate system is halfway the line connecting the left and right ear coil. The X-Y plane is defined by the 3 coils. The Z-axis starts in the same origin and is perpendicular to the X-Y plane. The Y-axis is defined as the *cross-product* of the Z-axis to the X-axis: Y = Z x X, such that the positive Y is directed to the left ear, and will probably not point directly at the left ear coil (VSM).

The azimuthal (ϕ) angle is defined as the angle in the X-Y plane, in the direction toward the +Y axis to the vector projected into the X-Y plane (see Fig. 1). The declination (θ) is the angle to the vector from the +Z axis. The coordinate system in this study may differ from other studies. The axes system i.e. used by Tecchio et al.,1998, where the positive y corresponds to the x in the VSM system. This is important to realise when describing dipole locations and comparing research results. Based upon the positions of these fiducials a head centred coordinate frame is defined and therefore the positions of all MEG sensors in head coordinates. We determined the best recording position, that position in which the smallest rotation and translations were necessary to align all data sets, using the coordinates of the sensors in multiple recording sessions corresponding to multiple head positions. The positional variations for the recordings per subject were quite small, the mean rotation angle amplitude was 3.8 degrees, the mean translation distance was 0.4 cm. For the recordings of the entire group the variations were larger, the mean rotation angle amplitude was 5.6 degrees, the mean translation distance was 0.8 cm. The average subjects head was positioned 0.02 cm left from the centre of the helmet. Recordings were performed in the synthetic 3rd-order gradient mode, using the manufacturers real-time software (Vrba,1996) and the system had a baseline of 5 cm. All volunteers were in the supine position. The MEG signals were sampled at 1250 Hz, triggered on the synchronization pulse of the electric stimulator. The peri-stimulus interval was 50 ms pre-trigger and 450 ms post-trigger. On-line filters were set at DC for high-pass and at 400 Hz (4th order Butterworth) for anti-aliasing low-pass. Off-line the MEG data were screened for artefacts, averaged and DC-corrected using the pre-trigger interval to determine the recording offset. Also +/- averages were calculated to obtain noise-level estimates. The estimated distance between two neighbouring sensors in the area of our interest is 2.67 cm.

Fig.1

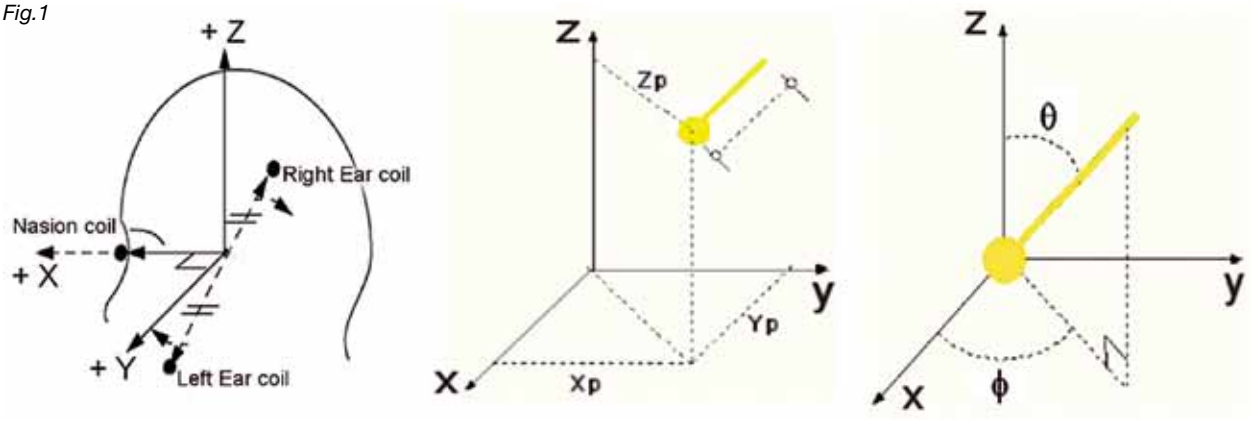

Fig. 1. The x, y and z axes are presented as the orientation parameters, declination and azimuth. Courtesy of VSM-systems; Canada.

MRI co-registration

Brain MRI' s were performed with a 1.5T 3d-MRI (Siemens Sonata). The following parameter settings were used: sagittal slice orientation, slice thickness 2 mm, FOV 256 mm, scanmode fl3d, scan technique 20 magnitude, TR 11.8 ms, echoes no. 1, TE 5ms, flip angle 30 degrees and contrast enhancement was applied. Lastly, the number of signals averaged was 2, scan matrix 256, reconstruction matrix 256, TI 0 and frequency 63.6 MHz. The MEG-MRI common reference system was defined on the basis of three anatomical landmarks (vitamin E capsules, 5 mm of diameter) fixed on nasion, left and right pre-auricular points. In this way, we achieved superimpositions on MR images with a precision of 2–3 mm as previously shown using simulations with artificial "dipoles" within a skull. The entire MRI procedure lasted about 30 min and was well tolerated by all subjects.

Compressed Waveform Profile (CWP), overlay and grand average plots

When the evoked responses of all 151 MEG sensors are superimposed, a butterfly-like display is produced which we termed the compressed waveform profile (CWP) from which the main peak activation stages were isolated. The somatosensory activities in the time domain were divided into three different phases, an early (<M50s), mid-latency (50-90 ms), and late (90-400 ms) phase. The CWP can effectively provide the individual characteristics of the brain dynamics of the sensory, motor and perceptual brain regions for the different subjects. After that, we produced an overlay plot and a grand average of the measurements of all subjects together. This was done with the responses both after median and ulnar nerve stimulation. The overlay plots of the individual subjects greatly accentuates the differences (see Fig. 2A) among the subjects while the grand averaged plots reveal the similarities (Fig. 2B).

Data management and statistical analysis

A small number (max 50) of events containing too much disturbances (movement artefact or blinking) was rejected manually in each dataset. All further data-analysis and presentation for graphical display was performed employing ASA software (Advanced Source Analysis, ANT A/S, The Netherlands). We studied the following parameters: latency and number of the (peak) stages, site of activity (x, y and z), dipole orientation and strength, focal activity (magnitude) and the patterns of activation (3D - topographic maps).

In order to compare the two hemispheres we derived the following parameters: latency differences, amplitudes (efflux and influx) and the coefficient of variation (cv), an index of measurement consistency for the magnitude. For comparison of the hemispheric activation in response to both right and left hand stimulation, only the contralateral activity was analysed in this study. A series of statistical analysis was conducted to compare these parameters in the hemispheres from right vs. left hand stimulation of the median and ulnar nerve. Two-way repeated ANOVA was conducted, with Tukey tests for post-hoc comparisons of the means to evaluate the studied effects, with alpha of 0.05 adopted as significant. The 95% Confidence Interval is defined as CI = mean ± 1.96 x Standard Error (SE).

Equivalent Current Dipole and Dipole Parameters

We applied the VSM (company) software to model the equivalent current dipole (ECD) sources. The head was approximated with a spherical volume conductor. The conventional single equivalent current (moving) dipole analysis (e.g. Lin et al., 2003; Fuchs et al., 2004) was used for data evaluation. The head model had to match the inner contour of the skull, matching was done visually. Epochs in the post stimulus 450 ms time

window, with clear SEF deflections were visually identified to select signals of interest for further analysis.

Results

A. Stimulus intensities under four different study conditions

The stimulus intensities required for eliciting the twitch thresholds of the relevant hand muscles were analysed and no statistical difference was demonstrated between the nerves and across the hands (Lhand/Median=6.28mA. Lh/Ulnar=5.49mA, Rh/M=5.75mA and Rh/U=5.15mA; $F_{1,9}$ = 2.653, p=0.14).

B. SEF waveform morphology (CWP) and peak consistency

We examined the CWPs based on the overlay plots of all healthy volunteers and the grand averaged plots. The profiles of the four study conditions for the overlay plots are displayed in Fig. 2A, and for the grand average in Fig. 2B. As shown in Fig. 2A, consistent initial peaks appeared in the first 50 ms, major activities in the middle latency period (50 -100 ms) and little activities in the late period (>100 ms). The number of peak stages is generally in the neighbourhood of 7-8. It is noticed that only M20, M30, M70 and M90 exhibit consistent activities in all subjects (10/10), while the late peaks were only observed in a subset of subjects (mostly 6-8/10 and one 3/10). No unique difference in the morphology between the median and ulnar CWP overlay plots can be shown in Fig. 2A.

In contrast, the grand averages of the four stimulated nerves produced a different picture (Fig. 2B). Only major activity is now apparent, the quality of the detailed information is diminished. The waveforms show little difference between the left and right grand average after median nerve (M) stimulation and ulnar nerve (U) stimulation.

C. SEF Peak Stages: Latency and Amplitude

Examining the individual overlay plots in Fig. 2A and the grand average plots in Fig. 2B, the higher variability of the late stages compared to the early stages is discernible. Applying a two-Way RM ANOVA on the full dataset at M20 and M30 (10/10 subjects), the latencies showed that only the M20 exhibited significant faster values after median nerve stimulation (21.225 ms) than after the ulnar nerve (21.920 ms) response and for both hemispheres ($F_{1,9}$=11.055, p<0.009).

As for the distribution of the amplitudes over the hemispheres, both the (positive: +) efflux and (negative: -) influx of the M20 and M30 was significantly larger after median nerve ($M20^+$ =189.21fT, $M20^-$ =-194.815fT, $M30^+$ = 236.25fT, $M30^-$ = -233.25fT) than after ulnar nerve stimulation ($M20^+$ =104,0fT, $M20^-$ =-108.085fT, $M30^+$ = 160.645fT and $M30^-$ = -152.86fT) in the responses across both hemispheres ($F_{1,9}$=30.123, p<0.01 in $M20^+$, $F_{1.9}$ = 10,592, p<0.01 in $M20^-$, $F_{1.9}$ = 33.058, p<0.01 in $M30^+$, $F_{1.9}$ = 10.526, < p<0.01 in $M30^-$).

D. Compressed Waveform Profiles and SEF characterization after median and ulnar stimulation for *individual volunteers*.

The characteristics of all volunteers included the CWP, peak latency, amplitude and 3D brain topography. For each subject and for all four stimulated nerves, the number of peak stages was assessed for each individual CWP and the results are presented in Table I. Fig. 3 depicts the CWPs of all 10 subjects in response to contralateral median and ulnar nerve stimulation. The results are shown of the left and right hemisphere CWPs and are presented as a pair, L-L and R-R. Peaks can be identified in all three periods, early,

middle late and late. As can be seen, after M150 differences between median and ulnar nerve stimulation are more clear. The M20, M30, M70 and M90 is present in all (10/10) subjects.

D1. CWPs Median nerve

Table IA (upper part) depicts the number of peak stages after electrical stimulation of the median nerve in both hemispheres. In the post stimulus period of 450 ms, 3 well known peak stages could be recognized, M20 (10/10 subjects), M30 (10/10) and M50 (8-10 /10). Major activity is reflected in the mid-latency M70 and M90 (50-100 ms, 10/10 subjects) component and late components are the M150 (110 –200 ms, 9-10/10 subjects) and M240 (200 –300ms, 6-8/10 subjects). A M300 component is present in 7-8/10 volunteers. Both late peaks can be identified in the LH and the RH. There is no unique pattern discernible over the group, each individual presented its own individual profile.

D2. CWPs Ulnar nerve

The results after ulnar nerve stimulation are shown in the lower part of Table IB. The ulnar M20, M30, M50, M70, M90 and M150 are seen in 8-10/10 subjects, the M225 only in 6/10 and the latest component (M30) in 3/10 subjects. Like after median nerve stimulation, the CWPs in the LH and RH depict no unique pattern.

The morphology of CWPs therefore in each hemisphere, both after median and ulnar stimulation, is generally more similar within the subjects than that between the subjects. Apart from the two well-known early components (M20 and M30), in all CWPs around 90 ms, a major area of neural activity is shown for both nerves. The amplitudes in the left hemisphere (LH) are not consistently larger than in the right hemisphere (RH), sometimes the reversed situation is present (see Fig. 3, subject HC-05). It is apparent that no identical CWP can be extracted across the subjects and each subject revealed his/her unique characteristics (8-10 /10).

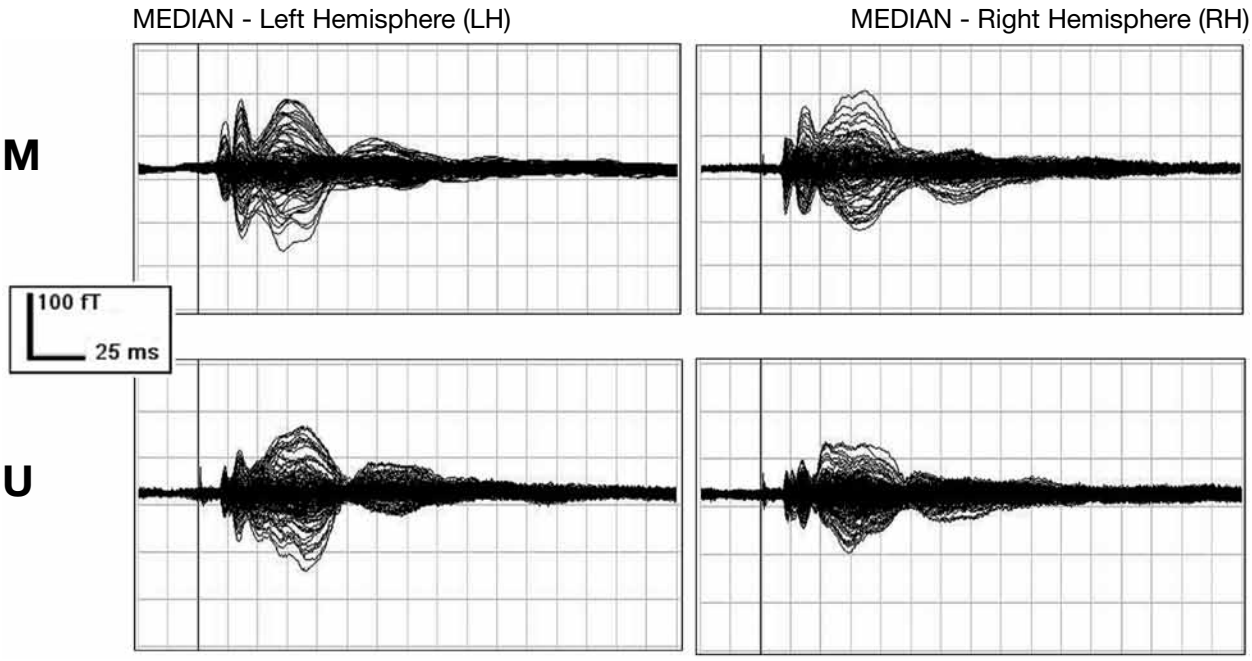

Fig. 2A. The grand averaged plots for median (M) and ulnar nerve stimulation (U) in both hemispheres. The upper part is after median nerve stimulation, the lower part after ulnar nerve stimulation.

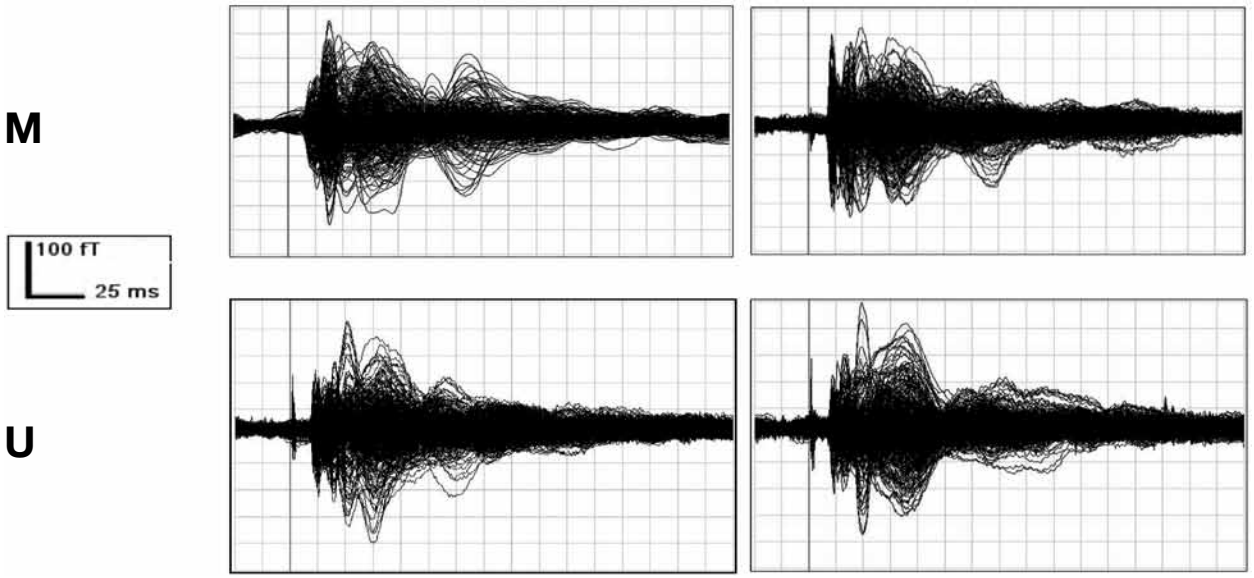

Fig. 2B. CWP overlay plots for median (M) and ulnar nerve stimulation (U) in both hemispheres. The upper two overlay plots, presenting all responses of the 151 sensors overlaid of the 10 healthy volunteers, are depicted. The ulnar plot is depicted in the lower part.

E. 3D Topography of SEFs

The 3D presentations of the evoked fields after median and nerve stimulation are depicted in Fig. 4, based on the overlay plots of all subjects in Fig. 2A. When comparing Fig. 4A and Fig. 4B, the morphological differences and similarities between the two sets of stimulated nerves can be evaluated. The evoked fields of both nerves present a dipolar configuration. The major activity is displayed in the first 150 ms.

In Fig. 4A (median) and 4B (ulnar), two polarity reversals are shown, a first and early one (M20/M30) and a second late one between 100 and 150 ms. After median nerve stimulation the first polarity reversal was observed in 9/10 subjects in the right hemisphere (RH) and 9/10 in the left hemisphere (LH). In one and the same subject (HC-04) the first polarity reversal in the LH and RH was not between M20/M30 but between M20/M50. The second polarity shift occurred between M100 and M150 in 10/10 subjects in both hemispheres.

After *ulnar stimulation* the situation was comparable. The first polarity shift was observed in the RH in 10/10 subjects and in 9 /10 in the LH after ulnar nerve stimulation. The second ulnar shift (see Fig. 4B) was at M90, a bit earlier than after median stimulation (at M100) but also in 10/10 subjects. This study demonstrated two polarity reversals after both median and ulnar nerve stimulation.

F. Dipole parameters

Six dipole parameters (3 position, 2 orientation and 1 the strength) were calculated from the measurement data. Based upon the literature we further studied the M20 and M30 dipoles

Median: Left Hemisphere							
20ms	30ms	50ms	70ms	90ms	150ms	240ms	330ms
10/10	10/10	8/10	10/10	10/10	10/10	6/10	7/10

Median: Right Hemisphere							
20ms	30ms	50ms	70ms	90ms	150ms	240ms	330ms
10/10	10/10	10/10	10/10	10/10	9/10	8/10	8/10

Ulnar: Left Hemisphere							
20ms	30ms	50ms	70ms	90ms	150ms	225ms	330ms
10/10	10/10	8/10	10/10	10/10	8/10	6/10	3/10

Ulnar: Right Hemisphere							
20ms	30ms	50ms	70ms	90ms	150ms	225ms	330ms
10/10	10/10	8/10	9/10	10/10	8/10	6/10	3/10

Tabel 1

The number of peak stages isolated for the LH vs. RH response. In this table the results after both median and ulnar nerve stimulation are presented. Time window is 500ms.

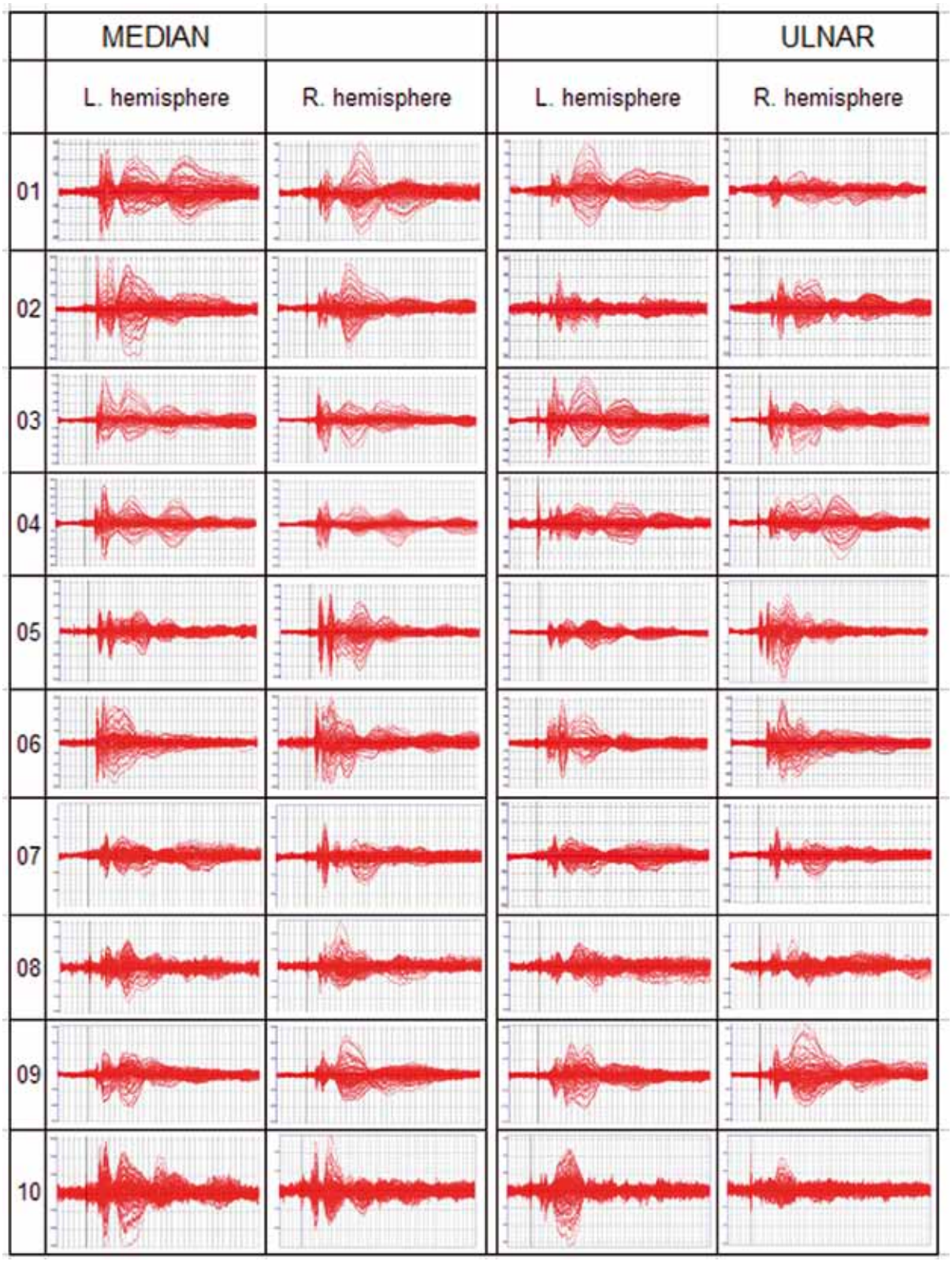

Fig. 3. Compressed waveform profiles (CWP) of 10/10 volunteers after median and ulnar nerve electrical stimulation. The time window is 50 ms pre-stimulus and 450 ms post-stimulus, the amplitudes are between 300 – 500fT. Contrast of CWPs between median and ulnar respectively for LH and RH both within the individual and across the subjects are presented.

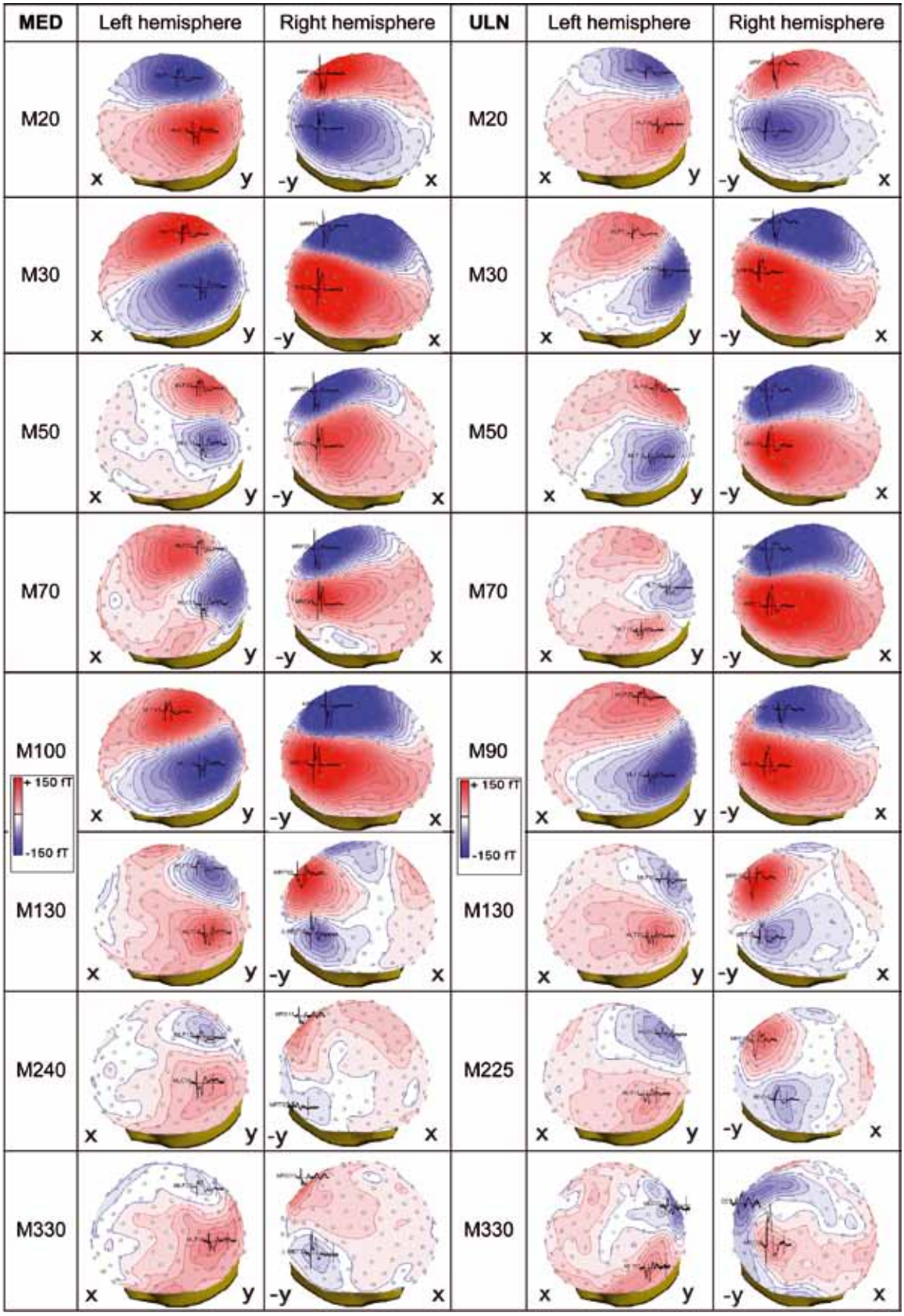

Fig. 4A. After electrical stimulation of the median nerves, the 3D brain maps comparing LH and RH at different peak stages are presented. The magnetic efflux is red, the influx is blue. Two polarity shifts can be observed, between M20s and M30 and a second one between M100 and M130. The magnetic contralateral hemisphere is exibited more clearly in the early stages than in the late stages. Amplitude scale on the vertical bar is between –150 to 150 fT.

LH - M20	x	y	z	declination	azimuth	strength
mean	3,5	42,3	86,0	74,9	345,4	29,9
Std	5,4	4,8	6,1	8,6	5,8	13,6
95% C.I.	-29,4 to 36,4	12,9 to 71,7	48,7 to 123,4	22,4 to 127,4	310 to 380,8	-53,9 to 113,2
C.V.	1,5	0,1	0,1	0,1	0,0	0,5
RH - M20	**x**	**y**	**z**	declination	azimuth	strength
mean	6,6	-39,8	84,7	72,47	19,47	25,28
Std	8,1	5,4	5,5	14,14	9,57	9,28
95% C.I.	-43,0 to 56,2	-72,9 to 6,7	51,2 to 118,2	-15,7 to 160,7	-39,13 to 78,07	-31,56 to 82,1
C.V.	1,2	-0,1	0,1	0,2	0,5	0,4

LH - U20	x	y	z	declination	azimuth	strength
mean	1,4	42,5	91,9	67,1	339,1	13,6
Std	6,9	7,4	6,4	11,1	16,1	5,0
95% C.I.	-31,4 to 34,3	-2,74 to 87,7	52,68 to 131,3	-0,96 to 135,3	240,39 to 437,8	-20,0 to 44,2
C.V.	4,8	0,2	0,1	0,2	0,04	0,4
RH- U20	**x**	**y**	**z**	declination	azimuth	strength
mean	2,95	-36,5	95,2	68,6	32,2	12,8
Std	6,4	5,9	8,7	8,6	20,9	5,8
95% C.I.	-41,9 to 45,5	-72,8 to -0,3	42,1 to 148,3	15,69 to 121,5	-96,03 to 160,5	-22,85 to 48,6
C.V.	2,18	0,16	0,09	0,1	0,6	0,5

Table 2A - Median and Ulnar M20

The dipole parameters and their statistical values at M20 in response to median and ulnar electrical stimulation.

LH - M30	x	y	z	declination	azimuth	strength
mean	4,5	42,3	90,0	107,8	173,1	29,6
Std	5,7	7,0	6,9	12,7	63,6	12,8
95% C.I.	-30,3 to 39,3	-0,4 to 85,0	47,7 to 132,3	30,0 to 185,6	-216,4 to 562,6	-48,8 to 108
C.V.	1,3	0,2	0,1	0,1	0,4	0,4
RH - M30	**x**	**y**	**z**	declination	azimuth	strength
mean	5,1	-40,7	89,4	108,8	180,4	30,0
Std	9,0	3,6	3,7	11,3	66,4	14,6
95% C.I.	-50,0 to 60,2	-62,7 to 18,65	66,7 to 112,1	41,1 to 176,4	-266,3 to 587,1	-69,4 to 119,4
C.V.	1,8	-0,1	0,0	0,1	0,4	0,5

LH - U30	x	y	z	declination	azimuth	strength
mean	2,1	39,1	91,9	103,8	182,3	20,3
Std	6,3	7,5	8,0	10,7	62,7	9,1
95% C.I.	-6,31 to 18,9	-6,8 to 84,96	42,9 to 140,91	38,3 to 169,15	-201,7 to 566,32	-35,7 to 76,3
C.V.	3,1	0,2	0,1	0,1	0,3	0,5
RH - U30	**x**	**y**	**z**	declination	azimuth	strength
mean	4,0	-38,3	94,0	107,0	226,4	19,0
Std	7,2	2,8	6,0	14,0	54,1	9,5
95% C.I.	-39,3 to 47,7	-65,34 to 11,18	63,81 to 124,21	21,39 to 192,59	-104,74 to 557,46	-38,87 to 76,93
C.V.	1,8	-0,07	0,06	0,13	0,23	0,49

Table 2B - Median and Ulnar M30

The dipole parameters and their statistical values at M30 in response to median and ulnar electrical stimulation.

after median and ulnar nerve stimulation only since these two dipoles are well described. Mean values, standard deviations, 95% Confidence Intervals (CI) and the Covariance (CV) are presented in Table II, the upper part for the M20 (II A) and the lower part for the M30(II B).

Two-Way (nerve and hemisphere) RM ANOVA revealed several significant findings as is presented in the following sections.

F-1. M20 dipole

The calculations of the six dipole parameters at 20 ms resulted in the following findings:

The x-values (mm) were larger in median nerve than ulnar nerve responses for both hemispheres (median vs. ulnar: $F_{1.9}$ =4.76, p=0.05), indicating a more anterior position of the median dipole position. (2) Larger y-values in median than ulnar nerve (median vs. ulnar: $F_{1.9}$ = 6.469, p<0.032), indicating a more lateral position of the median dipole than the ulnar dipole for both hemispheres. (3) The z-value of the median dipole was smaller (i.e. more inferior) to that of the ulnar. 4) Both orientation parameters, declination and azimuth, were significantly larger in median than ulnar dipoles for both hemispheres, indicating a more lateral and superior orientation of the median dipoles (see Fig. 1). Larger declination in median than ulnar nerve (median vs. ulnar: $F_{1,9}$ = 65,114, p<0,001).5). In addition, the dipole moments (strength in nAm) were larger after median than after ulnar nerve stimulation, both in the LH and RH for both nerves. (median vs. ulnar: $F_{1,9}$ = 8.225, p=0,019).

F-2. M30 dipole

The dipole position at 30 ms displayed similar characteristics. (1) The x-values were larger in median nerve than ulnar nerve responses for both hemispheres (median vs. ulnar: $F_{1,9}$ =14.332, p=0,004). (2) Greater z-values in ulnar than median nerve (ulnar vs. median: $F_{1,9}$ = 6,204, p<0.034). (3) Higher dipole moments values (median vs. ulnar: $F_{1,9}$ = 51.464, p=0,001) in median as compared to ulnar dipoles. When comparing the dipole values between M20 and M30, no location difference was noted, but the orientation of dipoles differed and the strength of the dipole at M20 was larger than at M30.

G. Inter-dipole distances between median and ulnar nerve

The inter-dipole distances in Table III could be calculated with the formula: the square root of the sum of the squares of the dipole differences of x, y and z. For the M20, the results of the inter-dipole differences were calculated to be at 11,17mm ± 4,93 at the left hemisphere (LH) and 16,73 ± 5,66mm on the right hemisphere (RH) respectively in response to right hand versus left hand stimulation. For the M30, the results of the inter-dipole differences were calculated to be at 9,8mm ± 4,7 at the left hemisphere (LH) and 10 ± 3mm on the right hemisphere (RH) respectively in response to right hand versus left hand stimulation. No statistical difference was observed between the hemispheres for both M20 and M30. Thus, no main effects of stage difference (F=4.51, p=0.066), or hemispheric difference (F-2.054, p-0.184) were found. However, the inter-dipole distance was larger for M20 than that of M30 (F-9.694, p-0.001). Table III lists detailed individual statistics and 95% confidence interval for establishment of normative data basis.

H. Inter-hemispheric dipole coordinate differences at M20 and M30 for median and ulnar nerve

When the absolute values of hemispheric differences of the dipole parameter in x, y, z were calculated, it was anticipated that the null hypothesis should indicate a full compliment if no location difference is ensured (i.e. a mirror image of the dipole location, respectively for M20

and M30). However, the values in the Table 4 indicated otherwise. Both the median and ulnar parameters yielded the mean values in the range of 3.75 to 10.44 (mm) between the left and right hemispheres. These individual values along with the 96% confidence intervals are listed in the Table 4 for further establishment of the normative data basis.

M20	Left Hem.	Right Hem.
S1	13,3	26,0
S2	12,5	11,1
S3	11,7	24,9
S4	13,7	20,5
S5	12,6	12,2
S6	13,3	13,3
S7	13,9	10,0
S8	2,0	13,6
S9	2,2	17,2
S10	16,5	18,4
Mean	**11,2**	**16,7**
Std	**4,9**	**5,7**
95% CI	**-18,8 to 41,2**	**-18,1 to 51,2**
CV (Std/Mean)	**0,44**	**0,34**

M30	Left Hem.	Right Hem.
S1	17,3	9,6
S2	8,2	5,9
S3	8,7	8,5
S4	4,4	9,7
S5	14,2	7,3
S6	11,0	9,8
S7	4,7	10,1
S8	7,5	12,3
S9	5,7	17,1
S10	16,3	9,2
Mean	**9,8**	**10,0**
Std	**4,7**	**3,0**
95% CI	**-19 to 38,6**	**-8,4 to 28,4**
CV	**0,48**	**0,30**

Table 3
The detailed individual statistics of the inter-dipole distance (mm) in both left-hemisphere (LH) and right hemisphere (RH) at M20 and M30 are presented for both nerves.

M20	Median			Ulnar		
	X	Y	Z	X	Y	Z
	LH - RH	LH-RH	LH - RH	LH - RH	LH - RH	LH - RH
S1	4,40	6,40	8,3	4,3	8,8	11,7
S2	1,90	5,00	2,9	1,1	5,8	12,5
S3	6,80	4,70	2,0	1,4	1,3	4,4
S4	9,90	4,90	5,9	9,9	14,1	3,2
S5	4,20	8,30	0,4	6,5	8,0	8,2
S6	8,80	1,20	1,4	5,5	1,2	1,9
S7	3,70	9,90	2,8	3,5	20,7	4,4
S8	4,80	9,50	5,3	3,9	10,2	4,3
S9	9,00	10,90	1,5	6,1	18,8	13,6
S10	6,40	13,80	7,0	9,0	15,5	15,6
Mean	5,99	7,46	3,75	5,12	10,44	7,98
Std	5,57	3,70	2,68	2,90	6,78	4,98
CV (Std/M)	0,93	0,49	0,71	0,57	0,65	0,62
95% C.I	2,54 to 9,44	5,17 to 9,75	2,09 to 5,41	3,33 to 6,91	6,23 to 14,64	6,41 to 9,55

M30	Median			Ulnar		
	X	Y	Z	X	Y	Z
	LH - RH	LH - RH	LH - RH	LH - RH	LH - RH	LH - RH
S1	6,6	10,80	1,00	5,6	2,1	6,2
S2	1,9	11,40	8,80	5,9	1,6	12,0
S3	5,6	1,40	0,80	1,4	4,1	0,9
S4	8,9	8,20	3,30	3,3	4,0	10,2
S5	2,2	7,40	7,70	3,0	10,4	2,5
S6	4,7	0,80	1,50	10,9	4,4	0,6
S7	2,8	1,20	0,60	5,7	3,3	12,1
S8	6,2	1,80	0,40	6,3	6,5	7,3
S9	6,8	5,00	11,20	5,6	6,4	4,2
S10	1,3	3,20	0,60	9,9	4,8	13,0
Mean	4,70	5,12	3,59	5,76	4,76	6,90
Std	2,54	4,07	4,07	2,92	2,54	4,76
CV (Std/M)	0,54	0,79	1,13	0,51	0,53	0,68
95% C.I	3,13 to 6,27	2,60 to 7,64	1,06 to 6,11	3,95 to 7,57	2,89 to 9,03	3,95 to 9,85

Table 4A en 4B

Absolute values of Inter-hemispheric differences (mm) of dipole parameters in the Individuals and in group statistics.

Discussion

Few comprehensive studies have analyzed the contralateral activities in response to both median and ulnar (or radial) nerve stimulation in great detail, though single nerve studies are reported (Slimp et al.,1986; Baumgartner et al.,1991; Buchner et al.,1994; Fujji et al.,1994; Grisolia et al.,1980; Huttunen et al.,1987 and 1992; Kaukoranta et al.,1986; Treede et al., 1995, Vanni et al.,1996; Tecchio et al.,2005).

We have systematically examined cortical topographic parameters and intra-cortical dipole features in both nerves. First, the *stimulus intensities* required for eliciting the twitch thresholds of the relevant hand muscles demonstrated no statistical difference in somatic sensitivity comparing the hand or the two different nerves. The *observed CWPs* for the median nerve was highly consistent with our recent publication (Theuvenet et al.,2005). The intra-subject (individual) CWP consistency, between the two hemispheres, was markedly smaller than the inter-subject differences (like Tecchio et al.,2005). The morphology of individual CWPs itself, overlay plots and grand averages are probably of less importance for assessing inter-hemispherical individual differences due to variation. In patients with different diseases however, CWPs still have to be studied carefully and therefore data from a healthy volunteer group will be of importance. Consistent peaks of SEFs observed for M20, M30 and M90 is in good accordance to the reported tangential current sources at M20 and M30 (Komssi et al., 2004). No difference in the number of the median and ulnar peaks in this study was observed and peak characteristics can be used in studying cortical responses for both nerves.

The median and ulnar *SEFs* showed dipolar configurations up to 330 ms at different latencies in nearly all the subjects including two polarity shifts. Its significance is not yet understood. Due to the fact that dipolar characteristics sofar have concentrated on the M20 and M30 (SI) and the M90 (SII), evoked fields and the derived six dipolar parameters have a place in describing interhemispheric differences. This dual observation for both median and ulnar has never been reported before. Focal extrema (*amplitudes*) at M20 and M30 were larger in both hemispheres after median stimulation. Based on the amplitudes however, no hemispherical preference could be established in this group (N=10). For the comparison of the two hemispheres in clinical practice, the amplitude differences between the two nerves can be used.

As for the *position* parameters, the median dipole displayed a more anterior (x-axis), more lateral (y-axis) and inferior (z-axis) compared to the ulnar one, this was true for both the M20 and M30 corresponding with the somatosensory anatomy. Thus, our results may not negate the assumption that M20 and M30 are from identical neuroanatomical site. The M30 dipole has been validated at the lateral shoulder of the inverted omega of the hand-digit somatosensory cortices by fMRI (Kumabe et al.,2000). Similarly, our observed dipole position of the median nerve (lateral inferior to the ulnar nerve dipole position) is likely in the posterior bank of the central fissure corresponding to area 3b for both (Baumgartner et al.,1991;Vanni et al. (1996). The *orientation* parameters of the M20, azimuth and declination (see Fig.1), were larger after median nerve stimulation. Lastly the *strength (moment)* of the median dipoles were larger at M20 than the ulnar ones, the LH values are predominantly larger too for both nerves than the RH. The strength of the M30 median dipole was larger too. All our subjects were right-handed and handedness related dipole differences were earlier described (Buchner et

al.,1995; Tsutada et al.,2002). This profile can be used for right-handed subjects, it is unknown how these parameters behave in left-handed subjects. Derived from the calculated parameters, our M20 *interdipolar distances* were in great agreement to the averaged 12-13mm for both nerves stimulated (Komssi et al.,2004). We extended these results to those of M30 and similar magnitude of inter-dipole differences in the neighborhood of 10mm at M30. No statistical difference was observed between the hemispheres for both M20 and M30. These values were somewhat larger than those reported of 7mm distance by Vanni et al.(1996).

Functional organization of the median and ulnar nerve dipoles can be detected by the different dipole parameters. Importantly, there is no full homology between the LH an RH. The parameters described are likely to be valuable for detecting for characterization of different disease states. Because of the lack of full homology between the LH and RH after median and ulnar electrical nerve stimulation, in patients with a unilateral disease, one cannot easily take the unaffected side as control.

The role handedness plays in the brain on inter-hemispherical differences and the results on cortical dominance after stimulation has not been fully established (White et al.,1997). Interhemispheric anatomical asymmetry was observed in the human *motor* cortex and was related to handedness and gender (Amunts et al., 2000). Functionally, a strong correlation was found (Soros et al.,1999) between handedness in humans and the extent (*distance*) of the area of cortical somatosensory representation of the hand representation in right-, but not in left-handers and that a functional hemispheric asymmetry also existed in primary sensory cortices. Jung et al. (2003) found a significant functional hemispheric asymmetry of the *amplitude* of N20 evoked potential at the cortical level, although there was no simple relation to handedness. Lifelong use of the dominant hand did not produce detectable changes in the cortical evoked activity (Niddam et al.,2000). Werner et al. (1996) described increased amplitudes of the left hemispheric responses in right handed workers. Asymmetry based upon *dipole moment* differences was described (Buchner et al.,1995; Tsutada et al.,2002). The observation of a functional interhemispheric difference was also made after cutaneous stimulation of the digits and using transcranial magnetic stimulation (Oliveri et al.,1999). Lastly, studying somatosensory processing of painful and non-painful stimuli with PET scans, Coghill et al. (2001) found evidence for hemispheric lateralised processing in some parts of the somatosensory system. A *latency shift* was described for the evoked potentials (P30) after painful stimulation (Niddam et al.,2000).

Several other factors contribute to differences in evoked responses. Stimulus intensity influenced dipole moment measures (Tsutada et al.,1999; Lin et al.,2003). The stimulus interval in MEG (Wikström et al.,1997) was equally relevant as the stimulus rate (Onishi et al.,1991) in SEPs and SEFs (Fujii et al.,1994). Differences between individuals are also dependant on the actual state of the somatosensory system (Buchner et al.,1999; Braun et al.,2002; Elbert et al.,1995; Noppeney et al.,1999, Liu et al.,2004). The results in this study therefore have to be understood within the framework of our measuring setup. Previous reports (Baumgartner et al.,1991; Buchner et al.,1994; Fujji et al.,1994; Huttunen et al, 1987 and 1992; Vanni et al.,1996) were based on group averages but for clinical applications the focus should rather be on the individual subject.

Injury and traumatic deafferentation of the human hand constitutes an important dysfunction and

impairment, confined at the wrist to the territories of median, ulnar and radial nerve or a combination of these nerves. *Amplitude* differences and changes at around 100ms were observed in peripheral traumatic nerve injury and the effects of a pain therapy, spinal cord stimulation (Theuvenet et. al., 1999). In patients with unilateral transections of the median or the ulnar nerve, *dipole source locations* exhibited somatotopic order with overlap between neighboring digits and in 2/3 nerve injured patients evidence for cortical reorganization was found. The *location* of sources related to digits neighboring differentiated digits was changed and their dipole *moments* were enhanced (Diesch et al.,2001). In patients with a Carpal Tunnel Syndrome (CTS), either an extended or a restricted *cortical representation* was shown along with the presence of paraesthesias or pain respectively (Tecchio et al.,2002). These few clinical studies sofar have shown that in different pathological disease states in patients, different changes in the type and magnitude of parameters were observed. Since no full inter-hemispheric homology exists, comparison of the responses in both hemispheres is still an issue for patients and requires careful examination. For clinical research, normative datasets as presented in this study are needed for evaluating cortical responses in pain syndromes.

Acknowledgements This study was supported by the MEG Centre, Royal Netherlands Academy of Science, Amsterdam, and Medtronic b.v., The Netherlands.

References

Amunts K, Jancke L, Mohlberg H, Steinmetz H and Zilles K. Interhemispheric asymmetry of the human motor cortex related to handedness and gender. Neuropsychologia, 2000, 3: 304 - 312.

Babiloni C, Babiloni F, Carducci F, Cincotti F, Rosciarelli F, Rossini PM, Arendt-Nielsen L, and Chen ACN. Mapping of early and late human somatosensory evoked brain potentials to phasic galvanic painful stimulation. Hum. Brain Mapp., 2001, 12: 168 -179.

Baumgartner C, Doppelbauer A, Deecke L, Barth DS, Zeitlhofer J, Lindinger G and Sutherling WW. Neuromagnetic investigation of somatotopy of human hand somatosensory cortex. Exp. Brain Res., 1991, 87: 641-648.

Baumgartner C, Doppelbauer A, Sutherling WW, Lindinger G, Levesque MF, Aull S, Zeitlhofer J and Deecke L. Somatotopy of human hand somatosensory cortex as studied in scalp EEG. Electroencephalogr. Clin. Neurophysiol.,1993, 88: 271-279.

Biermann K, Schmitz F, Witte OW, Konczak J, Freund HJ and Schnitzler A. Interaction of finger representation in the human first somatosensory cortex: a neuromagnetic study. Neurosci. Lett., 1998, 17: 13-16.

Braun C, Haug M, Wiech K, Birbaumer N, Elbert T and Roberts LE. Functional organization of primary somatosensory cortex depends on the focus of attention. NeuroImage, 2002, 3: 1451-1458.

Buchner H, Adams L, Müller A, Ludwig I, Knepper A, Thron A, Niemann K and Scherg M. Somatotopy of human hand somatosensory cortex revealed by dipole source analysis of early somatosensory evoked potentials and 3D-NMR tomography. Electroencephalogr. Clin. Neurophysiol., 1995, 96: 121-134.

Buchner H, Reinartz U, Waberski TD, Gobbele R, Noppeney U and Scherg M. Sustained attention modulates the immediate effect of de-afferentation on the cortical representation of the digits: source localization of somatosensory evoked potentials in humans. Neurosci. Lett.,1999, 260: 57-60.

Buonomano DV and Merzenich MM. Cortical plasticity: from synapses to maps. Annu. Rev. Neurosci. ,1998, 21: 149-86.

Chen ACN, Wang L and Arendt-Nielsen L. Cortical Plasticity in 3D Topography (ECD) of Thumb and Little Finger: Hand-Extension in Homunculus Cortex. NeuroImage. 2005, Abstract 505,

Coghill RC, Gilron I and Iandarola MJ. Hemispheric Lateralization of Somatosensory Processing. Am. Physiol. Soc., 2001: 2602-2613.

Diesch E, Preissl H, Haerle M, Schaller HE and Birbaumer N. Multiple frequency steady-state evoked magnetic field mapping of digit representation in primary somatosensory cortex. Somatosens. Mot. Res., 2001,18: 10-18.

Druschky K, Kaltenhäuser M, Hummel C, Druschky A, Pauli E, Huk WJ, Stefan H and Neundörfer B. Somatotopic Organization of the Ventral and Dorsal Finger Surface Representations in Human Primary Sensory Cortex Evaluated by Magnetoencephalography. NeuroImage, 2002, 15: 182-189.

Elbert T, Pantev C, Wienbruch C, Rockstroh B and Taub E. Increased cortical representation of the fingers of the left hand in string players. Science, 1995, 13, 270: 305-307.

Forss N, Merlet I, Vanni S, Hämäläinen M, Mauguiere F and Hari R. Activation of human mesial cortex during somatosensory target detection task. Brain Res., 1996, 23: 229-235.

Forss N, Hietanen M, Salonen O and Hari R. Modified activation of somatosensory cortical network in patients with right-hemisphere stroke. Brain, 1999,122: 1889-1899.

Fuchs M, Wagner M and Kastner J. Confidence limits of dipole source reconstruction results. Clin. Neurophysiol., 2004, 6: 1442-1451.

Fujii M, Yamada T, Aihara M, Kokubun Y, Noguchi Y, Matsubara M and Yeh MH. The effects of stimulus rates upon median, ulnar and radial nerve somatosensory evoked potentials. Electroencephalogr. Clin. Neurophysiol.,1994, 92: 518-526.

Garraghty PE, Hanes DP, Florence SL and Kaas JH. Pattern of peripheral deafferentation predicts reorganizational limits in adult primate somatosensory cortex. Somatosens. Mot. Res.,1994, 11: 109-117.

Geyer S, Schormann T, Mohlberg H and Zilles K. Areas 3a, 3b and 1 of Human Primary Somatosensory Cortex, NeuroImage, 2000, 11: 684 - 696

Grisolia JS and Wiederholt WC. Short latency somatosensory evoked potentials from radial, median and ulnar nerve stimulation in man. Electroencephalogr. Clin. Neurophysiol., 1980, 50: 375-381.

Hämäläinen M, Hari R, Ilmoniemi RJ, Knuutila J and Lounasmaa J. Magnetoencephalography – theory, instrumentation and application to non-invasive studies of the working human brain. Rev. Mod. Phys.,1993, 65: 413-497.

Hari R and Forss B. Magnetoencephalography in the study of human somatosensory cortical processing. Philos. Trans. R Soc. Lond. B Biol. Sci., 1999, 354: 1145-1154.

Huttunen J, Hari R and Leinonen L. Cerebral magnetic responses to stimulation of ulnar and median nerves. ElectroencephalogrClin.Neurophysiol.,1987,66:391-400.

Huttunen J, Ahlfors S and Hari R. Interaction of afferent impulses in the human primary sensorimotor cortex. ElectroencephalogrClin.Neurophysiol.,1992,82:176-181.

Inui K, Wang X, Tamura Y, Kaneoke Y and Kakigi R. Serial Processing in the Human Somatosensory System. Cerebral Cortex, 2004, 14: 851-857.

Liu L. and Ioannides AA. MEG Study of Short-Term Plasticity Following Multiple Digit Frequency Discrimination Training in Humans. Brain Topography, 2004, 16: 239-243(5)

Jung P, Baumgärtner U, Bauermann T, Magerl W, Gawehn J, Stoeter P and Treede RD. Asymmetry in the human primary somatosensory cortex and handedness. NeuroImage, 2003, 19 : 913-923.

Kaas JH. Plasticity of sensory and motor maps in adult mammals. Annu. Rev. Neurosci. 1991, 14: 137-167.

Kaas JH, Florence SL and Jain N. Subcortical Contributions to Massive Cortical Reorganizations. Neuron, 1999, 22: 657-660.

Kakigi R. Somatosensory evoked magnetic fields following median nerve stimulation. Neurosci. Res., 1994, 20: 165-174.

Kaukoranta E, Hämäläinen J, Sarvas J and Hari R. Mixed and sensory nerve stimulation activate different cytoarchitectonic areas in the human primary somatosensory cortex SI. Exp. Brain Res. 1986, 60-66.

Kawamura T, Nakasato N, Seki K, Kanno A, Fujita S, Fujiwara S and Yoshimoto T. Neuromagnetic evidence of pre- and post-central cortical sources of somatosensory evoked responses. Electroencephalogr. Clin. Neurophysiol. 1996, 100: 44-50.

Komssi S, Huttunen J, Aronen HJ and Ilmoniemi RJ. EEG minimum-norm estimation compared with MEG dipole fitting in the localization of somatosensory sources at S1. Clin Neurophysiol., 2004,115: 534-42.

Kumabe T, Nakasato N, Inoue T and Yoshimoto T. Primary thumb sensory cortex located at the lateral shoulder of the inverted omega-shape on the axial images of the central sulcus. Neurol Med Chir., 2000,40: 393-401; discussion 402-3.

Lin YY, Shih YH, Chen JT, Hsieh JC, Yeh TC, Liao KK, Kao CD, Lin KP, Wu ZA and Low-Ho LT. Differential effects of stimulus intensity on peripheral and neuromagnetic cortical responses to median nerve stimulation. NeuroImage, 2003, 20: 909-917.

Nakamura A, Yamada T, Goto A, Kato T, Ito K, Abe Y, Kachi T and Kakigi R. Somatosensory homunculus as drawn by MEG. NeuroImage, 1998, 7: 377-86.

Niddam DM, Arendt-Nielsen L and Chen AC. Cerebral dynamics of SEPS to non-painful and painful cutaneous electrical stimulation of the thenar and hypothenar. Brain Topogr., 2000, 13: 105-114.

Noppeney U, Waberski TD, Gobbele R and Buchner H. Spatial attention modulates the cortical somatosensory representation of the digits in humans. Neuroreport, 1999,10: 3137-3141.

Nuwer MR, Aminoff M, Desmedt J, Eisen AA, Goodin D, Matsuoka S, Mauguiere F, Shibasaki H, Sutherling W and Vibert JF. IFCN recommended standards for short latency somatosensory evoked potentials. Report of an IFCN committee. International Federation of Clinical Neurophysiology. Electroencephalogr. Clin. Neurophysiol., 1994, 91: 6-11.

Oliveri M, Rossini PM, Pasqualetti P, Traversa R, Cicinelli P, Palmieri MG, Tomaiuolo F and Caltagirone C. Interhemispheric asymmetries in the perception of unimanual and bimanual cutaneous stimuli. A study using transcranial magnetic stimulation. Brain, 1999,122: 1721-1729.

Onishi H, Yamada T, Saito T, Emori T, Fuchigami T, Hasegawa A, Nagaoka T and Ross M. The effect of stimulus rate upon common peroneal, posterior tibial, and sural nerve somatosensory evoked potentials. Neurology, 1991,41: 1972-1977.

Parra J, Kalitzin SN and da Silva FH. Magnetoencephalography: an investigational tool or a routine clinical technique? Epilepsy Behav., 2004, 5: 277-285.

Riddle DR and Purves D. Individual variation and lateral asymmetry of the rat primary somatosensory cortex. J Neurosci., 1995,15: 4184-4195.

Rossini PM, Martino G, Narici L, Pasquarelli A, Peresson M, Pizzella V, Tecchio F, Torrioli G and Romani GL. Short-term brain 'plasticity' in humans: transient finger representation changes in sensory cortex somatotopy following ischemic anaesthesia. Brain Res., 1994,11,642: 169-77.

Rossini PM, Narici L, Martino G, Pasquarelli A, Peresson M, Pizzella V, Tecchio F and Romani GL. Analysis of interhemispheric asymmetries of somatosensory evoked magnetic fields to right and left median nerve stimulation. Electroencephalogr Clin Neurophysiol.,1994, 91: 476-482.

Rossini PM, Tecchio F, Pizzella V, Lupoi D, Cassetta E and Pasqualetti P. Interhemispheric differences of sensory hand areas after monohemispheric stroke: MEG/MRI integrative study. NeuroImage. 2001, 14 : 474-485. Erratum in: Neuroimage 2001, 14: 1230. Paqualetti P.

Slimp JC, Tamas LB, Stolov WC and Wyler AR. Somatosensory evoked potentials after removal of somatosensory cortex in man. Electroencephalogr. Clin. Neurophysiol., 1986, 65: 111-7.

Soros P, Knecht S, Imai T, Gurtler S, Lutkenhoner B, Ringelstein EB and Henningsen H. Cortical asymmetries of the human somatosensory hand representation in right- and left-handers. Neurosci. Lett., 1999, 271: 89-92.

Tecchio F, Rossini PM, Pizzella V, Cassetta E and Romani GL. Spatial properties and interhemispheric differences of the sensory hand cortical representation: a neuromagnetic study. Brain Res., 1997, 767: 100-108.

Tecchio F, Rossini, P.M. ,Pizella V, Cassetta E, Pasqualetti P and Romani G. A neuromagnetic normative data set for hemispheric sensory hand cortical representation and their interhemispheric differences. Brain Res. Protoc., 1998, 2: 306- 314.

Tecchio F, Pasqualetti P, Pizzella V, Romani G and Rossini PM. Morphology of somatosensory evoked fields: inter-hemispheric similarity as a parameter for physiological and pathological neural connectivity. Neurosci Lett., 2000, 287: 203-206.

Tecchio F, Padua L, Aprile I and Rossini PM. Carpal tunnel syndrome modifies sensory hand cortical somatotopy: a MEG study. Hum. Brain Mapp., 2002, 17: 28-36.

Tecchio F, Zappasodi F, Pasqualetti P and Rossini PM. Neural connectivity in hand sensorimotor brain areas: an evaluation by evoked field morphology. Hum. Brain Mapp., 2005, 24: 99-108.

Theuvenet PJ, Dunajski Z, Peters MJ and van Ree JM. Responses to median and tibial nerve stimulation in patients with chronic neuropathic pain. Brain Topogr., 1999, 11: 305-313.

Theuvenet PJ, van Dijk BW, Peters MJ, van Ree JM, Lopes da Silva FL and Chen AC. Whole-head MEG analysis of cortical spatial organization from unilateral stimulation of median nerve in both hands: no complete hemispheric homology. NeuroImage, 2005, 28: 314-325.

Toga AW and Thompson PM. Temporal dynamics of brain anatomy. Annu. Rev. Biomed. Eng., 2003, 5:119-45.

Toga AW and Thompson PM. Mapping brain asymmetry. Nat. Rev. Neurosci., 2003, 4: 37-48.

Treede RD and Kunde V. Middle-latency somatosensory evoked potentials after stimulation of the radial and median nerves: component structure and scalp topography. Clin. Neurophysiol., 1995,12: 291-301.

Tsutada T, Tsuyuguchi N, Hattori H, Shimada H, Shimogawara M, Kuramoto T, Haruta Y, Matsuoka Y and Hakuba A. Determining the appropriate stimulus intensity for studying the dipole moment in somatosensory evoked fields: a preliminary study. Clin. Neurophysiol., 1999, 12: 2127-2130.

Vanni S, Rockstroh B and Hari R. Cortical sources of human short-latency somatosensory evoked fields to median and ulnar nerve stimuli. Brain Res., 1996, 21: 25-33.

Vrba J and Robinson SE. Signal Processing in Magnetoencephalography. Methods 2001, 249-271.

Wall JT, Xu J and Wang X. Human brain plasticity: an emerging view of the multiple substrates and mechanisms that cause cortical changes and related sensory dysfunction after injuries of sensory inputs from the body. Brain Res. Rev., 2002, 39: 181-215.

Werner RA and Franzblau A. Hand dominance effect on median and ulnar sensory evoked amplitude and latency in a-symptomatic workers. Arch. Phys. Med. Rehabil., 1996, 77: 473-476.

White L, Andrews TJA, Hulette C, Richards A, Groelle M, Paydarfar J and Purves D. Structure of the Sensorimotor System. I: Morphology and Cytoarchitecture of the Central Sulcus. Cerebral Cortex, 1997, 7: 18-30.

White L, Andrews TJA, Hulette C, Richards A, Groelle M, Paydarfar J and Purves D. Structure of the Human Sensorimotor System. II: Lateral Symmetry. Cerebral Cortex, 1997, 7: 31-47.

Wikström H, Roine RO, Salonen O, Aronen HJ, Virtanen J, Ilmoniemi RJ and Huttunen J. Somatosensory evoked magnetic fields to median nerve stimulation: interhemispheric differences in a normal population. Electroencephalogr Clin. Neurophysiol., 1997, 104: 480-487.

Ziemus B, Huonker R, Haueisen J, Liepert J, Spengler F and Weiller C. Effects of passive tactile co-activation on median and ulnar nerve representation in human SI. Neuroreport, 2000, 27: 1285-1288.

Chapter 7

Sensory handedness is not reflected in cortical responses after basic nerve stimulation. A MEG study.

Andrew C. Chen, Peter J. Theuvenet, Jan C. de Munck, Maria J. Peters, Jan M. van Ree, Fernando L. Lopes da Silva.

Brain Topography, 2011 Nov 12 [Epub a head of print]

Abstract

Motor dominance is well established, but sensory dominance is much less clear. We therefore studied the cortical evoked magnetic fields using magnetoencephalography (MEG) in a group of 20 healthy right handed subjects in order to examine whether standard electrical stimulation of the median and ulnar nerve demonstrated sensory lateralization. The global field power (GFP) curves, as an indication of cortical activation, did not depict sensory lateralization to the dominant left hemisphere. Comparison of the M20, M30, and M70 peak latencies and GFP *values* exhibited no statistical differences between the hemispheres, indicating no sensory hemispherical dominance at these latencies for each nerve. Field maps at these latencies presented a first and second polarity reversal for both median and ulnar stimulation. Spatial dipole position parameters did not reveal statistical left-right differences at the M20, M30 and M70 peaks for both nerves. Neither did the dipolar strengths at M20, M30 and M70 show a statistical left-right difference for both nerves. Finally, the Laterality Indices of the M20, M30 and M70 strengths did not indicate complete lateralization to one of the hemispheres. After electrical median and ulnar nerve stimulation *no* evidence was found for sensory hand dominance in brain responses of either hand, as measured by MEG. The results can provide a new assessment of patients with sensory dysfunctions or perceptual distortion when sensory dominance occurs way beyond the estimated norm.

Introduction

Hand dominance generally refers to the unequal distribution of motor skills and manual preference. In humans it has been found, based on several qualities, that right handedness is present in around 90% of the population (Hatta, 2007; Siengthai et al., 2008; Gardener et al., 2009) and left handedness in about 8% (Reiss et al., 2002). While mixed handedness is the ability to perform certain tasks better with one of the two hands, ambidexterity is the ability, in a minority of people, to use both the right and left hand for all tasks. Handedness therefore relates to the ability to perform some motor tasks better and is the result of a highly integrated (including visual and auditory) somatosensory - motor response (Annett, 2000; Reiss et al., 2000; Inoue et al., 2001; Haaland et al., 2004; Shinoura et al., 2005; Gentilucci et al., 2008). The question has arised whether asymmetry also exists in the representation of elementary sensory functions.

To address these issues, several characteristics of the somatosensory cortex have been examined. Right handedness was not correlated to gross lateral asymmetry in the *neuroanatomy* of the somatosensory system (White et al., 1997[a,b]) but several *functional* differences were described. In humans, strong correlation between handedness and the extent of the cortical hand representation in right-, but not in left-handers was found (Sörös et al.,1999). Jung et al. (2003; 2008), further reported that asymmetry of the cortical evoked responses appeared to be independent of motor function. Sensory lateralization to the right hemisphere was found in a large group of healthy individuals after *painful stimulation* and was unrelated to motor lateralization (Lugo et al., 2002). Finally, Zappasodi et al. (2006) observed some interhemispheric differences, but such differences were non-dependent on age and gender. In the study of handedness, non invasive imaging techniques are increasingly used. The cortical evoked responses, using electroencephalography (EEG) and magnetoencephalography (MEG) respectively, after standard electrical median and ulnar nerve stimulation have been studied (Babiloni et al., 2009; Darvas et al., 2004). Responses in the first 40 milliseconds (ms) post stimulus period were reproducible (Hari et al., 1993; Theuvenet et al., 1999; Kakigi et al., 2000; Castillo et al., 2005) and subsequently these responses have been in basis of many patient studies, including stroke (Goto et al., 2008), extremity amputation (Flor, 2003) or after painful stimuli (Treede et al., 2000). Evoked magnetic fields, measured by MEG arise when electrical stimulation elicits a contra-lateral cortical evoked response. MEG is known for its high temporal (< 1 msec) and good spatial accuracy (1-2 mm), moreover fissural cortical activity is better observed (Hari and Forss, 1999; Papadelis et al., 2011). Therefore, MEG is a highly appropriate technique to study sensory handedness, by detecting possible systematic differences in cortical responses due to left and right hand stimulation of median or ulnar nerve.

The aim of this study was to assess whether in a group of twenty right handed healthy subjects, after electrical median and ulnar nerve stimulation, the cortical evoked magnetic field characteristics would demonstrate sensory lateralization in the 400 ms post stimulus time window. We hypothesize that if right hand dominance would imply right sensory lateralization, this would be expressed in a systematic difference in lateralization of magnetic field characteristics generated by either left or right hand stimulation. The focus was on (1) the peak latencies, (2) the Global Field Power (GFP), (3) topographical maps of the somatosensory evoked fields, (4) equivalent current dipole (ECD) characteristics. Further, if evidence for asymmetry

of sensory fields existed, this might in turn affect the magnitude of responses to sensory input.

Materials and Methods

Healthy subjects

Twenty subjects (12 males and 8 females, range 27- 48 years, mean 34.1 and s.d. ± 6.1 years, all Caucasian right handed) were recruited from two hospital staffs. The Medical Ethical Committee of the Medical Center Alkmaar (NH04-196) and the VU University medical center approved of this study. All subjects were adequately informed, prior to the measurements an informed consent was obtained. The Edinburgh handedness inventory (Oldfield, 1971) was used to assess handedness.

Counter balanced electrical median and ulnar nerve stimulation.

Electrical stimulation of all four hand nerves was performed for each subject. The four nerves received a number, the left median nerve a "1" and the left ulnar a "2", for the right side "3" and "4" respectively. The order of stimulation was randomized for each subject (i.e. 1,3,2 and 4). Nerve stimulation with a bipolar electrode (cathode proximal) was performed at the wrist, according to the IFCN Guideline (Nuwer et al.,1994). An electrical stimulator (Grass, USA; model S48), using a photoelectric stimulus isolation unit (Grass, USA; model SIU7), was employed. LH means response in the Left Hemisphere after right hand stimulation, RH after left hand stimulation. All subjects were studied a single session that lasted approximately 45 minutes while between the measurements, enough recovery time (5 -10 minutes) was ensured. The stimulation current was pulsed, with a repetition rate of 2 Hz and pulse duration 0.2 ms. Stimulus intensity was adjusted to the individual twitch level using the threshold of thenar muscle, a clear painless twitch of either the thumb or the little finger was produced (Tsutada et al., 1999). Stimulations were well tolerated, per nerve five hundred stimulations were recorded. After each 100 stimulations, electronic repositioning of the head to the magnetic measuring system was performed to improve position accuracy. All subjects were asked to relax, to keep the eyes open, to focus on a fixed point on the ceiling and to refrain from blinking as much as possible.

Magnetoencephalography (MEG) and Magnetic Resonance Imaging (MRI) recordings.

All recordings were performed in a 3-layer magnetically shielded room (Vacuum Schmeltze GmbH, Germany), using a 151-channel whole-head gradiometer system (VSM - CTF, Canada) in the synthetic 3rd-order gradient mode with a gradiometer baseline of 5 cm. The x, y and z coordinate system, common to the MEG and MRI, was based on three anatomical landmarks fixed on nasion, left and right pre-auricular points and applied to all subjects. Using the positions of these fiducials, a head centered coordinate frame was defined. The (+) x-axis was directed to the nose, the (+) y-axis to the left ear and the (+) z-axis to the vertex. The head centered coordinate frame, defined by using the positions of these fiducials is based on each individual MRI. Using the coordinates of the sensors in multiple recording sessions, we determined the best recording position as the position in which the smallest rotation and translations were necessary to align all data sets. For the recordings per subject the positional variations were quite small; the mean rotation angle amplitude was 3.8 degrees, the mean translation distance was 0.4 cm. The average subjects head was positioned 0.02 cm left from the centre of the helmet. In order to increase accuracy, after each 100 stimulations the position of the head to the helmet was

electronically assessed.

MEG signals were sampled at 1250 Hz and triggered on the synchronization pulse of the electric stimulator. The peri-stimulus interval consisted of a 50 ms pre-trigger and a 400 ms post-trigger period. On-line filters were set at DC for high-pass and at 400 Hz (4^{th} order Butterworth) for anti-aliasing low-pass. Off-line the MEG data were screened for artifacts, averaged and DC-corrected using the pre-trigger interval to determine the recording offset. A small number (max 50) of events containing too much disturbances due to movement or blinking was rejected manually from all measurements. Also the +/- averages were calculated to obtain noise-level estimates. MRI' s of the brain were performed with a 1.5T 3d-mri (Siemens Sonata) and the MRI scan planes were set parallel to the MEG coordinate system. In this way, we achieved MEG superimpositions on MRI images with a precision of 2–3 mm as previously shown by simulation with artificial "dipoles" within a skull.

Global Field Power (GFP).
In MEG, the GFP expresses the cortical spatial magnetic energy distribution during the measurement and reflects underlying hemispherical neural activity at each time point (Lehmann et al., 1980; Skrandies, 1990). Off line the GFP (in femtoTesla^2 = fT^2) was assessed for all eighty measurements. Asymmetry of GFP distribution indicates lateralization of hemispheric activation. In MEG, and also in EEG (Hamburger et al., 1991), the GFP together with the Compressed Waveform Profile (CWP) is used to identify peak latencies. A peak was identified by visual inspection and defined by an amplification factor (= post stimulus amplitude / the prestimulus root mean square value as an indication of noise) > 3. In the temporal domain, hemispheric lateralization in timing of activation will be expressed in the peak latencies and may indicate a difference in transmission and / or activation time (Chapman et al., 1985).

Equivalent Current Dipole (ECD) characteristics.
VSM - CTF software (Vrba, 2001) was used to obtain ECD data from the MEG measurements.
A conventional single equivalent current (moving) dipole analysis (e.g. Lin et al., 2003; Fuchs et al., 2004) was used for data evaluation. The head model, based on individual MRI's, was chosen to match the inner contour of the skull, matching was done visually. Peaks in the post stimulus 400 ms time window, were analyzed. At each major peak, representing a cortical area of interest, six dipole characteristics (3 location, 2 orientation and strength) were determined. In particular, dipole strength was earlier described as a reliable quantitative index of cortical response to a somatosensory stimulus (Tsutada et al., 2002).

Data processing and statistical analysis.
This study was designed as an explorative study for the parameters that describe the cortical evoked differences between twenty healthy subjects. Since ample experimental and quantitative results as to the magnitude of the expected effects for sensory lateralization were available, a formal calculation of a prespecified power was not possible. Absence of an a priori power analysis indicates that negative statistical results have to be interpreted with caution since an existing difference may not be detected. Experimental design consisted in all cases of two-groups comparisons. Comparisons were made between the Left Hemisphere (LH) and Right Hemisphere (RH) for each nerve, as well as intra-hemispherical comparisons (LH or RH) between the two nerves. Effect sizes and p-values are reported wherever relevant magnitudes of effects existed. Whereby:

$$\text{Effect Size (E.S.)} = \frac{\text{mean experimental group} - \text{mean control group}}{\text{standard deviation control group}}$$

The effect size (Olejnik et al., 1999; Nakagawa et al., 2007) is a numerical way of expressing the strength or magnitude of a reported relationship, be it causal or not. An E.S. near 0.0 means that, on average, the experimental group and control group performed the same, a negative E.S., on average, means that the control group performed better. A positive E.S. means that the experimental group performed better than the control group. The more effective the intervention, or in our context, the more prevalent sensory dominance of the right hand, the higher the positive E.S. value. Statistical tests used were the independent groups t-test (or its non-parametric equivalent the Mann-Whitney rank sum test) for between groups comparisons, and the paired t-test (or its non-parametric equivalent the Wilcoxon signed ranks test) for within groups comparisons. Pearson correlation analyses were conducted to examine the association of the handedness values with respective laterality indices of strength. A p-value less than 0.05 was considered as a statistically significant rejection of the null-hypothesis specified with two-tailed alternative hypotheses. Statistical analysis was performed using SigmaStat 3.5 software. Manufacturers VSM - CTF software 4.6 (Vrba, 2001) was used to perform online data-analysis during all measurements and off line averaging. All further data-analysis (i.e. latencies, GFP values) and graphical display was performed employing ASA software (Advanced Source Analysis, ANT A/S, Enschede, The Netherlands).

By comparing the left and right cortical evoked field characteristics, laterality dominance could be confirmed if the Laterality Index (L.I.) favored one hemisphere more than the other. Here, the L.I. is determined for various parameters characterizing the cortical responses. When a parameter due to left hand stimulation equals RHp (largest response expected at the right hemisphere) and the corresponding parameter due to right hand stimulation equals LHp, the LI is defined as (Jung et al., 2003; Theuvenet et al., 2005; Hatta, 2007).

$$L.I. = (LH_p - RH_p) / (LH_p + RH_p).$$

The laterality index was determined for the *strength* of the dipoles (nanoAmperemeter = nAm) at the latencies of 20 ms, 30 ms and 70 ms post-stimulus (M20, M30 and M70 respectively). Moreover, *stimulation thresholds* were determined for all subjects and nerves since stimulus intensity may affect cortical responses (Torquati et al., 2002).

Results

I. Psychophysics

I A. Sensory sensitivity in both hands to electrical stimulation (milliAmpere - mA)

Handedness of the subject group, according to the Edinburgh inventory, presented a mean value of 71.4 and standard deviation (s.d.) of ± 11.0 confirming dexterity.

After left median nerve stimulation, the mean twitch threshold was 5.5 mA (s.d. ± 1.7 mA), and after right median stimulation 5.8 mA (s.d. ± 1.6 mA). For the left ulnar nerve values were, mean 5.8 mA (s.d. ± 2.0 mA) and the right nerve 5.9 mA (s.d. ± 1.6 mA). Individual data of the subjects are presented in Fig. 1A and 1B. Between the left and right median nerve no significant statistical difference *($p = 0.16$; E.S.= - 0.13*) in thresholds was found, neither after ulnar nerve stimulation *($p = 0.26$; E.S.= -0.06).*

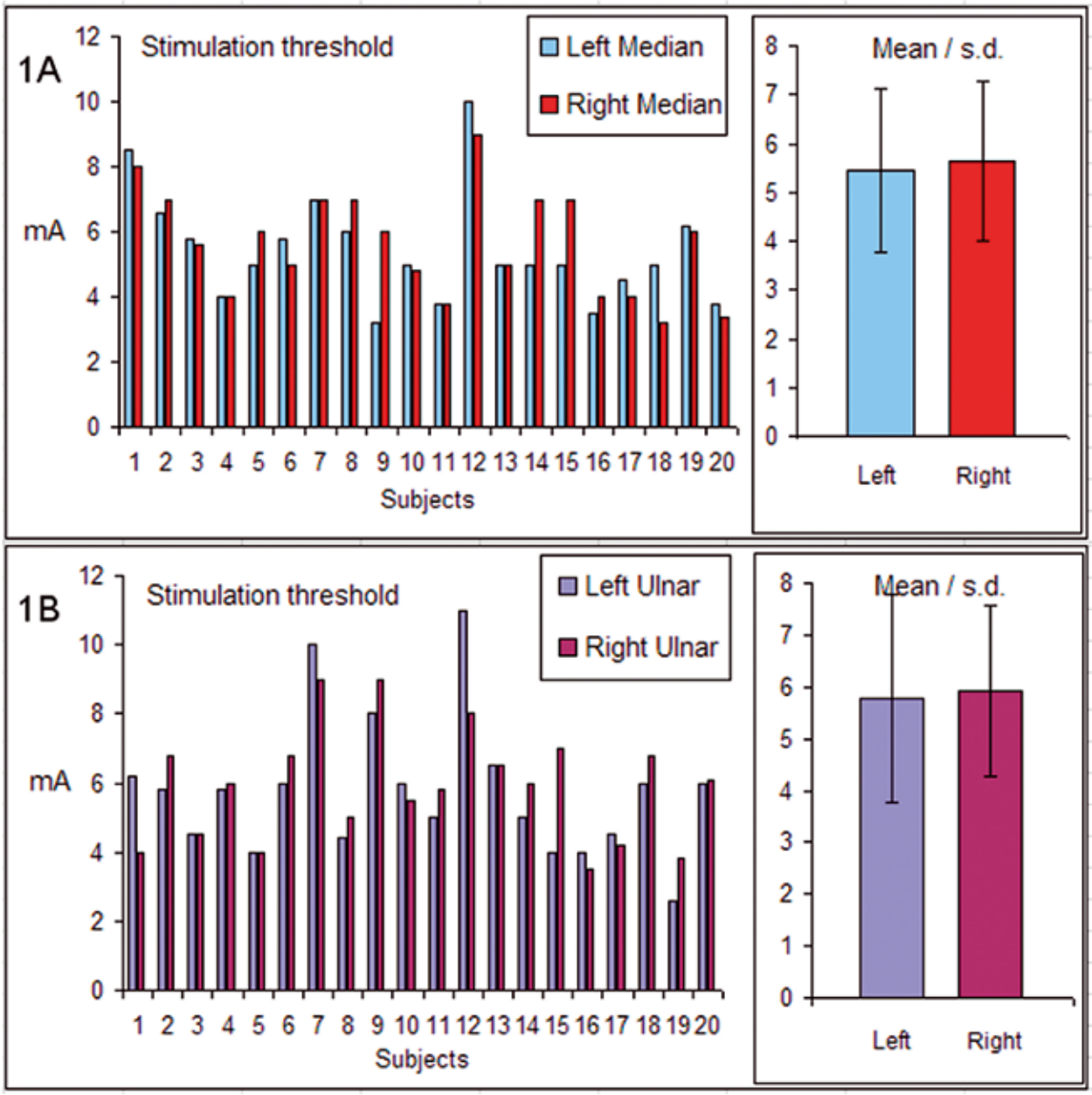

Fig. 1A. Median nerve: consistency of individual sensory sensitivity and comparisons after electrical median nerve stimulation of both hands is displayed. The right side depicts means and standard deviations (s.d.) between left and right hand thresholds. Fig. 1B. Ulnar nerve: stimulation thresholds for both hands are presented. On the right side means and standard deviations (s.d). Stimulation thresholds (y-axis) in milliAmpere (mA).

I B. Peak latencies and Global Field Power (GFP)

Fig. 2 displays the mean GFP overlay curves for all four stimulated nerves in the 400 ms post-stimulus period of both hemispheres. *Morphologically*, left and right median GFP curves (black and red) run parallel and the same is observed for the ulnar curves (blue and green). *Peaks*: in the *early stage* (<50 ms), a small M20 but larger M30 peak is observed. Apart from faster ulnar transmission to the RH at M30, no statistical peak latency

differences were found inter-hemispherically for both nerves of both hands. At M20, median intra-hemispherical transmission (LH or RH), was significantly faster than for the ulnar nerve. In the *middle stage* (50 - 90 ms) a dominant peak for both nerves is present, further referred to as the M70. At M70, there were no significant latency differences between the LH and RH for both nerves. Nor was transmission intra- hemispherically to either the LH or RH different between the nerves (see Table 1A, B and C, Supplementary Digital Content 1, latency & statistical data).

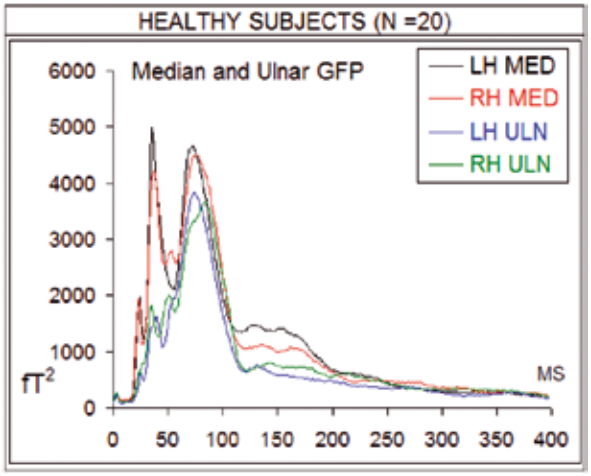

Fig. 2. The GFP overlay curves for all four stimulated nerves in the 400 ms time window are displayed. Each colored line represents the mean GFP values of a stimulated nerve. LH means Left Hemispheric response to right hand nerve stimulation (either median or ulnar), RH the same but for the left hand. The top two lines (black and red) depict the mean GFP values for the median nerve, the lower two lines (blue and green) for the ulnar nerve. Median induced GFP curves displayed higher components in the first 90 ms. The Power is in femtoTesla2, time in milliseconds (MS).

GFP values: at M20, M30 and M70, no significant GFP value differences were found between the LH and RH for either nerve (see Table 1A, 1B). At M20 and M30, in the LH or the RH, the median values were significantly larger than the ulnar GFP values (Table 1C). For the M70 peaks, there was *no* statistical significant intra-hemispherical (either LH or RH) GFP difference between the median and ulnar GFP values.

II. 3D Cortical topography of Somatosensory Evoked Fields

II A. Cortical field maps.

In Fig. 3, the cortical maps of a typical subject (HC-15), representing cortical activation at different peak latencies for each of the four stimulated nerves, are depicted. M-LH and M-RH depict the hemispherical evoked fields after right en left median nerve stimulation respectively. Between M20 and M30 an early dipole polarity reversal is seen as the second reversal around M150. Both reversals were found in > 85% of the subjects. After ulnar stimulation a comparable situation was observed in the left and right hemisphere (U-LH and U-RH), here also two reversals in over 85% of the subjects. The dipolar magnetic field distributions between the LH and RH for both nerves were visibly not different and are complementary. See Table Supplementary Digital Content 2 for data overview.

III Equivalent Current Dipole (ECD) characteristics

IIIA. Location parameters (x, y and z)

The six dipole parameters for the median and ulnar nerve at three latencies were calculated. For both nerves, M20, M30 and M70 data indicated that there was no statistical difference for both nerves and both hemispheres for the location parameters, except for the M20 ulnar x-value *(p = 0.013 and Effect Size 0.5).* The ulnar M20 was in the LH more posteriorly located.

At M70 in the LH and RH, *only* those single moving dipoles with a low residual error (< 8%) were included for presentation. For the median nerve

Table 1. GFP data and statistics are presented at M20, M30 and M70.

1A) SUBJECTS mean GFP values (fT^2)					
Median	M20		M30		M70
LH (20/20)	2988.9	LH (19/20)	5740.6	LH (20/20)	5701.3
s.d.	3445.6	s.d.	4954.1	s.d.	3814.6
RH (20/20)	2206.0	RH (19/20)	5283.3	RH (20/20)	6720.5
s.d.	2812.3	s.d.	3137.7	s.d.	5086.5
diff. RH-LH*	-782.9	diff. RH-LH*	-457.3	diff. RH-LH*	1019.2
Effect Size (E.S.)	-0.2	E.S.	-0.09	E.S.	0.27

1B) SUBJECTS (N=20) GFP values (fT^2)					
Ulnar	M20		M30		M70
LH (19/20)	1163.2	LH (19/20)	2458.3	LH (18/20)	4813.8
s.d.	1136.3	s.d.	2043.3	s.d.	4100.9
RH (18/20)	1116.2	RH (19/20)	3031.4	RH (19/20)	5764.4
s.d.	1225.8	s.d.	2969.2	s.d.	5098.7
diff. RH-LH*	-47.0	diff. RH-LH*	573.1	diff. RH-LH*	950.6
Effect Size (E.S.)	-0.04	E.S.	0.28	E.S.	0.23

1C) SUBJECTS (N=20) GFP values (fT^2)					
	M20		M30		M70
MLH - ULH*	P <0.001		P = 0.005		P = 0.431
Effect Size (E.S.)	1.6	E.S.	1.6	E.S.	0.21
MRH - URH*	P = 0.002		P <0.001		P = 0.347
Effect Size (E.S.)	0.89	E.S.	0.76	E.S.	0.18

Table 1. The M20, M30 and M70 mean GFP peak values, standard deviations (s.d.) and Effect Size values (E.S.) after median (1A) and ulnar (1B) stimulation of both hands are presented. Numbers between brackets indicate the number of peaks at each latency present out of twenty subjects. In 1C differences between the median and ulnar GFP groups are presented. MLH and ULH are the median and ulnar response in the Left Hemisphere (LH), MRH and URH indicate the same in the Right Hemisphere (RH). Peak GFP values are in femtoTesla^2 (fT^2).

13 / 20 and ulnar nerve 16 / 20 met this criterion (see Table 2) and were localized in SI. In Fig. 4, an example is presented of the M70 dipoles of subject HC-03. The M70 dipoles are depicted in three directions after stimulation of the median and ulnar nerve.

The M70 spatial coordinates (x, y and z) for the median nerve were (in mm): *LH* : x = -1.6; y = 40.3, z = 82.0; *RH* : x = -8.6; y = -43.2; z = 78.8. For the ulnar M70: *LH* : x = 4.2; y = 39.7; z = 81.0. The *RH* coordinates: x = 1.9; y = 39.3; z = 83.6 mm. The median and ulnar dipoles of subject HC-03 are located in the primary somatosensory cortex (SI).

Table 2 presents the dipole parameters at M20, M30 and M70 in both hemispheres for the two nerves.

2A MEDIAN			res. error	x	y	z	declination	azimuth	strength
LH	M20	mean	6,2%	2,1	42,4	84,9	75,6	323,4	25,3
		s.d.	2,1%	8,2	4,8	4,4	8,3	89,0	13,0
RH	M20	mean	6,4%	4,1	-42,1	84,5	68,9	21,6	21,9
		s.d.	1,5%	9,5	4,4	6,1	10,6	5,6	8,3
LH	M30	mean	4,3%	2,8	41,9	87,5	107,2	181,1	28,7
		s.d.	1,9%	7,8	6,4	6,4	12,7	63,8	9,8
RH	M30	mean	4,1%	3,7	-40,1	88,7	106,6	181,2	28,3
		s.d.	2,0%	9,9	4,1	4,8	13,0	64,3	13,7
LH	M70	mean	5.7%	-3,3	39,4	87,6	104,4	172,7	28,7
		s.d.	2.2%	9,3	5,8	6,4	9,7	15,7	9,0
RH	M70	mean	5.3%	2,2	-40,9	85,0	108,0	198,3	30,2
		s.d.	1.6%	9,4	5,3	4,7	9,3	18,3	8,1
2B ULNAR			res. error	x	y	z	declination	azimuth	strength
LH	M20	mean	6,1%	-0,7	35,5	87,9	67,9	331,0	13,4
		s.d.	1,8%	7,3	10,2	7,4	10,3	15,9	4,9
RH	M20	mean	7,2%	1,3	-35,5	92,5	79,0	84,2	14,7
		s.d.	2,9%	6,9	5,9	5,9	15,8	85,8	8,7
LH	M30	mean	5,9%	0,4	38,1	91,4	107,4	175,0	19,1
		s.d.	1,8%	6,9	5,6	5,8	13,3	65,6	8,2
RH	M30	mean	5,1%	2,9	-37,8	93,9	104,7	210,6	18,8
		s.d.	2,5%	6,3	4,3	5,7	11,7	41,7	8,9
LH	M70	mean	5,5%	-5,1	39,1	88,6	108,9	165,9	27,7
		s.d.	2,2%	8,3	4,3	7,8	8,7	18,3	14,5
RH	M70	mean	4,8%	1,4	-40,9	90,0	109,7	206,2	26,3
		s.d.	1,8%	8,1	5,9	6,3	8,9	25,6	9,9

IIIB. Orientation.

There was no statistical difference between the LH and RH for the spatial orientation parameters declination and azimuth, for the azimuthal differences after normalization.

III C. Strength.

At M20, M30 and M70, between the LH and RH, the dipolar strength (in nAm = nanoAmperemeter) for the median and ulnar nerve exhibited no significant statistical differences. However, the median dipolar strengths at M20 and M30 but not at M70, were significantly larger (paired t-test) than the ulnar ones for both hemispheres (see Table 3A, 3B and 3C).

III D. Laterality Indices (L.I.) of strength.

Laterality Indices of dipolar strengths (Fig. 5 A-F), assessed for both hemispheres and for both nerves at M20, M30 and M70, presented large individual variability between subjects. For both nerves, the sets of L.I. of dipole strengths at M20, M30 and M70 exhibited no particular trends, with no significant statistical differences (Fig. 5). In Table 3D relevant data for correlation between handedness and L.I. values are presented for

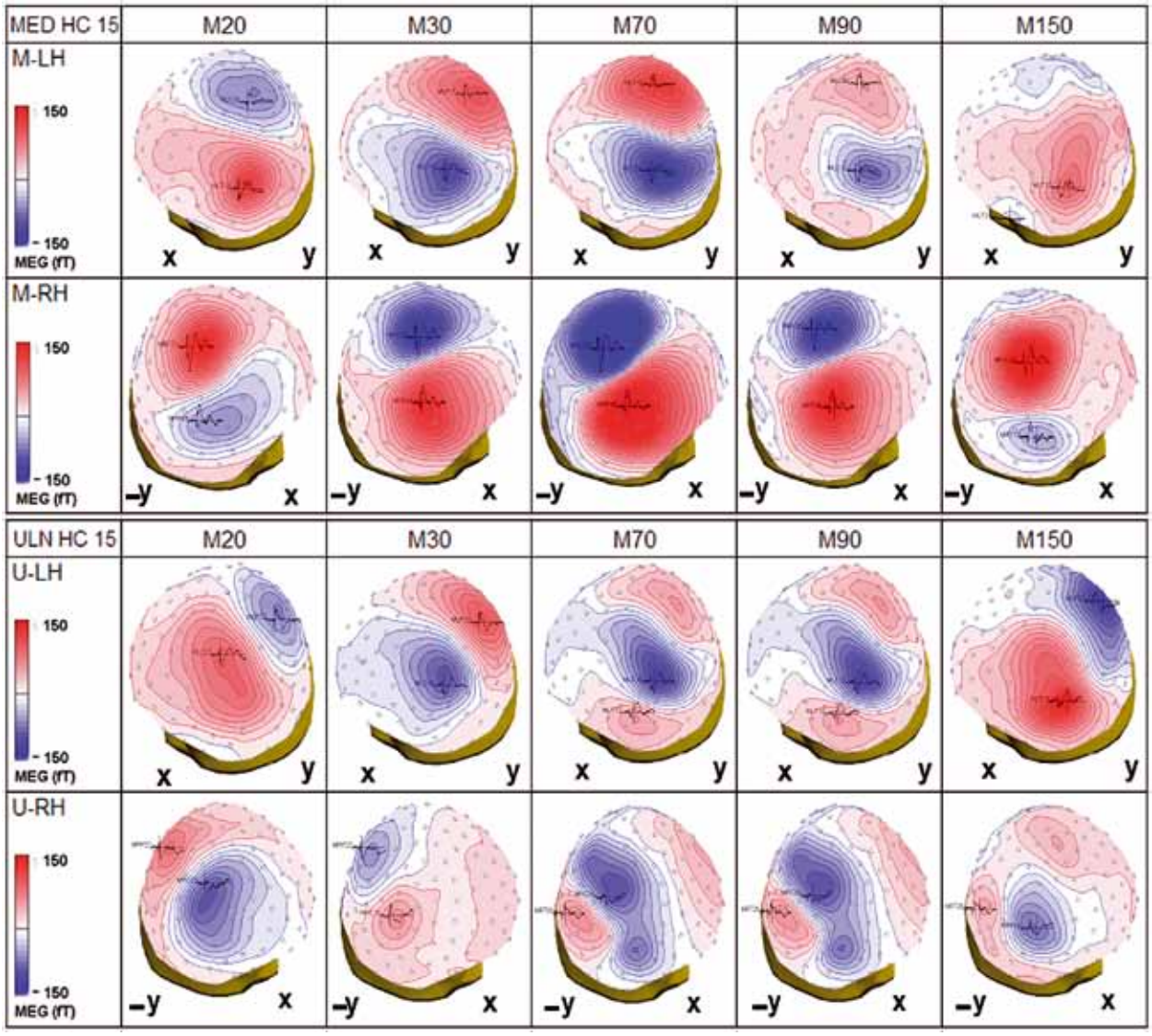

Fig. 3. Cortical maps at M20 and M30 (1st polarity reversal) and M90 and M150 (2nd reversal) after median nerve stimulation are presented of the subject HC-15 in the two top rows. Cortical maps at M20 and M30 (1st polarity reversal) and M90 and M150 (2nd reversal) after ulnar nerve stimulation are presented in the lower two rows. Amplitude settings: ± 150 fT. Less color intensity, red or blue, corresponds with lower amplitudes.

the median and ulnar nerve. Pearson correlation coefficient values (r-value) and p-values indicate their associated probabilities. No significant association between the handedness scores and the respective measured M20, M30 and M70 L.I. values were found. It appeared that this feature of handedness does not suggest an actual difference in the laterality index, indicating no lateralization in somatosensory processing to dominant LH.

3A	*MEDIAN*		*ULNAR*		MEDIAN versus ULNAR	
M20		strength	M20	strength	M20	
	LH mean*	25.3	LH mean*	13.4	MLH - ULH*	MRH - URH*
	s.d.	13.0	s.d.	4.9		
	RH mean	21.9	RH mean	14.7		
	s.d.	8.3	s.d.	8.7		
	p-value	p = 0.354	*p-value*	p = 0.754	p = <0.001	p = <0.001
	stat. test	*M-W rst*		*M-W rst*	*Paired t-test*	*Paired t-test*
	Effect Size	-0.26	E.S.	0.27	2.43	0.82
3B	*MEDIAN*		*ULNAR*		MEDIAN versus ULNAR	
M30		strength	M30	strength	M30	
	LH mean*	28.7	LH mean*	19.1	MLH - ULH*	MRH - URH*
	s.d.	9.8	s.d.	8.2		
	RH mean	28.3	RH mean	18.8		
	s.d.	13.7	s.d.	8.9		
	p-value	p = 0.252	*p-value*	p = 0.899	p = <0.001	p = 0.003
	stat. test	*Wilcox. srt*		*M-W rst*	*Paired t-test*	*Paired t-test*
	Effect size	-0.04	E.S.	-0.04	1.17	1.07
3C	*MEDIAN*		*ULNAR*		MEDIAN versus ULNAR	
M70		strength	M70	strength	M70	
	LH mean*	28.7	LH mean*	27,7	MLH - ULH*	MRH - URH*
	s.d.	9.0	s.d.	14,5		
	RH mean	30.2	RH mean	26,3		
	s.d.	8.1	s.d.	9,9		
	p-value	P = 0.674	*p-value*	P = 0.843	P = 0.482	P = 0.207
	stat. test	*M-W rst*		*M-W rst*	*M-W rst*	*M-W rst*
	Effect size	0.16	E.S.	-0.10	0,07	0.39
3D	M20 MED L.I.	M20 ULN L.I.	M30 MED L.I.	M30 ULN L.I.	M70 MED L.I.	M70 ULN L.I.
handedness	r = 0.072	r = 0.36	r = 0.147	r = 0.042	r = 0.197	r = 0.00
p-value	p = 0.75	p = 0.11	p = 0.52	p = 0.85	p = 0.39	p = 0.97

Table 3A-C. Mean strength values (in nanoAmperemeter) and standard deviations (s.d.) for the M20,M30 and M70 peaks, after median and ulnar nerve stimulation, are presented. MLH means the response in the Median Left Hemisphere, ULH means Ulnar Left Hemisphere. Comparable abbreviations for the right hemisphere. Significant p-values are in grey fields. Statistics: M-W rst = Mann-Whitney rank sum test; Wilcox srt = Wilcoxon signed rank test. Table 3D presents the Pearson correlation (r) values between handedness and Laterality Index (L.I.).

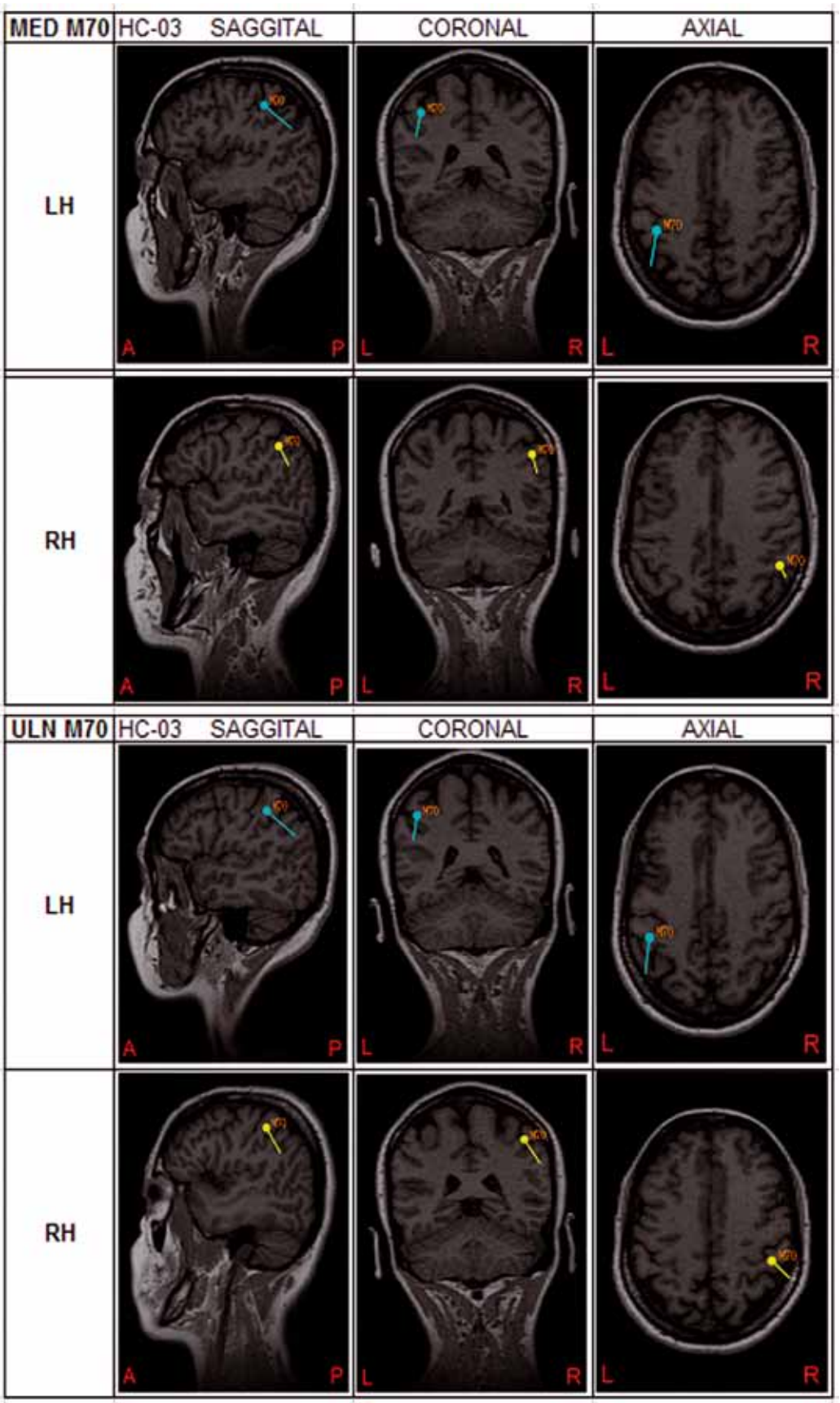

Fig. 4. The M70 dipoles after median and ulnar nerve stimulation (subject HC-03) are depicted in three directions: sagittal, coronal and axial. Both dipoles are located in the primary somatosensory cortex.

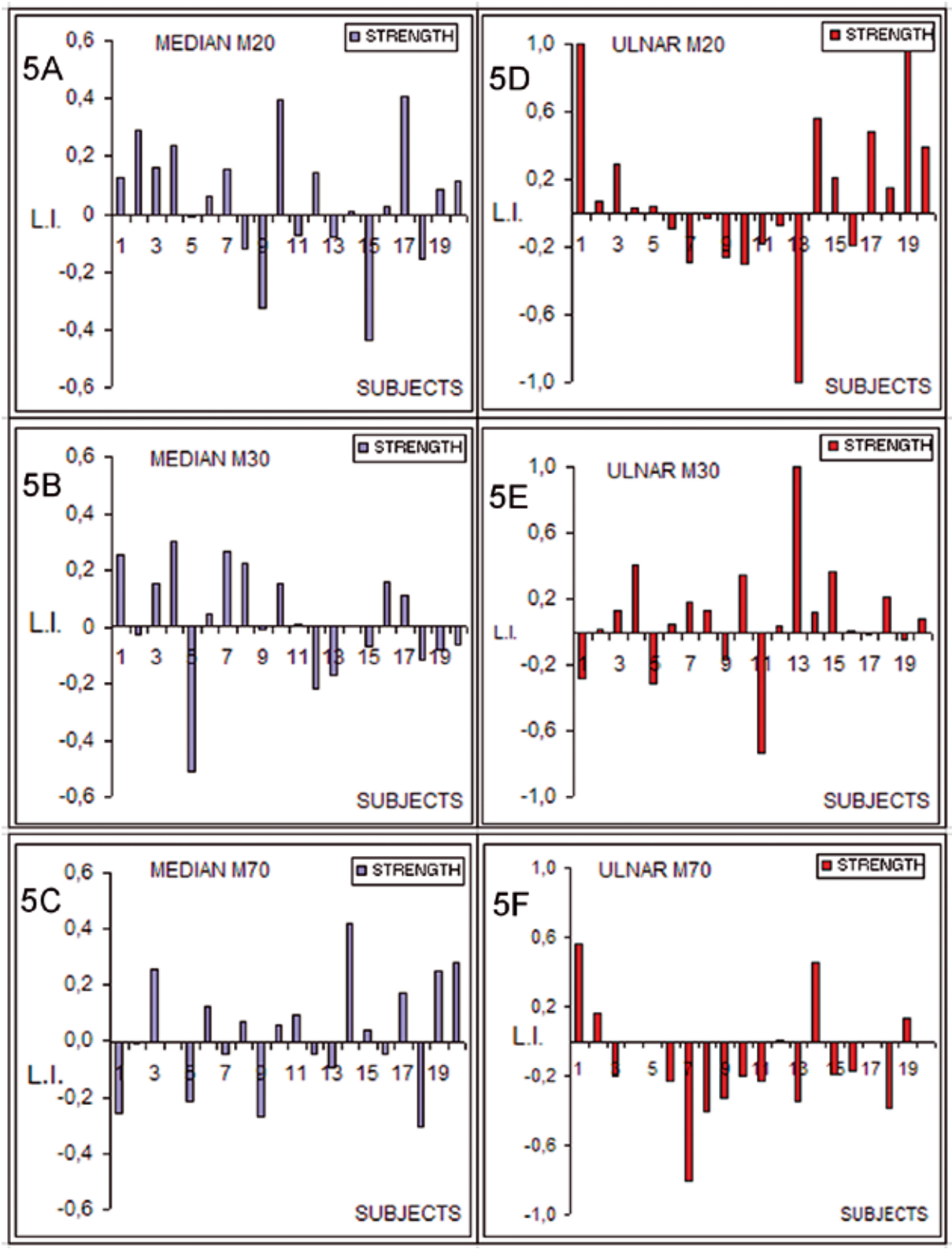

Fig. 5A. The Laterality Indices (L.I.) at M20 after median nerve stimulation are presented for all subjects, 13/20 had a positive L.I. and 7/20 a negative L.I. Fig. 5B. The results after median nerve stimulation at M30 are presented, 11/20 had a positive L.I. and 9/20 a negative L.I.. Fig. 5C. At M70 for the median nerve in 10/20 a positive L.I., 8/20 a negative L.I. and 2/20 with a L.I. of zero. Fig. 5D. The L.I. values at the Ulnar M20 are depicted, 11/20 had a positive L.I. and 9/20 a negative L.I. Fig. 5E. For the ulnar nerve at M30, 14/20 with a positive L.I., 4/20 a negative and two with a zero L.I. were found. Fig. 5F presents for the ulnar nerve at M70, 4/20 a positive L.I., in 11/20 a negative L.I. and 5/20 a zero L.I.. No hemispherical sensory lateralization could be demonstrated for both nerves.

Discussion

We stimulated in a healthy subject group (N=20) all four hand nerves in a randomized way, and applied a standard protocol (motor twitch level producing a clear painless twitch of either the thumb or the little finger and 500 stimulations at each nerve). Statistical analyses demonstrated that in the median or ulnar groups, no statistical significant threshold differences were found. Comparison of the median versus ulnar thresholds of both hand demonstrated the same. Cortical evoked responses relate to stimulus type and intensity (Tsutada et al., 1999) and responses in the *primary and secondary somatosensory cortices* (SI and SII respectively) vary from non-painful to painful stimulation (Torquati et al., 2002). In this study, no significant statistical left - right stimulus (threshold) intensity differences were found after standard electrical median and ulnar nerve stimulation. Therefore, the measured cortical evoked responses and derived main functional indices of hemispherical (a)symmetry are not influenced by intensity differences.

Based on the *GFP curves* and related *GFP peak values* for both the median and ulnar nerve, major cortical activation was demonstrated in the early (< 50 ms) and middle stage (50 - 90 ms). No significant lateralization of cortical activation to the dominant LH occurred in these stages. The median GFP peak values at M20 and M30 were significantly larger compared to the ulnar peak values. Based on the GFP definition, this indicates that after electrical median nerve stimulation, a relatively larger cortical area is activated compared to ulnar stimulation, possibly due to a larger spatial cortical presentation of the median nerve. Based on the morphological cortical GFP distributions after median and ulnar nerve stimulation, we have only studied the major peaks at M20, M30 and M70. Based on individual data, in the late stage in this study a M150, M180 and M240 peak with dipolar field characteristics was found. However, at the GFP group level after 90 ms, cortical magnetic distribution as indicated by the GFP curves, did not display major differences in activation. We are aware of the fact that there is in MEG a lack of sensibility for radial oriented dipoles. The lack of sensibility to detect the effect of handedness in the late stage (left hand vs. right hand) in the MEG sources can be contrasted with the cortical SEP maps. This was shown in Fig.1 of our earlier report (Niddam et al., 2001). The early and middle stage components (C4'/P25, F2/N35, C4'/P45, Fc2/N65), exhibited no differences between left-hand and right hand stimulations. The peak SEP topography was vividly shown with its largest magnitude at 240 ms, among all peak components. In the EEG-SEP, the 240 ms peak is much bigger than the early and middle stage components (20-90 ms), but shows relatively little activity in the late MEG-SEF. Thus, the influence of radial dipoles on late components (> 90 ms) is evident.

The *six ECD characteristics* of the M20 and M30 dipoles, which reside in SI, demonstrate no lateralization for both nerves. However, the ulnar dipole is more medially positioned, the median dipole more laterally. The only significant difference was found at M20 for the ulnar nerve, on the x-axis the dipole in the LH was located more posteriorly. Accurate characterization of the dipolar magnetic fields and related parameters at M70 still suffer from the absence of a reliable model for multiple ECD calculations, more generators are activated simultaneously. However, using a single moving dipole model for subjects with low residual errors of fit (< 8%) at M70 for both nerves, dipoles are localized in SI. Activity after M70 is commonly attributed to the secondary somatosensory cortex - SII (Hari et al., 1993, 1999; Simões et al., 2002; Castillo et al., 2005), notwithstanding

the large latency difference of activation (around 40 ms) with SI (Kawamura et al., 1996; Frot et al., 1999). The M70 dipoles in this study displayed only contralateral activity which makes localization in SII unlikely, bilateral activation for both nerves appeared after 90 ms post stimulus. This study also demonstrates that after electrical median and ulnar nerve stimulation, contralateral somatosensory processing in SI starts as early as M20 and continues to the middle stage at M70 in both hemispheres and for both nerves. The combination of CWPs and GFPs, in assessing the major peak latencies, produced a more accurate picture at M70 compared to a previous study (Theuvenet et al., 2005). Peak latencies at M20, M30 and M70 were not significantly different, supported by the Effect Size data and indicated no lateralization of transmission time or reaction time (Brancucci, 2010).

3D cortical mapping revealed dipolar fields at the major peak latencies with an early and late polarity reversal for both nerves, the significance for brain processing and accurate somatotopic organization is unknown but was observed earlier (Theuvenet et al., 2006). The spatial dipole localization parameters (x, y and z values) differed little, the only significant difference was found at M20. The Laterality Indices combined with statistical data of the dipole strengths at M20, M30 and M70 for the median and ulnar nerve did not provide evidence for sensory lateralization to the dominant LH. This indicates that in both hemispheres at these three major peak latencies, synchronous activation of a higher number of SI neurons occurs and agrees with the GFP curves of both nerves found in this study. In a recent EEG study in a group of 50 subjects (20-70 years), using intraclass correlation coefficient and correlation coefficient between GFP of left and right median nerve somatosensory evoked potentials, a high symmetry was found in healthy subjects (Van den Wassenberg et al., 2008). This situation changes essentially as soon as tasks are executed. In a group of right handed subjects it was demonstrated that depending on the complexity of the executed tasks, different parts of the dominant and non-dominant hemisphere cooperate, making handedness a relative quality (Halsband et al., 2006; Gut et al., 2007; Brenneman et al., 2008). New insights into the ability of the human brain to adapt during life (Rossini et al., 2004), as demonstrated in healthy humans like violin players (Schwenkreis et al., 2007), patients and animals (Kaas et al., 1983), the connecting functional principle between motor and sensory system still has to be elucidated. Handedness may prove to be a quality that can best be understood within the context of the tasks performed. Hemispherical asymmetry is possibly best correlated with the motor cortex (Volkmann et al., 1998), more observed in task dependant studies and as supported by this study to a far lesser extent with the elementary aspects of the somatosensory system.

This non-task dependant study certified that the cortical evoked field characteristics after standard electrical median and ulnar nerve stimulation, using a whole-head 151 channel MEG system, did not demonstrate sensory lateralization to the left dominant hemisphere in a group of twenty right handed subjects. Peak latencies, MEG field distribution (GFP) and dipole source parameters exhibited comparable values in the right and left hemispheres in response to contra lateral hand stimulation and did not differ significantly. Hence, the hypothesis that "hemispherical right motor dominance would be represented in the characteristics of the sensory evoked magnetic fields", has to be rejected. Any intra- and inter-individual comparison between studies requires at least the same or a comparable measuring protocol since the human somatosensory cortex

SI varies topographically to a certain extent (Geyer et al., 2000). In the past, several studies on cortical evoked responses in patients were published without a healthy control group studied for comparison. Statements on brain structure-functional relationships, without taking into consideration variation in hemispheric (a) symmetry, will remain incomplete (Birklein et al., 2005; Hugdahl, 2010). In addition, the effect of handedness on the sensory-motor system of the human hands is not yet fully understood. This study was restricted to right-handed subjects while the effect of handedness on the left-handed subjects requires further study to reinforce the main findings. On the level of the brain function in the interaction of SEF with alpha rhythms, alpha rhythm may interact the activation of SEP (e.g. Reinacher et al., 2009). However, it is not in the scope of current study. This study strictly focused on the M20-M30-M70 peaks. The influence of gender differences was studied by Zappasodi et al., 2006. Cortical interhemispheric differences after electrical nerve stimulation were quite symmetrical in the two hemispheres, making the interhemispheric differences relatively non-dependent of gender. In a broader perspective, final conclusions on the neurophysiological dominance vs. non-dominance of somatosensory systems requires further confirmation in future studies including brain rhythms, radial sources of evoked EEG responses, long-latency evoked responses and sensorimotor gating effects. Of note, these mentioned limitations do not drop down the importance of the present findings also for future clinical applications.

Conclusion

From the psychophysical evidence and responses to the contralateral global field power or the peak and peak potentials of early dipoles in SEF, it is concluded that there is no sensory dominance of human hands in a group of right-handed subjects. In contrast to the apparent motor dominance (dexterity, strength) of the right hand. Little depiction of sensory lateralization to the dominant left hemisphere is shown, both hemispheres are equal in sensory reactivity.

Acknowledgements. This study was made possible by a grant from Medtronic Tolochenaz (Switzerland) and technically supported by the MEG Centre (B.W. van Dijk, PhD), Dept. of Clinical Neurophysiology (Head: Prof. C.Stam), VU Hospital, Amsterdam. Clinical support by Mrs. M.A. Dekkers, MSc, Medical Center Alkmaar, The Netherlands. In addition, this research project has also been supported by a Grant from the Chinese National Science Fund (NSF 30770691).

References

Annett M (2000). Predicting combinations of left and right asymmetries. Cortex 36:485-505.

Birklein F, Rowbotham MC (2005). Does pain change the brain? Neurology 13:666-667.

Babiloni C, Pizella V, Del Gratta CD, Feretti A, Romani GL (2009). Fundamentals of electroencephalography magnetoencephalography, and functional magnetic resonance imaging. Int Rev of Neurobiol 86:67-81.

Brenneman MH, Decker S, Meyers J, Johnson K (2008). Does a continuous measure of handedness predict reading processes and reading-related skills across the lifespan ? Laterality 13:481-503.

Brancucci A (2010). Electroencephalographic and Magnetoencephalographic Indices of Hemispheric Asymmetry. In: Hugdahl K and Westerhausen R (ed) The two Halves of the Brain: Information Processing in the Cerebral Hemispheres. The MIT Press, Cambridge, pp 211-251.

Castillo EM, Papanicolaou AC (2005). Cortical representation of dermatomes: MEG-derived maps after tactile stimulation. NeuroImage 25:727-733.

Chapman RC, Schimek F, Colpitts YH, Gerlach R, Dong WK (1985). Peak Latency Differences in Evoked Potentials Elicited by Painful Dental and Cutaneous Stimulation. Int J Neurosci 27:1-12.

Darvas F, Pantazis D, Kucukaltun-Yildirim E, Leahy RM (2004). Mapping human brain function with MEG and EEG: methods and validation. NeuroImage Suppl 1:S289-99.

Flor H (2003). Remapping somatosensory cortex after injury. Adv Neurol 93:195-204.

Frot M, Mauguière F (1999). Timing and spatial distribution of somatosensory responses recorded in the upper bank of the sylvian fissure (SII area) in humans. Cereb Cortex 9:854-863.

Gardener H, Munger K, Chitnis T, Spiegelman D, Ascherio A (2009). The relationship between handedness and risk of multiple sclerosis. Mult Scler 15:587-592.

Gentilucci M, Dalla Volta R (2008). Spoken language and arm gestures are controlled by the same motor control system. Q. J Exp Psychol 61:944-957.

Geyer S, Schormann T, Mohlberg H, Zilles K (2000). Areas 3a, 3b, and 1 of human primary somatosensory cortex. Part 2. Spatial normalization to standard anatomical space. Neuroimage 11: 684-96.

Goto T, Saitoh Y, Hashimoto N, Hirata M, Kishima H, Oshino S, Tani N, Hosomi K, Kakigi R, Yoshimine T (2008). Diffusion tensor fiber tracking in patients with central post-stroke pain; correlation with efficacy of repetitive transcranial magnetic stimulation. Pain 140:509-18.

Gut M, Urbanik A, Forsberg L, Binder M, Rymarczyk K, Sobiecka B, Kozub J, Grabowska A. (2007). Brain correlates of right-handedness. Acta Neurobiol Exp (Wars) 67:43-51.

Haaland KY, Prestopnik JL, Knight RT, Lee RR (2004). Hemispheric asymmetries for kinematic and positional aspects of reaching. Brain 127:1145-1158.

Halsband U, Lange RK (2006). Motor learning in man: a review of functional and clinical studies. J Physiol Paris 99:414-424.

Hamburger HL, vd Burgt MA (1991). Global field power measurement versus classical method in the determination of the latency of evoked potential components. Brain Topogr 3:391-396.

Hari R, Karhu J, Hämäläinen M, Knuutila J, Salonen O, Sams M, Vilkman V (1993). Functional organization of the first and second somatosensory cortices: a neuromagnetic study. Eur J Neurosci 5:724-734.

Hari, R., Forss, N., (1999). Magnetoencephalography in the study of human somatosensory cortical processing. Philos trans R Soc Lond B Biol Sci 354:1145-1154.

Hatta T (2007). Handedness and the brain: a review of brain-imaging techniques. Magn Reson Med Sci 2:99-112.

Hugdahl K (2010). Introduction and overview. In: Hugdahl K, Westerhausen R (ed) The Two Halves of the Brain. MIT Press, Massachusetts, pp 1-18.

Inoue K, Kawashima R, Sugiura M, Ogawa A, Schormann T, Zilles K, Fukuda H (2001). Activation in the ipsilateral posterior parietal cortex during tool use: a PET study. NeuroImage 14:1469-1475.

Jung P, Baumgärtner U, Bauermann T, Magerl W, Gawehn J, Stoeter P, Treede RD (2003). Asymmetry in the human primary somatosensory cortex and handedness. NeuroImage 19:913-923.

Jung P, Baumgärtner U, Magerl W, Treede RD (2008). Hemispheric asymmetry of hand representation in human primary somatosensory cortex and handedness. Clin Neurophysiol 119:2579-2586.

Kaas JH, Merzenich MM, Killackey HP (1983). The reorganization of somatosensory cortex following peripheral nerve injury in adult and developing mammals. Ann Rev Neurosci 6:325-356.

Kakigi R, Hoshiyama M, Shimojo M, Naka D, Yamasaki H, Watanabe S, Xiang J, Maeda K, Lam K, Itomi K, Nakamura A (2000).The somatosensory evoked magnetic fields, Progress in Neurobiology 61:495 - 523.

Kawamura T, Nakasato N, Seki K, Kanno A, Fujita S, Fujiwara S, Yoshimoto T (1996). Neuromagnetic evidence of pre- and post-central cortical sources of somatosensory evoked responses. Electroencephalogr Clin Neurophysiol 100:44-50.

Lehmann D, Skrandies W (1980). Reference-free identification of components of checkerboard - evoked multichannel potential fields. Electroencephal. Clin Neurophysiol 48:609-621.

Lugo M, Isturiz G, Lara C, Garcia N, Eblen-Zaijur A (2002). Sensory lateralization in pain subjective perception for noxious heat stimulus. Somatosens Mot Res 19:207-212.

Nakagawa S, Cuthill IC (2007). Effect size, confidence interval and statistical significance: A practical guide for biologists". Biological Reviews Cambridge Philosophical Society 82:591-605

Niddam DM, Graven-Nielsen T, Arendt-Nielsen L, Chen AC (2001). Non-painful and painful surface and intramuscular electrical stimulation at the thenar and hypothenar sites: differential cerebral dynamics of early to late latency SEPs. Brain Topogr 13:283-92.

Nuwer MR, Aminoff M, Desmedt J, Eisen AA., Goodin D, Matsuoka S, Mauguière F, Shibasaki H, Sutherling W, Vibert JF (1994). IFCN recommended standards for short latency somatosensory evoked potentials. Report of an IFCN committee. International Federation of Clinical Neurophysiology. Electroencephalogr Clin Neurophysiol 91:6-11.

Oldfield RC (1971). The assessment and analysis of handedness: the Edinburgh inventory. Neuropsychologia 9:97-113.

Olejnik S., Algina J (2000). Measures of Effect Size for Comparative Studies: Applications, Interpretations and Limitations. Contemporary Educational Psychology 25:241-86.

Papadelis C, Eickhoff SB, Zilles K, Ioannides AA (2011). BA3b and BA1 activate in a serial fashion after median nerve stimulation: direct evidence from combining source analysis of evoked fields and cytoarchitectonic probabilistic maps. NeuroImage 54:60-73.

Reinacher M, Becker R, Villinger A, Ritter P (2009). Oscillatory brain states interact with late cognitive components of the somatosensory evoked potential. J Neurosci Methods 183:49-56.

Reiss M, Reiss G (2000). Motor asymmetry. Fortschr Neurol Psychiatr 68:70-79.

Reiss M, Reiss G (2002). Medical problems of handedness. Wien Med Wochenschr 2002;152:148-152.

Rossini PM, Dal Forno G (2004). Integrated technology for evaluation of brain function and neural plasticity. Phys Med Rehabil Clin N Am 15:263-306.

Schlereth T, Baumgärtner U, Magerl W, Stoeter P, Treede RD (2003). Left-hemisphere dominance in early nociceptive processing in the human parasylvian cortex. NeuroImage 20:441-454.

Siengthai B, Kritz-Silverstein D, Barrett-Connor E (2008). Handedness and cognitive function in older men and women: a comparison of methods. J Nutr Health 12:641-647.

Shinoura N, Suzuki Y, Yamada R, Kodama T, Takahashi M, Yagi K (2005). Fibers connecting the primary motor and sensory areas play a role in grasp stability of the hand. NeuroImage 25:936-941.

Simões C, Alary F, Forss N, Hari R (2002). Left-hemisphere-dominant SII activation after bilateral median nerve stimulation. NeuroImage 15:686-690.

Skrandies W (1990). Global field power and topographic similarity. Brain Topogr 3:137-141.

Sörös P, Knecht S, Imai T, Gurtler S (1999). Lutkenhoner B, Ringelstein EB, Henningsen H. Cortical asymmetries of the human somatosensory hand representation in right- and left-handers. Neurosci Lett 271:89-92.

Schwenkreis P, El Tom S, Ragert P, Pleger B, Tegenthoff M, Dinse HR. (2007). Assessment of sensorimotor cortical representation asymmetries and motor skills in violin players. Eur J Neurosci 26:3291-3302.

Theuvenet PJ, Dunajski Z, Peters MJ, van Ree JM (1999). Responses to median and tibial nerve stimulation in patients with chronic neuropathic pain. Brain Topogr 11:305-13.

Theuvenet PJ, van Dijk BW, Peters MJ, van Ree JM, Lopes da Silva FL, Chen AC (2005). Whole-head MEG analysis of cortical spatial organization from unilateral stimulation of median nerve in both hands: no complete hemispheric homology. NeuroImage 1:314-325.

Theuvenet PJ, van Dijk BW, Peters MJ, van Ree JM, Lopes da Silva FL, Chen AC (2006). Cortical characterization and inter-dipole distance between unilateral median versus ulnar nerve stimulation of both hands in MEG. Brain Topogr 19: 29-42.

Torquati K, Pizzella V, Della Penna S, Franciotti R, Babiloni C, Rossini PM, Romani GL (2002). Comparison between SI and SII responses as a function of stimulus intensity. Neuroreport 7:813-9.

Treede RD, Apkarian AV, Bromm B, Greenspan JD, Lenz FA (2000). Cortical representation of pain: functional characterization of nociceptive areas near the lateral sulcus. Pain 87:113-9.

Tsutada T, Tsuyuguchi N, Hattori H, Shimada H, Shimogawara M, Kuramoto T, Haruta Y, Matsuoka Y, Hakuba A (1999). Determining the appropriate stimulus intensity for studying the dipole moment in somatosensory evoked fields: a preliminary study. Clin Neurophysiol 110:2127-30.

Tsutada T, Ikeda H, Tsuyuguchi N, Hattori H, Shimogawara M, Shimada H, Miki T (2002). Detecting functional asymmetries through the dipole moment of magnetoencephalography. J Neurol Sci 198:51-61.

Van de Wassenberg WJ, van der Hoeven JH, Leenders KL, Maurits NM (2008). Quantifying interhemispheric symmetry of somatosensory evoked potentials with the intraclass correlation coefficient. J Clin Neurophysiol 25:139-46.

Volkmann J, Schnitzler A, Witte OW, Freund H (1998). Handedness and asymmetry of hand representation in human motor cortex. J Neurophysiol 79:2149-2154.

Vrba J, Robinson SE (2001). Signal Processing in Magnetoencephalography. Methods 25:249-271.

White L, Andrews TJA, Hulette C, Richards A, Groelle M, Paydarfar J, Purves D (1997a). Structure of the Sensorimotor System. I: Morphology and Cytoarchitecture of the Central Sulcus. Cerebral Cortex 7:18-30.

White L, Andrews TJA, Hulette C, Richards A, Groelle M, Paydarfar J, Purves D (1997b).
Structure of the Human Sensorimotor System. II: Lateral Symmetry. Cerebral Cortex 7:31-47.

Zappasodi F, Pasqualetti P, Tombini M, Ercolani M, Pizzella V, Rossini PM, Tecchio F (2006). Hand cortical representation at rest and during activation: gender and age effects in the two hemispheres.
Clin Neurophysiol 11:1518-1528.

Chapter 8

Anesthetic Block of Pain-related Cortical Activity in Patients with Peripheral Nerve Injury Measured by Magnetoencephalography.

Peter J. Theuvenet, M.D., Jan C. de Munck, Ph.D., Maria J. Peters, Ph.D., Jan M. van Ree, Ph.D., Fernando L. Lopes da Silva, Ph.D., Andrew C. N. Chen, Ph.D.

Anesthesiology 2011; 115: 375-386

Abstract

Background

This study examined whether chronic neuropathic pain, modulated by a local anaesthetic block, is associated with cortical magnetic field changes.

Methods

In a group of twenty patients with pain due to unilateral traumatic peripheral nerve injury, a local block with Lidocaine 1% was conducted and the cortical effects were measured and compared to a control group. The Global Field Power (GFP), describing distribution of cortical activation after median and ulnar nerve stimulation, was plotted and calculated. The effects on the Affected Hemisphere (AH) and the Unaffected Hemisphere (UH), before and after a block of the injured nerve were statistically evaluated.

Results

Major differences based on the GFP curves, at a component between 50 ms - 90 ms (M70), were found in patients: in the Affected Hemisphere the M70 GFP peak values were statistically significantly larger compared to the UH and the GFP curves differed morphologically. Interestingly, the mean UH responses were reduced compared to the control group and suggests that the UH is also part of the cortical changes. At M70, the GFP curves and values in the Affected Hemisphere were modulated by a local block of the median or the ulnar nerve. The most likely location of cortical adaptation is in the primary somatosensory cortex.

Conclusions

Cortical activation is enhanced in the Affected Hemisphere compared to the UH and is modulated by a local block. The UH In neuropathic pain changes as well. Evoked fields may offer an opportunity to monitor the effectiveness of treatments of neuropathic pain in humans.

Introduction

Traumatic peripheral nerve injury (PNI) may produce a variety of symptoms including neuropathic pain, autonomic dysfunction and disability.[1-3] Functionally, neuropathic pain may result from abnormal peripheral inputs and/or abnormal central processing.[4-8] The continuous volleys of ectopic afferent inputs produce central adaptive changes.[9-16] Neurophysiological parameters that characterize these cortical changes range from peak latency differences to cortical map reorganization.[17-20] Anatomical changes by sprouting and growth into the deafferentiated area, were found in animals after sensory loss of a forelimb.[21,22] In humans, electroencephalography studies showed functional changes in cortical evoked responses in amputees [19,23-25] after nerve injuries[10,26,27] and after stroke using magnetoencephalography.[28] After nerve injury in humans, cortical changes whereby recruitment from neighbouring cortical areas occurred, were reported as well.[2,15,29-31]

Nonetheless, central adaptations and sensitization in humans are difficult to demonstrate and pain modulation at the cortical level is not well established.[32-34] In this study, we hypothized that the volley of impaired afferent information in the PNI group, as soon as it was interrupted by a local anaesthetic block, would result in detectable cortical changes. Advances in magnetoencephalography, characterized by its accurate detection of fissural generators and undisturbed by reference activity, provides a better temporal resolution of the functional brain changes than functional Magnetic Resonance Imaging (fMRI). The aim of this study was to explore the cortical effects of local anaesthesia at the site of the nerve injury and to test the reversibility of the functional cortical changes using magnetoencephalography. We compared the characteristics of the evoked cortical fields after electrical stimulation of the median and/or ulnar nerve in two groups: (1) a group of healthy subjects, (2a) a group of patients, with traumatic PNI in one upper extremity, and (2b) the same patient group re-measured after local anaesthesia in the pain free condition.

Materials and Methods

The study was approved by the Medical Ethical Committee Alkmaar (NH04-196) and the VU Hospital Amsterdam. All healthy subjects and patients were adequately informed and gave their written consent. *Twenty healthy subjects* (13 males and 7 females, age range 27- 48 years, mean 34.1, standard deviation ± 6.1 years), all Caucasian and right handed) were recruited from two hospital staffs. *Twenty patients*, with a traumatic nerve injury and continuous pain were studied. Table 1 presents demographic data of the PNI group. Although variation of the nerve injuries is observed, all were in pain.

The group consisted of 5 male and 15 female right handed patients, the age was between 22 and 69 years (mean 48.3 and s.d. ± 14.7 years). In all patients, neuropathic pain had been present between 1 - 25 years (mean 5.4 s.d. ± 6.5 years). In 13/20 patients traumatic nerve injury was assessed during microsurgical repair, secondary neurolysis after a Carpal Tunnel Syndrome (N=2), after a M. Quervain operation and neuroma forming (N=3) or after a metacarpal fracture (N=2). Neuroanatomical damage varied from full nerve transection to digital nerve injury. In 5 patients, after major nerve injury (A1, A3, A4, A6, A11) partial paralysis or paresis was found, patient A3 also suffered from spasms. Mechanical allodynia was present in all patients, the severity changed with the level of activity. Other sensory symptoms included: hyperalgesia, hypoaesthesia and paraesthesia. All patients complained of

Patient	age	sex	injured nerve	etiology & operation	Number*	Onset of pain	pain duration (years)
A-1	35	F	median nerve	glass wound wrist, subtotally transected	3	immediately after trauma	4
A-2	43	M	radial nerve	sharp trauma, wrist, secondary entrapment correction	3	immediately after suture	3
A-3	47	M	median nerve	glass wound, total transection, median repair	1	2-3 months after injury	7
A-4	54	M	median nerve	glass wound, primary suture, neuroma removal	2	few weeks later	9
A-5	29	F	radial nerve	3 x ganglion operation at wrist, radial nerve neuroma	1	few weeks later	10
A-6	30	F	median nerve	glass wound, 50% transection	2	1 month later	1
A-7	63	F	radial nerve	de Quervain, wrist, nerve branch transection, neurolysis	4	immediately after operation	22
A-8	22	F	ulnar nerve	blunt trauma, ulnar transposition right	2	before 1st operation	3
A-9	49	M	radial nerve	sharp trauma: neurolysis right hand	2	2 months	3
A-10	61	F	radial nerve	de Quervain, wrist, pain and sensory loss	1	immediately after operation	1
A-11	55	M	ulnar nerve	neurinoma excision above elbow, infection wound	3	before 1st operation	4
A-12	63	F	radial nerve	de Quervain, wrist, radial nerve branch entrapment	5	immediately after operation	25
A-13	69	F	digit II nerve	neuroma excision twice	2	immediately after operation	2
A-14	67	F	digit V nerve	metacarpal fracture, neuroma forming digital nerve	2	immediately after operation	3
A-15	53	F	median nerve	CTS operation	1	before 1st operation	4
A-16	60	F	digit II nerve	matacarpal fracture, sensory loss and pain	0	within weeks	2
A-17	48	F	median nerve	CTS operation	1	before 1st operation	4
A-18	49	F	digit II nerve	digital nerve, local exploration and infection	1	before 1st operation	2
A-19	36	F	ulnar nerve	knife wound at wrist	2	immediately after operation	4
A-20	25	F	digit II nerve	knife wound at butchery	1	within weeks	2

Table 1. Demographic data of all twenty PNI patients. Age, gender, injured nerve and etiology are presented. Onset of pain after nerve injury and pain duration in years. CTS = Carpal Tunnel Syndrome. Number = number of operations after trauma. PNI** = Peripheral Nerve Injury.*

a cold hand, in particular during severe pain. Trophic changes included hyperhidrosis. The diagnose Complex Regional Pain Syndrome (CRPS) is based on signs and symptoms.[35,36] At the time of the measurements in 5 / 20 patients, this syndrome was diagnosed. Patient A-7 who only had a radial branch injury after a M. Quervain operation, suffered 22 years from pain. Intermittently, considerable edema, dystonia and loss of function was present. The Verbal Rating Score before the measurements ranged from 4 to 9 (mean 7.0, s.d. ± 1.0), after the local block each patient had to be pain free. At the time of admission to the pain clinic, analgesics (non-opioids and opioids) and anti-epileptics all had been used without good results. Patients used their different medications randomly like paracetamol, Non-Steroidal Anti-Inflammatory Drugs (NSAIDs) and opioids like tramadol or morphine. Three to seven days before the measurements, patients were free of pain medication. No neurological diseases were present and no medication was used that might bias cortical results (i.e. anti-epileptics).

Measurements

In the *subject group*, the four possible stimulation sites of both hands received a number, the left median nerve a "1" and the left ulnar a "2", for the right side "3" and "4" respectively. Stimulation order of the median or ulnar nerve was performed in a randomized way (i.e. 4,2,1,3 for subject HC-04) with a bipolar electrode at the wrist and the cathode placed proximally.[37] *Patients*: in order not to induce additional pain, we stimulated the nerves parallel to the injured nerves, e.g. after median / radial nerve injury we studied the ulnar evoked responses. Stimulation of the nerve parallel to the injured painful nerve is supported by experiments in squirrel monkey and in human subjects where dominance of the adjacent intact nerve emerged cortically.[38-40] *Subjects and patients* were measured in the supine position under identical conditions, lasting about 45 minutes with the head well positioned in the helmet. Foam rubber and the position of the bed close to the helmet stabilized the head in the helmet without much space left to move which might alter the position. A resting period between stimulation sessions of 5-10 minutes was ensured. An electrical nerve stimulator (Grass, model S48, Pegasus Scientific Inc., Rockville, Maryland, USA) and photoelectric stimulus isolation unit (Grass, model SIU7, USA) was employed. The stimulation current was pulsed at a repetition rate of 2 Hz with a pulse duration of 0.2 milliseconds (ms). In 10 / 20 patients median nerve stimulation and in 10 / 20 patients ulnar nerve stimulation was performed. Patients were measured three times: firstly the unaffected side, secondly the affected side before and thirdly after the administration of a local anaesthetic block (2 ml Lidocaine 1%) subcutaneously at the painful site (AH block). Full pain alleviation was achieved in 16/20 patients after 15 minutes. In four patients, a 4th measurement was performed since full pain alleviation required a 2nd block. A distinction was made between the affected hemisphere (AH) and unaffected hemisphere (UH), the AH and UH correspond to the contralateral side of affected and unaffected extremity, respectively. Stimulus intensity threshold reached a 1.5 times motor twitching level.[41] Five hundred stimuli were recorded from each nerve, after 100 stimuli the position of the head to the helmet was electronically reassessed for accuracy. The peri-stimulus interval was 50 - 100 ms pre-trigger and 400 ms post-trigger. During measurements, subjects and patients were asked to ignore the stimuli and refrain from blinking as much as possible, to keep eyes open and fixate a point on the ceiling. Stimulations were tolerable for both groups during all measurements. Two patients were unable to maintain their position and were left out of the study.

Magnetoencephalographic – MRI recordings

A 151-channel whole-head magnetoencephalography system (VSM - CTF, Port Coquitlam, Canada) was used and measurements were performed in a 3-layer magnetically shielded room (Vacuum Schmeltze GmbH, Hanau, Germany). The x, y and z coordinate system, common to each individual magnetoencephalography and MRI, was based on three anatomical landmarks and fixed to nasion, left and right pre-auricular points. Using the positions of these fiducials a head centred coordinate frame was defined. The (+) axis was directed to the nose, the (+) y-axis to the left ear and the (+) axis to the vertex. Magnetoencephalographic signals were sampled at 1250 Hz, triggered by the synchronization pulse of the electric stimulator. On-line, filters were set at direct current for high-pass and at 400 Hz (4th order Butterworth filter - IMST GmbH, Kamp-Lintfort, Germany) for anti-aliasing low-pass. Off-line the magnetoencephalographic data were screened for artefacts, averaged and direct current-corrected using the pre-trigger interval to determine the recording offset. Furthermore, +/- averages were calculated to obtain noise-level estimates. The raw data were visually inspected after data acquisition. Trials showing clear artefacts caused by eye blinks or by muscle activity, e.g. due to swallowing, were removed from the dataset. MRI registration was performed with a 1.5T 3d-MRI (Siemens Sonata, Erlangen, Germany).

Data management and statistical analysis

This study was designed as an explorative study for the parameters that describe the cortical evoked differences between healthy subjects and PNI patients. Since no prior experimental and quantitative results as to the magnitude of the expected effects were available, a formal calculation of a prespecified power was not possible. Absence of an a priori power analysis indicates that negative statistical results have to be interpreted with caution since an existing difference may not be detected. Based on the low availability of PNI patients *with* continuing pain, groups of twenty subjects and patients were selected. Experimental design consisted in all cases of simple two-group comparisons. Statistical tests used were the independent groups t-test (or its non-parametric equivalent the Mann-Whitney test where appropriate) for between groups comparisons, and the paired t-test (or its non-parametric equivalent the Wilcoxon signed ranks test where appropriate) for within groups comparisons. A p-value less than 0.05 was considered as a statistically significant rejection of the null-hypothesis specified with two-tailed alternative hypotheses. Effect sizes and p-values are reported wherever relevant magnitudes of effects existed. Whereby:

$$\text{Effect Size (E.S.)} = \frac{\text{mean experimental group} - \text{mean control group}}{\text{standard deviation control group}}$$

The effect size[42,43] is a numerical way of expressing the strength or magnitude of a reported relationship, be it causal or not. An E.S. near 0.0 means that, on average, the experimental group and control group performed the same, a negative E.S., on average, means that the control group performed better. A positive E.S. means that the experimental group performed better than the control group. The more effective the intervention, the higher the positive E.S. value. Statistical analysis was performed using SigmaStat 3.5v software (Systat Software Inc., Point Richmond, CA, USA). Control for multiple testing was deemed unnecessary since in this explorative study no common hypothesis or theory covering two or more individual statistical tests was present. Control for the family wise error rate is important only when a conclusion based on several statistical tests is falsified, if at most one of the underlying tests is

negative.[44] Given the clinical significance of our results and the likelihood of an increase of type II errors, control for the family wise error rate, i.e. a Bonferroni correction, was not performed.[45,46] Only contralateral hemispherical activity was analyzed in this study for comparison of the subject and patient groups. A Compressed Waveform Profile (CWP), the butterfly-like display of the superimposed evoked responses of all sensors of all subjects and patients was made. Of each subject and patient, the Global Field Power (GFP) curves and peak values after nerve stimulation of each hand were plotted and calculated in order to identify power differences and changes after the blocks. The GFP (in femtoTesla^2) was computed for each individual as the sum of squares over all channels, divided by the number of channels (N=151). For magnetoencephalography, the GFP is a measure of the variability of the magnetic field energy distribution and reflects neuronal activity.[47,48,49] Together with the CWPs, peak stages and peak latencies were identified. Three stages were defined: an early (<50 ms), middle (50 ms - 90 ms) and a late stage (90 ms - 400 ms). Peaks in the post stimulus 400 ms time window, with clear dipolar somatosensory evoked field activity were selected as the cortical areas of interest for analysis. A peak was identified by visual inspection and defined by an amplification factor (= post stimulus amplitude / the pre stimulus root mean square value as an indication of noise) > 3. Peaks in each of these stages are presented as i.e. M20 for the peak around 20 milliseconds etc. 3D cortical maps were made for all subjects (Left Hemisphere and Right Hemisphere) and patients (UH, AH and AH block) at different latencies. VSM - CTF (Port Coquitlam, Canada) software[50] was used to model the single equivalent current dipole (ECD) sources and Advanced Neuro Technology software (ANT A/S, Enschede, The Netherlands) for graphical display. The conventional single moving dipole analysis[51] was used for magnetoencephalographic data evaluation and based on individual MRI's.

Results

Stimulus intensities: in the *subject and patient* group and, between the two groups, no significant threshold differences were found between the left and right hand for all stimulated nerves and for all conditions ($p>0.05$ and E.S. values). *Somatosensory evoked field peak stages*: the incidences and latencies of the peaks in the early, middle and late stages for subjects and patients were assessed. The number of peaks demonstrated high consistency for both groups. Between the subject and patient groups, at M20, M30 and M70, no consistent significant latency differences were found that indicated facilitation of nerve transmission for patients (see Supplementary Digital Content I, listing the number of peaks and peak latencies for both groups).

Characteristics of the CWP

The CWP morphologies of all *subjects and patients*, after median and ulnar nerve stimulation, demonstrated large inter-individual variation but fewer intra-individual hemispherical differences. The CWPs of two patients are presented in Fig. 1, each from the median and ulnar group, and displayed different profiles. In patient A-10 (Fig. 1A-C), the CWPs after median nerve stimulation of both hands, before and after the anaesthetic block of the affected hand are presented. After ulnar stimulation in patient A-1 (Fig. 1D-F) a similar configuration was observed.

The effect of the anaesthetic block on the amplitude (reduction) once the patient was pain free, is observed in the middle stage in both patients (Fig. 1C and Fig. 1F).

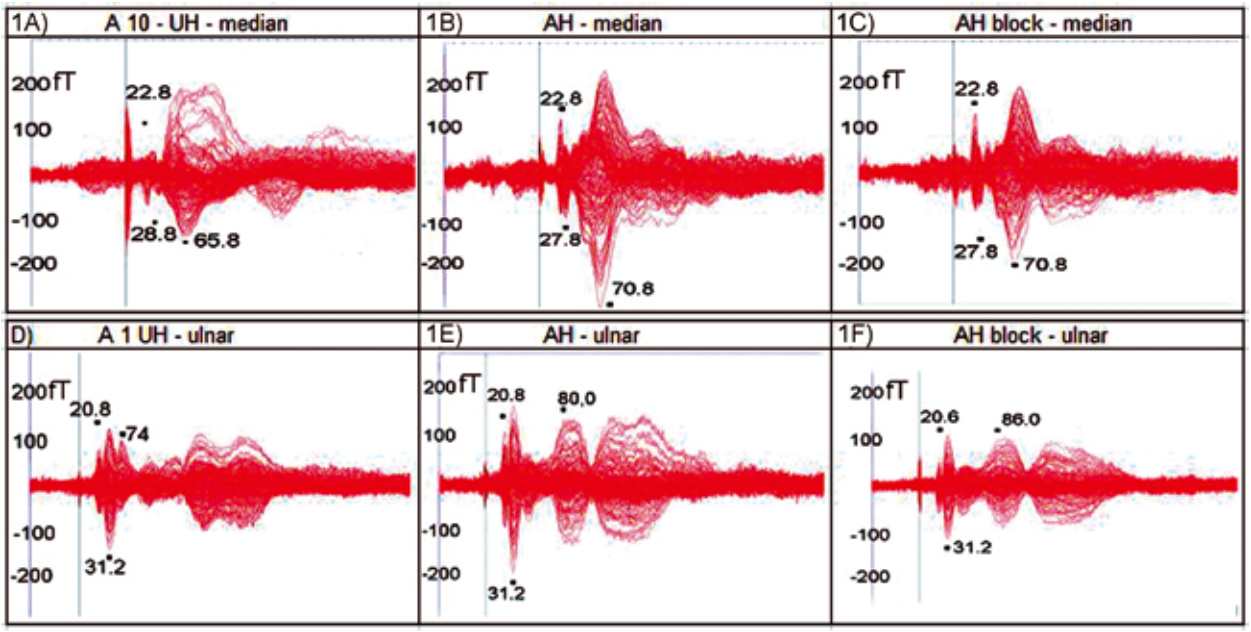

Fig. 1. CWPs after median (A–C) and ulnar nerve (D–F) stimulation are presented of the UH, AH, and AH block of two patients (A-10 and A-1). The AH block depicts the cortical evoked effects of the block on the affected hemisphere, in the pain-free state. Numbers at various peaks depict the latencies, in A the first peak is at 22.8 MS, etc. On the y-axis, the amplitude in femtoTesla (fT) is depicted on the x-axis, time in milliseconds (0–400 MS). AH= affected hemisphere; AH-block= affected hemisphere after a local block; CWPs. Compressed waveform profiles; UH=unaffected hemisphere.

Global Field Power (GFP) morphology

For the *subject and patient groups*, GFP plots were made of the 400 ms post-stimulus time window. Results are depicted in Fig. 2. *Subjects*: LH Med denotes the mean Left Hemispherical GFP response after stimulation of the right median nerve, RH Med the Right Hemispherical GFP response after left median nerve stimulation etc.

Fig. 2A presents the mean GFP overlay curves of the subject group after nerve stimulation. The top two curves (black and red) for the median nerve are morphologically slightly different; the same applies for the ulnar nerve (blue and green). The distribution (curves) of the power for both nerves in the entire time window is highly congruous with three distinct peaks in the first 90 ms: at M20, M30 and M70.

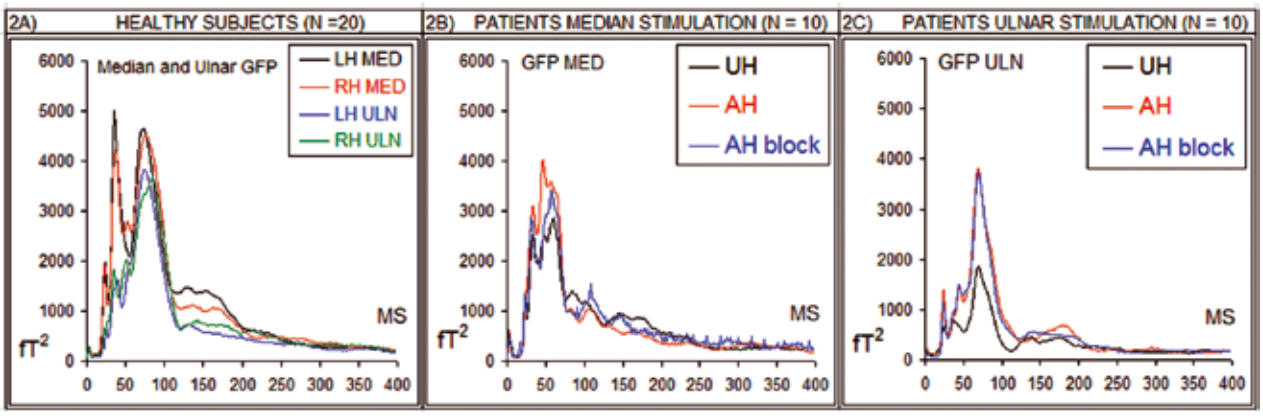

Fig. 2. The mean GFP curves of all subjects (N = 20) depict the power distribution (2A) over the LH and RH after stimulation of the median and ulnar nerves of both hands. LH MED or LH ULN indicate the response in the LH after median or ulnar stimulation, for the RH the same meaning. Fig. 2B and 2C depict the three mean GFP curves after median and ulnar stimulation of the patient groups. The UH curve (black), the AH curve (red), and the AH after the anesthetic block (blue) are depicted. Vertical is the power in fT^2 ($femtoTesla^2$) and horizontal is the time in milliseconds (0–400 MS). AH=affected hemisphere; AH-block=affected hemisphere after a local block; GFP=global field power; GFP MED and GFP ULN=GFP after median and ulnar nerve stimulation, respectively; LH=left hemisphere; RH=right hemisphere; UH=unaffected hemisphere.

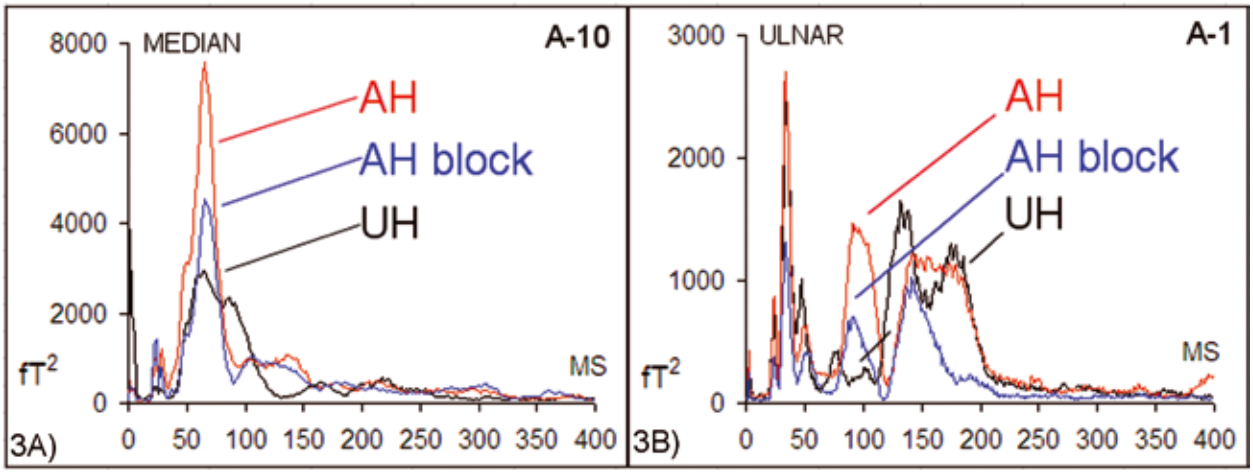

Fig. 3. Global field power (GFP) curves of patient A-10 (3A) and patient A-1 (3B) after median and ulnar nerve stimulation, respectively, are presented. Unaffected hemisphere (UH) (black) and affected hemisphere (AH) (red) represent the GFP curves after stimulation of the unaffected hand and affected hand; AH block (blue) depicts the GFP curve after an anesthetic block. Power differences and changes are clearly discernable after the block. Vertical is the power in fT^2 (femtoTesla^2) and horizontal is the time window in milliseconds (0–400 MS).

Patients: the morphology of the median and ulnar GFP curves (Fig. 2B and 2C) differed from the subject group. In the *median* group, the M20 and M30 peaks are part of a broad complex. In the middle stage the power in the AH is larger than in the UH, after the block the power decreases. In the *ulnar* group small M20 and M30 peaks are present. At M70, AH power is larger than in the UH but after the block no difference is recognized. Strikingly in the first 90 ms post stimulus, for both for the median and ulnar group the GFP peaks in the AHs are higher, particularly between 50 ms - 90 ms compared to the UH. *Subjects versus patients*: for both patient groups the GFP peaks at M20 are hardly distinguishable but lower compared to subjects. In the patient groups all the median and ulnar, M30 and M70 GFP peaks, especially in the UH, were lower compared to subjects.

Patients: GFP after the local block (AH block)

For the same two patients as in Fig. 1, the GFP curves including the effects of the anaesthetic block are presented in Fig. 3.

The GFP curves of the responses on the AH, AH block and UH of patient A-10, after median nerve stimulation are depicted in Fig. 3A. In the middle stage, around the M70 peak clear differences are visible. After a local block, with 1-2 ml of Lidocaine 1%, magnetoencephalography was repeated in the pain free state. As shown, there is a considerable reduction in GFP peak value (blue) of the AH block at 68.8 ms. The individual GFP profiles in patient A-1 (Fig. 3B) after ulnar stimulation differ and, power changes are observed between 30-130 ms. After the block, a considerable GFP reduction for both peaks is observed. Most consistent finding after the block for the patient group were GFP changes during the middle stage.

GFP values at M20, M30 and M70

Based on the GFP curves of each individual subject and patient, the peak values (fT^2) were assessed. GFP data were statistically compared in and between the subject and patient groups (median and ulnar). At M20 in both groups, no statistical differences were found. No statistical differences comparing the LH and Right Hemisphere were found between the GFP values (in fT^2) at M30 and M70 in the *subject group* either (Table 2). The E.S. data, the LH as dominant hemisphere was taken as control in the equation, indicate that there is hardly any difference between the Right Hemisphere and LH. However no complete

SUBJECTS

Median nerve mean GFP values (Paired t-test)

Peaks	M30 (fT^2)	Peaks	M70 (fT^2)
LH (20/20)	5740.6	LH (20/20)	5701.3
s.d.	4954.1	s.d.	3814.6
RH (20/20)	5283.3	RH (20/20)	6720.5
s.d.	3137.7	s.d.	5086.5
diff. RH-LH[1]	-457.3	diff. RH-LH[1]	1019.2
Effect Size (E.S.)	-0.09	E.S.	0.27

Ulnar nerve mean GFP values (Paired t-test)

Peaks	M30 (fT^2)	Peaks	M70 (fT^2)
LH (18/20)	2458.3	LH (19/20)	4813.8
s.d.	2043.3	s.d.	4100.9
RH (20/20)	3031.4	RH (20/20)	5764.4
s.d.	2969.2	s.d.	5098.7
diff. RH-LH[1]	573.1	diff. RH-LH[1]	950.6
Effect Size (E.S.)	0.28	E.S.	0.23

Table 2. Mean GFP peak values (in femtoTesla^2 - fT^2) and SD at two latencies (M30 and M70) are presented for the subject group in both hemispheres. ES data, numeric values, were calculated for the differences between the RH and LH. LH [1] is the dominant hemisphere and in the E.S. formula taken as control. Numbers between brackets indicate the number of peaks in each hemisphere at M30 and M70. ES=effect size; GFP=global field power; LH=left hemisphere; RH=right hemisphere.

homology of GFP values in healthy subjects for both nerves were found.

In the middle stage, the *patient groups* demonstrated a significant change. At M70, after median and ulnar nerve stimulation the AH values were significantly larger compared to the UH and AH block values for both nerves (Table 3). After the block in the pain free state no statistical difference of GFP values between the UH and the AH block, was found for both nerves ($p>0.05$). Effect Size data support these findings and accentuate the effectiveness of the block.

Subjects versus patients: statistical analysis of the individual GFP data between both groups and for both hemispheres, demonstrated no significant differences at M20. Table 4 presents the M30 and M70 GFP values, statistical differences and E.S. data for both groups.

These data support the morphology of the GFP curves in Fig. 2 where in the patient groups, the M30 and M70 peaks were lower compared to subjects. For both patient groups, significant lower GFP values of the UHs at M30 and M70, in comparison to subjects, is demonstrated. In conclusion, significant power changes in the patient groups were found at M70 before and after the block. In contrast, between subjects and patients at M30 and M70, significant statistical power differences occur.

3D Topography of somatosensory evoked fields

3D cortical maps were made for all subjects and patient's at all major peak latencies (see Supplementary Digital Content 2 and 3, presenting Median and Ulnar brain maps respectively for two patients). In the *Subject group and patient groups*, the 1st (M20 / M30) polarity reversal for both nerves was highly consistently found (> 90-95%). The 2nd polarity reversal in the subject group

PATIENTS

Median nerve mean GFP values (Paired t-test)			
Peaks	**M30 (fT^2)**	**Peaks**	**M70 (fT^2)**
UH - AH (10/10)	2759.5	UH (9/10)	***2826.4 ****
Effect Size (E.S.)	0.17	E.S.	*1.93*
AH - AH block (9/10)	3532.0	AH (9/10)	***5822.3 ****
E.S.	-0.08	E.S.	-0.75
UH - AH block (9/10)	3180.0	AH block (9/10)	4109.4
E.S.	0.09	E.S.	0.83

Ulnar nerve mean GFP values (Wilcoxon SRT)			
Peaks	**M30 (fT^2)**	**Peaks**	**M70 (fT^2)**
UH (10/10)	555.8	UH (10/10)	***1875.4 ****
Effect Size (E.S.)	0.66	E.S.	*1.76*
AH (10/10)	880.3	AH (10/10)	***4750.2 ****
E.S.	0.00	E.S.	*-0.22*
AH block (9/10)	876.0	AH block (10/10)	3477.1
E.S.	0.65	E.S.	0.98

*Table 3. GFP values for the median and ulnar patient groups are presented at three stages, (UH, AH, and AH block). Numbers between brackets indicate the number of M30 and M70 peaks in each hemisphere. * A significant statistical difference was found at M70 between the UH - AH and AH - AH block values (in bold). After the block there was no significant difference between the UH - AH block values for both patient groups. AH=affected hemisphere; AH block=affected hemisphere after the local block; ES=effect size (numeric values); GFP=global field power, values in femtoTesla^2 (fT^2); UH=unaffected hemisphere.*

was present between M90 - M180 (>90%). In the *patient group* for all three stages and for both nerves the 2nd reversal differed and ranged from no to even three reversals (from M50 to M180). In the middle stage reversals occurred several times. In the late stage (M90, M150 and M180) no 2nd reversal between 20% - 80% for both nerves was present which indicates wide variation.

Equivalent Current Dipole (ECD) characteristics

Subjects: at M20 and M30, for the *median and ulnar nerve*, after mirroring the dipoles to the same hemisphere, only the ulnar nerve ECD at M20 demonstrated a significant different x-value inter-hemispherically. In the LH, the ulnar ECD was positioned more posterior (p=0.013). The M70 ECDs in the subject groups with a low residual error (<6%), for both nerves present in 12-14 / 20, were located in the contralateral primary somatosensory cortex. Patients: statistical analysis of M20 and M30 dipole parameters did not show any significant difference. At M70, only those ECDs with a low residual error (< 6 %) for all stages (before and after block) were studied.

Figure 4 A presents four measurements of patient A-8 after median nerve stimulation. Patient A-8 is an example of the 4 of 20 patients (see Materials) in whom a second anesthetic block was needed. The red curve depicts the GFP curve of the patient in pain. After the first block, pain was hardly present but the injured hand felt painfully cold (green curve).

SUBJECTS versus PATIENTS

Median nerve mean GFP values (t-test / Mann Whitney RST)			
Peaks	**M30 (fT^2)**	**Peaks**	**M70 (fT^2)**
Mean LH + RH	5489.5	Mean LH + RH	6210.9
s.d.	4101.0	s.d.	4461.1
UH (10/10)	***2759.5****	UH (9/10)	***2826.4 ****
Effect Size (E.S.)	*-0.67*	E.S.	*0.76*
AH (9/10)	3532.0	AH (9/10)	**5822.3 ***
ES	-0.48	E.S.	-0.09
AH block (9/10)	***3180.0****	AH block (9/10)	4109.4
ES	*-0.6*	E.S.	-0.47

Ulnar nerve mean GFP values (t-test / Mann Whitney RST)			
Peaks	**M30 (fT^2)**	**Peaks**	**M70 (fT^2)**
Mean LH + RH	2737.1	Mean LH + RH	5301.3
s.d.	2517.0	s.d.	4641.4
UH (10/10)	***555.8****	UH (9/10)	***1875.4 ****
Effect Size (E.S.)	*-0.87*	E.S.	*-0.70*
AH (9/10)	***880.3****	AH (9/10)	4750.2
E.S.	*-0.74*	E.S.	-0.005
AH block (9/10)	*876.0*	AH block (9/10)	***3477.1****
E.S.	*-0.74*	E.S.	*-0.31*

*Table 4. Between the subject and patients groups, at M30 and M70, GFP values were calculated. Significant differences are presented (in bold) with an asterix * for both nerves. In the ES formula, the mean SD of the LH and RH was used. AH=affected hemisphere; AH block=affected hemisphere after the block; ES=effect size (values are numeric); GFP=global field power, in femtoTesla^2 (fT^2); LH=left hemisphere; RH=right hemisphere; UH=unaffected hemisphere.*

M30	latency (ms)	residual error	x (mm)	y (mm)	z (mm)	declination	azimuth	strength (nAm)
UH	32.0	1.4%	11.0	-45.2	72.5	118.4	208.8	52.9
AH	34.4	3.8%	2.9	36.5	82.3	93.2	172.7	52.8
AH - 1st block	33.6	3.3%	2.8	35.9	82.6	95.0	171.0	57.7
AH - 2nd block	33.6	2.8%	1.8	34.5	81.7	96.5	171.1	67.0
M70		residual error	x (mm)	y (mm)	z (mm)	declination	azimuth	strength (nAm)
UH	60.4	4.2%	11.5	-42.1	73.6	118.3	212.2	36.0
AH	63.4	4.0%	4.7	32.4	85.2	106.3	153.5	34.3
AH - 1st block	62.4	2.9%	3.5	31.9	82.0	101.0	162.6	44.4
AH - 2nd block	64.0	5.1%	3.4	31.7	83.3	105.2	157.3	39.9

Table 5. The latencies, residual errors, and six dipole parameters of patient A-8 are presented at M30 and M70. Position values (x, y, and z) in millimeters (mm), declination and azimuth in degrees, strength in nanoAmperemeter (nAm). AH=affected hemisphere; AH block=the hemispherical response after a first and second local anesthetic block; UH=unaffected hemisphere.

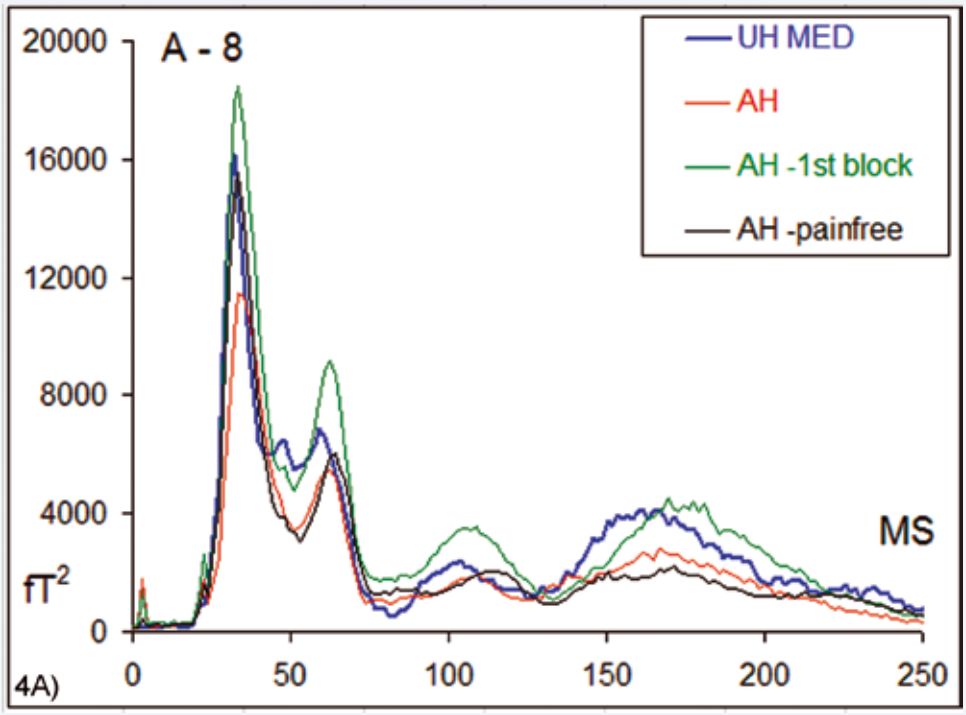

*Fig. **4A**. Four GFP curves of patient A-8 after four different measurements are presented. The UH curve (blue), AH in pain (red), AH first block without pain but unpleasant cold hand (green), and AH-pain free after the second block without pain (black) are depicted in a 250-ms (MS) time window; vertical is the power in fT² (femtoTesla²). Major power changes for patient A-8 are observed in the early (M30) and middle stage (M70). AH=affected hemisphere; AH-1st block= affected hemisphere after 1st local block; AH-pain free=affected hemisphere after 2nd local block; GFP=global field power; UH MED=unaffected hemisphere response after median nerve stimulation.*

The AH GFP peaks at M30 and M70 after the 1st block are relatively the highest. After the second block (black curve), the AH-pain free M30 GFP peak value decreases and is comparable to the UH M30 peak (UH = 16198.2 fT², AH second block = 15525.7 fT²). In the full pain-free state, the UH (blue curve) and AH second block (black) peaks at M30 and M70 are morphologically nearly identical. In the late stage (more than 90 ms), changes are relatively low.

Fig. 4B and 4C present a one dimensional image of the MRI of patient A-8 with all four dipoles projected over both hemispheres at M30 and M70 respectively. The UH dipole at M30 and M70 is depicted in blue, the AH dipoles in red. The dipole depicting the 1st block is green and yellow after the 2nd block. Both at M30 and M70, the UH dipole is located more anterior, lateral and inferior compared to all AH stages. The spatial data of the M30 and M70 dipoles in the AHs indicate that the dipoles hardly changed their positions (Table 5). Combining the dipole localizations in Fig. 4C with the two other 3-D spatial images (coronal, sagittal) indicates that M70 activity is localized in the primary somatosensory cortex (see Supplementary Digital Content 4, presenting a 3-dimensional overview of the M70 dipole characteristics of patient A-8). After selection, in 6 / 10 patients (median nerve) and 5 / 10 (ulnar nerve) with a low residual error (<6%) the dipoles were, compared to subjects, also located in the

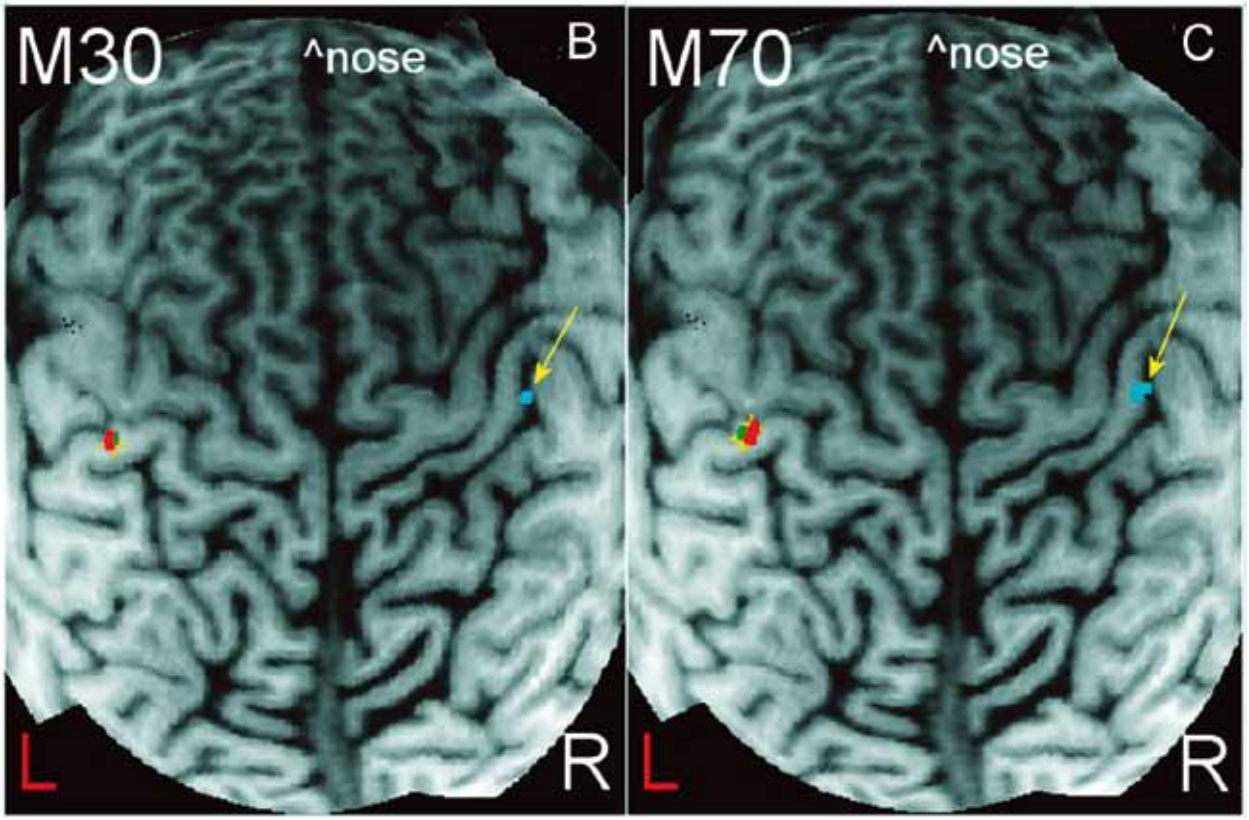

*Fig. **4B** and **4C**. The ECD localizations at M30 (**B**) and M70 (**C**) of patient A-8 are presented in the UH, AH, and AH after the first and second anesthetic block. The M30 and M70 dipoles in the UH are depicted in blue, in the AH in red. The green AH dipole depicts the dipole after the first block, minimal pain but still with an unpleasant cold hand. Yellow depicts the dipole localization after the second block. The nose is depicted in white and marks the (+) x axis. AH=affected hemisphere; AH-1st block=affected hemisphere after a first local block; AH pain free after second block; ECD=equivalent current dipole; L=Left; M30=ECD at 30 ms; M70 the ECD at 70 ms; R=right; UH=unaffected hemisphere.*

primary somatosensory cortex. In 9 / 20 M70 dipoles were not included since modelling with a single moving dipole was not possible or for residual error reasons (> 6%). Combining subjects and patient data at M70, no significant statistical differences were found.

Discussion

Cortical plasticity has been defined as the central nervous systems ability to adapt to environmental challenges or compensate for lesions.[52,53] Plasticity resulted in an *enhancement* of cortical activity after nerve injury or amputation in humans[29-31,54] or a shrinkage of the somatosensory hand representation in Complex Regional Pain Syndrome I.[55] Before the present study, stability and repeatability of the cortical evoked responses after median, ulnar and posterior tibial nerve stimulation was assessed in subjects and PNI patients.[56,57] In this study, magnetic evoked responses in and between subjects and PNI patients were compared, before and after an anaesthetic block. The *GFP curves*, presenting cortical activation in the subject and patient groups, differed morphologically and indicated: (a) decreased cortical activity in the UH of both patient groups compared to the AH and AH block phase; (b) decreased cortical activity in patients in the AH, AH block but in particular in the UH compared to subjects. These findings are

consistent with the interpretation that smaller or larger GFPs correspond to smaller or larger neural areas of activation. Therefore, our results suggest that in unilateral nerve injury of an upper extremity and continuous pain, both hemispheres are involved in cortical adaptations and hemispherical differences have to be compared with a healthy control group. The UH cannot simply serve as control to the AH. This is consistent with the observation that deafferentation in a body part elicits reorganizational changes in the sensorimotor cortex in both the contralateral and ipsilateral hemisphere.[58] Bilateral cortical reorganizational changes have been described after acute limb deafferentation[52] and in patients with non-painful phantom limb phenomena after upper extremity amputation.[25] The mechanisms underlying these functional changes in both hemispheres were ascribed to changes in inhibitory transcallosal transmission.[52] In the patient groups, significant power changes occurred in the middle stage around M70 after the anaesthetic block. In absence of the constant volley of impaired afferent information in patients with chronic neuropathic pain, central functional processes were reversible within 15 minutes even after years of chronic pain. Noteworthy, at M70 after the anaesthetic block and in the pain free condition, the significant differences in GFP values between the UH and AH disappeared. The high GFP response in patient A-8 after the first block (Fig. 4A –green curve) is very interesting since it may reflect the cortical effects of sympathetic involvement in neuropathic pain.[59]

Since there were no significant *stimulation threshold differences* in both groups after standard electrical median and ulnar nerve stimulation at all stages of the measurements, threshold differences did not contribute to the cortical evoked magnetic responses. The *CWP* inter- and intra-individual *morphology* differences of subjects and patients are supported by earlier work.[56,60-62] CWP morphology and GFP curves, indicated that the peak latencies and number of peaks of the subject and patient groups were highly consistent in the first 90 ms post-stimulus period. Altered temporal processing of afferent information (facilitation) in this group of pain patients could not be demonstrated. *Polarity reversals* of the 3D brain maps mainly reflect change in dipole orientation and are an indication of spatial somatosensory processing. The *first and second polarity reversals*, consistently seen in the 3D maps in subjects and described earlier[63], differed in the two groups. The significance of the finding that in the patient group, both reversals were less consistently observed and moreover at different latencies, is yet unknown. It may however indicate altered cortical processing in the patients. These findings in patients are in agreement with experimental changes described in brain maps due to PNI in animals.[9,30,64,65]

Dipole parameters at M20 and M30 indicated that there were few differences between subjects and patients at these latencies. The difference between the two hemispheres at M20 for the ulnar nerve in subjects (the ulnar M20 in the LH more posterior) was not found in patients. This was in contrast with a small magnetoencephalographic study where in a group of three patients after median or ulnar transection, enlarged dipole moments were found between the unaffected and affected side.[66] For all patients after median and ulnar nerve stimulation, the M70 dipoles with a low residual error (< 6 %), before and after the anaesthetic block were located in the contralateral primary somatosensory cortex. The latency and position of these dipoles are in agreement with earlier studies on somatosensory processing in healthy subjects.[67-70] At M70, no bilateral hemispherical dipolar activity was found in the present study after unilateral electrical stimulation

but occurred later (> 90 ms post stimulus). This agrees with other magnetoencephalographic studies[71,72] and excludes involvement of the second somatosensory cortex.[73,74] Finally, cortical interhemispheric differences after electrical nerve stimulation were quite symmetrical in the two hemispheres, making the interhemispheric differences non-dependent on age and gender.[75,76]

We conclude that in patients with neuropathic pain due to nerve injury, major cortical changes measured by magnetoencephalography at M70, reside in the primary somatosensory cortex and may represent altered activation in the affected but also unaffected hemisphere after peripheral median and ulnar nerve stimulation. The functional cortical changes in neuropathic pain, after the modulatory effects of an anaesthetic block, were found to be reversible. In these patients, an anaesthetic block can valuable for the study of contralateral activation in neuropathic pain using magnetoencephalography. PNI with neuropathic pain in humans, studied with non invasive diagnostic devices, may provide a pain model to study and monitor the effects of treatments.

Acknowledegments. This study was made possible by a grant from Medtronic Europe (Tolochenaz – Switzerland).
Technical support was provided by Bob W. van Dijk, Ph.D. and Kees Stam, Ph.D., Professor and Head Department of Clinical Neurophysiology and MEG Centre, VU Hospital, De Boelelaan 1117, 1081 HV Amsterdam, The Netherlands. Clinical support provided by Monique A. Dekkers, M.Sc., Medical Center Alkmaar, The Netherlands. We are grateful for all support.

A) Subjects	*< early >*		*< middle >*			*< late >*			
	M20	**M30**	**M40**	**M50**	**M70**	**M90**	**M150**	**M180**	**M240**
Median									
LH (number of peaks)	20 / 20	20 / 20		15 / 20	20 / 20	18 / 20	15 / 20	7 / 20	14 / 20
mean latency (ms)	*22.2*	*34.5*		*48.7*	*71.9*	*91.5*	*146.5*	*179.8*	*233.7*
s.d.	*1.6*	*2.9*		*4.2*	*3.9*	*5.0*	*8.1*	*7.6*	*14.2*
RH (number of peaks)	20 / 20	20 / 20		19 / 20	20 / 20	17 / 20	16 / 20	8 / 20	16 / 20
mean latency (ms)	*22.1*	*34.8*		*49.1*	*70.9*	*92.7*	*152.7*	*183.2*	*248.8*
s.d.	*1.6*	*2.2*		*5.1*	*4.2*	*8.7*	*10.5*	*8.3*	*21.1*
Ulnar	*< early >*		*< middle >*			*< late >*			
LH	19 / 20	20 / 20		16 / 20	18 / 20	18 / 20	14 / 20	12 / 20	13 / 20
mean latency (ms)	*23.6*	*35.5*		*50.5*	*70.6*	*91.1*	*151.2*	*180.5*	*228.1*
s.d.	*1.9*	*2.5*		*3.6*	*4.5*	*7.5*	*9.0*	*9,.4*	*21.6*
RH	19 / 20	19 / 20		16 / 20	19 / 20	20 / 20	15 / 20	14 / 20	14 / 20
mean latency (ms)	*23.4*	*34.4*		*51.5*	*72.0*	*93.4*	*154.9*	*187.3*	*237.1*
s.d.	*1.9*	*2.8*		*3.6*	*4.9*	*6.3*	*9.4*	*9.3*	*23.6*

B) PNI	*< early >*		*< middle >*			*< late >*			
	M20	**M30**	**M40**	**M50**	**M70**	**M90**	**M150**	**M180**	**M240**
Median (10/20)									
UH	10 / 10	10 / 10	4 / 10	9 / 10	7 / 10	20 / 20	7 / 10	4 / 10	9 / 10
mean latency (ms)	*22.3*	*32.2*	*39.6*	*52.7*	*68.0*	*94.0*	*160.9*	*175.0*	*228.2*
s.d.	*1.3*	*2,.4*	*2.4*	*4.7*	*7.5*	*8.6*	*6.7*	*3.8*	*16.8*
AH	10 / 10	10 / 10	4 / 10	8 / 10	9 / 10	20 / 20	7 / 10	5 / 10	6 / 10
mean latency (ms)	*22.6*	*32.0*	*40.8*	*50.7*	*70.2*	*98.2*	*158.9*	*188.0*	*237.3*
s.d.	*1,.9*	*2.8*	*3.1*	*3.7*	*5.2*	*11.7*	*6.4*	*7.8*	*16.4*
AH block	10 / 10	10 / 10	3 / 10	6 / 10	9 / 10	20 / 20	7 / 10	3 / 10	5 / 10
mean latency (ms)	*22.5*	*32.0*	*37.3*	*51.1*	*71.5*	*96.0*	*157.8*	*184.2*	*233.3*
s.d.	*1.6*	*4.3*	*0.9*	*3.7*	*6.3*	*12.5*	*11.2*	*7.7*	*17.5*
	M20	**M30**	**M40**	**M50**	**M70**	**M90**	**M150**	**M180**	**M240**
Ulnar (10/20)	*< early >*		*< middle >*			*< late >*			
UH	10 / 10	9 / 10	6 / 10	9 / 10	8 / 10	4 / 10	8 / 10	4 / 10	4 / 10
mean latency (ms)	*23.2*	*34.2*	*42.5*	*52.9*	*70.7*	*89.5*	*152.4*	*179.8*	*229.0*
s.d.	*1.8*	*3.8*	*3.4*	*6.4*	*8.0*	*10,.3*	*11.4*	*6.3*	*19.7*
AH	10 / 10	10 / 10	8 / 10	9 / 10	10 / 10	7 / 10	8 / 10	2 / 10	1 / 10
mean latency (ms)	*22.0*	*32.5*	*39.8*	*50.2*	*67.7*	*93.9*	*153,.3*	*183.2*	*233.6*
s.d.	*1.5*	*3.0*	*2,.6*	*2.8*	*4.2*	*10.2*	*9.3*	*8.7*	*6.8*
AH block	10 / 10	9 / 10	8 / 10	8 / 10	8 / 10	6 / 10	9 / 10	4 / 10	4 / 10
mean latency (ms)	*22.4*	*31.7*	*40.8*	*52,1*	*70.7*	*90.2*	*155,.7*	*184.0*	*225.8*
s.d.	*1.2*	*1.8*	*2.9*	*4.3*	*3.8*	*6.6*	*10.1*	*7.6*	*16.2*

Supplementary Digital Content 1. Panel (A) depicts the incidences of the various peaks in the early, middle and late stage for Subjects (N=20) after electrical stimulation of the median and ulnar nerve. Also the mean latencies (milliseconds) and standard deviations (s.d.). After M150, for both nerves peaks are not as consistently observed as in the early and middle stage. Panel (B) for the Peripheral Nerve Injury (PNI) group after median (N=10) and ulnar nerve (N=10) stimulation. In the late stage, after median stimulation the M70 and M150 peaks are more present compared to ulnar nerve stimulation. For the ulnar nerve, the M180 is relatively more frequently observed than the median nerve. For all panels the latency is in milliseconds (ms), the Effect.Size (E.S.) is a numerical value. E.S. is defined as the mean of the experimental group minus the mean of the control group and divided by the mean s.d.of the control group.

Supplemental Digital Content 2. Patient A-10 - MEDIAN

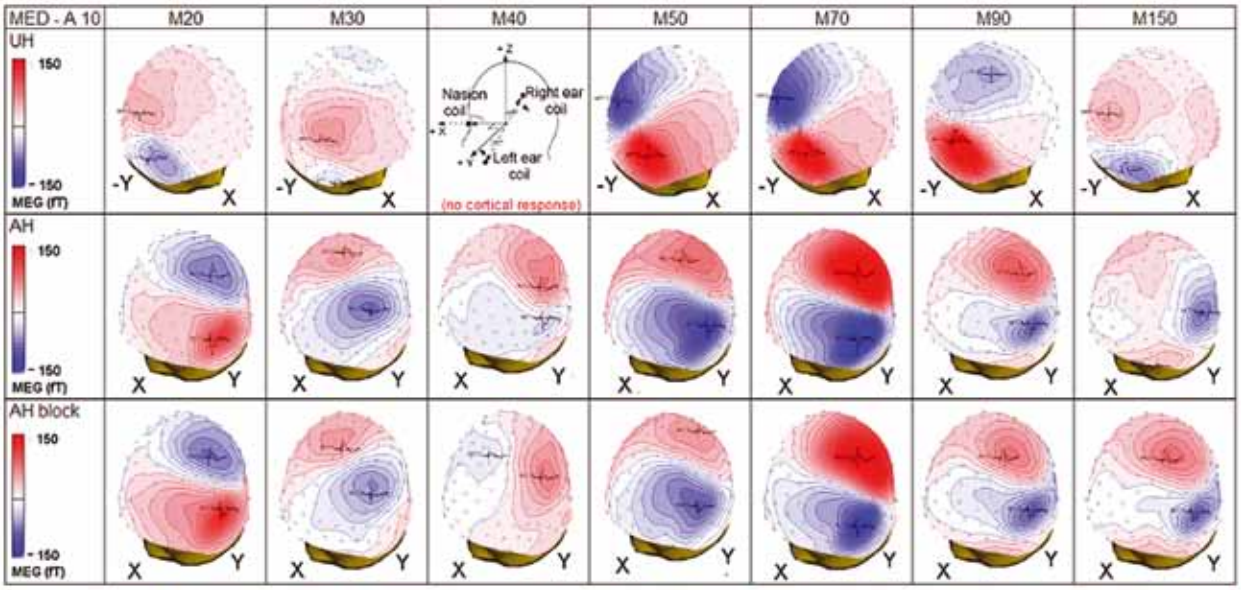

Brain maps of Patient A-10, after electrical median nerve stimulation, are presented at 3 stages in a 150 millisecond (ms) time window. The spatial orientation of the X, Y and Z axes are depicted under the UH M40 sub-panel. The MEG scale is from - 150 to +150 femtoTesla (fT). Unaffected Hemisphere (UH) and Affected Hemisphere (AH) depict the contralateral evoked responses after stimulation of the unaffected and affected nerve, respectively. In the UH two polarity reversals are observed, between M20 / M30 and M90 / M150. In the AH, a first polarity reversal is present between M20 / M30, no second reversal between M90 / M150. For the AH block, a first reversal is seen between M20 / M30, a second between M40 / M50. No reversal between M90 and M150 here. The M stands for magnetic peaks at different latencies, from M20 to M150 (20 ms to 150 ms).

Supplementary Digital Content 3. Patient A-1 – ULNAR

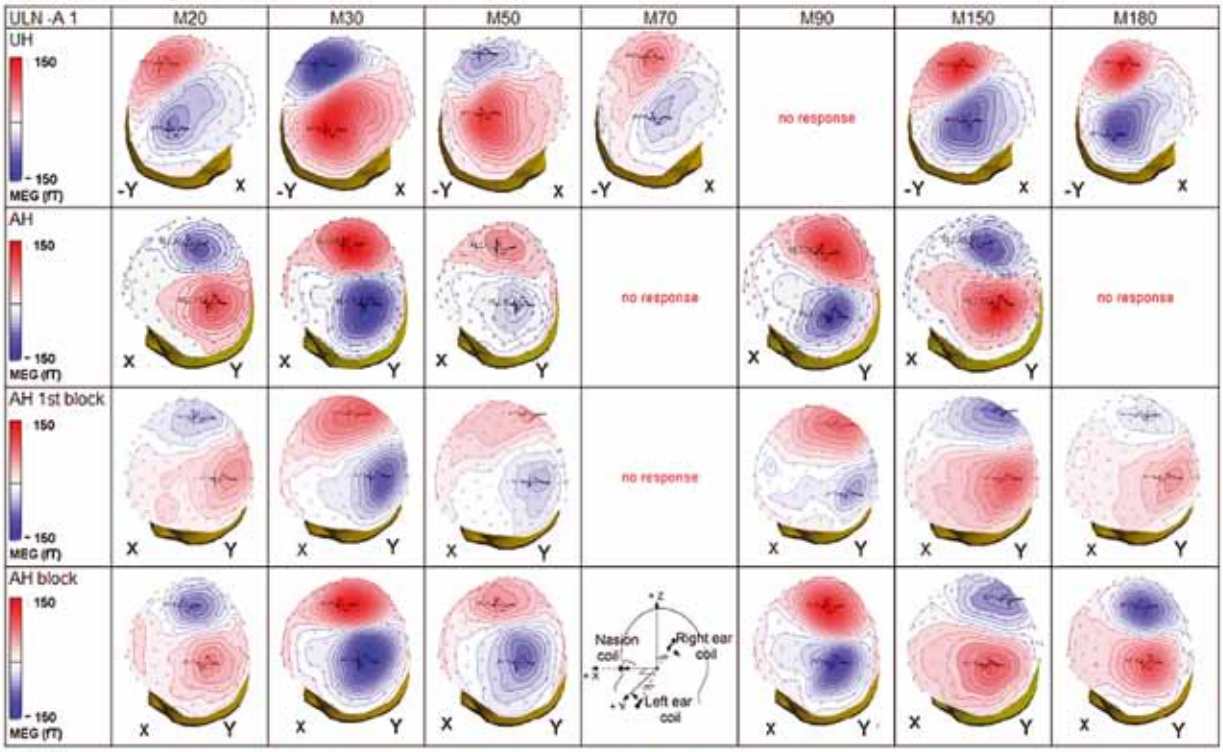

Brain maps of Patient A-1 are presented in a 180 millisecond (ms) time frame after ulnar nerve stimulation during 4 measurement phases. The X, Y and Z – axes system is depicted at the bottom of M70 - AH block, here no brain response either. The MEG scale ranges from -150 femtoTesla (fT) to + 150 fT. Unaffected Hemisphere (UH) and Affected Hemisphere (AH) depict the evoked responses after stimulation of the contralateral unaffected ulnar nerve and contralateral affected ulnar nerve, respectively. In the UH, there is no 2nd polarity reversal at M90 / M150. The AH 1st block maps are after the first anaesthetic block with hardly pain but still with an unpleasant cold hand. AH pain free is after the 2nd block with a complete pain free warm hand. In the UH a 1st polarity reversal at M20/M30 and a 2nd one at M50/M70. For all other three measurements (AH, AH 1st block and AH block), a M20/M30 and M90/M150 polarity reversal is present.

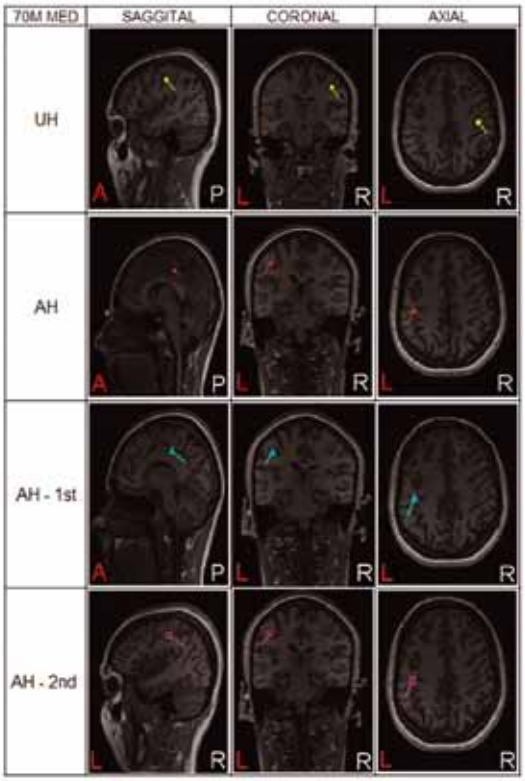

Supplemental Digital Content 4 depicts the M70 dipoles of patient A-8 after four different measurements. Patient A-8 suffered from the sequelae of a traumatic ulnar nerve injury at the right elbow which required ulnar transposition and secondly a neurolysis. Neuropathic pain had been present since 3 years at the time of the measurements.

The Equivalent Current Dipole (ECD) in the Unaffected Hemisphere (UH) at M70 is depicted in YELLOW. The M70 response in the Affected hemisphere (AH) in RED. After the 1st block, the pain nearly vanished after 1 cc Xylocaine 1% injected at the painful site, but the patient reported that the hand was still unpleasantly cold (CYAN). After an additional 2nd anesthetic block, with 1cc Xylocaine 1%, not only the coldness disappeared but the affected hand became comfortably warm and completely pain free (PINK). The cortical response at M70 after the 4th measurement is depicted in the AH pain free panel. The ECD parameters at M70, based on a single moving dipole were as follows:

M70	residual error	x (mm)	y	z	declination	azimuth	strength (nAm)
UH	4,2%	11,5	- 42,1	73,6	118,31	212,24	36,0
AH	4,0%	4,7	32,4	85,2	106,25	153,53	34,3
AH -1st block	2,9%	3,5	31,9	82,0	100,97	162,64	44,4
AH - pain free	5,1%	3,4	31,7	83,3	105,23	157,29	39,9

The difference between the spatial position of the UH and AH dipole indicates that the UH M70 dipole, compared to the AH M70 dipole, is positioned more anterior, more lateral and less inferior to the AH spatial position. Azimuthal orientation of the UH M70 dipole differs 58,7 degrees maximal from the AH dipoles, declination of all dipoles is about the same. The UH and AH dipoles are all posteriorly and inferiorly directed. It indicates that the M70 AH dipoles at three stages are quite stable. The strength in the AH -1st block, is the largest of all four stages.

References

1. Baron R: Peripheral neuropathic pain: From mechanisms to symptoms. Clin J Pain 2000; 16: 12-20

2. Baron R: Mechanisms of disease: Neuropathic pain, a clinical perspective.Nat Clin Pract Neurol 2006; 2: 95-106

3. Treede RD, Jensen TS, Campbell JN, Cruccu G, Dostrovsky JO, Griffin JW, Hansson P, Hughes R, Nurmikko T, Serra J: Neuropathic pain: Redefinition and a grading system for clinical and research purposes. Neurology 2008; 29: 1630-35

4. Bridges D, Thompson SW, Rice AS: Mechanisms of neuropathic pain. Br J Anaesth 2001; 87: 12-26

5. Chen R, Cohen LG, Hallett M: Nervous system reorganization following injury. Neuroscience 2002; 111: 761-73

6. Woolf CJ: Dissecting out mechanisms responsible for peripheral neuropathic pain: Implications for diagnosis and therapy. Life Sci 2004; 74: 2605-10

7. Costigan M, Scholz J, Woolf CJ: Neuropathic pain: A maladaptive response of the nervous system to damage. Annu Rev Neurosci 2009; 32: 1-32

8. Latremoliere A, Woolf CJ: Central sensitization: A generator of pain hypersensitivity by central neural plasticity. J Pain 2009; 10: 895-926

9. Dykes RW: Central consequences of peripheral nerve injuries. Ann Plast Surg 1984; 13: 412-22

10. Das A: Plasticity in adult sensory cortex: A review. Network: Comput Neural Syst 1997; 8: 33-76

11. Tinazzi M, Fiaschi A, Rosso T, Faccioli F, Grosslercher J, Aglioti SM: Neuroplastic changes related to pain occur at multiple levels of the human somatosensory system: A somatosensory-evoked potentials study in patients with cervical radicular pain. J Neurosci 2000; 20: 9277-83

12. Malmberg A: Central Changes. Pain in Peripheral Nerve Diseases, 1st edition. Edited by Reichmann H. Basel, Karger, 2001, pp 149-67

13. Stern J, Jeanmonod D, Sarnthein J: Persistent EEG overactivation in the cortical pain matrix of neurogenic pain patients. NeuroImage 2006; 31: 721-31

14. Schaible HG: Peripheral and central mechanisms of pain generation. Handb Exp Pharmacol 2007; 177: 3-28

15. Navarro X, Vivó M, Valero-Cabré A: Neural plasticity after peripheral nerve injury and regeneration. Prog. Neurobiol 2007; 82: 163-201

16. Jarvis MF, Boyce-Rustay JM: Neuropathic pain: Models and mechanisms. Curr Pharm Des 2009; 15: 1711-16

17. Pons TP, Garraghty PE, Ommaya AK, Kaas JH, Taub E, Mishkin M: Massive cortical reorganization after sensory deafferentation in adult macaques. Science 1991; 252: 1857-60

18. Tinazzi M, Zanette G, Volpato D, Testoni R, Bonato C, Manganotti P, Miniussi C, Fiaschi A: Neurophysiological evidence of neuroplasticity at multiple levels of the somatosensory system in patients with carpal tunnel syndrome. Brain 1998; 121: 1785-94

19. Karl A, Birbaumer N, Lutzenberger W, Cohen LG, Flor H: Reorganization of motor and somatosensory cortex in upper extremity amputees with phantom limb pain. J Neurosci 2001; 21: 3609-18

20. Hansson T, Brismar T: Loss of sensory discrimination after median nerve injury and activation in the primary somatosensory cortex on functional magnetic resonance imaging. J Neurosurg 2003; 99: 100-105

21. Kaas JH, Collins CE: Anatomic and functional reorganization of somatosensory cortex in mature primates after peripheral nerve and spinal cord injury. Adv Neurol 2003; 93: 87-95

22. Jain N, Florence SL, Qi HX, Kaas JH: Growth of new brainstem connections in adult monkeys with massive sensory loss. Proc Natl Acad Sci USA 2000; 97: 5546-50

23. Borsook D, Becerra L, Fishman S, Edwards A, Jennings CL, Stojanovic M, Papinicolas L, Ramachandran V, Gonzalez RG, Breiter H: Acute plasticity in the human somatosensory cortex following amputation. Neuroreport 1998; 9: 1013-17

24. Schwenkreis P, Witscher K, Janssen F, Pleger B, Dertwinkel R, Zenz M, Malin JP, Tegenthoff M: Assessment of reorganization in the sensorimotor cortex after upper limb amputation. Clin Neurophysiol 2001; 112: 627-35

25. Flor H, Muhlnickel W, Karl A, Denke C, Grusser S, Kurth R, Taub E: A neural substrate for non-painful phantom limb phenomena. Neuroreport 2000; 11: 1407-11

26. Assmus H: Somatosensory evoked cortical potentials (SSEP) in regenerating nerves following suture. Elektroenzephalogr Elektromyogr Verwandte Geb 1978; 9: 167-71

27. Tecchio F, Padua L, Aprile I, Rossini PM: Carpal tunnel syndrome modifies sensory hand cortical somatotopy: a MEG study. Hum Brain Mapp 2002; 17: 28-36

28. Rossini PM, Dal Forno G: Integrated technology for evaluation of brain function and neural plasticity. Phys Med Rehabil Clin N Am 2004; 15: 263-306

29. Wiech K, Preissl H, Lutzenberger W, Kiefer RT, Topfner S, Haerle M, Schaller HE, Birbaumer N: Cortical reorganization after digit-to-hand replantation. J Neurosurg 2000; 93: 876-83

30. Florence SL, Boydston LA, Hackett TA, Taub Lachoff H, Strata F, Niblock MM: Sensory enrichment after peripheral nerve injury restores cortical, not thalamic, receptive field organization. European Journal of Neuroscience 2001; 13: 1755-66

31. Stendel R, Jahnke U, Straschill M: Changes of medium-latency SEP components following peripheral nerve lesion. J. of Brachial Plexus and Peripheral Nerve Injury 2006; 20: 1-4

32. Ji RR, Kohno T, Moore KA, Woolf CJ: Central sensitization and LTP: Do pain and memory share similar mechanisms? Trends Neurosci 2003; 26: 696-705

33. Ohara PT, Vit JP, Jasmin L: Cortical modulation of pain. Cell Mol Life Sci 2005; 62: 44-52

34. Ochoa JL: Neuropathic pain: Redefinition and a grading system for clinical and research purposes (comment). Neurology 2009; 72: 1282-83

35. Bruehl S, Harden RN, Galer BS, Saltz S, Bertram M, Backonja M, Gayles R, Rudin N, Bhugra MK, Stanton-Hicks M: External validation of IASP diagnostic criteria for Complex Regional Pain Syndrome and proposed research diagnostic criteria. International Association for the Study of Pain. Pain 1999; 81: 147-54

36. Bruehl S: An update on the pathophysiology of complex regional pain syndrome. Anesthesiology 2010; 113: 713-25

37. Nuwer MR, Aminoff M, Desmedt J, Eisen AA, Goodin D, Matsuoka S, Mauguière F, Shibasaki H, Sutherling W, Vibert JF: IFCN recommended standards for short latency somatosensory evoked potentials. Report of an IFCN committee. International Federation of Clinical Neurophysiology. Electroencephalogr. Clin. Neurophysiol 1994; 91: 6-11

38. Schroeder CE, Seto S, Garraghty PE: Emergence of radial nerve dominance in median nerve cortex after median nerve transection in an adult squirrel monkey. J Neurophysiol 1997; 77: 522-26

39. Weiss T, Miltner WH, Huonker R, Friedel R, Schmidt I, Taub E: Rapid functional plasticity of the somatosensory cortex after finger amputation. Exp Brain Res 2000; 134: 199-203

40. Weiss T, Miltner WH, Liepert J, Meissner W, Taub E: Rapid functional plasticity in the primary somatomotor cortex and perceptual changes after nerve block. Eur J Neurosci 2004; 20: 3413-23

41 Tsutada T, Tsuyuguchi N, Hattori H, Shimada H, Shimogawara M, Kuramoto T, Haruta Y, Matsuoka Y, Hakuba A: Determining the appropriate stimulus intensity for studying the dipole moment in somatosensory evoked fields: A preliminary study. Clin Neurophysiol 1999; 110: 2127-30

42 Olejnik S, Algina, J: Measures of Effect Size for Comparative Studies: Applications, Interpretations and Limitations. Contemporary Educational Psychology 2000; 25: 241-86

43. Nakagawa S, Cuthill IC: Effect size, confidence interval and statistical significance: A practical guide for biologists". Biological Reviews Cambridge Philosophical Society 2007; 82: 591-605

44. Benjamini Y, Hochberg Y: Controlling the False Discovery Rate: A practical and Powerful Approach to Multiple testing. The Journal of the Royal Statistical Society. Series B (Methodological) 1995; 57: 289-300

45. Perneger TV: What's wrong with Bonferroni adjustments. BMJ 1998; 18: 1236-38

46. Hatem SM, Attal N, Ducreux D, Gautron M, Parker F, Plaghki L, Bouhassira D: Clinical, functional and structural determinants of central pain in syringomyelia. Brain 2010; 133: 3409-22

47. Lehmann D, Skandries W: Reference-free identification of components of checkerboard-evoked multichannel potential fields. Electroencephal Clin Neurophysiol 1980; 48: 609-21

48. Skrandies W: Global field power and topographic similarity. Brain Topogr 1990; 3: 137-41

49. Maurer K, Dierks Th: Data acquisition and signal analysis, Atlas of Brain Mapping, 1st edition. Edited by Maurer K, Dierks Th. Berlin, Springer Verlag, 1991, pp 23-37

50. Vrba J, Robinson SE: Signal Processing in Magnetoencephalography. Methods 2001; 25: 249-71

51. Fuchs M, Wagner M, Kastner J: Confidence limits of dipole source reconstruction results. Clin Neurophysiol 2004; 6: 1442-51

52. Hummel F, Gerloff C, Cohen LG: Modulation of Cortical Function and Plasticity in the Human Brain, Neural plasticity in adult somatic sensory-motor systems, 1st edition. Edited by Ebner FF. Boca Raton, Taylor & Francis Group, 2005, pp 207-27

53. Kaas JH: Functional implications of plasticity and reorganizations in the somatosensory and motor systems of developing and adult primates, The somatosensory system. Edited by Nelson RJ. Boca Raton, CRC Press, 2001, pp 367-82

54. Elbert T, Sterr A, Flor H, Rockstroh B, Knecht S, Pantev C, Wienbruch C, Taub E: Input-increase and input-decrease types of cortical reorganization after upper extremity amputation in humans. Exp Brain Res 1997; 117: 161-64

55. Maihöfner C, Handwerker HO, Neundörfer B, Birklein F: Patterns of cortical reorganization in complex regional pain syndrome. Neurology 2003; 61: 1707-15

56. Theuvenet PJ, Dunajski Z, Peters MJ, van Ree JM: Responses to median and tibial nerve stimulation in patients with chronic neuropathic pain. Brain Topogr 1999; 11: 305-13

57. Theuvenet PJ, van Dijk BW, Peters MJ, van Ree JM, Lopes da Silva FL, Chen AC: Whole-head MEG analysis of cortical spatial organization from unilateral stimulation of median nerve in both hands: No complete hemispheric homology. NeuroImage 2005; 28: 314-25

58. Werhahn KJ, Mortensen J, van Boven RW, Zeuner KE, Cohen LG: Enhanced tactile spatial acuity and cortical processing during acute hand deafferentation. Nat Neurosci 2002; 5: 936-38

59. Maihöfner C, Seifert F, Decol R: Activation of central sympathetic networks during innocuous and noxious somatosensory stimulation. NeuroImage 2011; 55: 216-24

60. Kakigi, R: Somatosensory evoked magnetic fields following median nerve stimulation. Neurosci Res 1994; 20: 165-74

61. Kakigi R, Hoshiyama M, Shimojo M, Naka D, Yamasaki H, Watanabe S, Xiang J, Maeda K, Lam K, Itomi K, Nakamura A: The somatosensory evoked magnetic fields, Progress in Neurobiology 2000; 61: 495-523

62. Tecchio F, Pasqualetti P, Pizzella V, Romani G, Rossini PM: Morphology of somatosensory evoked fields: Inter-hemispheric similarity as a parameter for physiological and pathological neural connectivity. Neurosci Lett 2000; 287: 203-06

63. Theuvenet PJ, Van Dijk BW, Peters MJ, Van Ree JM, Lopes da Silva FL, Chen AC: Cortical characterization and inter-dipole distance between unilateral median versus ulnar nerve stimulation of both hands in MEG. Brain Topogr 2006; 19: 29-42

64. Garraghty PE, Hanes DP, Florence SL, Kaas JH: Pattern of peripheral deafferentation predicts reorganisation limits in adult primate somatosensory cortex. Somatosens Mot Res 1994; 11: 109-17

65. Wall JT, Xu J, Wang X: Human brain plasticity: An emerging view of the multiple substrates and mechanisms that cause cortical changes and related sensory dysfunction after injuries of sensory inputs from the body. Brain Research Reviews 2002; 39: 181-215

66. Diesch E, Preissl H, Haerle M, Schaller HE, Birbaumer N: Multiple frequency steady-state evoked magnetic field mapping of digit representation in primary somatosensory cortex. Somatosens Mot Res 2001; 18: 10-8

67. Jones AK, Brown WD, Friston KJ, Qi LY, Frackowiak RS: Cortical and subcortical localization of response to pain in man using positron emission tomography. Proc R Soc Lond B Biol Sci 1991; 244: 39-44

68. Hari R, Karhu J, Hämäläinen M, Knuutila J, Salonen O, Sams M, Vilkman V: Functional organization of the first and second somatosensory cortices: a neuromagnetic study. Eur J Neurosci 1993; 5: 724-34

69. Hari R, Forss N: Magnetoencephalography in the study of human somatosensory cortical processing. Philos Trans R Soc Lond B Biol Sci 1999; 354: 1145-54

70. Huttunen J, Komssi S, Lauronen L: Spatial dynamics of population activities at S1 after median and ulnar nerve stimulation revisited: an MEG study. Neuroimage 2006; 32: 1024-31

71. Simões C, Alary F, Forss N, Hari R: Left-hemisphere-dominant SII activation after bilateral median nerve stimulation. NeuroImage 2002; 15: 686-90

72. Simões C, Hari R: Relationship between Responses to Contra- and Ipsilateral Stimuli in the Human Second Somatosensory Cortex SII. NeuroImage 1999; 10: 408-16

73. Schnitzler A, Ploner M: Neurophysiology and functional neuroanatomy of pain perception. Clin Neurophysiol 2000; 17: 592-603

74. Nieuwenhuys R: The Neocortex. The Human Central Nervous System, 4th edition Edited by Nieuwenhuys R, Voogd J, Huijzen van, Chr. Berlin, Springer Verlag, 2008, pp 683-714

75. Zappasodi F, Pasqualetti P, Tombini M, Ercolani M, Pizzella V, Rossini PM, Tecchio F: Hand cortical representation at rest and during activation: Gender and age effects in the two hemispheres. Clin Neurophysiol 2006; 117: 1518-28

76. Rossini PM, Rossi S, Babiloni C, Polich J: Clinical neurophysiology of aging brain: From normal aging to neurodegeneration. Prog Neurobiol 2007; 83: 375-400

CHAPTER 9

Cortically evoked responses and 3D mapping in Complex Regional Pain Syndrome I and II

SUBMITTED FOR PUBLICATION

Peter J. Theuvenet, MD [a,], J.C. de Munck [b], PhD , Maria J. Peters [c],PhD, Jan M. van Ree [d], PhD, Fernando L. Lopes da Silva [e], PhD and Andrew CN. Chen [f, CA], PhD.

Abstract

Complex Regional Pain Syndrome (CRPS) I and II are well known chronic pain syndromes. No objective tests are available to study the syndromes, which hampers the diagnosis and treatment. Cortically evoked responses were measured after standard electrical median and ulnar nerve stimulation using magnetoencephalography. Three groups were compared (a) 20 healthy subjects (b) 20 CRPS I and (c) 20 CRPS II patients. The responses studied were: peak latencies, number of peaks, compressed waveform profiles (CWP), global field power (GFP) curves and values, and six dipole characteristics. In the subject group, GFP curves as an indication of cortical activation were highly symmetrical for both nerves. In CRPS I, a significant decrease and in CRPS II an increase of GFP values was observed compared to subjects in the Affected Hemisphere (contralateral to the affected hand). In both patient groups the Unaffected Hemispheres were part of the cortical plasticity changes, decreased cortical activation presents a shrinkage of the activated somatosensory area compared to subjects. Significant latencies differences at M30 may indicate facilitation of nerve transmission and central processing. For all groups at 30 ms and 70 ms post stimulus, major cortical activation was observed in the primary somatosensory cortex. Evoked magnetic responses offer an objective approach to study CRPS I and CPRS II. Since in both CRPS syndromes, a difference in cortical activation exists as compared to subjects measured under identical circumstances, the two syndromes may require a different treatment approach.

INTRODUCTION

CRPS I and II are two well known chronic pain syndromes with comparable symptomatology[1] and may result in severe disability.[2] There is accumulating evidence that in both syndromes, neuroanatomical[3,4,5], neurochemical [6,7,8,9,10,11] , autonomic and adaptive functional changes occur along the neuraxis.[12,13,14,15,16,17,18,19,20,21,22, 23,24,25]

CRPS I is diagnostically still based on clinical symptoms which may change during the disease. In CRPS I symptoms like pain, edema, vasomotor and sudomotor disturbances may develop.[26, 27,28, 29,30,31,32,33] Interestingly, peripheral neuropathological changes displaying abnormal thin fibre axons in skin and vascular bed were described in CRPS I[34] and a genetic predisposition is suspected.[35] Objective tests to diagnose CRPS I are still unavailable hampering proper diagnosis and treatment.

CRPS II is caused by peripheral nerve injury (PNI), of e.g. the median or ulnar nerve but the incidence of CRPS II is relatively low, ranging from 2 - 2,5%.[36,37] PNI not necessarily results in CRPS II or neuropathic pain and may present less severe forms comparable to CRPS I.[36] Neuropathic pain was recently redefined as, “pain arising as a direct consequence of a lesion or disease affecting the somatosensory nervous system.[38] Even though CRPS II patients share comparable symptoms as CRPS I patients, their sensory profiles differed supporting the concept of different underlying mechanisms leading to chronic pain in PNI patients.[3,39] Functionally, neuropathic pain in PNI may be due to abnormal peripheral input and/or abnormal central processing.[40,41,42,43] Abnormal peripheral inputs may begin shortly after the nerve injury when ectopic discharges start to produce pain. This discharge may result from cross-talk with sympathetic fibres and produces

autonomic dysfunction.[20,44] Adaptive cortical evoked responses after nerve injury in humans were described.[14,45,46,47]

This study compared the characteristics of evoked cortical fields, after standard electrical median or ulnar nerve stimulation in three groups: a healthy subject group (N=20) and two patient groups (each N=20) with either CRPS I or II and continuous pain, using magnetoencephalography (MEG). We hypothized that patients with CRPS I or II produce functional hemispherical differences, due to altered cortical processing of impaired afferent sensory information. Further, that these cortical functional effects might differentiate the two groups from healthy subjects.

MATERIALS AND METHODS

All subjects and patients were adequately informed and gave their written consent. The study was approved by the Ethical Committee of the Medical Center Alkmaar (NH04-196) and the VU University Medical Center. The measuring setup in the subject and patient groups was identical. Taken the three groups together, a total of 184 measurements were performed.

Subjects and patient groups

The healthy subject group was recruited from the hospital staffs and 80 measurements were performed. *CRPS I patient group*: twenty patients who met the CRPS I criteria based on the description by Bruehl and coworkers[27] were included, and 40 measurements were performed. Continuous pain had to be present with a pain intensity of 5 or larger on the Verbal Rating Scale (VRS). In this group of patients no intervention was performed during the measurements. The choice between median or ulnar stimulation was based on the place of the initial trauma, e.g. after a metacarpal V fracture median nerve stimulation was chosen.

CRPS II - PNI group. Twenty patients with a unilateral peripheral nerve injury (PNI) at the upper extremity were measured, after stimulation of the unaffected and affected hand. Stimulation was conducted on the nerve parallel to the injured nerve. No other neurological diseases were present that might bias study outcome. The patient group consisted of 5 male and 15 female patients, age was between 22 and 69 years (mean 48.3 and s.d. ±14.7 years). Only patients with continuous pain and a pain duration of at least one year were included in the study. In all patients neuropathic pain was present between 1 and 25 years (mean 5.7 s.d. ± 6.5 years). In 13 patients nerve injury (knife or glass) was assessed during surgical repair, during neurolysis (N=3) after a recurrent carpal tunnel syndrome (CTS), after M. de Quervain operation and neuroma forming (N=2) or after a metacarpal fracture with nerve injury (N=2). Nerve damage differed from nearly full transection to digital nerve injury. The VRS before the measurements ranged from mean 7.0 and s.d. ± 1.0. Motor loss / weakness was present in all patients with major nerve injury and in the CTS group (N=8/20). In contrast to hyperalgesia and hypoaesthesia, allodynia was present in all patients. Autonomic dysfunction was present in half of the group, mostly a cold feeling.

PAIN (unrelated to the inciting event)		20/20		
SYMPTOMS	Sensory	*Reports of hyperalgesia*		
		20 / 20		
	Vasomotor	*Temperature asymmetry*	*Skin colour changes*	*Skin colour asymmetry*
		18 / 20	15 / 20	15 / 20
	Sudomotor / edema	*Edema*	*Changes in sweating*	*Asymmetry in sweating*
		18 / 20	15 / 20	15 / 20
	Motor / trophic	*Functio laesa*		
		20 / 20		
		Weakness	*Tremor*	*Dystonia*
		20 / 20	5 / 20	14 / 20
		Trofic changes		
		Increased hairgrowth	*Increased nailgrowth*	Skin changes
		9 / 20	7 / 20	10 / 20
SIGNS	Sensory	*Allodynia and / or hyperalgesia*		
		20 / 20		
	Vasomotor	*Temperature asymmetry*	*Skin colour changes*	*Skin colour asymmetry*
		20/20	20/20	20/20
	Sudomotor / edema	*Edema*	*Changes in sweating*	*Asymmetry in sweating*
		19 / 20	14 / 20	13 / 20
	Motor / trophic	*Functio laesa*		
		20 / 20		
		Weakness	*Tremor*	*Dystonia*
		20 / 20	5 / 20	12 / 20
		Trofic changes		
		Increased hairgrowth	*Increased nailgrowth*	*Skin changes*
		9 / 20	6 / 20	8 / 20

Table 1. An overview is presented of the inclusion data for the CRPS I group (N=20). For the Symptoms and Signs incidences out of 20 patients are presented.

MEASUREMENTS

Standard electrical median and/or ulnar nerve stimulation was performed at the wrist with a bipolar electrode, the cathode proximal.[48] In the subject group, nerve stimulation of the median and ulnar nerve of both hands was performed in a randomized way. The four nerves received a number, the left median nerve a “1” and the left ulnar a “2”, for the right nerves “3” and “4” respectively. The order of stimulation was randomized for each subject (i.e. 1, 4, 2 and 3). An electrical nerve stimulator

(Grass, USA; model S48) was employed using a photoelectric stimulus isolation unit (Grass, USA; model SIU7). The stimulation current was pulsed, at a repetition rate of 2 Hz and with a pulse duration of 0.2 ms. All subjects and patients were studied in a single session, lasting about 45 minutes. Between stimulations a resting period of 5-10 minutes was ensured. Stimulus intensity was tailored to the individual twitching level of each separate hand and reached a 1.5 x motor twitching level. The twitch threshold varied with the subject and was tolerated. Five hundred stimuli were recorded from each nerve, after 100 stimuli the position of the head to the helmet was electronically reassessed for accuracy. The peri-stimulus interval was 50-100 ms pre-trigger and 400 ms post-trigger.

MEG Recordings

A CTF MedTech (Canada) 151-channel whole-head system was used inside a 3-layer magnetically shielded room (Vacuum Schmeltze GmbH, Germany). The x, y and z coordinate system was based on the nasion, left and right ear. The coil locations (nose, right and left ear coils) were used to determine the distance between the head and the measurement system and gave rise to the axes system. Using the positions of these fiducials a head centred coordinate frame was defined. The (+) x-axis was directed to the nose, the (+) y-axis to the left ear and the (+) z-axis to the vertex. The system has a 5 cm baseline. Recordings were performed in the synthetic 3rd-order gradient mode, using the manufacturer's real-time software. All measurements were performed in the supine position. The MEG signals were sampled at 1250 Hz, triggered on the synchronization pulse of the electric stimulator. The peri-stimulus interval was 50 -100 ms pre-trigger and 400 ms post-trigger. On-line filters were set at DC for high-pass and at 400 Hz (4th order Butterworth) for anti-aliasing low-pass. Off-line the MEG data were screened for artefacts, averaged and DC-corrected using the pre-trigger interval to determine the recording offset.

MRI registration

Brain MRIs were performed with a 1.5T 3d-MRI (Siemens Sonata). The following parameter settings were used: slice orientation sagittal, slice thickness 2 mm, FOV 256 mm, scan mode fl 3d, scan technique 20 magnitude, TR 11.8 ms, echoes no. 1, TE 5 ms, flip angle 30 degrees and contrast enhancement was applies. Lastly the number of signals averaged was 2, scan matrix 256, reconstruction matrix 256, TI 0 and frequency 63.6 MHz. The MEG-MRI common reference system was defined on the basis of three anatomical landmarks fixed on nasion, left and right pre-auricular points. The MRI scan planes were set parallel to the above defined localization coordinate system (vitamin E capsules, 5 mm of diameter on the same coil locations that were marked with a fibre-tip pen). In this way, we achieved superimpositions on MR images with a precision of 2-3 mm as previously shown by simulation with artificial 'dipoles' within a skull. The entire MRI procedure lasted about 30 min.

Compressed Waveform Profile (CWP)

A butterfly-like display is produced when the SEFs of all sensors are superimposed, the compressed waveform profile (CWP). It was used to identify the main peak latencies. In subjects, cortical responses in the Left Hemisphere are abbreviated as LH, in the Right Hemisphere as RH. In patients, UH and AH mean the hemispherical response after stimulation of the contralateral unaffected and affected extremity, respectively. The CWP demonstrates the individual characteristics of the brain dynamics of the sensory, motor and perceptual brain regions. In the time domain, somatosensory activities were divided into three

different stages with peaks, an early (<50 ms), middle (50-90 ms), and late stage (90-400 ms). Peaks at various latencies are further indicated by the letter M for magnetic response, i.e. at 30 ms as M30 etc. 3D cortical maps were made for all subjects (LH and RH) and patients (UH and AH) at different peak latencies.

Global Field Power (GFP)

The GFP expresses the spatial magnetic energy distribution during the whole timeframe of the measurement and reflects the underlying hemispherical neural activity at each time point and was produced for all 184 measurements.[49] In MEG but also in EEG measurements[50], the CWP and GFP are further used to identify major peak latency components. A peak was defined by an amplification factor (= post stimulus amplitude / the prestimulus root mean square value as an indication of noise) > 3. In the temporal domain, hemispheric lateralization in timing of activation will be expressed in the peak latencies and may indicate a difference in transmission and / or activation time.[51]

Equivalent Current Dipole (ECD) and Dipole Parameters

CTF software was used to model the equivalent current dipole (ECD) sources to MEG and for statistical analysis. The head was approximated with a spherical volume conductor. The conventional single equivalent current (moving) dipole analysis[52,53] was used for the data evaluation. MEG data were co-registered with MR images using fiducial coils and vit. E markers. The head model was chosen to match the inner contour of the skull, matching was done visually. Peaks in the post stimulus 400 ms time window, with clear SEF deflections (as judged by comparison of average and plus minus average signal amplitudes), were visually identified to select the cortical areas of interest for further analysis. At each of the peak latencies the dipole characteristics were determined.

Data management and statistical analysis

This study was designed as an explorative study for the parameters that describe the cortical evoked differences between healthy subjects, CRPS I and CRPS II – PNI patients. Since no prior experimental and quantitative results as to the magnitude of the expected effects were available, a formal calculation of a prespecified power was not possible. Absence of an a priori power analysis indicates that negative statistical results have to be interpreted with caution since an existing difference may not be detected. Therefore posterior powers have been calculated where appropriate. Based on the low availability of PNI patients with continuing pain, groups of twenty subjects and patients were selected. Experimental design consisted in all cases of simple two-group comparisons. Statistical tests used were the independent groups t-test (or its non-parametric equivalent the Mann-Whitney rank sum test where appropriate) for between groups comparisons, and the paired t-test (or its non-parametric equivalent the Wilcoxon signed ranks test where appropriate) for within groups comparisons. A p-value less than 0.05 was considered as a statistically significant rejection of the null-hypothesis specified with two-tailed alternative hypotheses. Effect sizes and p-values are reported wherever relevant magnitudes of effects existed. Whereby:

$$\text{Effect Size (E.S.)} = \frac{\text{mean experimental group} - \text{mean control group}}{\text{standard deviation control group}}$$

The effect size is a numerical way of expressing the strength or magnitude of a reported relationship, be it causal or not. An E.S. near 0.0 means that, on average, the experimental group and control group performed the same, a negative E.S., on

average, means that the control group performed better. A positive E.S. means that the experimental group performed better than the control group. The more effective the intervention, the higher the positive E.S. value. Statistical analysis was performed using SigmaStat 3.5v software (Systat Software, Inc. Point Richmond, CA, USA). Control for multiple testing was deemed unnecessary since in this explorative study no common hypothesis or theory covering two or more individual statistical tests was present. Control for the family wise error rate is important only when a conclusion based on several statistical tests is falsified, if at most one of the underlying tests is negative.[44] Given the clinical significance of our results and the likelihood of an increase of type II errors, control for the family wise error rate, i.e. a Bonferroni correction, was not performed. Only contralateral hemispherical activity was analyzed in this study for comparison of the subject and patient groups. CTF (Port Coquitlam, Canada) software was used to model the single equivalent current dipole (ECD) sources and Advanced Neuro Technology software (ANT A/S, Enschede), The Netherlands for graphical display.

RESULTS

Stimulus intensities under different study conditions

The stimulus intensities required for eliciting the twitches were analysed for all three groups. Stimulation thresholds producing a clear twitch in the subject and two patient groups were compared. No statistical significant differences were found after comparison within and between the three groups ($p>0.05$).

CWP and peak consistency

The CWPs of the subjects and patient groups were studied for morphology, number of peaks and peak latencies. In Fig. 1, the CWPs of a subject after median (1A) and ulnar nerve (1B) stimulation, are presented. The median amplitudes are clearly larger than the ulnar ones in the first 90 ms post stimulus. Only those peaks displaying a dipolar field configuration were included for further analysis.

Fig. 2AB. In the panels 2A and 2B, the CWPs of two patients with CRPS I are presented after median and ulnar nerve stimulation of the Unaffected Hemisphere (UH) and Affected Hemisphere (AH). Amplitude and morphology differences are clearly visible. Intra-individual less differences are present. The highest CWP peaks are identified in the first 90 ms post stimulus. CWPs have a rather qualitative value in comparison of individuals. The GFP of these two patients display power (in femtoTesla^2) differences between the UH and the AH. For patient C-06 and C-11, the major GFP peaks and differences between the UH and AH are clearly visible.

In contrast to the GFP curves of subjects in Fig.

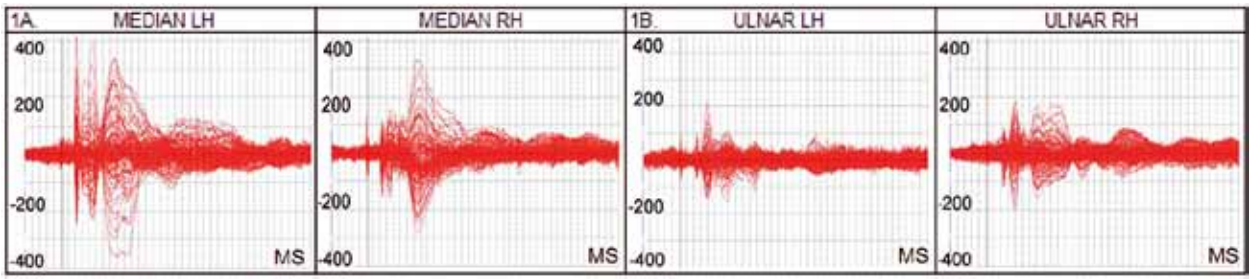

Fig. 1. CWPs after median (1A) and ulnar nerve (1B) stimulation of a healthy subject (HC-02) of the LH and RH. Median amplitudes, especially in the first 90 ms post stimulus are larger compared to the ulnar ones. Vertical: the amplitude in fT and horizontal the time in milliseconds (MS). Time window is 400 ms post stimulus, amplitude scales are ± 400 fT. CWPs = Compressed Waveform Profiles; fT=femtoTesla; LH = Left hemispheres; RH = right hemisphere.

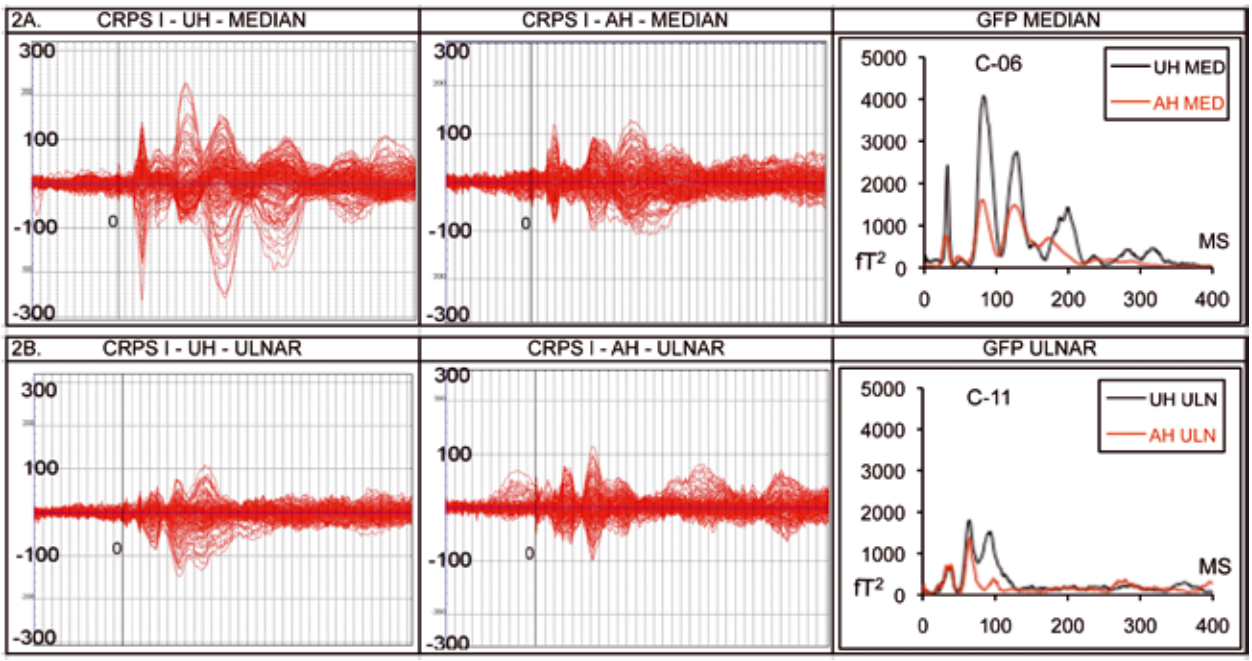

Fig. 2AB. The CWPs and GFPs of two patients with CRPS I are presented after median (2A) and ulnar (2B) nerve stimulation. In the GFP panels after median and ulnar nerve stimulation, responses in the UH are larger compared to the AH. Vertical is the amplitude in fT and horizontal the time in milliseconds (MS). AH = affected hemisphere; amplitude scales are ± 300 fT; fT=femtoTesla; power in fT^2 = femtoTesla^2 in the GFP median and ulnar curves, the zero indicates the stimulation onset; time in the GFP panels is in milliseconds (MS); UH = Unaffected hemisphere.

3A, the GFP in the AH for both patients display low values. The GFP curves in the UH of patient C-06 but especially in patient C-11, are low compared to subjects. Major activation is observed in the first 100 ms post stimulus.

Fig. 2CD depicts the CWPs and GFPs after median (2C) and ulnar nerve stimulation (2D) in two patients with a PNI. The CWPs presented several peaks, amplitude differences are visible in the 90 ms time window of major activation. Comparing the CWPs of all subjects and patients, large inter-individual differences were revealed but intra-individual differences were less.

Major GFP differences between the UH and AH are observed in the first 90 ms, large peaks at M30 and M70 are visible. In comparison with the GFP curves of the subjects in Fig. 3A, it is apparent that in the AHs of the two PNI patients, cortical activation is altered and displays relatively high values.

SEF Peak Stages: number and latencies

The M20 and M30 peaks in the early stage were consistently seen in all groups. A M40 is only observed in patients, not in subjects. For the CRPS I group at 41.0 ms ± 1.3 ms, the PNI group at 39.2 ± 1.8 ms and the peaks in the middle stage (50 ms - 90 ms), further referred as M50 and M70, are present in all groups. In the late stage (> 90 ms), apart from the M150 peak, late peaks are less frequently observed.

Comparison of the major peak latencies within the three groups, from M20 to M90, no statistical significant differences were found except for the ulnar M30 in the subject group where transmission to the RH was faster ($p = 0.005$). Between the three groups (Healthy Subjects (HS) – CRPS I and CRPS II), the observed latency differences were as follows:

(a) At M30, peak latencies between the CRPS I group and HS, for the median and ulnar

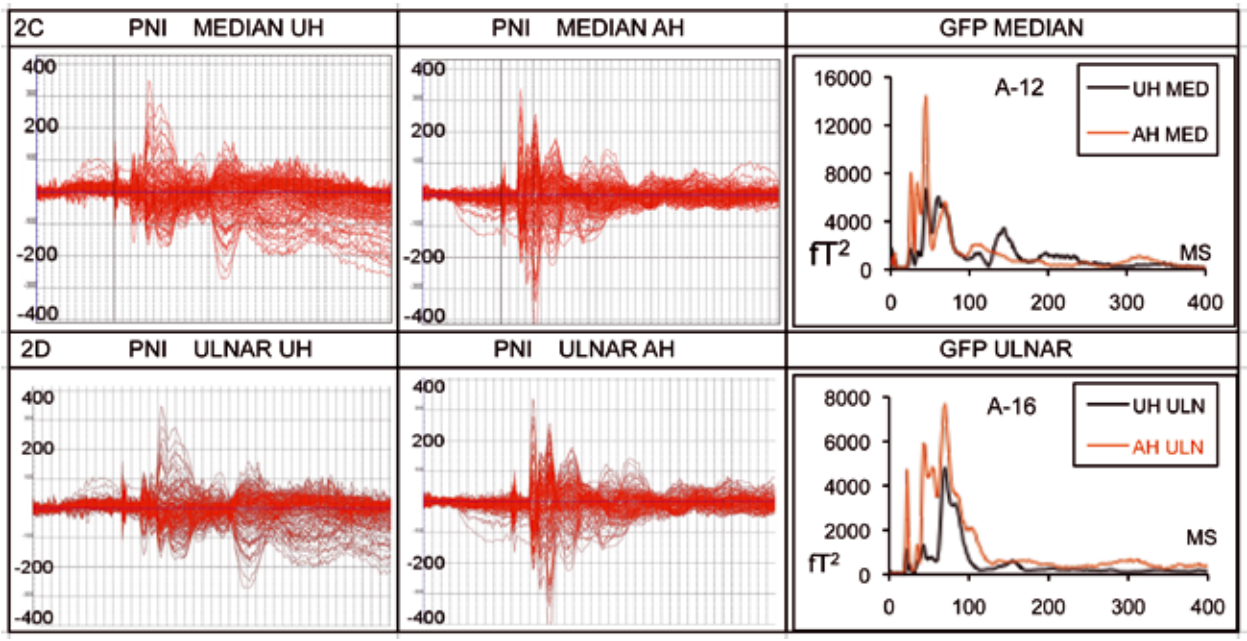

Fig. 2CD. The CWPs and GFPs of two patients with a PNI are depicted. The top three panels (2C) after median nerve stimulation. The lower three panels (2D) after ulnar nerve stimulation. Vertical is the amplitude in fT (fT=femtoTesla) and horizontal the time in milliseconds (MS). AH = affected hemisphere; amplitude scales are ± 400 fT; power in femtoTesla² in the GFP median and ulnar curves, the zero indicates the stimulation onset; time in the GFP panels is in milliseconds (MS); UH = Unaffected hemisphere.

nerves, were significantly shorter for the CRPS I UH and AH groups compared to HS (p = < 0.001 – p=0.006). At M70, the UH and AH peak latencies for both nerves did not differ compared to subjects.

(b) At M30, for the median nerve, in the CRPS II group and HS, the UH and AH, peak latencies were significantly shorter for the CRPS II group (p = 0.007 – 0.022). For the ulnar nerve, only transmission to the AH was faster. At M70, the UH peak latency was significantly shorter (p=0.033).

(c) At M30, CRPS I versus CRPS II: comparison of the UH/UH peak latencies revealed that for the median nerve, latency in CRPS I group was significantly shorter (p = 0.014) at M30, for the AH/AH no difference was found. For the ulnar nerve, at M30 UH/UH and AH/AH latencies were not different. The M70 latency did not differ for both groups.

Supplementary Digital Content 2 presents the incidences of the major peaks for the three groups.

GFP curves of the three groups

For all three groups, the mean GFP curves, after median and ulnar nerve stimulation, were produced as an overlay plot. *Subject group* (Fig. 3A left panels), black and red depict the median responses (N=20) and blue and green the ulnar responses (N=20). For the median and ulnar nerve in the first 90 ms post-stimulus, the M20 peak is relatively small but two major peak activations at M30 and M70 were found. Around M70 for both nerves major activity is observed, the median response is 4650 fT² and the ulnar between 3808 and 4193 fT². At all times the median GFP curves were higher compared to the ulnar ones.

CRPS I group: a different situation is found as depicted in the upper panels

(Fig. 3B-C). For the median group (N=12), the UH and AH curves are lower compared to subjects,

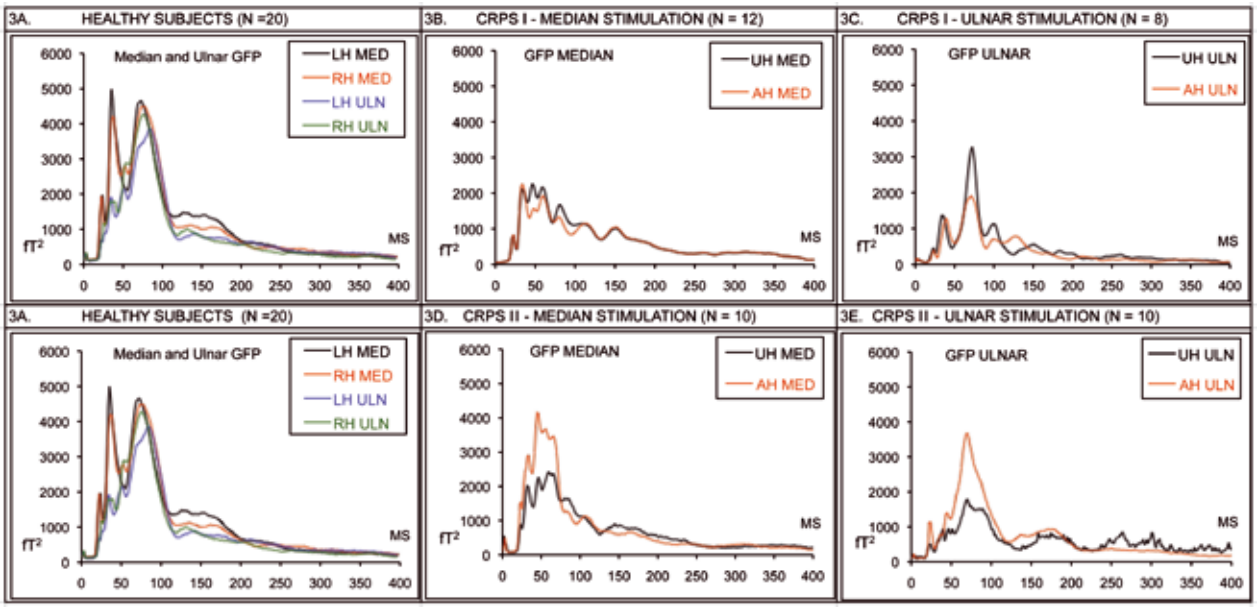

Fig. 3A-E depict the GFP curves after median and ulnar nerve stimulation for (Fig. 3A) the healthy subject group in the left top and lower panel; (Fig. 3B-C) after stimulation in the CRPS I group and (Fig. 3D-E) after stimulation in the PNI group. In the CRPS I group, GFP curves in the median group are comparable but in the ulnar group the UH curve is higher compared to the AH curve. In the CRPS II group, in the median and ulnar groups, the AH curves are higher compared to the UH curves. Power in femtoTesla² (fT²) on the y-axis, time on the x-axis from 0 to 400 milliseconds (MS).

for the ulnar group (N=8) the UH is higher compared to the AH curve. For the median and ulnar nerve, UH and AH are lower compared to subjects. A M70 peak (Fig. 3B) is missing in the median group.

CRPS II group: the GFP curves (Fig. 3D-E), after median (N=10) and ulnar (N=10) nerve stimulation, demonstrate a clear difference between the UH and the AH. For the median nerve, the mean GFP curve in the AH at M30 and M70 is higher compared to the UH. At this stage, mean GFP curves for patients remain lower compared to the subjects. The median and ulnar UH response in the *CRPS II* group is much lower compared to subjects.

Statistical analysis of the GFP peak values at M30 and M70

In Subjects, the M30 and M70 GFP peak values, for the median and ulnar nerves were statistically not different (paired t-test) and supported by the Effect Size data (Table 2A).

CRPS I. At M30 and M70, no statistical differences were found between the UH and AH after stimulation of both nerves (Table 2B). Statistical analysis of the peak values (Table 2C) between subjects and patients revealed that the median M30 UH and AH were significantly smaller compared to subjects. At M70, the median UH and AH GFP values also were significantly smaller. Ulnar M30 values were not different compared to subjects. At the ulnar M70 GFP peak, values of the UH and AH, values were significantly smaller compared to subjects.

CRPS II group. In the CRPS II group, GFP values at M70 between the UH and AH differed statistically for the median and ulnar nerve (Fig. 2C), AH peak values were significantly larger.

Comparison of the GFP data with the subject data at M30 and M70 revealed that for the median and ulnar nerve, the UH was significantly smaller

SUBJECTS

2A) Median nerve mean GFP values (Paired t-test)			
Peaks	M30 (fT²)	Peaks	M70 (fT²)
LH (20/20)	5740,6	LH (20/20)	5701,3
s.d.	4954,1	s.d.	3814,6
RH (20/20)	5283,3	RH (20/20)	6720,5
s.d.	3137,7	s.d.	5086,5
diff. RH-LH[1]	-457,3	diff. RH-LH[1]	1019,2
Effect Size (E.S.)	-0,09	E.S.	0,27
Ulnar nerve mean GFP values (Paired t-test)			
Peaks	M30 (fT²)	Peaks	M70 (fT²)
LH (18/20)	2585,1	LH (19/20)	4813,8
s.d.	2024,2	s.d.	4100,9
RH (20/20)	3031,4	RH (20/20)	5764,4
s.d.	2969,2	s.d.	5098,7
diff. RH-LH[1]	446,3	diff. RH-LH[1]	950,6
Effect Size (E.S.)	0,22	E.S.	0,23

Table 2A presents the mean GFP value data at M30 and M70 after median and ulnar nerve stimulation in the subject group (N=20). LH represents the response in the Left hemisphere after right median nerve stimulation, RH after left median stimulation. S.d. is the standard deviation. The superscript [1] indicates that in the ES formula, the LH values were taken as control. Numbers between brackets present the number of subjects out of 20 for both nerves with a M30 or M70 peak. GFP values are in fT² (femtoTesla²).

CRPS I PATIENTS

2B) Median nerve mean GFP values (Paired t-test)			
Peaks	M30 (fT²)	*Peaks*	M70 (fT²)
UH (11/12)[1]	3445,0	UH (10/12)[1]	2574,8
s.d.	3619,2	s.d.	1887,2
AH (11/12)	2445,3	AH (11/12)	3040,5
s.d.	2302,0	s.d.	2224,6
Effect Size (E.S.)	*-0,28*	*E.S.*	*0,25*
Ulnar nerve mean GFP values (Wilcoxon SRT)			
Peaks	M30 (fT²)	Peaks	M70 (fT²)
UH (8/8)[1]	2360,1	UH (8/8)[1]	3430,1
s.d.	2869,8	s.d.	5245,0
AH (8/8)	2135,5	AH (8/8)	2961,7
s.d.	3657,2	s.d.	4017,8
Effect Size (E.S.)	*-0,07*	*E.S.*	*-0,08*

Table 2BC. Table 2B: in the CRPS I groups, numbers between brackets present the numbers of M30 or M70 peaks in each hemisphere. GFP value data, mean and standard deviations (s.d.) in the UH and AH for the median and ulnar nerve are presented. Effect size (E.S.) data were included, the UH[1] indicates that the UH for both nerves in the E.S. formula was used as control.

2C) SUBJECTS versus CRPS I			
Median nerve mean GFP values (t-test / Mann Whitney RST)			
Peaks	M30 (fT²)	Peaks	M70 (fT²)
Mean LH & RH[1]	5489,5	Mean LH & RH[1]	6210,9
mean s.d.	3412,1	mean s.d.	4095,7
UH (11/12)	3445,0	UH (10/12)	2574,8**
Effect Size (E.S.)	*-0,59*	*E.S.*	*-0,89*
AH (11/12)	2445,3**	AH (11/12)	3040,5**
ES	*-0,89*	*E.S.*	*-0,77*
Ulnar nerve mean GFP values (t-test / Mann Whitney RST)			
Peaks	M30 (fT²)	Peaks	M70 (fT²)
Mean LH & RH[1]	2808,2	Mean LH & RH[1]	5534,3
s.d.	2226,8	s.d.	3978,2
UH (8/8)	2360,1	UH (8/8)	3430,1**
Effect Size (E.S.)	*-0,14*	*E.S.*	*-0,53*
AH (8/8)	2135,5	AH (8/8)	2961,7**
Effect Size (E.S.)	*-0,30*	*E.S.*	*-0,65*

*Table 2C presents the outcome of comparisons between the Subjects and CRPS I patients for both nerves at M30 and M70. In the E.S. formula, the mean LH and RH[1] and s.d. was used as control. GFP values are in femtoTesla2. Numbers between brackets indicate the numbers of a M30 or M70 peak out of the group. ** in light blue panels indicate statistical differences.*

CRPS II PATIENTS

2D) Median nerve mean GFP values (Paired t-test)			
Peaks	M30 (fT²)	Peaks	M70 (fT²)
UH (10/10)	2759,5	UH (9/10)	2826,4 **
Effect Size (E.S.)	*0,17*	*E.S.*	*1,93*
AH (9/10)	3532,0	AH (9/10)	5822,3 **
E.S.	*-0,08*	*E.S.*	*-0,75*
Ulnar nerve mean GFP values (Wilcoxon SRT)			
Peaks	M30 (fT²)	Peaks	M70 (fT²)
UH (10/10)	555,8	UH (10/10)	1875,4 **
Effect Size (E.S.)	*0,66*	*E.S.*	*1,76*
AH (10/10)	880,3	AH (10/10)	4750,2 **
E.S.	*0,00*	*E.S.*	*-0,22*

SUBJECTS versus PATIENTS

2E) Median nerve mean GFP values (t-test / Mann Whitney RST)			
Peaks	M30 (fT²)	Peaks	M70 (fT²)
Mean LH + RH[1]	5489,5	Mean LH + RH[1]	6210,9
s.d.	4101,0	s.d.	4461,1
UH (10/10)	2759,5**	UH (9/10)	2826,4 **
Effect Size (E.S.)	*-0,67*	*E.S.*	*0,76*
AH (9/10)	3532,0	AH (9/10)	5822,3
ES	*-0,48*	*E.S.*	*-0,09*
Ulnar nerve mean GFP values (t-test / Mann Whitney RST)			
Peaks	M30 (fT²)	Peaks	M70 (fT²)
Mean LH + RH[1]	2737,1	Mean LH + RH[1]	5301,3
s.d.	2517,0	s.d.	4641,4
UH (10/10)	555,8**	UH (9/10)	1875,4 **
Effect Size (E.S.)	*-0,87*	*E.S.*	*-0,70*
AH (9/10)	880,3**	AH (9/10)	4750,2
E.S.	*-0,74*	*E.S.*	*-0,005*

*Table 2DE. In Table 2D the statistical results of the comparison of the GFP values between the CRPS II groups are presented at M30 and M70, in Fig. 2E between the PNI group and subjects. Effect size (E.S.) data were included, the superscript[1] indicates that the mean LH & RH for both nerves in the E.S. formula was used as control. Numbers between brackets indicate the numbers of a M30 or M70 peak out of the group. ** in light blue panels indicate statistical differences.*

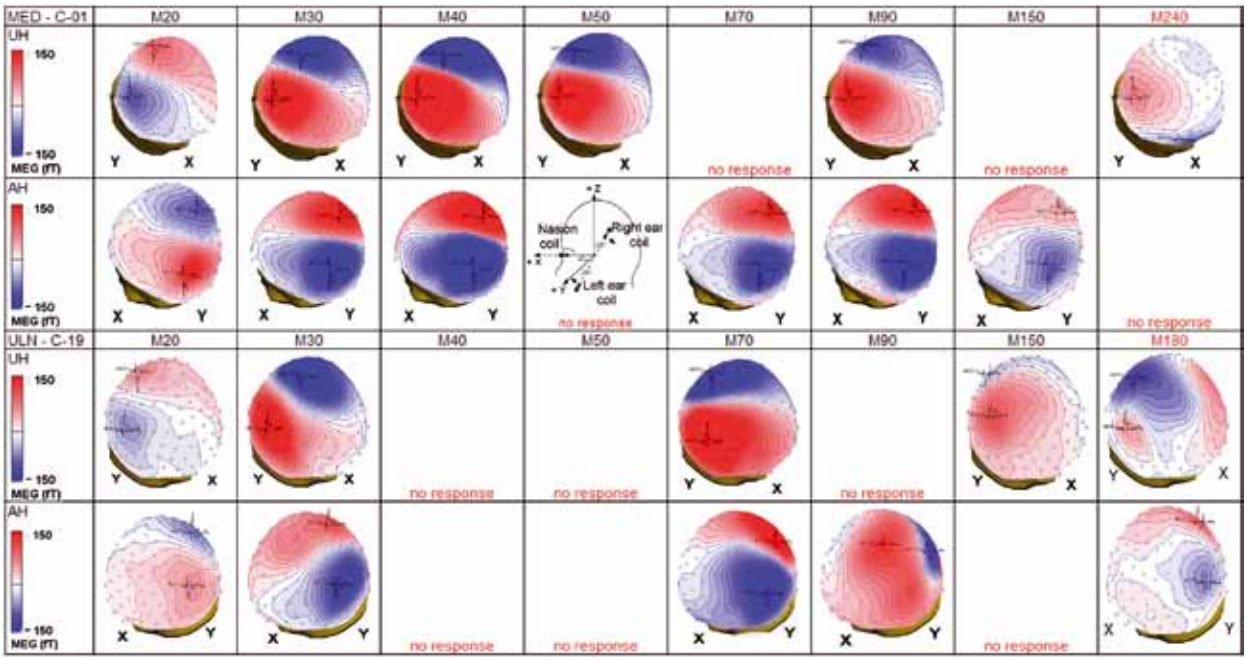

Fig. 4A. The brain maps of two CRPS I patients, C-01 and C-19, after median and ulnar nerve stimulation respectively, are presented in the 240 ms and 180 ms time window. In patient **C-01**, *in the UH and AH, after the first polarity reversal between M20/M30, no second polarity reversal in the 240 ms time window in discernable. In patient* **C-19**, *in the UH and AH, the reversal pattern is highly irregular and peaks are missing. Both reversals, at M20/M30 and M70/M150 can be observed. The amplitude scale is depicted in the first column and is between – 150 femtoTesla (fT) to + 150 fT. No response indicates that at that latency no peak has been identified.*

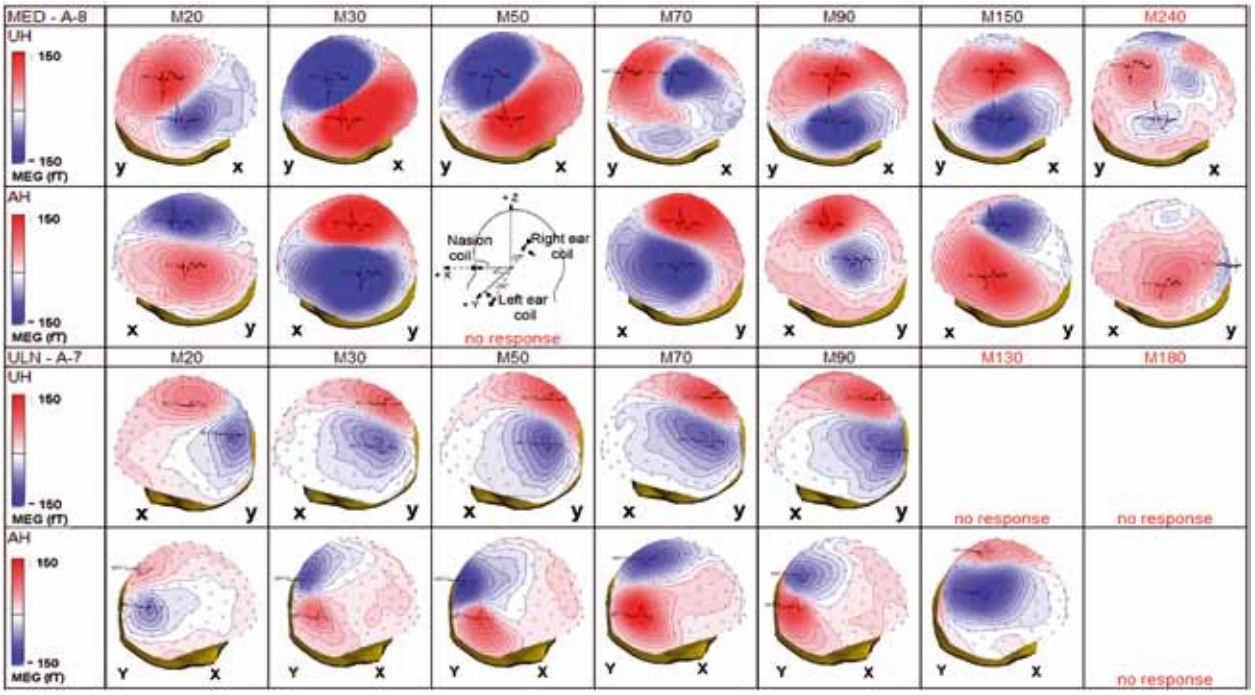

Fig. 4B. The brain maps of two CRPS II patients, A-8 and A-7, after median and ulnar nerve stimulation respectively, are presented in the 240 ms and 180 ms time window. The amplitude scale is depicted in the first column and ranges from – 150 femtoTesla (fT) to + 150 fT. In patient **A-8** *after median nerve stimulation, in the UH after the first polarity reversal between M20/M30, between M50/M70 and M70/M150 a gradual reversal occurs with changes in orientation. In the AH, a first reversal between M20/M30 and a second between M70/M150 is observed. In patient* **A-7** *after ulnar nerve stimulation in the UH, no first or second polarity reversal is observed. In the AH at M20/M30 a first reversal, and a second after M90/M150. The amplitude scale is depicted in the first column and is between – 150 femtoTesla (fT) to + 150 fT. No response indicates that at that latency no peak has been be identified.*

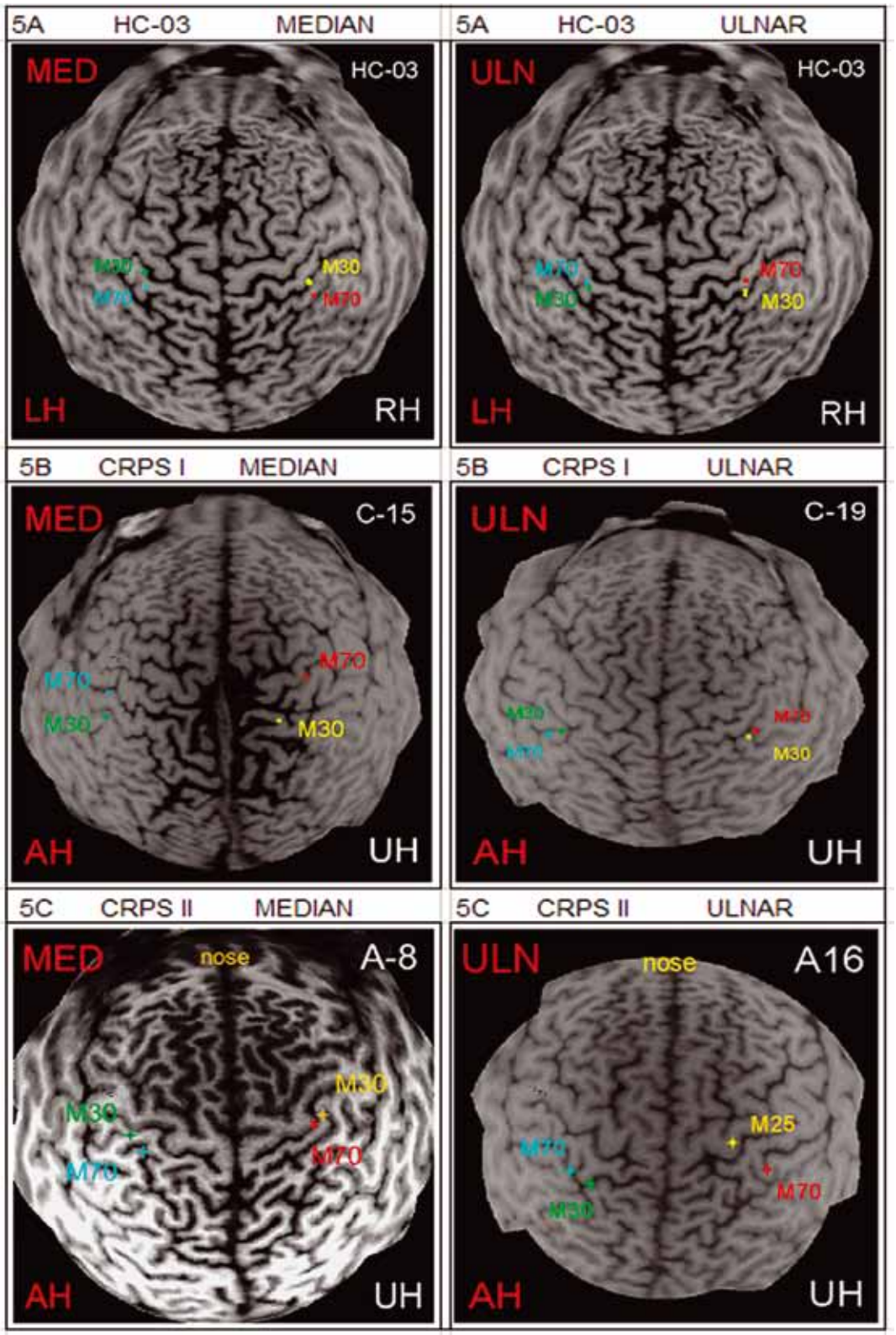

Fig. 5A-C. In Fig. 5 the M30 and M70 dipoles are depicted for all three figures with the same color code: M30 and M70 in the left hemisphere in green and cyan respectively, in the right hemisphere the M30 and M70 are in yellow and red respectively. In Fig. 5A the ECD localizations at M30 and M70 of healthy subject HC-03 after median and ulnar nerve stimulation are depicted. In Fig. 5B the ECD localizations at M30 and M70 two CRPS I patients are presented after median (HC-15) and ulnar (HC-19) nerve stimulation. In Fig. 5C two patients of the CRPS II group after median (A-8) and ulnar (A-16) nerve stimulation. The nose is depicted and marks the (+) x-axis. AH=affected Hemisphere; ECD=equivalent current dipole; LH=Left Hemisphere; M30=ECD at 30 ms; M70 the ECD at 70 ms; RH=right hemisphere; UH=Unaffected Hemisphere.

compared to subjects. The ulnar AH M30 value was also significantly smaller. Significant p-values were supported by ES data.

Comparison between the three GFP value groups
The GFP value profiles between the three groups differ in various ways. Table 2A-C demonstrates that in the CRPS I group, GFP values in the UH and AH are statistically not different at M30 and M70. CRPS I versus subjects demonstrates that at M70, the UH and AH are significantly smaller compared to subjects. Retrograde power values did not alter significances. Table AD-E for the CRPS II group demonstrates that the GFP values of the UH compared to the AH at M70 for both nerves, are significantly smaller. Comparison with subjects demonstrates that for both nerves at M30 and M70, all four UHs are significantly smaller compared to subjects. Only the AH GFP values at M30 for the ulnar nerve are smaller compared to subjects. The median M30 AH and the median and ulnar M70 AH are not significantly different compared to subjects.

3D Topography of SEFs
For all three groups brain maps were produced at the major peak latencies. The sequence of all brain maps exhibited a dynamic view of the cortical magnetic field changes in the 400 ms post stimulus time window. The first polarity reversal between M20 and M30 is consistently present in all groups. In a minority (3 /20) the reversal appeared between M30 – M50. The second polarity reversal in the subject group, for both nerves and both hands was found in 19 / 20 subjects between M90 and M150. In the CRPS I and II group, the second reversal appeared earlier, or there was a third reversal or the reversal was absent. A much less consistent presence of the second reversal in both patient groups was observed. Fig. 4A depicts two examples of the CRPS I group after median and ulnar nerve stimulation in patients C-1 and C-19, respectively.

Fig. 4B depicts of the CRPS II group, patients A-8 and A-7 after median and ulnar nerve stimulation, respectively. Fig. 4A and 4B demonstrate, compared to healthy subjects, that brain dynamics in both CRPS groups differ with respect to number of polarity reversals, latency of the reversals and direction of the dipolar fields.

Dipole characteristics
Description of the dipole characteristics for all three groups focuses on the M30 and M70 dipole, only the dipoles presenting a low residual error (<7%) were included for further study. M70 dipoles still suffer from the fact that multiple dipoles are active at the same time and a reliable multi-dipole model is not yet available. Fig. 5 depicts the M30 and M70 dipoles for a subject (5A), a CRPS I patient (5B) and a CRPS II (PNI) patient (5C). In Fig. 5A the M30 and M70 dipoles after median and ulnar stimulation are depicted in the LH and RH. The position at M30 and M70 in each hemisphere for the median nerve are reversed compared to the ulnar nerve. As can already be observed from the “axial pancake images”, while in the subjects groups M30 and M70 are closely positioned, in the CRPS groups there is wider variation.

Supplementary Digital Content 3 presents the dipole data of three representatives of the Subject, CRPS I and CRPS II groups in Fig.5. Based on these data, at M30 and M70, dipoles were located in the primary somatosensory cortices after inspection of the saggital and coronal views. Residual errors (res.err) are presented in percentages, positions in millimeters, orientation in degrees and strength in nanoAmperemeter (nAm).

Position data, orientation and strength
At M30 and M70, dipole data were compared in and between the groups.
Subjects: the M30 and M70 dipoles after median and ulnar stimulation were located in the primary somatosensory cortex. For the median and ulnar nerve, no significant dipole differences were found in the LH and RH. The median M30 dipole was anterior to the M70 dipole in the LH and RH, the reversed positions for the ulnar dipoles. *CRPS I*: at M30 and M70, for all dipole characteristics and for both nerves, no significant differences were found. *CRPS II*: comparison of the spatial positions of the UH and AH at M30 and M70, orientation and strength does not reveal a statistical difference for the median and ulnar nerves. *Between groups*: comparison of the subjects data with the CRPS I data for all six dipole characteristics, no significant differences were found. For the data between subjects and CRPS II, also no statistical differences were found. Dipole positions in the two patients groups demonstrated wider variation but dipoles with a low residual error were mainly located in the primary somatosensory cortex. At M70 for all three groups no ipsilateral activation was observed.

DISCUSSION

The continuous flow of afferent sensory information influences somatotopy during developing and adult life in a dynamic way.[54,55,56] Any change in input, both in animals and humans under physiological or pathological circumstances, will induce cortical plasticity, these mechanisms will last throughout human life span.[57,58,59,60,61]

In this study, interesting new differences were found in and between the CRPS type I and II patient groups compared to subjects in response to standard electrical nerve stimulation. The stimulation intensities to evoke a clear twitch in all three groups did not differ significantly, indicating that evoked responses were not affected by stimulation differences.

The GFP curves

In *healthy subjects*, the GFP curves displaying the spatial magnetic energy distribution (area of cortical activation) after median and ulnar nerve stimulation are highly congruous in the 400 ms post stimulus time window, two major peaks at M30 and M70 are identified. At these two peaks of highest power, cortical activation is largest The median evoked curves are higher compared to the ulnar curves, possibly the result of a larger cortical presentation of the median nerve compared to the ulnar nerve.

The distribution of cortical activation in the present study indicates that in the *CRPS I and II groups*, after long periods of continuous pain, cortically evoked activation changed compared to healthy subjects. For both groups, the *UH and AH GFP curves* are lower compared to subjects and indicate decreased cortical activation. The cortical responses in the UH indicate that the UH is part of hemispherical adaptive changes in these two pain syndromes. Therefore, the UH in these

two patients groups cannot simply be taken as control for the AH of each individual. The largest cortical changes are observed in the early and middle stage (0-90 ms).

The UH / AH GFP curves of the CRPS I and II group differed. The AH curves in CRPS I and II patients were all lower compared to subjects, the median and ulnar evoked responses presented differences. In the ***CRPS I*** group, the ulnar UH curve is higher compared to the AH, for the median nerve comparable. It suggests that in *CRPS I*, decreased cortical activation in the AH is balanced with a relatively higher UH activation, the AH curve at M30 and M70 presents a large decrease in cortical activation. In ***CRPS II***, the opposite is found. For both nerves the AH is higher compared to the UH. Possibly in the chronic state, peripheral injury (reflected in the AH) drives the contraleral hemispherical response but also the ipsilateral UH response is affected and is lower compared to the AH.

The GFP values

In the *subject groups*, after median and ulnar nerve stimulation, at M30 and M70 no significant statistical differences were found which indicates comparable cortical activation which supports the morphology of the GFP curves. In the ***CRPS I*** *group*, the UH and AH GFP values at M30 and M70, present statistically comparable values. Compared to subjects however, for the median nerve at M30 and M70 and for the ulnar nerve at M70, the UH and AH GFP values are significantly smaller. This implies for the CRPS I group that the UH and AH present a significant *shrinkage* of evoked cortical activation compared to subjects. In the ***CRPS II*** *group*, at M30 and M70, the AH GFP values for the median nerve were significantly larger compared to the UH values, for the ulnar nerve only at M70. This indicates altered cortical activation at these two major areas of cortical activation. Compared to subjects, in these patients the UH and AH demonstrated decreased activation. Therefore, in the *CRPS II* group in contrast to the CRPS I group, cortical activation in the AH is significantly larger compared to the UH.

Involvement of the UH in this study of both CRPS groups is an intriguing observation. The UH responses for both patient groups are lower for both nerves compared to healthy subjects. The GFP value differences at M30 and M70, largest areas of cortical activation, support these differences. It indicates that the UH in a patient with a unilateral affected upper extremity, is part of the functional cortical plasticity changes in the AH. Interhemispheric processing of somatosensory information was described in animals[62,63] and human studies [64,65,66,67,68] and it was concluded that global sensory processing was created by combining activity in each cerebral hemisphere through the corpus callosum. Whereby at this higher cortical level of integration, the flow of afferent information to the cortices is continuously balanced by inhibitory and/or excitatory interhemispheric somatosensory processing. This can result from adjusting the responsiveness of ascending sensory pathways, and includes altered interhemispheric transfer of callosal information: the periphery drives the cortical responses.[66,68,69,70] It indicates that adaptations to the interhemispheric transfer of information in humans is part of cortical plasticity mechanisms.[69,70]

Since the somatosensory and motor cortex are anatomically interconnected[54], altered somatosensory inputs will affect sensory-motor coupling. This may offer an explanation for dystonia found in CRPS.

The data at the group level in the present study suggest that balancing the somatosensory inputs in order to maintain the body schema

as in CRPS patients, includes changes in interhemispheric information processing which is supported by human studies.[63,64,65,66] Changes in callosal processing can be expressed in latency differences at comparable peaks. Study of the latency differences between the groups demonstrated that at M30 in the CRPS I group, median and ulnar peak latencies were significantly shorter compared to subjects but not at M70. This was to some extent present at M30 in CRPS II, only for the median nerve. Therefore, some indication of facilitation of nerve transmission is present in both groups but limited at M30 for the median nerve.

There is still debate on the true difference between CRPS I and II. In recent studies, evidence was presented for abnormal thin caliber NF positive/ MBP-negative axons innervating hair follicles and a decrease in epidermal, sweat gland and vascular innervation in CRPS I[2,4,5] These findings may relate to the complete functional loss of cutaneous sympathetic vasoconstrictor activity.[71,72] The question remains whether these neuropathological changes refer to a common cause (peripheral nerve injury) for both syndromes and whether in CRPS I these changes are primary or secondary. It also raises the question whether nerve injury of very small peripheral fibres, which are difficult to diagnose, is able to set into motion the cascade of changes that are observed in CRPS I. Bilateral involvement of the hemispheres in order to maintain the body schema[67,68], as demonstrated in this study, may alter physical training and rehabilitation strategies. Or the study of the cortical effects of medication that influence interhemispheric transmission. In CRPS II, reducing the drive of impaired inputs to the AH, due to the nerve injury, is directed at reducing pain and peripheral and central sensitization[70] as is performed by using electrical spinal cord stimulation. In short: the present study suggest that in CRPS I, relatively decreased impaired afferent inputs are balanced with the UH. In CRPS II, relatively increased impaired inputs are equally balanced. For this reason, therapeutic strategies will differ.

Conclusion

The changes in cortical activation in CRPS I and II, after standard median and ulnar nerve stimulation, demonstrate differences in cortical activation that indicate plasticity changes. Cortical reorganization in this study was best monitored using the GFP. In *CRPS I*, in the UH and AH relatively decreased cortical activation was found, as indicated by the GFP curves and values. In *CRPS II* the reversed situation was found, AH activation was larger compared to the UH. Involvement of the UH may indicate that in both pain syndromes, bilateral compensatory mechanisms are operational probably through altered inter-hemispherical information processing. At the individual and group level, non-invasive imaging techniques like magnetoencephalography and using standard electrical stimulation may further elucidate the mechanisms operational in CRPS I and II and facilitate effective treatment.[73]

Acknowledgements.
This study was made possible by a grant from Medtronic Europe(Tolochenaz – Switzerland). Technical support was provided by Bob W. van Dijk, Ph.D. and Kees Stam, Ph.D., Professor and Head Department of Clinical Neurophysiology and MEG Center, VU University Medical Hospital, Amsterdam, The Netherlands. Clinical support provided by Monique A. Dekkers, M.Sc., Medical Center Alkmaar, The Netherlands. We are grateful for all support.

Patient	age	sex	injured nerve	etiology & operation	Number*	Onset of pain	pain dura-tion (years)
A-1	35	F	median nerve	glass wound wrist, subtotally transected	3	immediately after trauma	4
A-2	43	M	radial nerve	sharp trauma, wrist,secondary entrapment correction	3	immediately after suture	3
A-3	47	M	median nerve	glass wound, total transection, median repair	1	2-3 months after injury	7
A-4	54	M	median nerve	glass wound, primary suture, neuroma removal	2	few weeks later	9
A-5	29	F	radial nerve	3 x ganglion operation at wrist, radial nerve neuroma	1	few weeks later	10
A-6	30	F	median nerve	glass wound, 50% transection	2	1 month later	1
A-7	63	F	radial nerve	de Quervain, wrist, nerve branch transection, neurolysis	4	immediately after operation	22
A-8	22	F	ulnar nerve	blunt trauma, ulnar transposition right	2	before 1st operation	3
A-9	49	M	radial nerve	sharp trauma: neurolysis right hand	2	2 months	3
A-10	61	F	radial nerve	de Quervain, wrist, pain and sensory loss	1	immediately after operation	1
A-11	55	M	ulnar nerve	neurinoma excision above elbow, infection wound	3	before 1st operation	4
A-12	63	F	radial nerve	de Quervain, wrist, radial nerve branch entrapment	5	immediately after operation	25
A-13	69	F	digit II nerve	neuroma excision twice	2	immediately after operation	2
A-14	67	F	digit V nerve	metacarpal fracture, neuroma forming digital nerve	2	immediately after operation	3
A-15	53	F	median nerve	CTS operation	1	before 1st operation	4
A-16	60	F	digit II nerve	matacarpal fracture, sensory loss and pain	0	within weeks	2
A-17	48	F	median nerve	CTS operation	1	before 1st operation	4
A-18	49	F	digit II nerve	digital nerve, local exploration and infection	1	before 1st operation	2
A-19	36	F	ulnar nerve	knife wound at wrist	2	immediately after operation	4
A-20	25	F	digit II nerve	knife wound at butchery	1	within weeks	2

Supplementary Digital Content 1 presents an overview of the demographic data of the patients included in the CRPS II group. The column "Number" presents the number of operations for each patients.

A) SUBJECTS	*< early >*			*< middle >*			*< late >*		
	M20	*M30*	*M40*	*M50*	*M70*	*M90*	*M150*	*M180*	*M240*
Median									
LH	20 / 20	20 / 20		15 / 20	20 / 20	18 / 20	15 / 20	7 / 20	14 / 20
RH	20 / 20	20 / 20		19 / 20	20 / 20	17 / 20	16 / 20	8 / 20	16 / 20
Ulnar	*< early >*			*< middle >*			*< late >*		
LH	19 / 20	20 / 20		16 / 20	18 / 20	18 / 20	14 / 20	12 / 20	13 / 20
RH	19 / 20	19 / 20		16 / 20	19 / 20	20 / 20	15 / 20	14 / 20	14 / 20
B) CRPS I	*< early >*			*< middle >*			*< late >*		
	M20	M30	M40	M50	M70	M90	M150	M180	M240
Median (12/20)									
UH	12/12	10/12	8/12	11/12	8/12	10/12	10/12	6/12	7/12
AH	12/12	10/12	8/12	8/12	10/12	10/12	11/12	8/12	6/12
Ulnar (8/20)	*< early >*			*< middle >*			*< late >*		
UH	8/8	7/8	4/8	5/8	7/8	8/8	4/8	3/8	3/8
AH	8/8	7/8	7/8	4/8	7/8	6/8	5/8	3/8	4/8
C) CRPS II	*< early >*		*< middle >*			*< late >*			
	M20	M30	M40	M50	M70	M90	M150	M180	M240
Median (10/20)									
UH	10 / 10	10 / 10	4 / 10	9 / 10	7 / 10	20 / 20	7 / 10	4 / 10	9 / 10
AH	10 / 10	10 / 10	4 / 10	8 / 10	9 / 10	20 / 20	7 / 10	5 / 10	6 / 10
	M20	M30	M40	M50	M70	M90	M150	M180	M240
Ulnar (10/20)	*< early >*		*< middle >*			*< late >*			
UH	10 / 10	9 / 10	6 / 10	9 / 10	8 / 10	4 / 10	8 / 10	4 / 10	4 / 10
AH	10 / 10	10 / 10	8 / 10	9 / 10	10 / 10	7 / 10	8 / 10	2 / 10	1 / 10

Supplementary Digital Content 2 presents for the three groups the incidences of the peaks in the 240 millisecond post stimulus time frame for both hemispheres.

HC-03

MED	M30 res. err.	lat.(ms)	x (mm)	y (mm)	z (mm)	declin.	azimuth	strength
LH	5,6%	31,2	5,4	44,3	83,5	102,8	158,9	30,4
RH	3,8%	32,0	-3,6	-38,4	80,1	117,6	204,2	27,7
	M70 res.err.							
LH	4,6%	70,4	-1,6	40,3	82,0	100,1	172,3	36,2
RH	6,7%	71,2	-8,6	-43,2	78,8	120,1	196,8	21,4
ULN			x (mm)	y (mm)	z (mm)	declin.	azimuth	strength
LH	5,2%	29,6	-1,6	38,6	80,2	103,1	168,7	39,6
RH	5,5%	28,8	-2,6	35,2	81,4	109,4	197,1	30,3
	M70 res.err.							
LH	1,9%	64,8	0,0	40,0	84,6	100,9	156,9	37,4
RH	2,8%	64,4	1,9	-39,3	83,6	116,7	212,7	32,4

CRPS I								
MED C-15	M30 res. err.	lat.(ms)	x (mm)	y (mm)	z (mm)	declin.	azimuth	strength (nAm)
UH	3,34%	25,6	-17,8	-39,1	76,0	94,7	210,7	18,7
AH	6,10%	30,4	11,9	36,4	79,1	86,2	166,4	10,8
	M70 res.err.							
UH	6,6%	60,8	12,8	-46,7	77,1	117,1	226,0	24,2
AH	6,5%	60,8	8,7	45,2	78,5	114,6	140,9	25,6

ULN C-19	M30 res. err.	lat.(ms)	x (mm)	y (mm)	z (mm)	declin.	azimuth	strength (nAm)
UH	4,1%	33,6	-0,0	-26,6	75,1	104,25	176,84	39,21
AH	10,4%	30,4	1,1	23,5	80,9	106,4	173,7	19,3
	M70 res.err.							
UH	4,0%	75,2	-0,0	-37,4	78,7	114,39	191,25	58,53
AH	6,9%	73,6	-6,3	40,2	79,9	133,0	150,4	36,9

CRPS II								
MED A-8	M30 res. err.	lat.(ms)	x (mm)	y (mm)	z (mm)	declin.	azimuth	strength (nAm)
UH	2,9	31,2	10,4	-43,0	73,8	114,4	207,7	56,4
AH	3,8%	34,4	2,9	36,5	82,3	93,2	172,7	52,8
	M70 res.err.							
UH	4,2%	65,6	9,5	-39,2	75,5	113,27	209,35	32,9
AH	5,0%	66,4	1,4	32,4	85,6	103,55	162,13	29,5

ULN A-16	M30 res. err.	lat.(ms)	x (mm)	y (mm)	z (mm)	declin.	azimuth	strength (nAm)
UH	6,6%	25,6	3,7	-30,1	91,8	92,6	181,0	9,2
AH	3,2%	33,6	-0,7	40,6	88,6	96,0	23,3	12,1
	M70 res.err.							
UH	4,83%	70,4	-10,6	42,3	83,5	115,4	183,6	30,9
AH	5,27%	70,4	11,3	38,8	93,6	109,0	179,8	35,9

Supplementary Digital Content 3 presents an overview of the dipole characteristics of a healthy subject, and two patients from the CRPS I and II group. Of each group at the M30 and M70 ECD after median and ulnar nerve stimulation. AH=Affected Hemisphere; azimuth= azimuth in degrees; decline.=declination in degrees; lat (ms)= the peak latency in milliseconds; LH=Left Hemisphere; MED= values after median nerve stimulation; res. err=residual error; RH=Right Hemisphere; Strength= strength in nanoAmperemeter (nAm); UH=Unaffected Hemisphere; x, y and z are the dipole positions in millimeter; ULN= values after ulnar nerve stimulation;

References

1. Merskey H (1994). Complex regional Pain Syndrome. In: Merskey H, Bogduk N (Ed), Classification of Chronic Pain, IASP Task Force on Taxonomy, International Association for the Study of Pain. IASP Press, Seattle, USA, pp. 40-4.

2. Albrecht PJ, Hines S, Eisenberg E, Pud D, Finlay DR, Connolly MK, Paré M, Davar G, Rice FL: Pathologic alterations of cutaneous innervation and vasculature in affected limbs from patients with complex regional pain syndrome. Pain 2006; 120:244-66.

3. Baron R: Peripheral neuropathic pain: From mechanisms to symptoms. Clin J Pain 2000; 16:12-20.

4. Oaklander AL, Rissmiller JG, Gelman LB, Zheng L, Chang Y, Gott R: Evidence of focal small-fiber axonal degeneration in complex regional pain syndrome-I (reflex sympathetic dystrophy). Pain 2006; 120:235-43.

5. Oaklander AL, Fields HL: Is reflex sympathetic dystrophy/complex regional pain syndrome type I a small-fiber neuropathy ? Ann Neurol 2009; 65:629-38.

6. Birklein F, Schmelz M, Schifter S and Weber M: The important role of neuropeptides in complex regional pain syndrome. Neurology 2001; 57:2179-84.

7. Birklein F: Complex regional pain syndrome. J Neurol 2005; 252:131-38.

8. Thacker MA, Clark AK, Marchand F, McMahon SB: Pathophysiology of peripheral neuropathic pain: immune cells and molecules. Anesth Analg 2007; 105:838-47.

9. Obata K, Noguchi K: Contribution of primary sensory neurons and spinal glial cells to pathomechanisms of neuropathic pain. Brain Nerve 2008; 60: 483-92.

10. Zhang YQ, Guo N, Peng G, Han M, Raincrow J, Chiu CH, Coolen LM, Wenthold RJ, Zhao ZQ, Jing N, Yu L: Role of SIP30 in the development and maintenance of peripheral nerve injury-induced neuropathic pain. Pain 2009; 146:130-40.

11. Baron R: Neuropathic pain, a clinical perspective. Handb Exp Pharmacol 2009; 194:3-30.

12. Guan X, Zhu X, Tao YX: Peripheral nerve injury up-regulates expression of interactor protein for cytohesin exchange factor 1 (IPCEF1) mRNA in rat dorsal root ganglion. Naunyn Schmiedebergs Arch Pharmacol 2009; 380:459-63.

13. Dykes RW: Central consequences of peripheral nerve injuries. Ann Plast Surg 1984; 13:412-22.

14. Das A: Plasticity in adult sensory cortex, A review. Network Comput Neural Syst 1997; 8:33-76.

15. Tinazzi M, Priori A, Bertolasi L, Frasson E, Mauguière F, Fiaschi A: Abnormal central integration of a dual somatosensory input in dystonia. Evidence for sensory overflow. Brain 2000; 123:42-50.

16. Juottonen K, Gockel M, Silén T, Hurri H, Hari R and Forss N: Altered central sensorimotor processing in patients with complex regional pain syndrome. Pain 2002; 98:315-23.

17. Schwenkreis P, Witscher K, Janssen F, Pleger B, Dertwinkel R, Zenz M, Malin JP and Tegenthoff M: Assessment of reorganization in the sensorimotor cortex after upper limb amputation. Clin Neurophysiol 2001; 112:627-35.

18. Maihöfner C, Handwerker HO, Neundörfer B, Birklein F: Patterns of cortical reorganization in complex regional pain syndrome. Neurology 2003; 61:1707-15.

19. Forss N, Merlet I, Vanni S, Hämäläinen M, Mauguière F, Hari R: Activation of human mesial cortex during somatosensory target detection task. Brain Res 1996; 734:229-35.

20. Devor M: Sodium channels and mechanisms of neuropathic pain. J Pain 2006; 7 (1 Suppl 1): S3-S12.

21. Stern J, Jeanmonod D, Sarnthein J: Persistent EEG overactivation in the cortical pain matrix of neurogenic pain patients. NeuroImage 2006; 31:721-31.

22. Krause P, Förderreuther S, Straube A: TMS motor cortical brain mapping in patients with complex regional pain syndrome type I. Clin Neurophysiol 2006; 117:169-76.

23. Larbig W, Montoya P, Braun C, Birbaumer N: Abnormal reactivity of the primary somatosensory cortex during the experience of pain in complex regional pain syndrome: a magnetoencephalographic case study. Neurocase 2006; 12:280-85.

24. Schaible HG: Peripheral and central mechanisms of pain generation. Handb Exp Pharmacol 2007; 177:3-28.

25. Navarro X, Vivó M, Valero-Cabré A: Neural plasticity after peripheral nerve injury and regeneration. Prog Neurobiol 2007; 82:163-201.

26. Veldman PH, Reynen HM, Arntz IE, Goris RJ: Signs and symptoms of reflex sympathetic dystrophy: prospective study of 829 patients. Lancet 1993; 342:1012-16.

27. Bruehl S, Harden RN, Galer BS, Saltz, S et al.: External validation of IASP diagnostic criteria for Complex Regional Pain Syndrome and proposed research diagnostic criteria. International Association for the Study of Pain. Pain 1999; 81:147-54.

28. Jänig W, Baron R: Complex regional pain syndrome: mystery explained? Lancet Neurol 2003; 2:687-97.

29. Stanton-Hicks M: Complex regional pain syndrome. Anesthesiol Clin North America 2003; 21:733-44.

30. Harden RN, Bruehl S, Stanton-Hicks M, Wilson PR: Proposed new diagnostic criteria for complex regional pain syndrome. Pain Med 2007; 8:289-92.

31. Schürmann M, Gradl G, Zaspel J, Kayser M, Lohr P, Andress HJ: Peripheral sympathetic function as a predictor of complex regional pain syndrome type I (CRPS I) in patients with radial fracture. Auton Neurosci 2000; 86:127-34.

32. Perez RS, Collins S, Marinus J, Zuurmond WW, de Lange JJ: Diagnostic criteria for CRPS I: differences between patient profiles using three different diagnostic sets. Eur J Pain 2007; 11:895-902.

33. Albazaz R, Wong YT, Homer-Vanniasinkam S: Complex regional pain syndrome: a review. Ann Vasc Surg 2008; 22:297-306.

34. Albrecht PJ, Hines S, Eisenberg E, Pud D, Finlay DR, Connolly MK, Paré M, Davar G, Rice FL: Pathologic alterations of cutaneous innervation and vasculature in affected limbs from patients with complex regional pain syndrome. Pain 2006; 120:244-66.

35. Birklein F, Schmelz M: Neuropeptides, neurogenic inflammation and complex regional pain syndrome (CRPS). Neurosci Lett 2008; 437:199-202.

36. Kline DG, Hudson AR: Basic considerations. Edited by Kline DG, Hudson AR. Nerve injuries. Operative Results for Major Nerve Injuries, Entrapments, and Tumors. W.B. Saunders Company. Philadelphia, London, 1995, pp 1-29.

37. Bryant PR, Kim CT, Millan R: The rehabilitation of causalgia (complex regional pain syndrome-type II). Phys Med Rehabil Clin N Am 2002; 13:137-57.

38. Treede RD, Apkarian AV, Bromm B, Greenspan JD, Lenz FA: Cortical representation of pain: functional characterization of nociceptive areas near the lateral sulcus. Pain 2000; 87:113-19.

39. Schüning J, Scherens A, Haussleiter IS, Schwenkreis P, Krumova EK, Richter H, Maier C: Sensory changes and loss of intra-epidermal nerve fibers in painful unilateral nerve injury. Clin J Pain 2009; 25:683-90.

40. McAllister RM, Calder JS: Paradoxical clinical consequences of peripheral nerve injury: a review of anatomical, neurophysiological and psychological mechanisms. Br J Plast Surg 1995; 48:384-95.

41. Costigan M, Scholz J, Woolf CJ: Neuropathic pain: A maladaptive response of the nervous system to damage. Annu Rev Neurosci 2009; 32:1-32.

42. Latremoliere A, Woolf CJ: Central sensitization: A generator of pain hypersensitivity by central neural plasticity. J Pain 2009; 10:895-926.

43. Woolf CJ. Central sensitization: implications for the diagnosis and treatment of pain. Pain 2011; 152:S2-15.

44. Baron R: Mechanisms of disease: Neuropathic pain, a clinical perspective. Nat Clin Pract Neurol 2006; 2:95-106.

45. Assmus H: Somatosensory evoked cortical potentials (SSEP) in regenerating nerves following suture. Elektroenzephalogr Elektromyogr Verwandte Geb 1978; 9:167-71.

46. Theuvenet PJ, Dunajski Z, Peters MJ, van Ree JM: Responses to median and tibial nerve stimulation in patients with chronic neuropathic pain. Brain Topography 1999; 11:305-13.

47. Tecchio F, Padua L, Aprile I, Rossini PM: Carpal tunnel syndrome modifies sensory hand cortical somatotopy: a MEG study. Hum Brain Mapp 2002; 17:28-36.

48. Nuwer MR, Aminoff M, Desmedt J, Eisen AA, Goodin D, Matsuoka S, Mauguière F, Shibasaki H, Sutherling W, Vibert JF: IFCN recommended standards for short latency somatosensory evoked potentials. Report of an IFCN committee. International Federation of Clinical Neurophysiology. Electroencephalogr Clin Neurophysiol 1994; 91:6-11.

49. Lehmann D, Skrandies W: Reference-free identification of components of checkerboard-evoked multichannel potential fields. Electroencephal Clin Neurophysiol 1980; 48:609-21.

50. Hamburger HL, vd Burgt MA.: Global field power measurement versus classical method in the determination of the latency of evoked potential components. Brain Topogr 1999; 3:391-96.

51. Chapman RC, Schimek F, Colpitts YH, Gerlach R, Dong WK: Peak Latency Differences in Evoked Potentials Elicited by Painful Dental and Cutaneous Stimulation. Int J Neurosci 1985;27:1-12.

52. Lin YY, Shih YH, Chang KP, Lee WT, Yu HY, Hsieh JC, Yeh TC, Wu ZA, Ho LT: MEG localization of Rolandic spikes with respect to SI and SII cortices in benign Rolandic epilepsy. NeuroImage 2003; 20:2051-61.

53. Fuchs M, Wagner M, Kastner J: Confidence limits of dipole source reconstruction results. Clin Neurophysiol 2004; 6:1442-51.

54. Kaas JH: Functional implications of plasticity and reorganizations in the somatosensory and motor systems of developing and adult primates, The somatosensory system. Edited by Nelson RJ. Boca Raton, CRC Press, 2001, pp 367-82

55. Kaas JH and Collins CE: Anatomic and functional reorganization of somatosensory cortex in mature primates after peripheral nerve and spinal cord injury. Adv Neurol 2003; 93:87-95.

56. Hummel F, Gerloff C, Cohen LG: Modulation of Cortical Function and Plasticity in the Human Brain, Neural plasticity in adult somatic sensory-motor systems, 1st edition. Edited by Ebner FF. Boca Raton, Taylor & Francis Group, 2005, pp 207-27

57. Schroeder CE, Seto S, Garraghty PE: Emergence of radial nerve dominance in median nerve cortex after median nerve transection in an adult squirrel monkey. J Neurophysiol 1997; 77:522-26.

58. Buonomano DV, Merzenich MM: Cortical plasticity: from synapses to maps. Annu Rev Neurosci 1998; 21:149-86.

59. Florence SL, Boydston LA, Hackett TA, Taub Lachoff H, Strata F, Niblock M M: Sensory enrichment after peripheral nerve injury restores cortical, not thalamic, receptive field organization. European Journal of Neuroscience 2001, 13:1755-66.

60. Hickmott PW and Merzenich MM: Local circuit properties underlying cortical reorganization. J Neurophysiol 2002; 88:1288-01.

61. Flor H: Remapping somatosensory cortex after injury. Adv Neurol 2003; 3:195-04.

62. Calford MB, Tweedale R: Interhemispheric transfer of plasticity in the cerebral cortex. Science 1990; 249:805-07.

63. Iwamura Y, Taoka M, Iriki A: Bilateral activity and callosal connections in the somatosensory cortex. Neuroscientist 2001; 7:419-29.

64. Disbrow EA, Roberts T, Poeppel D, Krubitzer L: Evidence for interhemispheric processing of inputs from the hands in human S2 and PV. J Neurophysiol 2001; 85:2236-44.

65. Li L, Ebner FF: Balancing bilateral sensory activity: callosal processing modulates sensory transmission through the contralateral thalamus by altering the response threshold. Exp Brain Res 2006; 172:397-15.

66. Hinkley LB, Krubitzer LA, Nagarajan SS, Disbrow EA: Sensorimotor integration in S2, PV, and parietal rostroventral areas of the human sylvian fissure. J Neurophysiol 2007; 97:1288-97.

67. Berlucchi G, Aglioti SM: The body in the brain revisited. Exp Brain Res 2010; 200:25-35.

68. Berlucchi G: What is callosal plasticity ?. Edited by Chalupa LM, Berardi N, Caleo M, Galli-resta L, Pizzorusso T: Cerebral Plasticity, new perspectives, 1st Edn. Massachusetts Institute of Technology, Toppan Best-set Premedia Limited, USA, 2011, pp 235-46.

69. Tinazzi M, Priori A, Bertolasi L, Frasson E, Mauguière F, Fiaschi A: Abnormal central integration of a dual somatosensory input in dystonia. Evidence for sensory overflow. Brain 2000; 123 (Pt 1):42-50.

70. Schwenkreis P, Scherens A, Rönnau AK, Höffken O, Tegenthoff M, Maier C: Cortical disinhibition occurs in chronic neuropathic, but not in chronic nociceptive pain. BMC Neurosci. 2010;11:73.

71. Wasner G, Heckmann K, Maier C, Baron R. Vascular abnormalities in acute reflex sympathetic dystrophy (CRPS I): complete inhibition of sympathetic nerve activity with recovery. Arch Neurol 1999; 56:521-2.

72. Wasner G, Schattschneider J, Heckmann K, Maier C, Baron R. Vascular abnormalities in reflex sympathetic dystrophy (CRPS I): mechanisms and diagnostic value. Brain 2001; 124:587-99.

73. Perez RS, Zollinger PE, Dijkstra PU, Thomassen-Hilgersom IL, Zuurmond WW, Rosenbrand KC, Geertzen JH; CRPS I task force. Evidence based guidelines for complex regional pain syndrome type 1. BMC Neurol. 2010; 31:10:20.

Chapter 10 DISCUSSION

The general aim of this study was to investigate the cortically evoked responses after standard electrical median and ulnar nerve stimulation in two patient groups with either a type I or a type II Complex Regional Pain Syndrome (CRPS) and to compare the results with those in healthy subjects using identical measuring procedures.

Chapter 2 presents the relevant neuroanatomy and functional neuroplasticity changes. Chapter 3 provides the backgrounds of magnetoencephalography (MEG), dipole localization and human cortical brain mapping. To answer the general research question of this study, five specific investigations were executed, which are presented in Chapters 4 to 9. In chapter 10, the 5 specific investigations are discussed and conclusions are drawn.

***Investigation I**: to examine the stability and repeatability of evoked responses after standard electrical median, ulnar and posterior tibial nerve stimulation in the cortex of the brain in two studies of patients with a unilateral peripheral nerve injury and neuropathic pain.*

It was hypothized that if abnormal peripheral and/or central inputs are an underlying cause in neuropathic pain resulting in central sensitization (Woolf, 1993), we would find evidence for this on the cortex. With the use of a 19-channel MEG and a 34-channel EEG (Twente University), the cortically evoked responses after standard electrical median, ulnar or posterior tibial nerve stimulation were measured in a group of eight patients with continuous neuropathic pain due to a unilateral peripheral nerve injury (arm or leg). All the patients were measured when in pain and in pain-free condition. When the patient was in pain, the cortically evoked responses demonstrated that an amplitude enhancement occurred in the affected hemisphere (AH), in contrast to the unaffected hemisphere (UH), between 80-150 ms post stimulus. In the pain free condition after Spinal Cord Stimulation (SCS), the enhancement rapidly decreased. We were first to demonstrate the pain blocking effects of SCS on the cortex (Theuvenet et al., 1999). In 3/8 patients, these MEG measurements were repeated after a longer period of SCS (1-12 months) using EEG, since the noise due to the pulse generator prevented the use of MEG. It was found that in the pain-free condition after SCS, the functionally enhanced cortical responses in the AH decreased (Chapter 4), confirming the stability and reversibility of cortically evoked responses in this group of patients. In a similar group of eight patients the measurements were repeated at the MEG center (Amsterdam) with a 151-channel whole-head MEG system. Instead of the SCS used in the pilot phase at Twente University, a local anesthetic was applied at the painful site to block the pain. Again the cortical differences between the AH and UH were observed, which decreased after a local anesthetic block (part of Chapter 8).
In conclusion, the observation proved consistent that cortically evoked responses in patients with neuropathic pain changed in a reproducible way when the pain was blocked (by SCS or a local anesthetic block). This finding initiated the main study.

***Investigation II**: to study the characteristics of the cortically evoked magnetic responses in healthy subjects after electrical median and ulnar nerve stimulation as a frame of reference for the measurements in the two patient groups.*
Cortically evoked magnetic responses were studied in 20 healthy subjects using a whole-head 151-channel MEG. Standard electrical median and ulnar nerve stimulation was performed in a randomized way. The parameters studied were: number of peaks, peak latencies, compressed waveform profiles (CWP), global field power (GFP),

3D-brain maps, and six equivalent current dipole (ECD) characteristics (3 location, 2 orientation and strength).

After median and ulnar nerve stimulation, cortically evoked responses revealed a number of characteristics in the 400 ms post stimulus. The number of peaks (6-8) and peak latencies in the 400 ms post stimulus were highly consistent for the median and ulnar nerve. At the inter-individual level for both groups, wide variation in CWPs was observed, which limits the use of the CWPs for peak number and latency identification. Transmission at the M20 peak after median nerve stimulation was significantly faster than after ulnar stimulation ($p<0.001$). As for the position parameters, the median dipole displayed a more anterior (x-axis), more lateral (y-axis) and inferior (z-axis) position than the ulnar dipole. This was found for both the M20 and M30 dipole, which corresponds with the somatosensory anatomy of the homunculus. The interpolar distances over the cortex between both nerves at M20 were calculated to be at 11.17 mm ± 4.93 after right hand stimulation and 16.73 mm ± 5.66 after left hand stimulation. Dipole strengths of the median dipoles were larger at M20 and M30 than those of the ulnar dipoles.

In the 400 ms post stimulus period, 3D brain maps of all the identified peaks for both nerves displayed a highly consistent pattern, which is supported in the literature by several other MEG studies (e.g. Hari et al., 1984; 1 Rossini et al., 1994; Vanni et al., 1996; Hari and Forss, 1999; Kakigi et al., 2000; Tecchio et al., 2000; Huttunen et al., 2006). Two polarity reversals were observed (M20/M30 and M90/M150) for both nerves. GFP curves, which display the spatial cortical magnetic energy distribution during 400 ms post stimulus and reflect underlying neural activity at each time point, were observed to be highly congruous for the median and ulnar nerve, although the median nerve displayed higher power than the ulnar nerve. Two major peaks were found, at M30 and M70. Based on the ECDs at M30 and M70, with a low residual error, neural sources for both nerves were positioned in the primary somatosensory cortex (SI). This indicates that somatosensory processing in SI takes place in the early and middle stage of the response (20-90 ms). No evidence was found for complete interhemispherical homology or sensory hand dominance in brain responses of either hand, as measured by MEG (Chapter 6 and 7).

In conclusion, in healthy subjects, the cortically evoked responses after standard electrical nerve stimulation revealed a high consistency of the responses. The results of this second investigation in healthy subjects provide a frame of reference for evaluating cortical changes in functional disorder and disease sequelae.

Investigation III*: to examine the characteristics of the cortically evoked responses in two patient groups: CRPS I and CRPS II.*

The cortically evoked magnetic responses in CRPS I and II patients with unilateral chronic pain in an upper extremity were compared on the basis of ten characteristic response parameters (Chapter 8 and 9). At the interindividual level for both groups, large variations in CWPs were observed, which limits the use of the CWPs for peak number and latency identification. Based on the *GFP curves and values* for median and ulnar nerve stimulation, it was found that cortical activation profiles differed for the CRPS I and II groups. In *the CRPS I* group, cortical activation in the AH was smaller than or comparable to cortical activation **in** the UH. In the *CRPS II* group, activation in the AH was significantly larger than in the UH for both nerves. This finding indicates that at the group level, a functional cortical difference is observed between CRPS I and II. In CRPS I, in contrast to CRPS II, a decrease of afferent somatosensory inputs to the AH may be present,

or inputs may be altered due to modulation (e.g. descending inhibition), or both. . This is supported by the fact that the CRPS II AH GFP value for the median nerve at M70 was significantly larger than the CRPS I UH and AH GFP value.

Compared with CRPS II, the peak latencies at M30 after median nerve stimulation of the UHs were significantly shorter in the CRPS I group, indicating faster transmission. At M70, no significant differences were observed for both nerves and both syndromes. At the M30 and M70 peaks for both patient groups, the *ECDs* with a low residual error were mainly localized in SI. After nerve stimulation, dipolar fields at M70 depicted contralateral activation only, excluding ipsilateral activation in SII.

Based on the GFP curves in the present study, our data suggest that SII is not the major site of change of activation. Brain maps depicted irregular patterns of cortical activation at all the identified peaks for both groups and both nerves. First and second polarity reversals appeared later, earlier or not at all. This suggests altered somatosensory processing in both patient groups. The generators of the second polarity reversal at M90/M150 are hard to localize, because the required source model does not have a stable inverse solution.

In the CRPS II group only (Chapter 8), measurements were repeated in the pain free state after a local anesthetic block (Theuvenet et al., 2011). After the block and in pain free condition, the GFP value differences for both nerves between the UH and AH at M70 disappeared (UH-AH block). In the CRPS II group, the altered cortical responses in the AH in the pain free state suggest a rapid reversibility of the functional cortical plasticity changes.

In conclusion, cortically evoked responses in CRPS I and II demonstrated different profiles in the spatial distribution of cortically evoked activation, and in both syndromes evidence for cortical plasticity was found. In the CRPS II group, the interhemispheric differences in pain and in pain-free condition indicate cortical functional reversibility even after many years of chronic neuropathic pain. These changes were comparable to the first observations presented in Chapter 4.

Investigation IV*: to compare the characteristics of the three groups: (a) healthy subjects; (b) CRPS I patients and (c) CRPS II patients.*

Comparison of the stimulation threshold intensities across the three groups at all stages of the measurements demonstrated no significant differences. This implies that the cortically evoked response differences cannot be ascribed to stimulation differences.

In contrast to healthy subjects, CRPS I and CPRS II patients presented *bilateral* altered cortically evoked responses in the early and middle stages after standard electrical nerve stimulation (0-90 ms post stimulus), which were located in SI. At M30 and M70 in CRPS I and II, and compared to healthy subjects, GFP differences in cortical activation were observed in the AH. After median and ulnar nerve stimulation, the UH and AH GFP values in *CRPS I* were both significantly lower than in healthy subjects. In *CRPS II*, the UH GFP values were also significantly lower than in healthy subjects, but the AH values did not differ significantly. In both patient groups, the cortical changes in the UH and AH indicate cortical plasticity changes. No specific pain intervention for the CRPS I group was employed in this investigation.

At *M30*, significant peak *latency differences* were found between healthy subjects and both CRPS groups: in patients, the peak latencies were shorter in the UH and AH. At *M70*, only the UH of the CRPS II group showed a significantly shorter latency than the one found in healthy subjects. A lower peak latency in CRPS patients may indicate faster transmission to the cortex. As was pointed

out in the third investigation, brain maps at all the identified peaks for both patient groups and both nerves depicted irregular patterns of cortical activation, in contrast to *healthy subjects*, and first and second polarity reversals appeared later, earlier or not at all.

In conclusion, cortically evoked plasticity changes dominate the responses in CRPS I and II. GFP value differences in the early and middle stages characterized these changes. Altered patterns of 3D brain mapping in the two patient groups support these observations. There is evidence for faster transmission to the cortex, which may indicate facilitation of transmission.

***Investigation V**: to assess the functional cortical differences between the three groups and to determine whether different cortical profiles exist.*

In healthy subjects, highly congruous distribution of cortical activation occurred in the 400 ms post-stimulus time window after electrical stimulation of the median and ulnar nerve, displaying two major areas of cortical activation at M30 and M70 in both hemispheres. This is in contrast with CRPS I and II, where, in the chronic pain state, both hemispheres were involved in cortical plasticity changes, and both displayed bilateral changes. In CRPS I, the cortically evoked responses after ulnar nerve stimulation were smaller in the AH than in the UH, whereas for median nerve stimulation this was less obvious. In CRPS II the opposite situation occured (Chapter 9), as responses at M70 in the AH were significantly larger than in the UH. Significantly decreased cortical activation in CRPS I and II compared with healthy subjects suggests decreased or modulated afferent somatosensory inputs along the neuraxis, or compensatory effects to these impaired inputs by altered interhemispheric transmission, or both (Hummel et al., 2005).

In the CRPS II group, a local anesthetic block was applied to test the changes in the AH (Chapter 8). In the pain-free condition after the block, a significant functional reduction of the cortical response in the AH was found. No intervention in the CRPS I group was employed in our study. In a MEG study of CRPS I patients with pain, a functionally significant shrunken hand area of the cortical hand representation was found in the AH, using air-puff-derived tactile finger stimulation (Maihöfner et al., 2003). In a second study employing the same finger-stimulation technique, pain interventions were performed using NSAIDs (non-steroidal anti-inflammatory drugs), amitryptiline and gabapentine (Chapter 9). After clinical improvement and pain reduction, cortical plasticity changes in the AH were reversible. The cortical reorganizational parameter that correlated best with the changes in cortical plasticity was the presence or absence of pain. However, functional restoration of the shrunken somatosensory hand area in CRPS I patients was observed after effective pain therapy (Maihöfner et al., 2004). In contrast with our present study, both studies by Maihöfner and coworkers included a comparison with the patients' UH, but not with healthy subjects. In our study, bilateral cortically evoked responses in CRPS I and II, in the UH and AH, were observed, which presented cortical plasticity changes in response to the disease. Therefore, the definition of the UH in the present study, the "evoked responses in the hemisphere contralateral to the unaffected extremity after electrical nerve stimulation", defines the hemisphere but does not exclude plasticity changes in the course of CRPS.

In conclusion, in healthy subjects highly congruous activation has been found after electrical median and ulnar nerve stimulation in the early and middle stage. CRPS I and II both demonstrated cortical plasticity changes as observed in the GFP curves and values at M30 and M70, basically in the same time frame as in healthy subjects. Unlike healthy subjects, both patient groups showed evidence of faster transmission at M30 in the UH and AH

for the median and ulnar nerve. In the UH at M30, transmission in the CRPS I group was significantly faster.

General conclusions, theoretical considerations and future perspectives

General conclusions

This study presents the first systematic evaluation and comparison of cortically evoked responses after standard electrical median and ulnar nerve stimulation in Complex Regional Pain Syndrome I and II, using MEG. Moreover, unlike several related publications in this field, our results are compared with a group of healthy subjects measured under identical conditions.

The results of the Study investigations 1 to 5 reveal differences in cortically evoked responses in CRPS I and II compared with healthy subjects. The overview in Chapter 2 outlines several aspects of importance for this study concerning the major afferent somatosensory pathways and the subcortical and cortical areas involved in somatosensory processing, including pain (Burton, 2005).

In response to altered environmental circumstances (e.g. physiological changes, tissue damage, infection), neuroplasticity occurs at the peripheral receptor, the dorsal root ganglion, and in subcortical and cortical areas. The afferent somatosensory pathways convey contralateral and ipsilateral information (Chapter 2). Therefore, the two cerebral hemispheres receive bilateral somatosensory inputs under physiological and pathological conditions. At the cortical level, interhemispheric transfer of somatosensory information in humans is facilitated by the corpus callosum and the commissura anterior (Bloom and Hynd, 2005). At higher cortical levels, processing of intra- and interhemispherical somatosensory information continuously maintains the body schema (Wyke, 1982; Schwoebel and Coslett, 2005; Berlucchi, 2010). In the present study, this was reflected in the highly congruous distribution of cortical activation over the left and right hemispheres in healthy subjects after median and ulnar nerve stimulation; there was a balance in the spread of cortical activation during the entire 400 ms post-stimulus time frame.

As was pointed out in Chapter 2, 8 and 9, interhemispheric transfer of information is influenced by inhibitory or excitatory changes, and probably both mechanisms are involved (Kaas, 1999; Burton, 2005; Bloom and Hynd, 2005). In an earlier human mechanism-based study, GABAergic drugs like benzodiazepines (e.g. lorazepam) released the inhibitory action of cortical inter-hemispheric transmission (Hummel et al., 2005) and influenced acute cortical plasticity changes as observed after an Ischemic Nerve Block or INB (2 Rossini et al., 1994; Werhahn et al., 2002). After INB in one hand, an improved tactile discrimination in the other, non-deafferentiated hand was observed, which only lasted for the duration of the INB. Therefore, under certain physiological and pathological circumstances homeostasis of the body schema will induce continuous cortical plasticity changes in both hemispheres (Li and Ebner, 2006; Berlucchi, 2010; Berlucchi and Aglioti, 2010).

Theoretical considerations

The present study is the first to demonstrate *bilaterally* decreased cortical activation in two chronic pain syndromes with *unilaterally* affected upper extremities, CRPS I and II, in comparison with healthy subjects. These bilateral cortical plasticity changes may provide an explanation for the clinical observation that CRPS, after starting in one extremity, ***spreads*** *seemingly spontaneously* to the opposite side and to another extremity (Maleki et al., 2000; van Rijn et al., 2011). The

seemingly unaffected hemispheres (UHs) in CRPS I and II patients may functionally be less able to process somatosensory afferent inputs and to integrate information interhemispherically in a normal way, due to their involvement in the disease process (Wyke, 1982; Berlucchi, 2010).

Even after years of chronic pain these functional cortical plasticity changes are rapidly reversible using SCS or a local block (Chapter 4 and 8). Not included in this study are plasticity changes due to sprouting of nerve fibres after injury and neurotransmitter changes that accompany pain syndromes (Florence, 2002). The latter, induced neuroplasticity changes are difficult to restore due to more permanent changes, which explains the difficulty of treating these patients. Another consequence of impaired afferent somatosensory integration and hemispherical involvement in CRPS is *dystonia*, which occurs in 25% of the cases (van Rijn et al., 2007; van Hilten, 2010; Munts et al., 2011). Impaired afferent somatosensory inputs produce altered and impaired somatosensory-motor coupling, which primarily affects the injured extremity (Tinazzi et al., 2000; Florence, 2002; Swart et al., 2009). Neither Tinazzi nor Swart observed bilateral hemispherical changes due to a different study design.

Future perspectives

The observed differences between CRPS I and II GFP distribution (curves and values) at M30 and M70 are an indication of changes in cortical neural activation. They suggest that in CRPS II, due to the changes after nerve injury described earlier, relatively larger areas of cortical neural activation are being processed than in CRPS I. Bilateral cortical changes due to a unilaterally affected upper extremity and chronic pain may require different approaches to treatment and to monitoring therapeutic effects in CRPS I and II (Bultitude et al., 2010; Rothgangel et al., 2011).

In the last Dutch “evidence based guideline Complex Regional Pain Syndrome, type I” (Geertzen et al., 2006) no objective diagnostic tests proved to be available, and the diagnosis remains largely dependent on questionnaires. Neurophysiological monitoring with evoked fields may offer an additional objective tool for further study of chronic pain. In CRPS, it is recommended to use a combination of contemporary stimulation techniques like Qualitative Sensory Testing (Hansson et al., 2007) and non-invasive neuroimaging techniques like magnetoencephalography. The added value of combinations of techniques, depending on the research question, may provide a more solid substantiation of the mechanisms operational in CRPS and chronic pain.

References

Bruehl S, Harden RN, Galer BS, Saltz, S. External validation of IASP diagnostic criteria for Complex Regional Pain Syndrome and proposed research diagnostic criteria. International Association for the Study of Pain. Pain 1999; 81: 147-154.

Bultitude JH, Rafal RD. Derangement of body representation in complex regional pain syndrome: report of a case treated with mirror and prisms. Exp Brain Res 2010; 04: 409-418.

Berlucchi G, Aglioti SM. The body in the brain revisited. Exp Brain Res 2010; 200: 25-35.

Berlucchi G (2011). What is callosal plasticity? In: Chalupa LM, Berardi N, Caleo M, Galli-resta L, Pizzorusso T (Ed), Cerebral Plasticity, new perspectives, 1st Edn. Massachusetts Institute of Technology, Toppan Best-set Premedia Limited, USA, pp 235-246.

Bloom JS, Hynd GW. The role of the corpus callosum in interhemispheric transfer of information: excitation or inhibition? Neuropsychol Rev 2005; 15: 59-71.

Burton H (2005). Cerebral cortical regions devoted to the somatosensory system. In: Nelson RJ (Ed), The somatosensory system: deciphering the brains own body image. Methods and new frontiers in neuroscience. CRC Press, Boca Raton, USA, pp 27-73.

Florence SL (2002). The changeful mind: Plasticity in the Somatosensory system. In: Nelson RJ (Ed), The somatosensory system. CRC Press, Boca Raton, pp 335-367.

Geertzen JHB, Perez RSGM (2006). Diagnostics, Epidemiology and Etiology. In: Geertzen JHB, Perez RSGM, Dijkstra PU, Kemler MA, Rosenbrand CJGM (Ed), Evidence Based Guideline Complex regional Pain Syndrome I. Van Zuiden, Utrecht, The Netherlands, pp 29-55. In Dutch.

Hansson P, Backonja M, Bouhassira D. Usefulness and limitations of quantitative sensory testing: clinical and research application in neuropathic pain states. Pain 2007; 129:256-259.

Hari R, Reinikainen K, Kaukoranta E, Hämäläinen M, Ilmoniemi R, Penttinen A, Salminen J, Teszner D. Somatosensory evoked cerebral magnetic fields from SI and SII in man. Electroencephalogr Clin Neurophysiol 1984; 57: 254-263.

Hari R, Forss N. Magnetoencephalography in the study of human somatosensory cortical processing. Philos Trans R Soc Lond B Biol Sci 1999; 1387: 1145-1154.

Hummel F, Gerloff C, Cohen LG (2005). Modulation of Cortical Function and Plasticity in the Human Brain. In: Ebner FF (Ed), Neural plasticity in adult somatic sensory-motor systems, 1st edition. Boca Raton, Taylor & Francis Group, USA, pp 207-227.

Kaas JH. Is most of neural plasticity in the thalamus cortical? Proc Natl Acad Sci 1999; 96: 7622-7623.

Kakigi R, Hoshiyama M, Shimojo M, Naka D, Yamasaki H, Watanabe S, Xiang J, Maeda K, Lam K, Itomi K, Nakamura A. The somatosensory evoked magnetic fields. Prog Neurobiol 2000; 61: 495-523.

Li L, Ebner FF. Balancing bilateral sensory activity: callosal processing modulates sensory transmission through the contralateral thalamus by altering the response threshold. Exp Brain Res 2006; 172: 397-415.

Maihöfner C, Handwerker HO, Neundörfer B, Birklein F. Cortical reorganization during recovery from complex regional pain syndrome. Neurology 2004; 63: 693-701.

Maleki J, LeBel AA, Bennett GJ, Schwartzman RJ. Patterns of spread in complex regional pain syndrome, type I (reflex sympathetic dystrophy). Pain 2000; 88: 259-266.

[1]Rossini PM, Narici L, Martino G, Pasquarelli A, Peresson

M, Pizzella V, Tecchio F, Romani GL. Analysis of interhemispheric asymmetries of somatosensory evoked magnetic fields to right and left median nerve stimulation. Electroencephalogr Clin Neurophysiol 1994; 91: 476-482.

[2] Rossini PM, Martino G, Narici L, Pasquarelli A, Peresson M, Pizzella V, Tecchio F, Torrioli G, Romani GL. Short-term brain 'plasticity' in humans: transient finger representation changes in sensory cortex somatotopy following ischemic anesthesia. Brain Res 1994; 642: 169-177.

Rothgangel AS, Braun SM, Beurskens AJ, Seitz RJ, Wade DT. The clinical aspects of mirror therapy in rehabilitation: a systematic review of the literature. Int J Rehabil Res 2011; 34: 1-13.

Schwoebel J, Coslett HB. Evidence for multiple, distinct representations of the human body. J Cogn Neurosci 2005; 17: 543–553.

Swart CM, Stins JF, Beek PJ. Cortical changes in complex regional pain syndrome (CRPS). Eur J Pain 2009; 13: 902-907.

Tecchio F, Pasqualetti P, Pizzella V, Romani G, Rossini PM. Morphology of somatosensory evoked fields: inter-hemispheric similarity as a parameter for physiological and pathological neural connectivity. Neurosci Lett 2000; 287: 203-206.

Theuvenet PJ, Dunajski Z, Peters MJ, van Ree JM. Responses to Median and Tibial Nerve Stimulation in Patients with Chronic Neuropathic Pain. Brain Topography 1999; 11: 305-313.

Theuvenet PJ, de Munck JC, Peters MJ, van Ree JM, Lopes da Silva FL, Chen AC: Anesthetic block of pain-related cortical activity in patients with peripheral nerve injury measured by magnetoencephalography. Anesthesiology 2011; 115: 375-386.

Tinazzi M, Priori A, Bertolasi L, Frasson E, Mauguière F, Fiaschi A: Abnormal central integration of a dual somatosensory input in dystonia. Evidence for sensory overflow. Brain 2000; 123: 42-50.

Vanni S, Rockstroh B, Hari R. Cortical sources of human short-latency somatosensory evoked fields to median and ulnar nerve stimuli. Brain Res 1996; 737: 25-33.

Van Hilten JJ. Movement disorders in complex regional pain syndrome. Pain Med 2010; 11: 1274-1277.

Van Rijn MA, Marinus J, Putter H, van Hilten JJ. Onset and progression of dystonia in complex regional pain syndrome. Pain 2007; 130: 287-293.

Van Rijn MA, Marinus J, Putter H, Bosselaar SR, Moseley GL, van Hilten JJ. Spreading of complex regional pain syndrome: not a random process. J Neural Transm 2011; 118: 1301-1309.

Werhahn KJ, Mortensen J, Kaelin-Lang A, Boroojerdi B, Cohen LG. Cortical excitability changes induced by deafferentation of the contralateral hemisphere. Brain 2002; 125: 1402-1413.

Woolf CJ. The pathophysiology of peripheral pain-Abnormal peripheral input and abnormal central processing. Neurochir Suppl Wien 1993; 58: 125-130.

Wyke M. Interhemispheric integration in man. Psychol Med 1982; 12: 225-230.

Acknowledgements

Courtesy M.A. Dekkers, MSc.
Former Coordinator Pain Clinic MCA

This thesis is dedicated to the Quality System Neuromodulation in The Netherlands. The development of a Quality System for Neuromodulation was proposed and developed by a number of medical specialists for the benefit of chronic non-oncological pain patients. In 2002, the Study "Quality System Neuromodulation" resulted in recognition by the Dutch Government as a requirement for reimbursement of this invasive and very costly therapy. The confidence and support of the Dutch Health Insurance Board – CVZ (Mr. R. Langenberg, Mr. H. Jansen, Drs. G. Gimbrere) and the Ministry of Health (VWS) over so many years (former Minister Prof. Dr. Mrs. E. Borst-Eilers and Drs. N. Oudendijk) couldn't be emphasized more. Without that support, the Quality System would never have been completed. To this day, it is still a standard, yet to be completed since the second and third level of organization have never been introduced. We promised a quality system Neuromodulation, guaranteeing a controlled and gradual implementation of this system but we *never even got close*.

I would like to thank Dr. G.H.J.J. Spincemaille, former neurosurgeon at the UMC-Maastricht. **Dear Geert**; history will not award us for all the efforts we made over nearly 20 years in supporting Neuromodulation, often working with empty hands. I would like to thank you and Rita for all your support, friendship and hospitality! Here I also would like to thank Mr. J. Merkun, former Vice-president Europe at Medtronic (Medtronic, Tolochenaz, Switzerland). **Dear Jo**, without the financial support, made available thanks to your personal efforts, this thesis wouldn't have been possible. Thank you for supporting Neuromodulation especially between 1990-2000, when there was no reimbursement whatsoever. We were simply living our professional life from one day to another.

In *chronological order*, it is my great pleasure to express my deep gratitude to all those who have made this thesis and my work in pain medicine possible.

Prof. dr. Jan M. van Ree, neuro-pharmacologist.
Dear Jan, basically this thesis started on Monday, the 17th of June 1991 in your room at the former Rudolf Magnus Institute, Vondelstraat 6 in Utrecht. You will probably never realize how big that step was for me at that time. The institute where, as a medical student, I spent so many hours learning from the teachings in Pharmacology by your predecessors, Prof. Dr. M. Tausk and Prof. Dr. D. de Wied. We met for the first time in January 1980, in Montpellier (France) where you presented a talk on endorphins that I will never forget. In history, the Rudolf Magnus Institute was a tiny bit too late to present beta-endorphin as an important medical discovery. Apart from your personal support over so many years in the interest of the basic science of pain medicine and Neuromodulation, I can only deeply cherish the friendship that underlies all of our cooperation, and I would like to thank you for that!

Prof. Dr. J.M (Riet) Peters, physicist.

Lieve Riet, in 1992 I was bewildered by your interview in Elsevier's Magazine, and so the choice for MEG was partially a coincidence. After a telephone call from our Day Care Hospital in Alkmaar, you showed much interest and since then I have always been welcome at the "Huisje", Low Temperature Division, University in Twente (1993-1999). The first MEG was measured on the 4th of March 1993. Our early work with Zbigniew Dunajski, is the basis of the present thesis. Above all, I am aware that I have been very fortunate that we met and that, within the limits of your financial budget in Twente, I was allowed to perform 34 measurements. Thank you very much for your support and for your friendship over nearly 20 years. Hopefully health care and our patients will benefit from our work! *Prof. Dr. Zbigniew Dunajski, physicist*. **Dear Zbigniew**, the support and kindness, not only from you as a scientist but also from your wife Christina, will never be forgotten. You have been at the basis of our pilot study at the University of Twente and I would like to express my gratitude for your lessons and support, not only over those six years but even until today. Thank you for showing me the historical part of Warschaw in 2010.

Prof. Dr. Fernando L. Lopes da Silva..

Dear Fernando, thank you for all your kindness, support and advice over so many years. You were among those who helped me to continue to keep confidence in this project. I will not forget the welcome at the Amsterdam University and your help with the second MEG study in 1999. We were able to perform eight measurements which enabled us to start the study.

Prof. Dr Andrew Chen (Aalborg Technical University, Denmark and Capital Medical University Beijing – China).

Dear Andrew, meeting you for the first time in the gloomy basement of the St. Lucas Hospital in Zavethem (Belgium) in December 1999 started a new chapter in my professional and personal life that I couldn't be more grateful for. Working with you in Aalborg and Beijing was sometimes like jumping on the high velocity train to Paris. Without your continuous support over the past 10 years, this thesis would have been very difficult to finish. On behalf of all our patients, thank you for helping me to try to study the basic cortical mechanisms underlying CRPS I and II. You came a long way in your own scientific life. First at John Bonica's University in Seattle, acknowledged and invited by Aalborg University and later by the Chinese Academy of Sciences to work in the Human Brain mapping Institute at the Capital Medical University in Beijing. I hope that we will be able to continue cooperation in the future. "Yellow river" was once a very popular pop song I liked a lot (Christie, 1970), so let's try to make it to the Yellow river before we have nothing to do anything else …..

Dr. B.W. van Dijk, physicist (MEG center, VU University Hospital, Amsterdam). **Dear Bob**, after meeting you in 1999, the pilot started that resulted in the present study. Thank you for all the technical support and advice during the study and all your help with our publications.

Dr. J.C. de Munck, physicist (VU University Medical Center (Amsterdam, Dept, Phys. Med. Technology). **Dear Jan**, in our study you proved to be of value and I am grateful for your contribution as my co-promotor. I can only hope that in the near future we will be able to continue our cooperation with MEG. Thank you for your pancake images in the end …which are, after all, a typically Dutch treat!

Dr. R. Oosterveld, physicist (Donders Institute Nijmegen).
Dear Robert: you advised and supported me at all those moments when I was unable to process the averaged MEG data, you provided me with software hyperlinks which enabled me to use the CTF program. Your willingness to travel to Alkmaar on Saturdays and all our communication by e-mail will not be forgotten. In my work at home on all the individual data sets, your support in processing the data was vital to me.

Medical Center Alkmaar (The Netherlands)
A great deal of what and who I became as a medical professional, I owe to my teachers in Alkmaar. In 1973 I worked as junior (co-assistant) in Neurology and Psychiatry especially with Dr. F. Appelman. **Dear Frank**, during my entire professional carrier I have learned and benefited from your great wisdom, starting in January 1973. After all our Sunday discussions in 1973 I started reading Jung's work. Life has awarded us greatly by providing us the opportunity to continue the discussions we started in 1973, and happily those discussions have never ended.

In 1975 I took up an internship (Wissel-assistenschap) for 18 months, mainly in Surgery (Jen Niebuurt, Dr. Ron Hiemstra, Aycke Smook, Jan Bonnier), Gynecology (Haye Hoekstra, Jaap Bennen, Dr. Jan Boodt) and Anesthesiology (Cas Zegveld, Frits Hirschmann and Pat Gijsberts). I am indebted to all my teachers, especially the late Cas Zegveld. **Dear Cas**, in 1968 you were one of the three initiators in our country of what today is called I "Pain Medicine" in Anesthesiology (Admiraal, Knape, Zegveld). I will never forget your value for pain medicine in The Netherlands and the way you encouraged me to become an anesthesiologist and a pain specialist. Your skillfulness and kindness to patients have been an example I will not forget. I hope you are doing well on your cloud, ……this time hopefully without your Camel cigarette.

P.J. Moens, economic director, Board of Directors, Medical Center Alkmaar. **Dear Piet**, up till now I consider you as the father of our hospital, the Medical Center Alkmaar. You were for me one of those in the management of our hospital who really cared for the interests of our hospital and personnel and I consider myself lucky that during my period 1984-1988 as Chairman of the Medical Staff, we were able to serve the interests of the Medical Center Alkmaar in close cooperation.

To our Neuromodulation team: Babetti van Wijngaarden Lindhout, Mariska Tesselaar, Monique Dekkers. **Dear all**, I cherish the memory of our work in Neuromodulation, it was highly professional and thanks to your efforts our hospital received full CVZ and SLKN recognition. Far beyond our work at that time, I cherish the respect and friendship that we share up until today.

To my paranymphs:
Dr. M.H. Hovingh. **Dear Menno**, I would like to not to express my deep gratitude for all that we were able to share since we met at the CBO. In your capacity as former CBO Board Member, you have been at the basis of what is known today as "The consensus Medical Specialists Guideline Developments (1996) ". Thank you for your friendship since those days.

Monique Dekkers, MSc. **Dear Mo**; I would like to thank you for all your support since 1988. In your former job as Coordinator of our Pain Clinic at the Medical Center Alkmaar, you stood at the very basis of Neuromodulation, in Alkmaar and elsewhere, and often in the theatre after working hours. I cannot but agree with those who once called you "the Dutch mother of Neuromodulation". In the

end, you deserved endlessly much better but you have been awarded with a “blessing in disguise”.

The DTP Department and the library: Mr. R.M. Blom. **Dear René**, thank you for helping me in a very professional and patient way. I am so glad we started years earlier to draft the lay-out of the thesis. The MCA Library. Dear Gertruud, Marc, Carla and Marjan. This thesis was effectively supported by our MCA library staff by providing articles electronically in such an unforgettably fast way, thank you all and hope to meet again soon!

The department of Radiology, MRI section. Dr. P. Algra, radiologist. **Dear Paul**, over many years and in many ways cooperation with your department has been very fruitful and I would like to thank you, also for your advice and support in completing my thesis. I also would like to thank our **radiology assistants** at the MRI department and especially all those who supported us in the pain clinic. Your level of care and kindness is still memorized by our patient ! Patients can tell the difference.

The department of Anesthesiology. Mr. H. Boerma, *Head of the Department*. **Dear Han**, by thanking you I would like to express my enormous gratitude to all the members of our department. Not only for their support in the operating room, but certainly for their contribution and benefit for pain medicine. Thank you for being such a good friend when I stumbled physically in 2009. *Mr. Martin Reij*. **Dear Martin**, thank you for all your lessons in PSP-7. It enabled me to process all graphics and images in this thesus independantly. *The MCA operating theater*. *Mrs. Sylvia Goosensen*. **Lieve Sylvia**, my gratitude for all the support and friendship I received from your staff over all the years that I worked as an anesthesiologist in Alkmaar is tremendous (!). This certainly includes my work at the POK (**Marjon van Denderen**). I hope to meet you in the St. Laurens Church! **Secretariat department of Anesthesiology**: I would like to express my gratitude for all your support and friendship over so many years, it has always been a pleasure to work at the POS. **To our recovery**: thank you all for all support and kindness. **Our receptionists and telephone operators**: I has always been a pleasure to talk to you and I am grateful for all your help over many years.

Now, before my gratitude will cover the length of another thesis, I would like, last but not least, to thank my **family** for supporting and enduring me over so many years. It is not easy to have an anesthesiologist / pain specialist as a father or brother, and certainly not me. As our uncle Mr. Piet van Rij once stated about me when I was about 4, “he looks so quiet, but believe me he’s an ever-slumbering volcano”. Probably that energy kept me going.

There are so many others to thank and possibly I have forgotten someone, human as I am. I will however make it up at the St. Laurens Church in Alkmaar and thank you there.

Curriculum Vitae

Naam Theuvenet

Voornamen Peter Johan

Geboren 17-12-1948.

Peter. J. Theuvenet, anesthesioloog – pijnspecialist

Uit een gezin van drie kinderen ben ik nog steeds de oudste en groeide op tijdens de wederopbouw van Nederland. Mijn vader was civiel ingenieur en mijn moeder was verpleegkundige in het toenmalige Clara Ziekenhuis in Rotterdam. Na de oorlog en na de soevereiniteitsoverdracht in 1949 van Indonesië, wij woonden destijds op Lombok en Bali, keerden mijn ouders terug naar Nederland. Op voordracht van MP Gerbrandy mocht mijn vader voor de Food and Agriculture Organization (FAO) van de Verenigde Naties gaan werken, hij was avant la lettre een “ontwikkelingshulpwerker” en het bijbehorende wereldbeeld in de 50er en 60er jaren ben ik nooit vergeten (de krentebol en de kaars met kerstmis). Het verging mij als mens niet anders, tegen de tijd dat je nog eens rustig om uitleg naar al die stappen zou willen vragen waren ze er allebei niet meer en was de deur naar mijn verleden dicht. Na 2 kleuterscholen, 3 lagere scholen en 3 middelbare scholen behaalde ik in Den Helder in 1967 mijn HBS-B diploma. Eeuwig onderweg, altijd afscheid nemen maar het maakte me wel flexibel. Den Helder voelt voor mij nog steeds een beetje als thuis, daar leerde ik van de zee houden. Mijn ouders hebben mij twee elementaire zaken voorgeleefd die in belangrijke mate hebben bepaald wie en wat ik later zou worden: een “Godsbesef” en “dat niets in het leven vanzelfsprekend is”. Daar zullen ongetwijfeld mede de fundamenten liggen waarop mijn streven naar het steeds blijven proberen de inhoud en de kwaliteit van de uitoefening van de medisch specialistische geneeskunst te helpen verbeteren, is gebaseerd. In goede samenhang met vele anderen heb ik daar inhoud en gestalte aan proberen te geven. Dit proefschrift markeert tevens mijn vertrek uit het MCA en is voor mij een moment van zeer grote dankbaarheid voor alles wat ik op mijn weg tegenkwam en ondervond in samenhang met heel veel andere mensen. “Opgeven” komt in mijn woordenschat niet voor.

• Artsendiploma, Rijksuniversiteit Utrecht	maart 1974
• Medisch Specialistendiploma Anestesiologie & Pijnbestrijding, Universiteit Leiden	oktober 1980

• Erelid van de Orde van Medisch Specialisten (OMS)	1997
• Koninklijke onderscheiding: Officier in de Orde Oranje Nassau	2007
• Erelid van het Petrus Camper Instituut	2008

• Militaire dienstplicht in Seedorf (West-Duitsland)	1974 - 1975
• Wisselassistentschap Centraal Ziekenhuis Alkmaar (MCA)	1975 - 1977
• Lid van de Medische Staf van het Medisch Centrum Alkmaar (MCA)	1980 - 2012
• Voorzitter van de Medische Staf van het MCA	1984 - 1988
• Lid van het Centraal Bestuur van de Landelijke Specialisten Vereniging (L.S.V.)	1988 - 1998
• Lid van de Raad van Toezicht van het CBO	1991 - 1995
• Lid van de Ziekenfondsraad werkgroep Accreditatie Ziekenhuizen (werd het NIAZ)	1991 - 1998
• Lid van het Bestuur van de Sectie Pijn van de Nederlandse Vereniging van Anesthesiologie	1992 - 1995
• Voorzitter Commissie Kankerpijnbestrijding (NVA))	1992 - 1995
• Lid Commissie ontwikkeling Richtlijnen Pijnbestrijding (o.a. CRPS I en Kankerpijnbestrijding)	1992 - 1995
• Lid van het Centraal Bestuur van de Europese Vereniging van Medisch Specialisten (UEMS)	1992 - 2006
• Lid van het bestuur van de Stichting Managementparticipatie Medisch Specialisten (SPMS)	1993 - 2006
• Hoofd LSV delegatie bij de Europese Vereniging van Ziekenhuisartsen (AEMH)	1993 - 2000
• Medeoprichter en initiatiefnemer Kwaliteitssysteem Neuromodulatie	1994 - 2006
• Vice-Voorzitter van de Landelijke Specialisten Vereniging (LSV)	1994 - 1998
• Voorzitter van het Platform Kwaliteit (LSV)	1994 - 1998
• Voorzitter van de Commissie Kwaliteit (LSV)	1994 - 1998
• Initiatiefnemer Pijnbestrijding Regionaal Beleid NHN	1994 - 2008
• Voorzitter van de Medisch Wetenschappelijke Raad van het CBO	1996 - 2006
• Adviseur van de Raad Wetenschap, Opleiding en Kwaliteit van de OMS	1997 - 2000
• Medeoprichter en bestuurslid Stichting Intranet Medisch Specialisten Nederland (SIMSN)	1997 - 2010
• Medeoprichter en secretaris van het Petrus Camper Instituut	1997 - 2008
• Bestuurslid Begeleidingscommissie SBW Art. 18 Voorzieningen CVZ	1998 - 2000
• Coördinator Pijnpolikliniek, Medisch Centrum Alkmaar	2000 - 2010
• Hoofd LSV delegatie bij de Europese Vereniging van Medisch Specialisten (UEMS)	2003 - 2006
• Secretaris Stichting Landelijk Kwaliteitssysteem Neuromodulatie (SLKN)	2006 - heden
• Vice-president van de Europese Vereniging van Medisch Specialisten (UEMS) (aandachtsgebieden Kwaliteitsbeleid en Europese elektronische communicatie)	2002 - 2006

Publikaties

Vielvoye-Kerkmeer AP, Theuvenet PJ. Is prescribing of opioïd analgesics such as morphine to patients with chronic benign pain (un)ethical? Ned. Tijdschrift van Geneeskunde 1992; 14: 2261-63.

Boersma FP, Bosma E, Giezen, Theuvenet PJ. Cancer Pain Control by Infusion Techniques. Journal of Pain and Symptom Management 1992; 7 : 155-9.

P.J. Theuvenet, Dr. A.P.P.M. Driessen, Dr. J.M.W.M. Merkus, Prof. Dr. A.F. Casparie, I. van de Wiel – Maas, Mevr. Mr. W.L.R. Kuipers. Kwaliteitsbeleid Medische Specialisten 1995. ISBN 90-70655-09-8. De Doelenpers, Alkmaar.

Lombarts M.J.M.H., Dr. van Everdingen J.J.E., Theuvenet, P.J., Prof. Dr. Casparie, A.F. Consensus over Medisch-Specialistische Richtlijnen 1996. ISBN 90-70655-10-1.

Theuvenet PJ, Dunajski Z, Peters MJ, van Ree JM. Responses to median and tibial nerve stimulation in patients with chronic neuropathic pain. Brain Topogr 1999; 11: 305-13.

P.J. Theuvenet, J.S. Burgers en N.S. Klazinga. Historisch perspectief van Richtlijnontwikkeling in Nederland. In: J.J.E van Everdingen (Ed) Evidence-based Richtlijnontwikkeling. ISBN 90-313 4209 2. Bohn, Stafleu, van Loghem, Houten, 2004; pp. 11-17.

A.F. Casparie, P.J. Theuvenet, N.S. Klazinga en A.E. Timmerman. Richtlijnontwikkeling als onderdeel van Kwaliteitssystemen. In: J.J.E van Everdingen (Ed) Evidence-based Richtlijnontwikkeling. ISBN 90-313 4209 2. Bohn, Stafleu, van Loghem, Houten, 2004; pp. 36-48.

M. Berg, D. de Vos, K.H. Njoo, P.J. Theuvenet. ICT-ondersteuning: de volgende stap in de evolutie van richtlijnen. In: J.J.E van Everdingen (Ed) Evidence-based Richtlijnontwikkeling. ISBN 90-313 4209 2. Bohn, Stafleu, van Loghem, Houten, 2004; pp. 272-280.

Geert H. Spincemaille, MD, PhD; Nicoline Beersen; Monique A. Dekkers, RN; Peter J. Theuvenet, MD. Neuropathic Limb Pain and Spinal Cord Stimulation: Results of the Dutch Perspective Study. Neuromodulation 2004; 7: 184-92.

Beersen N, Bart de Bruijn JH, Dekkers MA, Ten Have P, Hekster GB, Redekop WK, Spincemaille GH, Theuvenet PJ, Berg M, Klazinga NS. Developing a national continuous quality improvement system for neuromodulation treatment in The Netherlands. Jt Comm J Qual Saf 2004; 30: 310-21.

P.J. Theuvenet, MD1, M.A. Dekkers, R.N1, N. Beersen, MSc, N.S. Klazinga, MD, PhD3, G.H.J.J. Spincemaille, MD., PhD4. The Development of a Quality System for Neuromodulation in the Netherlands. Neuromodulation, 2005, 8: 28-35.
Beersen N, Redekop WK, de Bruijn JH,

Theuvenet PJ, Berg M, Klazinga NS. Quality based social insurance coverage and payment of the application of a high cost medical therapy: the case of spinal cord stimulation for chronic non-oncologic pain in The Netherlands. Health Policy 2005; 71: 107-15.

Peter J. Theuvenet, Bob W. van Dijk, Maria J. Peters, Jan M. van Ree, Fernando L. Lopes da Silva and Andrew CN. Chen.. Whole head MEG analysis of cortical spatial organization from unilateral stimulation of median nerve in both

hands: No complete hemispheric homology. NeuroImage 2005; 28: 314-325.

Peter J. Theuvenet, Bob W. van Dijk, Maria J. Peters, Jan M. van Ree, Fernando L. Lopes da Silva and Andrew CN. Chen. Hemispheric Discrimination in MEG between median versus ulnar nerve in unilateral stimulation of left and right hand. Brain Topography 2006; 19: 29-42.

Sensory handedness is not reflected in cortical responses after basic nerve stimulation. A MEG study. Chen ACN, Theuvenet PJ, de Munck JC, Peters MJ, van Ree JM, Lopes da Silva FL. Brain Topography; 2011: Nov 12 [Epub ahead of print].

Anesthetic Block of Pain-related Cortical Activity in Patients with Peripheral Nerve Injury Measured by Magnetoencephalography. Theuvenet PJ, de Munck JC, Peters MJ, van Ree JM, Lopes da Silva FL, Chen ACN. Anesthesiology 2011; 115; 375-386.

Samenvatting

Inleiding

Complex Regionaal Pijn Syndroom (CRPS) type I stond voorheen bekend als posttraumatische dystrofie of Südeck atrofie en CRPS type II als causalgie (brandende, continue pijn). CRPS I kan ontstaan na een polsfractuur met vaak als klacht knellend gips of na een enkelverstuiking. Soms lijkt het pijnsyndroom spontaan te zijn ontstaan. Het enige verschil met CRPS II is dat er bij dit type per definitie sprake is van een perifeer zenuwletsel (b.v bij de pols of enkel). Beide CRPS typen werden in 1994 gedefinieerd door de International Association for the Study of Pain (IASP) en zijn in Nederland bekende chronische pijnsyndromen. De IASP beschrijving van CRPS I en II laat identieke symptomen zien. Er kan sprake zijn van langdurig veel pijn, oedeem, een koude of juist warme hand of voet, funktieverlies en invaliditeit wat in zeldzame gevallen kan leiden tot (gedeeltelijke amputatie) van een arm of been. Bij de laatste herziening van de Nederlandse “Evidence based richtlijn” CRPS I in 2006 werd wederom vastgesteld dat de diagnose grotendeels gesteld wordt op basis van symptomen en dat objectieve onderzoeksmethoden niet voorhanden zijn. De reden hiervoor is dat onbekend is wat CRPS I veroorzaakt, hoe het in stand gehouden wordt en waarom de ene patiënt na een polsfractuur wel CRPS krijgt en de andere niet.

Plasticiteit

In de laatste decennia werd steeds duidelijker dat er bij chronische pijn continu pijnprikkels naar de hersenen worden gestuurd die daar funktionele veranderingen veroorzaken. Dit soort blijvende veranderingen in de hersenen wordt aangeduid met plasticiteit (Hoofdstuk 2). Plasticiteit in het zenuwstelsel stelt ons gedurende ons hele leven in staat tot aanpassingen aan de zich steeds veranderende omstandigheden en eisen van het leven. Plasticiteit in de hersenen ziet men niet alleen bij patiënten met bijvoorbeeld chronische pijn maar ook bij gezonde mensen, zoals bij sporters of musici. Hierbij worden specifieke hersengebieden die veel gebruikt worden in een bepaalde beroepsgroep vergroot. Pijn en pijnprikkels worden bij de mens verwerkt in het gevoelszenuwstelsel (het somatosensorische zenuwstelsel). Het gevoelszenuwstelsel is één van onze vijf zintuigen. Het zorgt er voor dat tast, koude en warmte, de stand van ons lichaam in de ruimte maar ook pijn in de hersenen geregistreerd wordt en het bevordert bovendien het in stand houden van ons lichaamsschema (Hoofdstuk 2). Meerdere hersengebieden zijn bij het verwerken van pijnprikkels en het gewaarworden van pijn betrokken en functionele veranderingen treden na een letsel snel op.

Bij de behandeling van CRPS I en II kan, bij patiënten waar geen andere behandeling meer mogelijk is, ruggenmergstimulatie worden toegepast of een morfinepomp worden geïmplanteerd (neuromodulatie). De in dit proefschrift beschreven onderzoeken begint bij de observatie dat het gunstige effect van ruggenmergstimulatie na verloop van tijd vermindert. Om hiervoor een verklaring te vinden werd met zeer gevoelige magnetoencephalografie (MEG) apparatuur de hersenactiviteit gemeten ten gevolge van elektrische stimulatie van de nervus medianus en nervus ulnaris. Deze metingen werden uitgevoerd in drie groepen, gezonde personen, een groep patiënten met een CRPS I en een groep met CRPS II. Door vergelijking van de hersenactiviteit tussen deze drie groepen werd in kaart gebracht in hoeverre plasticiteit van de hersenen een rol speelt. Toen aan deze studie werd begonnen (1993), was er nog relatief weinig bekend over het meten van opgewekte corticale activiteit met MEG bij de mens, laat staan bij patiënten met chronische pijn.

De meetmethode

Magnetoencephalografie (zie Hoofdstuk 3) is een relatief nieuwe niet-invasieve meetmethode. De zenuwcellen in de hersenen veroorzaken elektrische activiteit waardoor een magnetisch veld wordt opgewekt. Zeer kleine veranderingen van het magnetische veld kunnen door MEG gemeten worden. Funktioneel menselijk hersenonderzoek wordt verder mogelijk gemaakt door het combineren van MEG meetgegevens met een MRI (Magnetic Resonance Imaging), dat de structuren in de hersenen in beeld brengt. Na elektrische stimulatie van een zenuw bij de pols (nervus medianus of nervus ulnaris), volgt een "opgewekte activiteit in de hersenen". Uitgangspunt was meer te weten te komen over de mechanismen die een rol spelen in de hersenen bij beide pijnsyndromen. Alleen patiënten met een CRPS I of II aan één arm werden bestudeerd. Bij alle patiënten met een CRPS II werd bovendien een derde of zelfs vierde MEG meting verricht na lokale verdoving op de plaats van het zenuwletsel. De meetopstelling was voor de drie groepen identiek (Hoofdstuk 3).
Om de opgewekte hersenactiviteit tussen verschillende groepen te kunnen vergelijken werden de reacties in de hersenen gekarakteriseerd door 10 parameters: de tijd na elektrische stimulatie waarbij een piek optrad (de latentietijd in ms), het aantal pieken in de periode van 0 tot 400 ms na stimulatie en de Compressed Waveform Profile (CWP), de vlinderfiguur (blz. 112) die ontstaat na over elkaar projecteren van de signalen van de 151 MEG kanalen. Verder werden bepaald de Global Field Power (GFP), die een maat is voor de distributie van zenuwcelactivering op de hersenschors (blz. 134), en de 6 dipool parameters (blz. 136) behorende bij de pieken M20, M30 en M70 (respectievelijk 20, 30 en 70 ms na begin van de stimulus). Een "3D-brain map" laat op grafische wijze bij een piek met een bepaalde latentie, op de hersenschors een bipolair magneetveld zien met veldlijnen evenals de efflux en de influx (blz. 92). Bestudering van de 20 gezonde personen op basis van de 10 parameters leverde een referentiekader op voor de onderzoeken bij patiënten. Bij gezonde personen werd onderscheid gemaakt tussen de LH (linker hemispheer) en de RH (rechter hemispheer) als aanduiding voor de hersenhelft waar een opgewekte reactie werd gemeten. Bij de patiënten werd onderscheid gemaakt tussen de Unaffected Hemisphere (UH), d.w.z. de reactie op de contralaterale hersenhelft na stimulatie van de gezonde arm en de Affected Hemisphere (AH), de reactie op de contralaterale hersenhelft na stimulatie van de aangedane arm. In de CRPS II groep werden bovendien metingen gedaan na een plaatselijke verdoving van de aangedane zenuw, die de pijn tijdelijk deed verdwijnen (de AH block waarden).

Wat hebben we gevonden?
Op basis van de resultaten (parameters en "3D-brain maps") kan geconcludeerd worden dat bij ***gezonde personen*** in zeer belangrijke mate sprake is van symmetrie in de opgewekte activiteiten in beide hersenhelften. Niet helemaal symmetrisch verdeeld zijn met name de amplitudes van de pieken bij M20 en M30 (Hoofdstuk 6). Voorzichtigheid bij het beoordelen van de meetresultaten blijft dus geboden. De GFP curves en waarden bij M20, M30 en M70 werden nader geanalyseerd (blz.135). Bij deze drie latenties na medianus en ulnaris stimulatie werden geen significante verschillen in GFP waarden gevonden in de gezonde personen.

Op basis van de GFP curves en waarden in de ***CRPS I groep*** werd gevonden dat de opgewekte activiteit in de UH en AH significant lager was vergeleken met gezonde personen. Na ulnaris stimulatie werd voor de GFP waarde een verlaging in de UH en AH bij M30 en M70 gevonden, na medianus stimulatie alleen bij M70. Binnen de CRPS I groep was de opgewekte reactie in de UH bij M30 en M70 niet significant groter dan in de AH, alhoewel de GFP curve na ulnaris stimulatie een hogere reactie in de UH laat zien dan op de AH (blz. 184).

Binnen de ***CRPS II groep*** werd in dit opzicht een andere situatie gevonden. De opgewekte reactie in de AH bij M70 was significant *groter* dan in de UH na stimulatie van zowel de nervus medianus als ulnaris (blz. 184). Ook in de CRPS II groep was, in vergelijking met gezonde personen, sprake van significant lagere UH waarden, echter voor de CRPS II AH waarden was geen verschil met gezonde personen. Dat betekent dat bij CRPS II het geactiveerde gebied in de AH funktioneel niet verkleind was t.o.v. gezonde personen. Verder waren de CRPS II AH waarden significant groter dan de AH en UH waarden in de CRPS I groep (Hoofdstuk 9).
In tegenstelling tot de CRPS I groep, is bij CRPS II het geactiveerde gebied op de hersenschors relatief intact gebleven. Voor zowel de CRPS I als de CRPS II groep geldt echter dat bij M30 en M70, zowel na nervus medianus als ulnaris stimulatie, de UH waarden significant lager waren dan bij gezonde personen. Dat betekent dat de hemispheer contralateraal aan de gezonde arm, functioneel betrokken is in het ziekteproces. Mogelijk veroorzaakt informatie-uitwisseling tussen de beide hersenhelften ervoor dat de balans in het lichaamsschema in stand wordt gehouden doordat de UH mee verandert.
Bij gezonde personen wordt na stimulatie van de nervus medianus en ulnaris, bij 400 ms na stimulatie, een eerste en tweede polariteitomslag gevonden van het bipolaire magneetveld (b.v. blz. 90 en 137). Bij de CRPS I en II groep is dat regelmatige beeld van polariteitomslagen verdwenen. Dit geeft aan dat in de 400 ms na elektrische stimulus van een zenuw de opgewekte activiteit in de hersenschors anders verloopt in de tijd en mogelijk ook qua plaats.
Bestudering van de dipolen bij de drie groepen laat zien, met name na observatie van de effekten op de hersenschors na een zenuwblokkade en meting in de pijnvrije toestand, dat de veranderingen voornamelijk plaats vinden in de primaire somatosensorische hersenschors en vooral bij 30 en 70 ms na het toedienen van een elektrische stimulus. Het is bekend dat in dat deel van de hersenschors onderscheid in gevoelskwaliteiten wordt gemaakt (somatosensorische discriminatie). Opmerkelijk daarbij is dat na een interventie als ruggenmergstimulatie of een lokaal verdovende blokkade (Hoofdstukken 4 en 8), de opgewekte hersenactiviteit zelfs na jaren van chronische pijn, nog functioneel beïnvloedbaar is.

Waar staan we?
Dit proefschrift presenteert voor het eerst systematisch onderzoek naar de opgewekte activiteit in de hersenschors bij CRPS I en II patiënten na standaard stimulatie van de nervus medianus en ulnaris. Van belang is dat in dit onderzoek de uitkomsten bij patiënten werden vergeleken met een groep gezonde personen die onder identieke onderzoek omstandigheden werd gemeten.
De bevindingen in dit onderzoek geven aan dat bij CRPS I en II corticale plasticiteit en reorganisatie in beide hersenhelften een rol spelen. Dit kan een verklaring geven voor de klinische waarneming dat bij een aantal patiënten na de aangedane arm, ogenschijnlijk spontaan de andere arm of een been betrokken wordt in het ziekteproces. Corticale *reorganisatie op de hersenschors* wordt bij patiënten met CRPS I en II het beste beschreven d.m.v. de GFP curves en waarden en het gegeven dat veranderingen vooral plaatsvinden in de eerste 70 ms na stimulatie. Doordat bij beide groepen patiënt er continu veranderde gevoelsinformatie aan de hersenen wordt aangeboden, zou een stoornis in de koppeling tussen het gevoelszenuwstelsel en het motorische zenuwstelsel dystonie kunnen veroorzaken. Daardoor is de spierspanning permanent verstoord wat tot een dwangstand kan leiden en invaliditeit. Voor verder basaal wetenschappelijk onderzoek naar de mechanismen die bij CRPS I en II werkzaam zijn, kunnen afhankelijk van de specifieke vraagstelling combinaties van technieken worden toegepast (Hoofdstuk 3.1.2).

Acronyms

AH = Affected Hemisphere
ALS = AnteroLateral System
CRPS = Complex Regional Pain Syndrome
CWP = Compressed Waveform Profile
EEG = Electroencephalography
ECD = Equivalent Current Dipole model
ES = Effect Size
fT = femto-Tesla (10^{-15} Tesla)
fT^2 = Power
GFP = Global Field Power
HD-EEG = High Definition EEG
IASP = International Association for the Study of Pain
IEEG = Intracranial EEG (with subdural electrodes)
LI = Laterality Index
MEG = Magnetoencephalography
MRI = Magnetic Resonance Imaging
fMRI = functional MRI
MRS = Magnetic Resonance Spectroscopy
MS = Milliseconds
PET = Positron Emission Tomography
PNI = Peripheral Nerve Injury
UH = Unaffected Hemisphere
SI = Primary somatosensory cortex
SII = Secondary somatosensory cortex
SMT = Spinomesencephalic Tract
SPECT = Single Photon Emission Computed Tomography
SQUID = Superconducting Quantum Interference Device
SRT = SpinoReticular tract
STT = SpinoThalamic Tract
TMS = Transcranial Magnetic Stimulation